



HAL
open science

L'inhibition du complexe I mitochondrial améliore l'organogenèse végétale in vitro

Fatima Aissa Abdi

► **To cite this version:**

Fatima Aissa Abdi. L'inhibition du complexe I mitochondrial améliore l'organogenèse végétale in vitro. Amélioration des plantes. Université Paris Saclay (COmUE), 2018. Français. NNT : 2018SACLS136 . tel-02426206

HAL Id: tel-02426206

<https://theses.hal.science/tel-02426206>

Submitted on 2 Jan 2020

HAL is a multi-disciplinary open access archive for the deposit and dissemination of scientific research documents, whether they are published or not. The documents may come from teaching and research institutions in France or abroad, or from public or private research centers.

L'archive ouverte pluridisciplinaire **HAL**, est destinée au dépôt et à la diffusion de documents scientifiques de niveau recherche, publiés ou non, émanant des établissements d'enseignement et de recherche français ou étrangers, des laboratoires publics ou privés.

Mitochondrial complex I dysfunction enhances *in vitro* plant organogenesis

Thèse de doctorat de l'Université Paris-Saclay
préparée à l'Université Paris-Sud

École doctorale n°567
Sciences Du Végétal : du gène à l'écosystème
Spécialité de doctorat : Biologie

Thèse présentée et soutenue à Versailles, le 28/05/2018, par

Fatima AISSA ABDI

Composition du Jury :

Abdelhafid BENDAHMANE Directeur de recherche, INRA, Institute of Plant Sciences Paris-Saclay	Président de jury
Frank VAN BREUSEGEM Professeur, VIB-UGent, Dept. of Plant Systems Biology	Rapporteur
Michel HERNOULD Professeur, Université de Bordeaux, Biologie du Fruit & Pathologie	Rapporteur
Manuelle BODIN Directrice adjointe, Vegenov BBV	Examineur
Pierre HILSON Directeur de recherche, Institut Jean-Pierre Bourgin	Directeur de thèse
Hakim MIREAU Directeur de recherche, Institut Jean-Pierre Bourgin	Invité

Abbreviations

A

ABA	ABscisic Acid
ADP	Adenosine Di-Phosphate
ATP	Adenosine Tri-Phosphate

B

BP	Biological Process
----	--------------------

C

C	Control
cI	complex I
CIM	Callus Induction Medium

D

D	Dilution
DMSO	DiMethyl SulfOxide
DTT	DiThioThreitol

E

ECIM	Embryogenic Callus Induction Medium
------	-------------------------------------

F

FAD	Flavin Adenine Dinucleotide
FADH2	DihydroFlavin Adenine Dinucleotide
FMN	Flavin-Mono-Nucleotide

G

GA	Gibberellic Acid
GL	L-Galactono- γ -Lactone
GLDH	L-Galactono- γ -Lactone Dehydrogenase
Grx1-roGFP2	Glutharedoxin1-reduction-oxidation Green Fluorescent Protein 2

M

MDM	Mitochondrial Dysfunction Motif
ml, mg, cm	millilitre, milligram, centimetre
mETC	mitochondrial Electron Transport Chain
MRR	Mitochondrial Retrograde Regulation

N

NAD(P)H	Nicotinamide Adenine Dinucleotide
NPA	N-1-Naphthylphthalamic Acid

O

OXPHOS	OXidative PHOSphorylation
--------	---------------------------

P

p	p-value
PCD	Programmed Cell Death
PSCT	Plant Stem Cells Technology
Pi	inorganic Phosphate
PPR	PentatricoPeptid Repeat

Q

QTL	Quantitative Trait Locus
-----	--------------------------

R

RH Relative air Humidity

S

SAM Shoot Apical Meristem

SEIM Somatic Embryogenesis Induction Medium

SIM Shoot Induction Medium

ROS Reactive Oxygen Species

T

T Transfer of calli

TCA Tricarboxylic Acid cycle

TDZ Thidiazuron

TSA Trichostatin A

Figures

Figure 1.1: Schematic representation of several regeneration modes.....	2
Figure 1.2: Differentiation, de-differentiation and trans-differentiation of a fertilized egg.....	4
Figure 1.3: WIND1-ESR1 pathway Model for shoot regeneration in Arabidopsis.....	14
Figure 1.4: Auxin and cytokinin interactions during SAM initiation.....	16
Figure 1.5: Schematic model of indirect somatic embryogenesis regulation in Arabidopsis.....	22
Figure 1.6: Auxin and cytokinin patterns during de novo shoot regeneration and SE regeneration.....	26
Figure 1.7: Representation of the protoplasts system.....	26
Figure 1.8: Eukaryotic cell mitochondrion.....	28
Figure 1.9: Simplified scheme of the mitochondrial respiration in plants.....	30
Figure 1.10: Schematic representation of the complex I modular design with core subunits in <i>Arabidopsis thaliana</i>	32
Figure 1.11: Schematic representation of electron and substrate transfer in the respirasome.....	40
Figure 1.12: PPR proteins in eukaryotic cells.....	42
Figure 1.13: Overview of ROS production and scavenging in plants.....	48
Figure 1.14: Foyer-Halliwell-Asada pathway for ROS scavenging.....	52
Figure 1.15: Cellular functions are conditioned by basal ROS level maintenance.....	60
Figure 1.16: Hypothetical model for nucleus-mitochondrion cross-talk in response to cI dysfunction.....	62
Figure 4.1: Shoot regeneration is not correlated with callus size at the transfer to the regeneration medium.....	111
Figure 4.2: Calli growth and regeneration after inhibition of the mitochondrial complex IV with cyanide and of AOX with SHAM.....	113
Figure 4.3: <i>In vitro</i> induced variations among calli derived from two pools of mother plants (wt 1 and wt 2) of the same ecotype (Col-0).	116
Figure 4.4: <i>In vitro</i> induced variation between three biological replicates.	117
Figure 4.5: Hypothetical relationship between inhibitor-mediated oxidative stress and <i>in vitro</i> shoot regeneration.....	119
Figure 5.1: Representation of the experimental setup showing treatments, genotypes and time points characterized through microarray transcriptome analysis.....	128
Figure 5.2: Early and late responses to complex I rotenone inhibition.....	134

Figure 5.3: Transcriptional signature of metabolism genes in rotenone treated calli.....	136
Figure 5.4. Transcriptional signature of cell response genes in rotenone treated calli.....	137
Figure 5.5: Comparison between two cI mutants (<i>mtl1</i> , <i>mtsfl</i>) and wild type in liquid culture.....	139
Figure 5.6: Transcriptional signature of metabolism in cI mutant calli.....	141
Figure 5.7: Transcriptional signature of cell response genes in cI mutant calli.....	142
Figure 5.8: Comparison between cI genetic defect (<i>mtl1</i> , <i>mtsfl</i>) and cI rotenone inhibition.	146
Figure 5.9: Comparison between response to the transfer in rotenone-treated calli and control calli.	149
Figure 5.10: Transcriptional signature of metabolism genes induced by callus transfer and depending on rotenone treatment.....	150
Figure 5.11: Transcriptional signature of cell response genes induced by callus transfer and depending on rotenone treatment.....	152
Figure 5.12: Transcriptional signature of metabolism genes induced by callus transfer in wild type and cI mutant calli.....	155
Figure 5.13: Transcriptional signature of cell response genes induced by callus transfer in wild type and cI mutant calli.....	157
Figure 5.14: Impact of cI genetic defects on the cell wall related genes.....	158
Figure 5.15: Impact of cI genetic defects on photosynthesis related genes.....	159
Figure 5.16: Expression patterns of cell cycle related genes.....	161
Figure 5.17: Expression patterns of cytokinin and auxin related genes.....	164
Figure 5.18: Expression patterns of alternative pathway genes.....	167
Figure 5.19: Expression profile of genes related with complex I impairment.....	169
Figure 5.18: Expression patterns of alternative pathway genes.....	171

Tables

Table 1.1: Complex I subunits in human, <i>Arabidopsis thaliana</i> and <i>Chlamydomonas reinhardtii</i>	34
Table 1.2: Properties, reactivity and production site of the main reactive oxygen species (ROS) in plants.....	46
Table 5.1: Number of differentially expressed genes (DEGs) for each pair-wise comparison.....	131

Contents

Chapter 1: General introduction	1
1. Regeneration	2
1.1. De-differentiation, differentiation and trans-differentiation.....	5
1.1.1. De-differentiation.....	5
1.1.2. Differentiation.....	7
1.1.3. Trans-differentiation.....	7
1.2. Higher plants regeneration.....	9
1.2.1. <i>In vitro</i> shoot regeneration.....	9
1.2.1.1. Hormonal regulation.....	11
1.2.1.2. Molecular regulation of de novo shoot regeneration.....	15
1.2.1.3. Epigenetic control.....	19
1.2.2. Somatic embryogenesis.....	21
1.2.2.1. Hormonal regulation.....	21
1.2.2.2. Molecular regulation of somatic embryogenesis.....	23
1.2.2.3. Epigenetic control.....	23
1.2.3. <i>De novo</i> shoot organogenesis versus somatic embryogenesis in Arabidopsis.....	25
1.3. The use of protoplasts-derived calli to study <i>in vitro</i> shoot regeneration.....	27
2. Mitochondrial respiration.....	29
2.1. The mitochondria	29
2.2. Oxidative phosphorylation system.....	31
2.2.1. Electron transport chain (ETC)	
2.2.1.1. Complex I (cI).....	33
2.2.1.1.1. cI structure and mechanism.....	33
2.2.1.1.2. cI impairment.....	33
2.2.1.2. Complex II (cII).....	35
2.2.1.3. Complex III (cIII).....	35
2.2.1.4. Complex IV (cIV).....	35
2.2.2. Alternative pathway.....	39
2.2.2.1. Rotenone-insensitive Type 2 NAD(P)H dehydrogenases (NADH2s).....	39

2.2.2.2.	Cyanide-insensitive alternative oxidase (AOX).....	39
2.2.3.	The respirasome.....	41
2.2.4.	ATP synthase (complex V, cV).....	41
2.3.	Pentatricopeptide Repeat (PPR) proteins.....	43
2.3.1.	PPR protein family.....	43
2.3.2.	PPR protein structure.....	43
2.3.3.	Arabidopsis PPR mutants affected in mitochondrial cI to study the link between respiration and development.....	45
3.	Redox signaling and plant development.....	47
3.1.	ROS production in plants.....	49
3.1.1.	Singlet oxygen ($^1\text{O}_2$)	49
3.1.2.	Hydroxyl radicals (OH)	49
3.1.3.	Superoxide (O_2^-).....	49
3.1.4.	Hydrogen peroxide (H_2O_2)	49
3.2.	ROS scavenging.....	51
3.2.1.	Anti-oxidant compounds.....	51
3.2.1.1.	Ascorbate-glutathione pathway.....	53
3.2.1.1.1.	Ascorbate (vitamin C).....	53
3.2.1.1.2.	Glutathione (GSH).....	53
3.2.1.2.	Tocopherols (vitamin E) and carotenoids.....	55
3.2.2.	Enzymatic ROS detoxification.....	55
3.2.2.1.	Superoxide dismutase (SOD).....	55
3.2.2.2.	Catalase (CAT).....	55
3.2.2.3.	Ascorbate peroxidase (APX).....	55
3.2.2.4.	Monodehydroascorbate reductase (MDHAR).....	57
3.2.2.5.	Dehydroascorbate reductase (DHAR).....	57
3.2.2.6.	Glutathione reductase (GR).....	57
3.2.2.7.	Guaiacol peroxidase (GPOX).....	57
3.2.2.8.	Thioredoxins (Trx) and glutaredoxins (Grx).....	57
3.3.	Mitochondrial ROS and anti-oxidant systems.....	59
3.4.	Redox regulation of plant development.....	61
3.4.1.	ROS and plant growth.....	61
3.4.2.	ROS and plant regeneration.....	63
3.4.3.	ROS and mitochondrial retrograde signals.....	63

Research outline	67
Chapter 2: Mitochondrial complex I genetic dysfunction enhances shoot regeneration in <i>Arabidopsis thaliana</i> protoplast-derived calli	69
Introduction.....	70
Methods.....	72
• Plant materials and growth conditions.....	72
• Protoplast culture, callus induction and shoot regeneration.....	72
• Growth analysis.....	73
• Total RNA isolation and RT-qPCR.....	73
Results.....	75
• CI genetic dysfunction results in smaller plants but does not prevent organogenesis..	75
• CI deficiency reduces cell proliferation in mutant protoplast-derived calli.....	75
• CI mutant tissues produce more shoot meristems than wild type.....	76
• Marker gene profiles indicate that CI mutants respond differently to tissue transfer than wild type.....	77
Discussion.....	79
Figures.....	82
References.....	85
Chapter 3: The chemical inhibition of the mitochondrial electron transport chain enhances <i>de novo</i> shoot regeneration in <i>Arabidopsis</i> protoplast-derived calli and results in cytosolic oxidative stress	88
Introduction.....	89
Materials and Methods.....	91
• Plant materials and growth conditions.....	90
• Protoplast culture, callus induction and shoot regeneration.....	91
• Rotenone treatment.....	91
• Growth quantification.....	92
• Total RNA isolation and RT-qPCR.....	92
• Redox state measurement.....	92
Results.....	94
• Inhibitory effect of rotenone on <i>Arabidopsis</i> callus growth.....	94
• Rotenone promotes organogenesis when applied at specific stages.....	94
• Rotenone inhibits cell proliferation and induces an oxidative stress in cultured calli..	95

• Mitochondrial complex I rotenone inhibition is rapidly relayed as an oxidative cytosolic signal and the redox shift patterns are cell-dependent.....	96
Discussion.....	99
Figures.....	102
Acknowledgments.....	104
References.....	104
Chapter 4: Variability hampers the functional analysis of bioactive molecules on in vitro development.....	107
Introduction.....	108
Results.....	109
1. Beyond viability, callus size is not a good predictor of <i>in vitro</i> organogenesis.....	109
2. The effect of complex IV and AOX inhibitors on callus growth and regeneration...	112
3. Sources of variability.....	115
Discussion.....	118
Materials and Methods.....	120
• Plant materials and growth conditions.....	120
• Protoplast preparation, callus induction and shoot regeneration.....	120
• Inhibitors preparation and application.....	120
• Cell growth quantification.....	120
• Total RNA isolation and RT-qPCR.....	121
References.....	122
Chapter 5: Transcriptional landscape of <i>in vitro</i> caulogenesis.....	123
Introduction.....	124
Materials and Methods.....	126
• Plant materials and growth conditions.....	126
• Rotenone application.....	126
• Total RNA isolation and microarray analysis.....	126
• Gene ontology (GO) enrichment analysis.....	127
• MapMan analysis.....	127
Results and discussion.....	129
• Experimental set up.....	129
• CI rotenone inhibition reduces the mitotic activity of proliferating protoplast-derived calli and induces genes associated with stress and hormone signaling.....	131

- Proliferating cI mutant calli *mtl1* and *mtsfl* are affected in photosynthesis, oxidative stress and hormonal responses.....138
- The difference between a constant genetic defect and a transient chemical defect...143
- The transfer of calli from callogenesis liquid medium to regeneration gelled medium prompts a major gene expression reprogramming, but cI genetic defects dampen the shock.....147
- Impact of rotenone on the callus transfer response.....147
- Impact of cI genetic defects on the transcriptional response to the transfer.....153
- Cell cycle transcriptional signatures indirectly report the dynamics of callus proliferation.....160
- Phytohormones metabolism and signaling.....162
- Induction of the alternative respiratory pathway.....166
- Comparison with previous reports investigating transcriptional responses to various mitochondrial dysfunctions.....168
- Induction of genes expressed in the shoot meristem.....170

Chapter 6: General discussion and perspectives.....176

References.....183

Chapter I:

General introduction

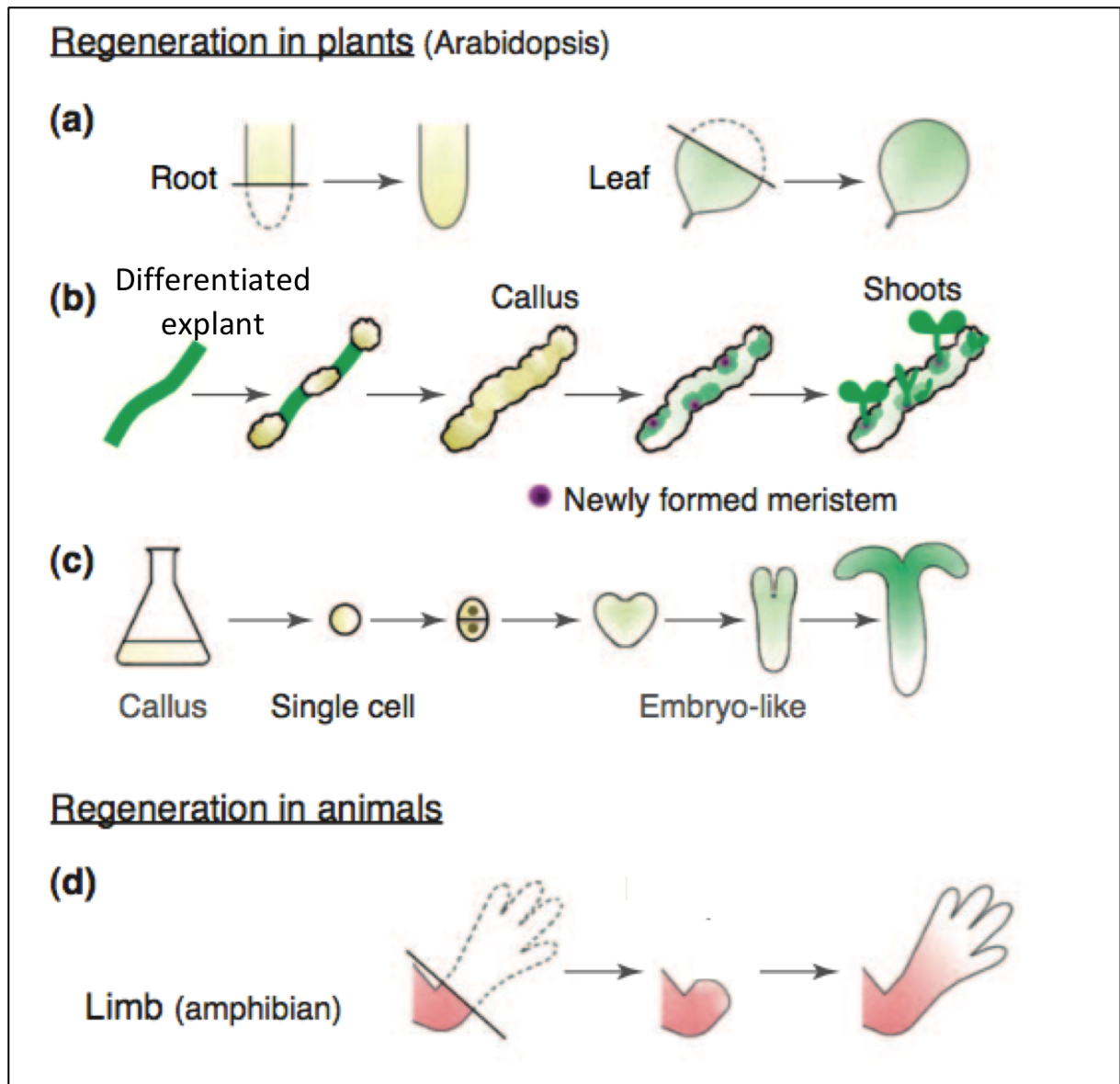


Figure 1.1: Schematic representation of several regeneration modes (Sugimoto et al., 2011). (a) Regeneration of the excised root and leaf parts in Arabidopsis. (b) Arabidopsis *in vitro* shoot regeneration after callus induction from differentiated explant. (c) Somatic embryogenesis from callus culture. (d) Regeneration of limbs in amphibians after amputation.

1. Regeneration

Regeneration is a common mechanism in all living organisms (Figure 1.1) that can happen naturally to face injuries and after amputations by developing new tissues and organs (Sugimoto et al., 2011; Ikeuchi et al., 2016). In humans, the regeneration is limited to very few specific organs, like liver, which regenerate its damaged parts through proliferation of differentiated cells (Jopling et al., 2011). Unlike animal regeneration, plant regeneration usually observed after injuries, could be induced to develop entire new plants. Another difference between animal and plant regeneration is the ability of animal stem cells to move to the damaged site for regeneration whereas plant cells can not; as a result, plants developed other strategies for their remedy without stem cells movement (Xu and Huang, 2014).

The understanding and improvement of plant regeneration have a great importance regarding its use in fundamental and applied biology. Regeneration is a critical step in plant transformation process, polyploidization and in micro-propagation industry (Motte et al., 2014b). In the last decade, a new wave of plant regeneration applications appeared with the use of plant stem cells cultures in cosmetics (Trehan, 2017). This recent technology called PSCT for Plant Stem Cells Technology (Moruš et al., 2014) emerged in cosmetic industries with the exploitation of calli regenerative-properties to deal with several human aging processes as skin aging (Trehan, 2017) or hair follicle aging (Moruš et al., 2014).

In land plants, the regeneration of an entire plant can be conducted *in vitro* through somatic embryogenesis or *de novo* shoot organogenesis followed by root organogenesis with differential auxin/cytokinin ratio to induce the specific biological process (Xu and Huang, 2014). Before *de novo* organogenesis, many species have to pass through a de-differentiation or *trans*-differentiation step. This mechanism can happen naturally after wounding (scar callus) or in the case of *in vitro* tissue culture, de-differentiation is induced by a high auxin/cytokinin ratio (Sugiyama, 2015).

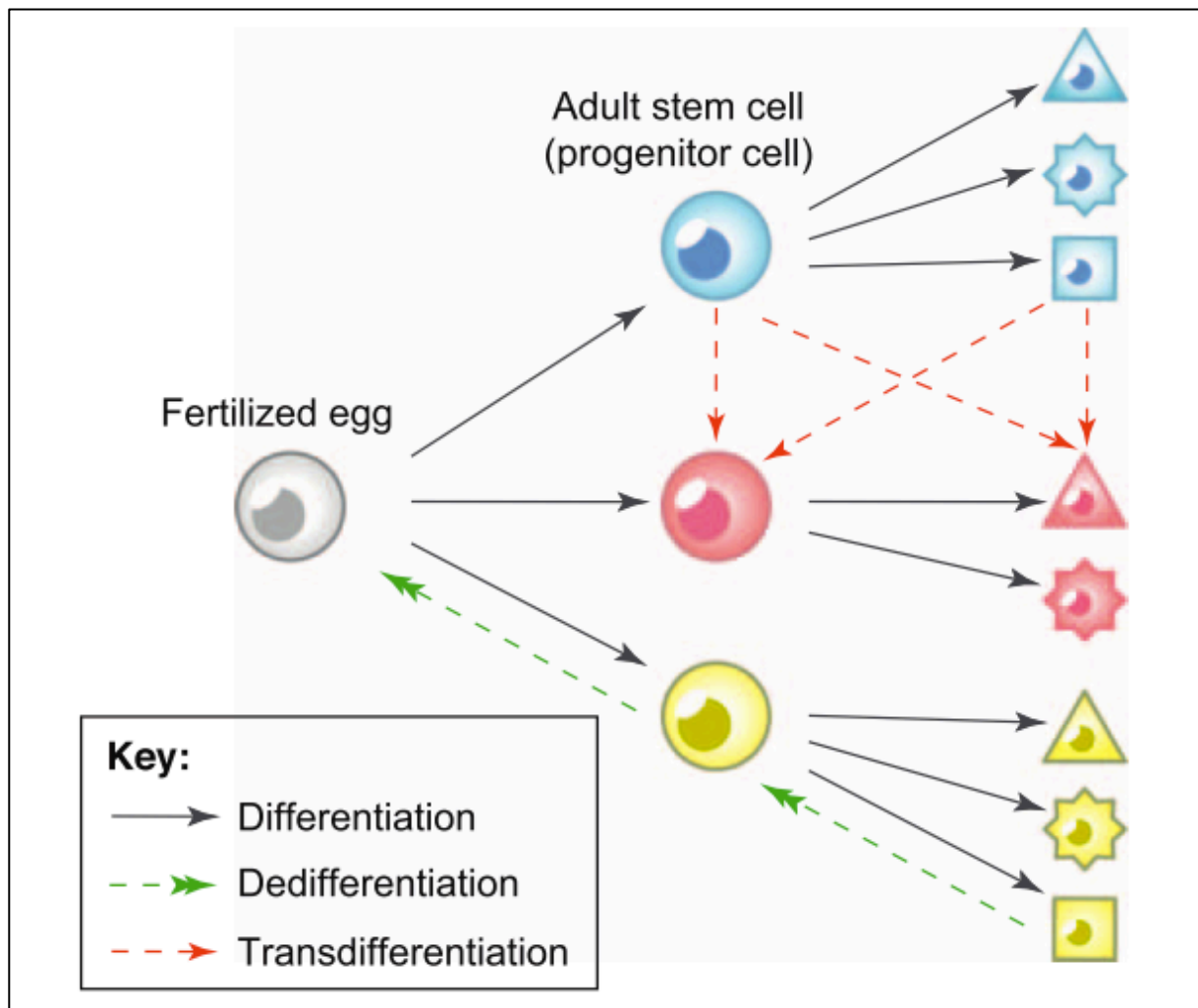


Figure 1.2: Differentiation, de-differentiation and trans-differentiation of a fertilized egg (Sugimoto et al., 2011). Different colours represent different cell lineage and the shapes represent different cell types. A cell de-differentiates when it returns to a more embryonic state; differentiate when it evolves to a special cell type and trans-differentiate when it switches into a different cell type.

1.1. De-differentiation, Differentiation and trans-differentiation

Regenerative faculty is due to the ability of some cells to de-differentiate (Williams et al., 2003). De-differentiation is the capacity of some mature cells to go back to their undifferentiated and non-specialised state as stem cells. This “stem-cells” like state confers pluripotency (ability to differentiate into different cell types) to the de-differentiated cells. Differentiation is a mechanism by which stem cells acquire a specialisation to form organs. Trans-differentiation involves a stepwise de-differentiation of a cell lineage to form an intermediate cell type that can then differentiate into another cell lineage (Grafi, 2004; Damri et al., 2009; Sugimoto et al., 2011; Sugiyama, 2015). Thanks to their potency, plant cells are able to de-differentiate or trans-differentiate from a differentiated state (Figure 1.2).

1.1.1. De-differentiation

De-differentiation process can occur naturally or it can be stimulated by a stress stimuli like pathogen attack, mechanic wounding or several other biotic and abiotic stresses (Damri et al., 2009; Grafi and Barak, 2015).

The first published reviews summarizing the cytological and physiological aspects of tissues de-differentiation were in 1941 and 1952 by Bloch describing scar callus after wounding as wound healing (Bloch, 1941; Bloch, 1952). With the development of *in vitro* culture, many studies were conducted afterwards on a potential “wound hormone” related to the initiation of callus formation (Sugiyama, 2015).

Several recent works demonstrated that the de-differentiation process is triggered by a “wound signal” responsible for the initiation of the first steps of de-differentiation like hormonal changes or genes expression modification (Xu and Huang, 2014). As for any developmental switch, de-differentiation implies drastic chromatin remodelling to modulate the expression of genes related with the previous differentiated state as well as the new cell fate related genes (Grafi and Barak, 2015).

De-differentiation is also characterised by a re-entry into the cell cycle and the activation of pluripotency-related genes like *NAM (NO APICAL MERISTEM)* (Grafi, 2004). Among the most characterised genes during de-differentiation process and described as wound-responsive genes are the WOUND INDUCED DE-DIFFERENTIATION (*WIND*) genes that encodes an AP2/ERF domain transcription factor. *WIND* expression is tightly related with callus formation in wounding sites and the over expression of *WIND1* result in callus formation without any wound stimuli (Iwase et al., 2015; Iwase et al., 2017).

1.1.2. Differentiation

After de-differentiation and with the re-entry into the cell cycle, cell divisions lead to the formation of meristems and stem cells niches. Differentiation process is tightly related with the existence of stem cell niches responsible of the production of several cell lineage types (Sugimoto et al., 2011; Ikeuchi et al., 2016). In plant cell culture, after callus formation, organs can be induced by adding specific phytohormones in the medium: auxin-rich medium to induce roots formation and cytokinin-rich medium to induce shoots formation. The differentiation mechanism will be discussed in some specific regeneration protocols in the upcoming sections.

1.1.3. Trans-differentiation

Trans-differentiation exists in both plants and animals. For a long time, it was assumed that the use of CIM (callus induction medium) is an indispensable step to acquire competence for shoot regeneration when calli are transferred on SIM (shoot induction medium) (Sugiyama, 2013). However, recent studies demonstrated that cells can trans-differentiate directly from a given lineage to another without the callus step. This direct conversion of a root meristem to a shoot meristem still require a two step culture system similar to CIM/SIM first on auxin-rich and second cytokinin-rich medium (Rosspopoff et al., 2017).

1.2. Higher plants regeneration

The *in vitro* plant regeneration establishment took half a century from the emergence of the idea of plant tissue culture made by Haberlandt in 1902 to the first hormone-based *in vitro* cell culture in 1957 (Haberlandt, 1902; Skoog and Miller, 1957). Since that, many works have been published on *de novo* shoot/root organogenesis and somatic embryogenesis using *in vitro* regeneration techniques to understand the cellular and molecular mechanisms underlying these developmental processes (Sugiyama, 2013; Motte et al., 2014b; Sugiyama, 2015; Radhakrishnan et al., 2018).

In general, there are three types of plant regeneration: tissue repair, *de novo* organogenesis and somatic embryogenesis (Figure 1.1). Plants can undergo regeneration process from relatively undifferentiated cells or through the reprogramming of differentiated cells. *De novo* plant organogenesis can happen either naturally or *in vitro* (Ikeuchi et al., 2016) and can be direct (directly from explant) or indirect (passing through a callus tissue) (Su and Zhang, 2014).

1.2.1. *In vitro* shoot regeneration

Different regeneration protocols are used to study plant *in vitro* organogenesis. The most used system for the study of *in vitro* shoot generation is the two steps protocol (Radhakrishnan et al., 2018). This protocol, commonly called CIM/SIM system was adapted to *Arabidopsis thaliana* by Feldman and Marks in the 80's (Feldmann and Marks, 1986). In general, part of root or leaf is used as an explant that is cultivated on auxin-rich callus induction medium (CIM) to activate the re-entry into the cell cycle of the differentiated cells in order to de-differentiate into a callus. Calli are then transferred to a cytokinin-rich regeneration medium called SIM for shoot induction medium (Che et al., 2002). When calli are transferred to the regeneration medium, the proliferation is arrested then it is reactivated in specific areas at the callus surface (Sugiyama, 2013).

Sugimoto and co-workers demonstrated a root-like developmental pathway for callus derived from three different *Arabidopsis* explants: roots, cotyledons and petals. This similarity was demonstrated by the expression of root-related molecular markers during callus formation (Sugimoto et al., 2010). In the two-step regeneration (CIM/SIM) protocol, the root-like trait of callus seems to be essential for the acquisition of shoot regeneration competence (Kareem et al., 2015).

1.2.1.1. Hormonal regulation

Auxin and cytokinin are the most used hormones during *in vitro* shoot regeneration steps since their use by Skoog and Miller 60 years ago in an *in vitro* regeneration protocol (Skoog and Miller, 1957). During the last decades, many works were conducted to understand how the hormonal network influence regeneration-related genes expression.

Mutant affected in the shoot regeneration capacity are often affected in auxin and cytokinin pathways (Xu and Huang, 2014). The first cytokinin-related mutant bearing a high caulogenesis rate was isolated by (Catterou et al., 2002). This mutant named *hoc* for “*high shoot-organogenic capacity*” showed a high cytokinin level in roots resulting in an *in vitro* supernumerary shoots without treatment of root-explants with any exogenous hormone. The observed phenotype results in a mutation in a gene encoding a class III type HD-ZIP transcription factor corresponding to the *ATHB15 / CORONA / INCURVATA4* protein (Duclercq et al., 2011). The class III HD-ZIP genes were previously described to direct cell differentiation for SAM establishment (Emery et al., 2003; Zhang et al., 2015). Conversely, mutants with high auxin level have a reduced shoot regeneration rate. For example, the overexpression of the auxin-biosynthesis gene *YUCCA1 (YUC1)* in rice resulted in a drastic inhibition of shoot regeneration of crown-roots derived calli (Yamamoto et al., 2007).

In vitro culture of mutants affected in hormones metabolism and signaling demonstrated that the endogenous hormonal balance is as much important as the hormonal balance in the culture media. In general, the exogenous auxin/cytokinin balance promotes the establishment of an endogenous hormonal balance leading to the induction of shoot regeneration (Peres et al., 1999).

Using root explants, Gordon and co-workers demonstrated that during callus induction on CIM, auxin responsive-signals progressively declined revealing the essential role of auxin during the first cell proliferation step of callus formation (Gordon et al., 2007). The TRANSPORT INHIBITOR RESPONSE 1 (TIR1) protein was described to participate to the cellular auxin signaling during shoot organogenesis. When calli are transferred to SIM, *TIR1* is induced in shoot initiation sites and its overexpression increased shoot regeneration frequency (Qiao et al., 2012).

De novo auxin biosynthesis is also important for *de novo* shoot regeneration. When calli are transferred on SIM, auxin biosynthesis genes YUCCA (YUCs) are induced in future SAM areas. Although auxin-responsive signals are almost undetectable in the newly formed SAM, the SAM surrounding-areas are marked by a strong auxin-responsive signal. This importance of auxin distribution for the SAM establishment was reported by Cheng and his collaborators who demonstrated that PIN1-mediated auxin polarised transport is essential for shoot meristem establishment. The use of N-1-naphthylphthalamic acid (NPA), an auxin polar-transport inhibitor, in the SIM impaired the initiation and development of shoot meristems through the disruption of the hormonal cross-talk between auxin and cytokinin. Auxin also interferes in cytokinin biosynthesis by repressing the expression of cytokinin-biosynthesis genes *ATP/ADP ISOPENTENYLTRANSFERASE (IPTs)* through the *AUXIN RESPONSE FACTOR 3 (ARF3)* (Gordon et al., 2007; Cheng et al., 2013).

During shoot establishment on SIM, the areas among callus marked by *AtIPT5* signals are the same where SAM are formed, demonstrating the importance of cytokinin biosynthesis during *de novo* shoot regeneration. Beside cytokinin biosynthesis, cytokinin signaling is also important during shoot organogenesis. Cytokinin response-genes implicated in the shoot meristem establishment are induced through the B-type ARABIDOPSIS RESPONSE REGULATORS (ARRs) transcriptional activators whereas A-type ARR are negative regulators of shoot regeneration (To and Kieber, 2008; Cheng et al., 2013). Overexpression of type-A ARR ARR7 and ARR15 resulted in a dramatic decrease in shoot regeneration frequency whereas the overexpression of type-B ARR ARR2 promoted shoot regeneration without exogenous cytokinin addition (Hwang and Sheen, 2001; Buechel et al., 2010).

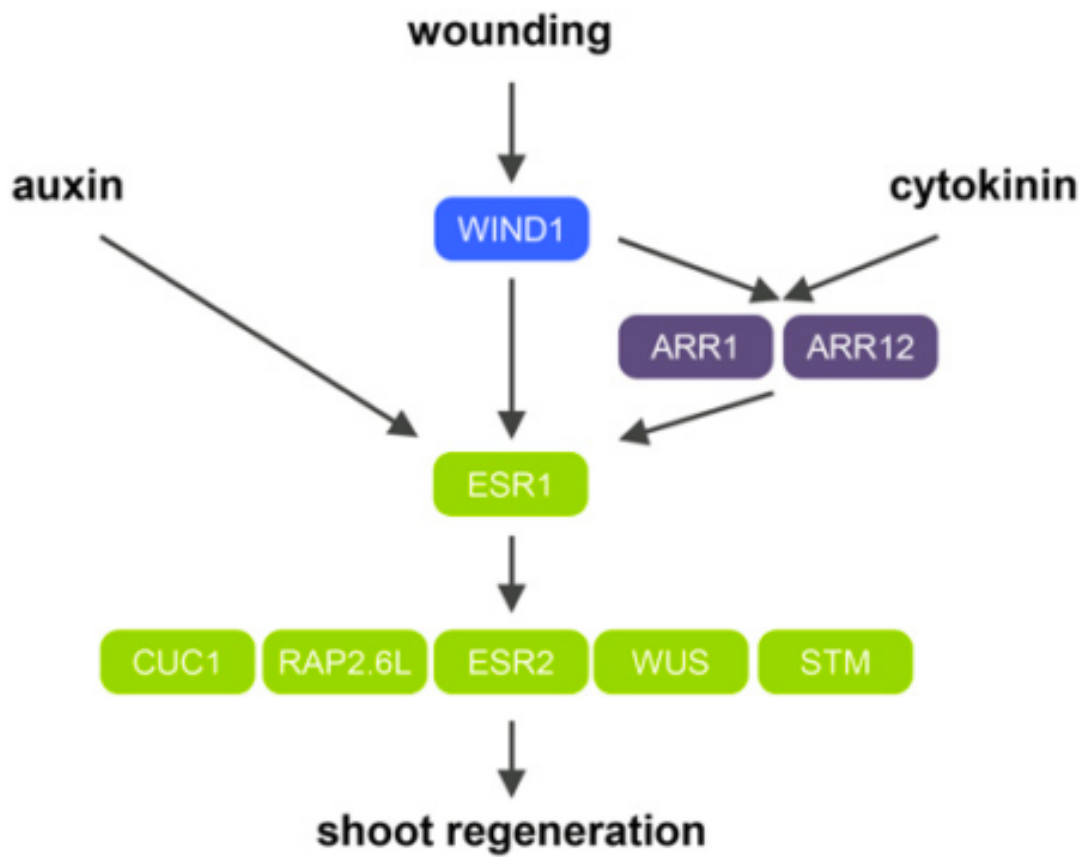


Figure 1.3: WIND1-ESR1 pathway Model for shoot regeneration in Arabidopsis (Iwase et al., 2017).

The implication of another hormone, ethylene, in *de novo* shoot regeneration was also reported in several studies. For example, on wheat, tobacco and brassica explants, the treatment with an ethylene inhibitor like AgNO₃ enhanced *de novo* shoot regeneration on calli from recalcitrant wheat and brassica cultivars as well as weakly-regenerating tobacco mutants (Purnhauser et al., 1987; Songstad et al., 1988; Chi et al., 1990).

1.2.1.2. Molecular regulation of de novo shoot regeneration

Using loss of function mutants, several transcription factors (TFs) were highlighted to complement the understanding of molecular regulation of *de novo* shoot regeneration (Radhakrishnan et al., 2018).

It was recently reported that the molecular mechanism of shoot regeneration through CIM/SIM protocol begins with a wound signal as the expression of the *WIND1* transcription factor is observed in callus with regenerative competence. *WIND1* together with auxin and cytokinin signaling pathways activate the *ENHANCER OF SHOOT REGENERATION 1 (ESRI)* that in turn induces *CUP SHAPED COTYLEDON 1 (CUC1)* and other regeneration-related TF (Figure 03). The areas where CUCs are highly expressed are marked by the formation of a pre-meristem followed by shoot regeneration (Sugiyama, 2013; Iwase et al., 2017).

As mentioned previously, Sugimoto and collaborators showed common molecular features between lateral root development and callus formation during the first step of the two-steps regeneration protocol. Callus formation from roots, cotyledons and petals undergo a similar molecular programme as lateral root formation and when some mutants were unable to form lateral roots they were also unable to form callus from the different explants (Sugimoto et al., 2010). Several root-related genes like *WUSCHEL-related homeobox 5 (WOX5)*, *PLETHORA 1 (PLT1)* and *PLT2* are expressed in callus independently from the explant origin (Sugimoto et al., 2010; Kareem et al., 2015).

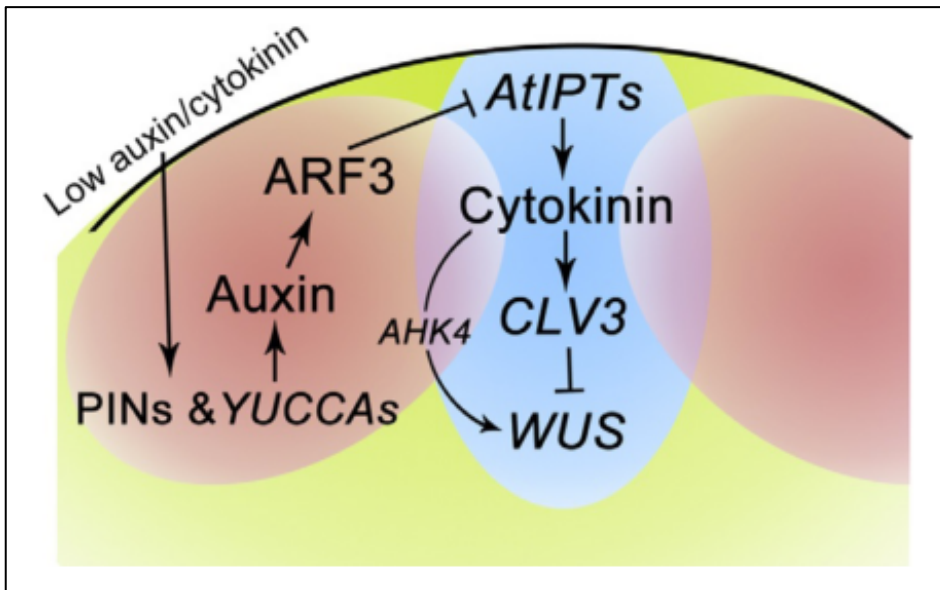


Figure 1.4: Auxin and cytokinin interactions during SAM initiation (Su and Zhang, 2014). Local auxin biosynthesis and transport mediated by YUCs and PINs regulate the local auxin response in regions surrounding SAM, which negatively regulates expression of cytokinin biosynthetic genes IPTs through the direct binding of ARF3 to their promoters. In the center region of SAM, cytokinin signaling may partially regulate *WUS* expression through a *CLV*-dependent pathway. Cytokinin-induced increase of *WUS* transcript levels is mediated primarily through an *AHK4*-dependent pathway. Red color indicates auxin-response regions, blue color indicates cytokinin-response regions, and yellow color indicates callus.

Callus formation is not sufficient for the acquisition of pluripotency to regenerate. This fact was observed in the PLT triple mutants *plt3; plt5-2; plt7* which develops callus formation but does not show any shoot formation when callus is transferred to the regeneration medium (Kareem et al., 2015).

Few days after the callus transfer on the regeneration medium, cytokinin induces the expression of Shoot Apical Meristem (SAM) related genes WUSCHEL (WUS) and SHOOT MERISTEMLESS (STM). In Arabidopsis, WUS induction depends on the spatiotemporal distribution of cytokinin within the callus. This distribution is controlled by auxin gradient and auxin-mediated negative regulation of cytokinin biosynthesis-genes IPTs through the response factor ARF3 (Figure 1.4). Cytokinin mediated WUS induction on the SIM is operated by the B-type ARRs: ARR1, ARR2, ARR10, and ARR12. These transcriptional activators interact with microRNA165/6 (miR165/6)-targeted HD-ZIP III transcription factors to induce a localised WUS expression (Cheng et al., 2013; Zhang et al., 2017; Radhakrishnan et al., 2018).

Genetic variations among different cultivars of the same species can have a considerable impact on shoot regeneration frequency. Motte and collaborators exploited the natural variability in shoot regeneration frequency among Arabidopsis accessions to identify a potential regeneration-related quantitative trait locus (QTL). The QTL analysis revealed a leucine-rich repeat receptor-like kinase, named RECEPTOR-LIKE PROTEIN KINASE1 (RPK1) as a major QTL affecting shoot regeneration in Arabidopsis (Motte et al., 2014a).

1.2.1.3. Epigenetic control

In normal conditions (absence of stress stimuli), Arabidopsis plant regeneration is repressed thanks to epigenetic regulations (Ikeuchi et al., 2015b). During the first step of regeneration (i.e. de-differentiation), for DNA accessibility, chromatin conformational changes are induced through post-translational histone modifications (Jopling et al., 2011). One of the histone modifiers is the polycomb group (PcG) complex which acts for genes silencing by the trimethylation of histone-3 lysine-27 (H3K27), dimethylation of H3K9 and ubiquitination of H2AK118/119 (de la Paz Sanchez et al., 2015). Many genes implicated in the wound-induced regeneration such as the *ENHANCER OF SHOOT REGENERATION 1* (*ESR1*), are rapidly induced after wounding through the removal of their epigenetic silencing by the polycomb-mediated histone modification (Ikeuchi et al., 2015a; Ikeuchi et al., 2015b).

Another epigenetic regulation was observed during the first step of *de novo* organogenesis (i.e. callus formation) in mutants affected in the Polycomb repressive complex 2 (PRC2). PRC2 is composed of three components: CURLY LEAF (CLF), SWINGER (SWN) and EMBRYONIC FLOWER 2 (EMF2) (Chanvivattana et al., 2004). *clf swn* and *emf2* both showed incapacity to form callus from leaf explants. In these mutants, the repressive mark H3H27m3 was reduced at many auxin-related genes suggesting an epigenetic regulation of callogenesis through auxin pathway (He et al., 2012).

It was recently reported that during the two-steps regeneration, the cytokinin-rich medium induces an important epigenetic modification to release WUS locus. The high number of shoot meristems in the *mtl1* (*methyltransferase 1*) mutant was linked with the absence of the repressive methylation in the regulatory regions of WUS and ARF3. Thus, mutations in some epigenetic-markers genes have a considerable impact on shoot regeneration (Li et al., 2011).

1.2.2. Somatic embryogenesis

The first published works on somatic embryogenesis (SE) were on carrot in the last 1950s, after the establishment of *in vitro* culture conditions. Since the publication of Reinert and co-workers in 1970 on SE derived from a single carrot cells, many protocols of SE were reported on several plant species (Sugiyama, 2015). Somatic embryogenesis can be induced directly (without callus step) or indirectly using an auxin-rich medium to induce embryogenic-callus formation followed by the transfer of competent calli on an auxin-free or low auxin-poor medium for somatic-embryos development (Thorpe and Stasolla, 2001).

1.2.2.1. Hormonal regulation

As for *de novo* shoot regeneration, SE is also induced using specific hormonal balance. After callus induction using an auxin-rich embryonic callus-inducing medium (ECIM), the formed embryonic calli become less dependant to the exogenous auxin, since auxin removal from the media permits the establishment of an endogenous auxin gradient. In fact, removal of exogenous auxin stimulates SE initiation and endogenous auxin biosynthesis. Auxin distribution and SAM-related TF expression permit the establishment of organizing centers (OCs) of the future somatic embryos. Somatic embryos are formed in areas where the auxin biosynthesis genes YUC 1 and YUC4 were expressed beforehand (Su et al., 2009; Bai et al., 2013; Su and Zhang, 2014).

Beside auxin and cytokinin, other phytohormones like abscisic acid (ABA) and gibberellic acid (GA) were also described as important factors in SE for some speices. ABA rich-medium induced SE in carrot seedling-explants without the addition of any other exogenous hormone in the medium (Nishiwaki et al., 2000). Another study reported the alteration of SE induction when Arabidopsis callus were treated with the ABA inhibitor fluridone (Su et al., 2013). In Loblolly pine, the use of GA inhibitor Paclobutrazol increased significantly SE regeneration in several genotypes (Pullman et al., 2005).

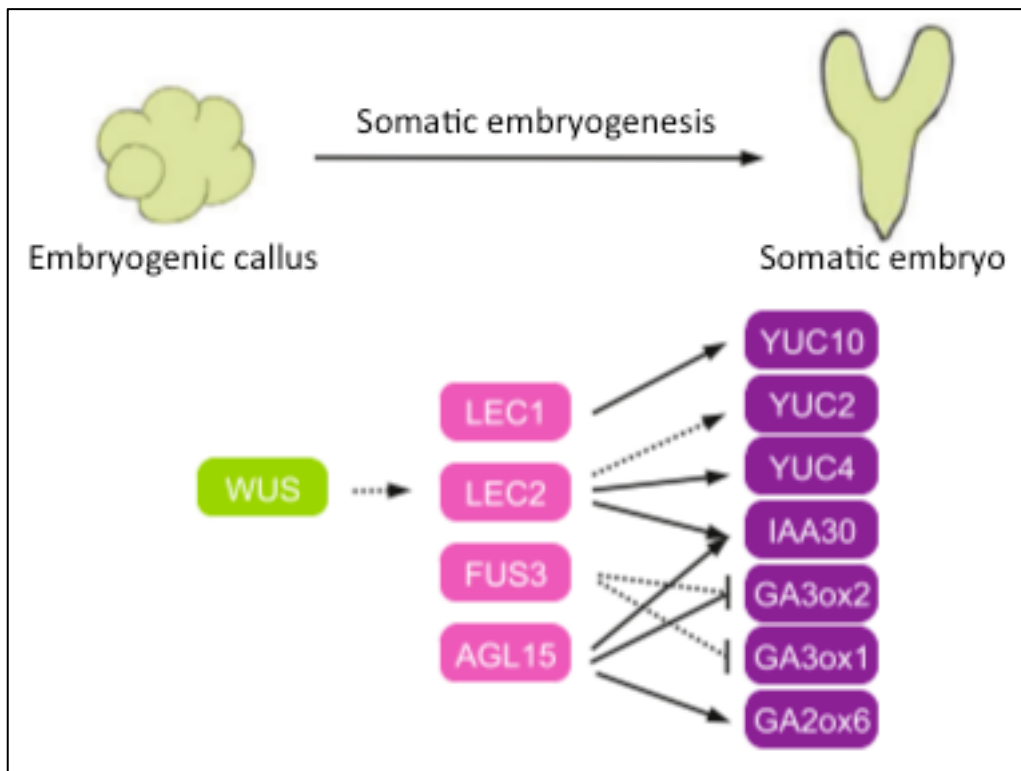


Figure 1.5: Schematic model of indirect somatic embryogenesis regulation in *Arabidopsis* (Ikeuchi et al., 2016). After WUS induction in low auxin response domains, the other TFs are subsequently induced by WUS. The resulting expression of LEC1, LEC2 and FUS3, together with AGL15 modulate the endogenous levels of auxin, GA and ABA to promote embryogenesis. Solid black lines indicate direct transcriptional regulation and dotted black lines indicate direct or indirect transcriptional regulation.

Ethylene was also described to influence somatic embryos regeneration. In rice and coffee, at certain concentrations, exogenous ethylene promoted SE in rice kernels-derived calli and coffee leaves-derived calli whereas the chemical inhibition of ethylene inhibited SE in coffee leaf explants (Cornejo-Martin et al., 1979; Hatanaka et al., 1995). However, for other species, ethylene has a negative effect on SE. For example, in carrot petiole-derived calli, ethylene treatment reduced SE regeneration (Tisserat and Murashige, 1977). Moreover, during *Arabidopsis* SE, ethylene related biosynthesis and signaling genes were down-regulated and mutants with high ethylene levels or enhanced ethylene signaling have disrupted SE (Bai et al., 2013).

1.2.2.2. Molecular regulation of somatic embryogenesis

After the transfer of *Arabidopsis* embryogenic calli to an auxin-free medium, the *de novo* auxin gradient results in *WUS* expression in low auxin response areas where SAM of future embryos will be formed (Su et al., 2009). Other embryogenesis-related TFs are then successfully induced for somatic embryos development (Figure 1.5). During somatic embryogenesis, the expression of LEAFY COTYLEDON1 (LEC1) induced the expression of auxin biosynthesis gene YUC10 whereas LEC2 induced YUC2 and YUC4. However, LEC2 is also implicated with AGL15 in the regulation of auxin signaling through the induction of the auxin signal-repressor INDOLE ACETIC ACID INDUCIBLE30 (IAA30) gene (Braybrook et al., 2006; Stone et al., 2008; Zheng et al., 2009; Junker et al., 2012). The other finely regulated hormonal balance is mediated by AGAMOUS-LIKE15 (AGL15) and FUSCA3 (FUS3). AGL15 and FUS3 reduce GA level by inducing GA degrading-enzyme GA2ox6 and repressing GA biosynthesis-genes GA3ox2, GA3ox1 and GA3ox2 (Curaba et al., 2004; Gazzarrini et al., 2004; Wang et al., 2004; Zheng et al., 2009).

1.2.3.3. Epigenetic control

As for *de novo* organogenesis, somatic embryogenesis is also marked at the beginning of the process by chromatin remodelling and heterochromatin decondensation (Sugiyama, 2015).

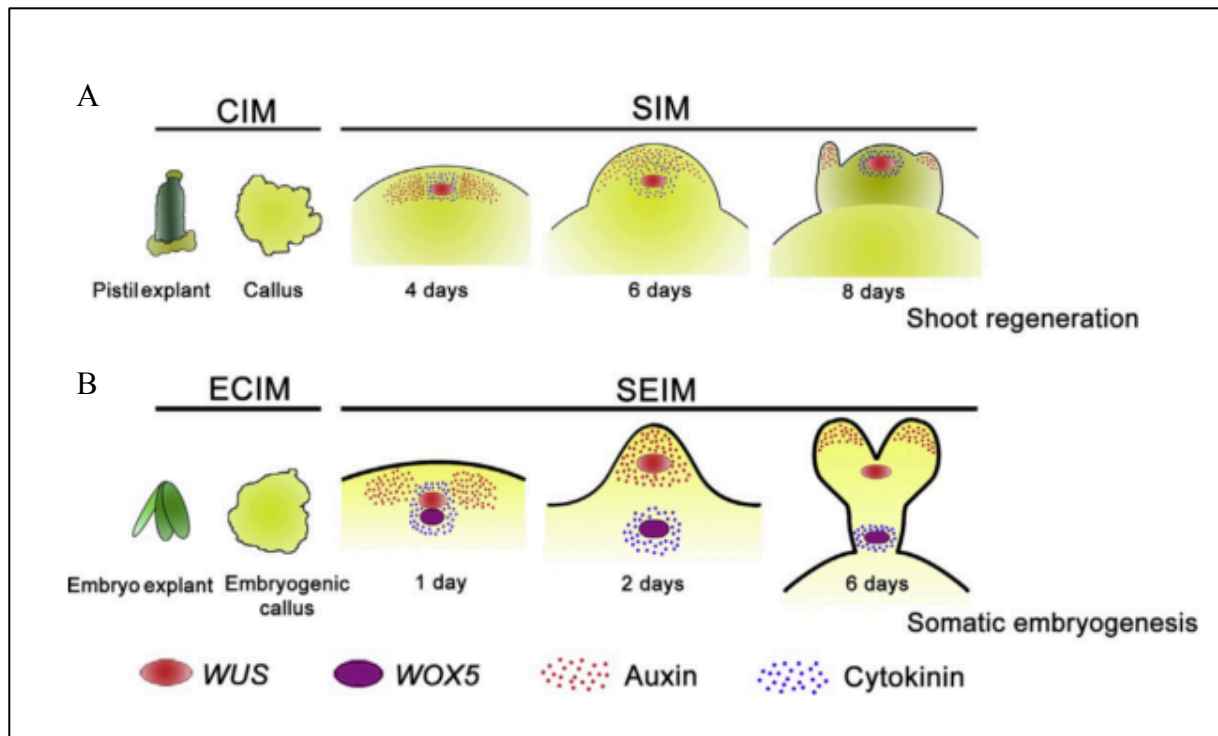


Figure 1.6: Auxin and cytokinin patterns during *de novo* shoot regeneration and SE regeneration (Su and Zhang, 2014). A, Callus formation on callus induction medium (CIM) from pistil explant, followed by shoot regeneration on shoot induction medium (SIM). B, Embryogenic callus obtention after embryo explant incubation on embryogenic callus induction medium (ECIM) and somatic embryos formation on somatic embryogenesis induction medium (SEIM).

The repressive epigenetic regulation through histone deacetylation was described to control SE. The chemical inhibition of histone deacetylases using trichostatin A (TSA) on *Arabidopsis* leaves resulted in embryo-like structures (Tanaka et al., 2008). On *Brassica* microspores, TSA application in association with a heat treatment greatly promoted somatic embryogenesis (Li et al., 2014).

1.2.3. *De novo* shoot organogenesis versus somatic embryogenesis in *Arabidopsis*

De novo shoot organogenesis and SE are under distinct mechanisms (Cheng et al., 2013). It was recently reported that the genetic programs for SAM establishment were different between embryogenesis and *de novo* shoot regeneration (Zhang et al., 2017). In SE, bipolar structure is formed very early in the course of the development and could be distinguished by *WUS* and *WOX5* domains, while only *WUS* is expressed in SAM of *de novo* shoot regeneration. Auxin and cytokinin responsive-signals distribution are also different between both systems (Figure 1.6). When calli are transferred to the regeneration medium, SAM cells expressing *WUS* are marked by cytokinin signals during all *de novo* shoot regeneration process whereas during SE regeneration, cytokinin encircle both *WUS* and *WOX5* in the beginning, later, it is co-localised just in cells surrounding the region of *WOX5* expression in the RAM. Auxin response is similar in early steps of development in both *in vitro* shoot regeneration and SE, it is observed surrounding the SAM. Auxin response is different in the later steps, with the emergence of the bud for the shoot regeneration, it is localised above SAM then in leaf primordia (Figure 1.6 A) and for SE at the top of the promeristem then in the margin of cotyledons of new formed somatic proembryo (Figure 1.6 B).

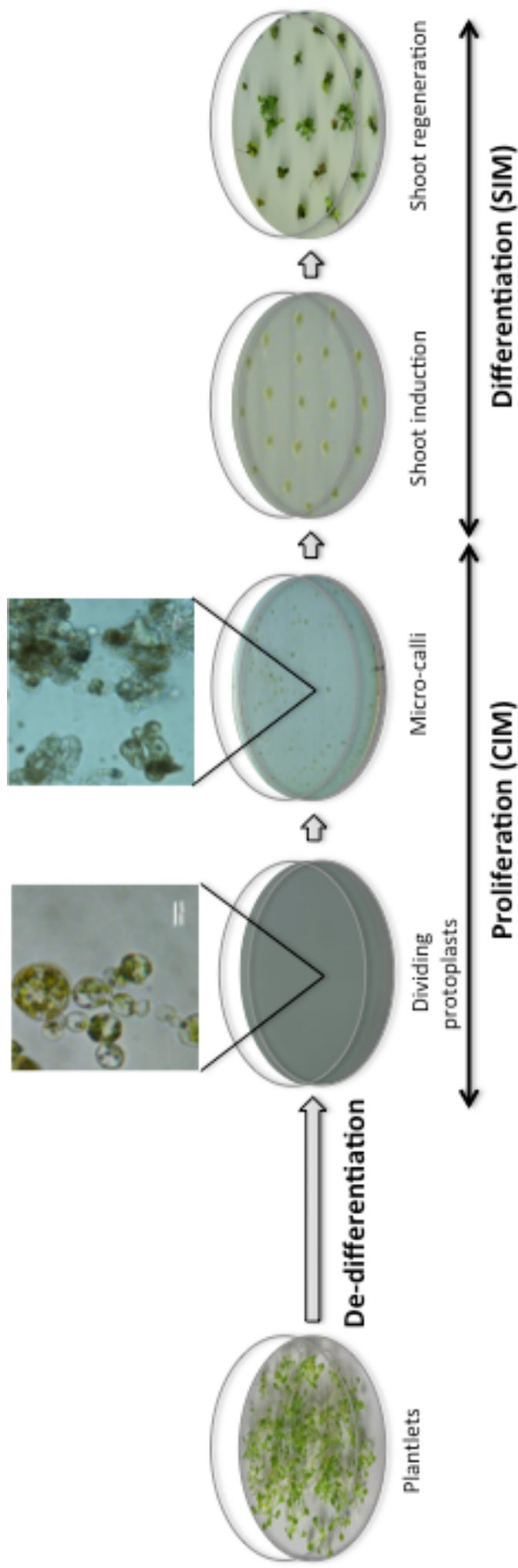


Figure 1.7: Representation of the protoplasts system. Some differentiated cells in the plant undergo a de-differentiation programme after enzymatic cell wall removal. The obtained protoplasts proliferate thanks to auxin and cytokinin in the callus induction medium (CIM) to form micro-colonies, micro-calli and then calli. On the shoot induction medium (SIM), some calli-cells undergo a differentiation programme to form shoots.

1.3. The use of protoplasts-derived calli to study *in vitro* shoot regeneration

Protoplasting (protoplasts isolation from differentiated tissues, organs or from an entire plant) is considered as the appropriate model to study de-differentiation (Chupeau et al., 2013). After the enzymatic cell wall removal, the obtained protoplasts acquire pluripotency and undergo callus formation by proliferation after exogenous phytohormones induction (Damri et al., 2009; Grafi and Barak, 2015). When transferred on a regeneration medium containing an appropriate cytokinin, some calli-cells undergo differentiation to form organs (Figure 1.7).

In 1960, Cocking isolated for the first time protoplasts after cellulose digestion of the cell wall. A decay later, Takebe and co-workers published an effective protocol for tobacco plant regeneration from mesophyll-isolated protoplasts (Takebe et al., 1971). Since that, the protoplast culture system was used for several purposes like protoplast fusion to create somatic hybrids (Sugiyama, 2015) and more recently for transgene-free genome editing in plants (Woo et al., 2015).

Protoplasts have a stem-cells like properties like the chromatin decondensation and a quiescent metabolism (Damri et al., 2009; Grafi and Barak, 2015). Thanks to the protoplast culture system, a lot of information about chromatin decondensation and epigenetic marks during de-differentiation were obtained (Sugiyama, 2015). Protoplasting is characterised by epigenetic marks related to genes activation like the acetylation of residues K9 and K11 of the histone H3 and also the DNA de-methylation of some specific genes (Williams et al., 2003; Avivi et al., 2004).

Protoplasts-derived calli regeneration system presents a good model to study organs differentiation, especially *de novo* shoot regeneration process since calli are obtained from proliferation of completely de-differentiated cells.

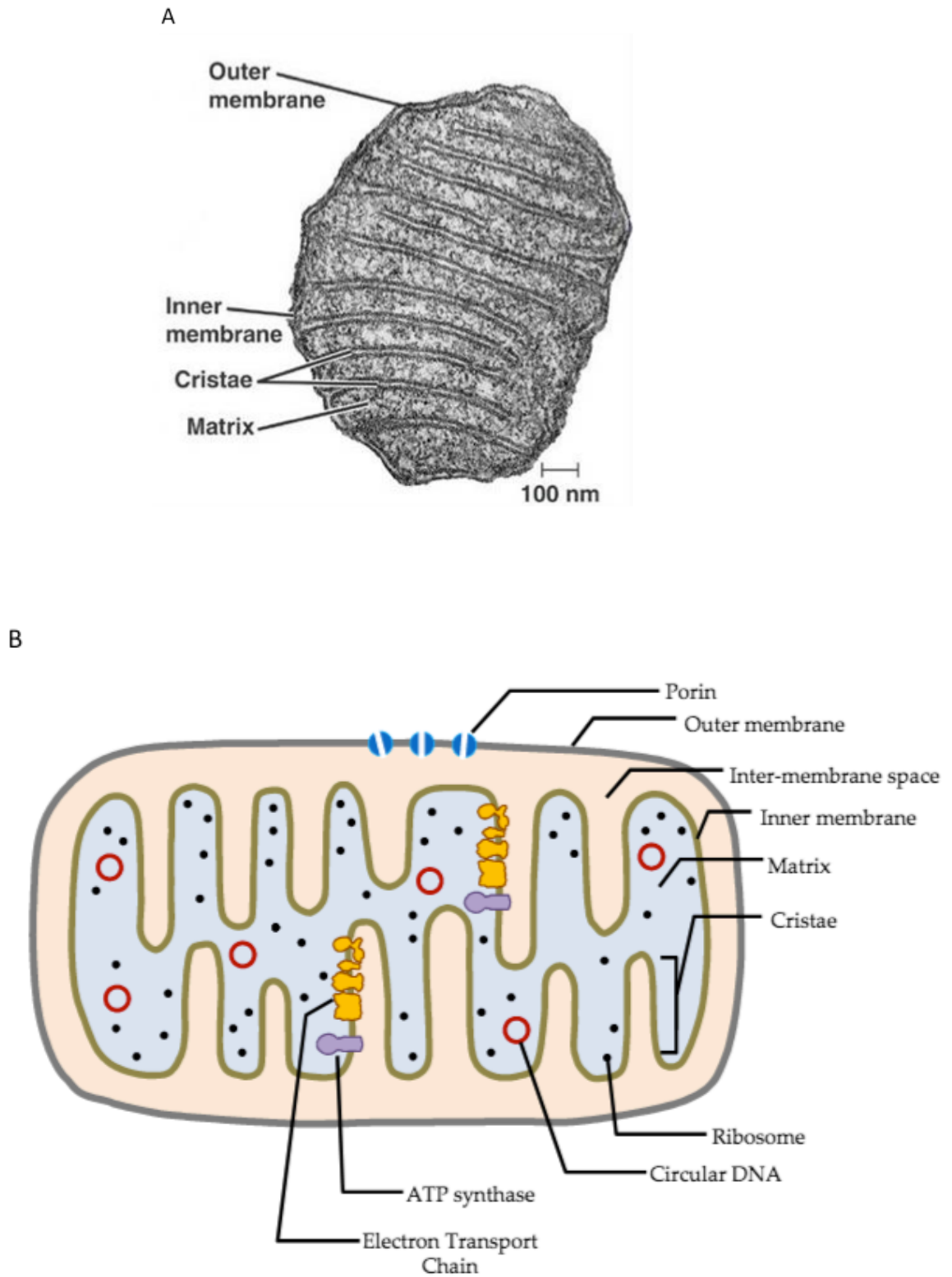


Figure 1.8: Eukaryotic cell mitochondrion. A, Electron microscopy image of a mitochondrion. B, Schematic illustration of the mitochondrion general structure (Yusoff et al., 2015).

2. Mitochondrial respiration

2.1. The mitochondria

Mitochondria are the central energy generator in many living organisms. They produce the adenosine triphosphate (ATP) necessary to fuel a wide range of biological processes. Since the publication in 1970 of the *Origin of Eukaryotic Cells* book by Lynn Margulis supporting a symbiotic origin of mitochondria and chloroplasts (endosymbiont hypothesis), multiple researchers investigated the evolution of the mitochondrial genomes and demonstrated the link between the α -proteobacteria order Rickettsiales and eukaryotic mitochondria. However, the present eukaryotes mitochondrial genome differs from its α -proteobacterial genitor genome because a considerable number of the proto-mitochondria genes was transferred to the nucleus after endo-symbiosis (Gray, 2012).

The first morphological description of the mitochondria structure was published in 1945 using an electronic microscope to image isolated rat mitochondria (Claude and Fullman, 1945). The detailed internal structure of the eukaryote mitochondria was further elucidated with the further development of electron microscopic tomography (Frey and Mannella, 2000). Mitochondria include two membranes (the outer and inner membranes) and a matrix, and contain multiple proteins and several copies of its circular genome DNA (Figure 1.8). Mitochondrial genome encodes few inner-membrane proteins. The majority of mitochondrial proteins are encoded in the nuclear DNA and imported to the mitochondria (Millar et al., 2011).

Plant cells contain hundreds of mitochondria with different morphologies depending on the physiological conditions and the developmental state of the cell (Welchen et al., 2014). A tight coordination between nucleus and mitochondria is essential for the sustainability and the integrity of the cell. This coordination is managed by retrograde (from organelle to nucleus) and anterograde (from the nucleus to the organelle) regulations (Millar et al., 2011).

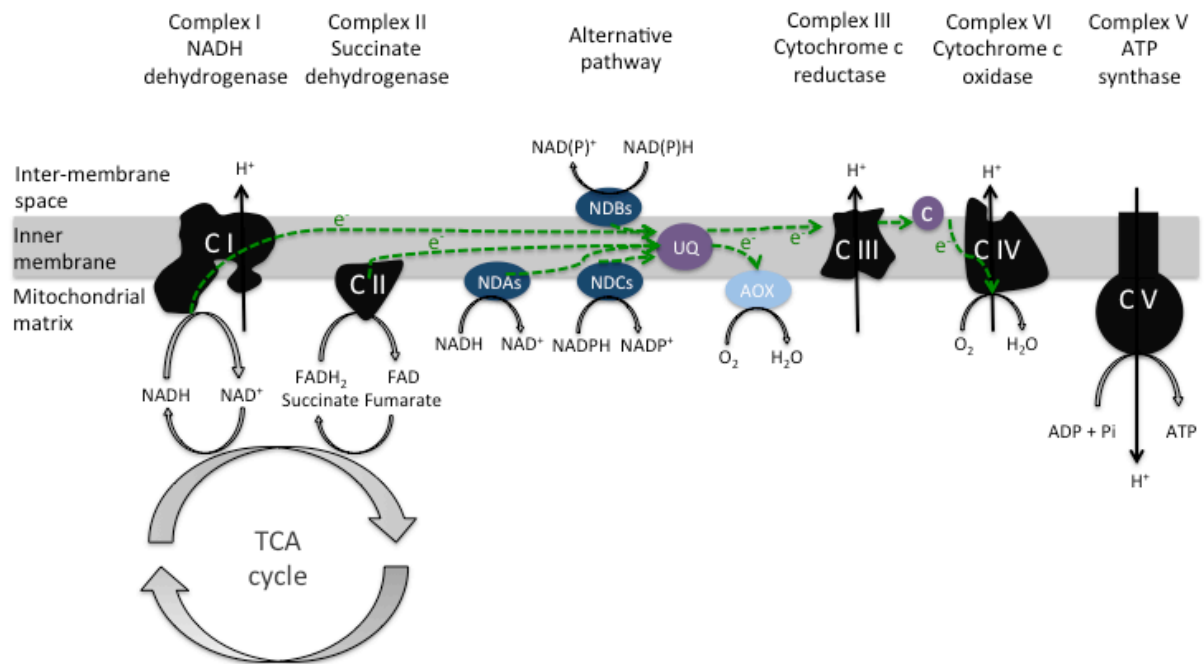


Figure 1.9: Simplified scheme of the mitochondrial respiration in plants. The mitochondrial respiratory chain uses the energy in NADH and succinate (produced in the tricarboxylic acid cycle, TCA cycle) to generate ATP. Electrons enter the electron transport chain (ETC) from NAD(P)H via Complex I (C I) and alternative NAD(P)H-dehydrogenases (NDAs, NDCs and NDBs) and also from succinate via cII (C II). Electrons are then transferred via the two mobile electron-transporters ubiquinone (CII to CIII) and cytochrome C (C III to C IV) to reduce molecular oxygen into water. When the alternative pathway is activated, AOX transfers directly electrons from ubiquinone to the molecular water. CI, III and IV pump protons from the mitochondrial matrix to the inter-membrane space. Then, protons flow back into the matrix via the complex V driving ATP production in the mitochondrial matrix. The five complexes of the mitochondrial respiratory chain are represented in black. The components of the alternative pathway are represented in blue: dark blue, NAD(P)H dehydrogenases type 2 (NDAs, NDBs and NDCs); light blue, alternative oxidase (AOX). Ubiquinone (UQ) and cytochrome c (C) are in purple. Black straight arrows represent proton flux across the inner membrane. Dotted green arrows represent electron flux.

Mitochondrial respiration involves two main processes. The first is the tricarboxylic acid (TCA) cycle where organic acids are oxidatively decarboxylated to reduce the co-enzymes NAD⁺ (nicotinamide adenine dinucleotide) and FAD (flavin adenine dinucleotide). The second is the oxidative phosphorylation (OXPHOS) where electrons resulting from NAD(P)H and FADH₂ oxidation are transferred through the mitochondrial electron transport chain (mETC) and used to reduce oxygen into water (Figure 1.9). For each NADH oxidation, 10 protons are translocated from the matrix to the inter-membrane space creating a proton gradient that powers the phosphorylation of ADP to produce ATP (Millar et al., 2011; Schertl and Braun, 2014; Sousa et al., 2018).

Beside ATP synthesis, mitochondria are implicated in co-factor, co-enzyme and lipid biosynthesis (Rao et al., 2017). These organelles play also a significant role in programmed cell death (Yao et al., 2004; Reape et al., 2008). Mitochondria are directly related to the redox homeostasis as the final step of ascorbate biosynthesis occurs in the mitochondrial inter-membrane space. This step concerns the conversion of L-galactono- γ -lactone (GL) to ascorbic acid by the L-galactono- γ -lactone dehydrogenase (GLDH). This enzyme is bound to the mitochondrial inner membrane and requires the electron transporter cytochrome c as an electron acceptor (Bartoli et al., 2000).

2.2. Oxidative phosphorylation system

The mitochondrial OXPHOS system is the main pathway for mitochondrial ATP production operated by the mitochondrial respiratory chain. Localized in the inner mitochondrial membrane, the plant respiratory chain includes four main complexes (complexes I–IV) involved in electron transport and proton translocation, the ATP synthase complex (complex V), two mobile electron carriers (co-enzyme Q [ubiquinone] and cytochrome c) and some additional components that are activated in particular conditions (Rasmusson et al., 2008). In normal conditions, after the oxidation of NADH and FADH₂ by the cI and the cII, respectively, electrons are transferred by the mobile ubiquinone to the cIII, then by the mobile cytochrome c from the cIII to the cIV and finally to O₂ to produce H₂O.

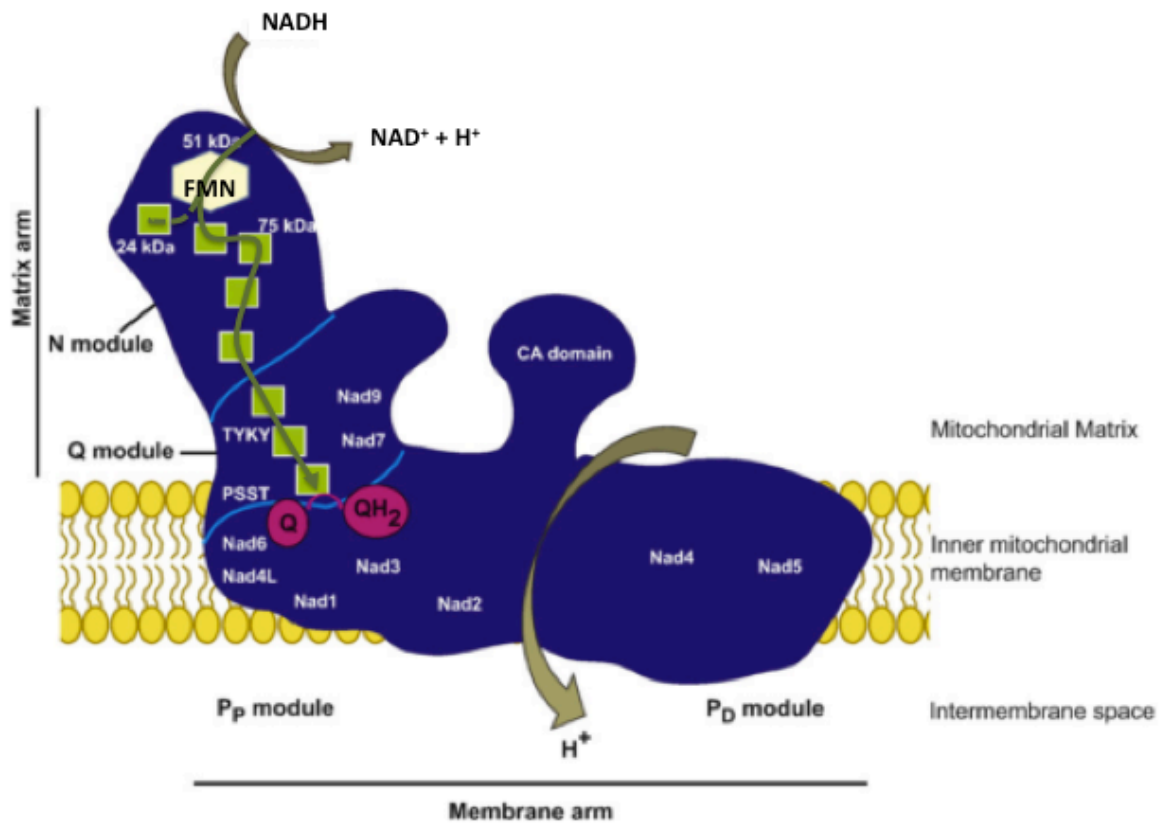


Figure 1.10: Schematic representation of the complex I modular design with core subunits in *Arabidopsis thaliana* adapted from (Subrahmanian et al., 2016). Electrons flow from NADH to ubiquinone (Q) via one FMN molecule and eight Fe-S clusters (green squares) is indicated by dark green arrow. CI is divided into three functional modules: NADH oxidation N-module, quinone reduction Q-module and finally the proton-translocating P-module which, in turn, includes the proximal section (P_p) and the distal section (P_d). Plant CI bears an additional domain called carbonic anhydrase (CA) domain.

2.2.1. Electron transport chain (ETC)

Plant mitochondria are characterized by two electron transport pathways: the “classical” cytochrome c oxidase (COX) pathway (cI to cIV) and the alternative oxidase (AOX) pathway called alternative pathway (type 2 NAD(P)H dehydrogenase and AOX). Plant ETC is characterized by several alternative points by which electrons enter and leave the respiratory chain (Millar et al., 2011; Schertl and Braun, 2014).

2.2.1.1. Complex I (cI)

The mitochondrial NADH:ubiquinone oxidoreductase (complex I, cI) was isolated for the first time from beef heart mitochondria in the 60's (Hatefi et al., 1962). In plants, the mitochondrial cI contains nearly 50 subunits and some of these proteins are specific to plants (Braun et al., 2014). The cI oxidizes NADH and transfers two electrons to the mobile electrons transporter ubiquinone. This oxido-reduction is coupled to the translocation of four protons across the inner membrane (Sousa et al., 2018).

2.2.1.1.1. cI structure and mechanism

The mitochondrial cI structure was elucidated using X-ray crystallography on the eubacterium *Thermus thermophilus* cI. CI has a L shape structure consisting of two arms: one called hydrophobic or membrane arm is inserted in the inner mitochondrial membrane; the other one is in the mitochondrial matrix side and is called hydrophilic or peripheral arm (Baradaran et al., 2013) (Figure 1.10). cI can be compartmented into 3 modules: module N for NADH oxidation module, module Q for quinone reduction module and finally module P for proton transfer module. NADH oxidation is catalyzed by a flavin-mono-nucleotide (FMN) located at the periphery of the hydrophilic arm (module N). Electrons are then carried out through modules N and Q by eight iron-sulfur (Fe-S) clusters to the quinone-binding site (Q site) at the interface with the membrane domain (Figure 1.10) (Verkhovskaya et al., 2008; Baradaran et al., 2013; Braun et al., 2014; Subrahmanian et al., 2016).

Table 1.1: Complex I subunits in human, *Arabidopsis thaliana* and *Chlamydomonas reinhardtii* (Subrahmanian et al., 2016).

<i>A. thaliana</i>		<i>C. reinhardtii</i>		<i>H. sapiens</i>	Localization	Module	Cofactor (s)
Name	Accession number	Name	Accession number				
Core subunits							
51 kDa	At5g08510	NUO6	Cre10.g422600	NDUPV1	matrix	N	FMN, N3
24 kDa	At4g02580	NUO5	Cre10.g450400	NDUPV2	matrix	N	N1a
75 kDa	At5g37510	NUO51	Cre12.g535950	NDUF51	matrix	N	N1b, N4, N5
TYKY/23 kDa	At1g16700, At1g79010	NUO8	Cre12.g496750	NDUF58	matrix	Q	N6a, N6b
P551/20 kDa	At5g11770	NUO10	Cre12.g492300	NDUF57	matrix	Q	N2
Nad9 ^m /30 kDa	AtMg00070	NUO9/ND9	Cre07.g527400	NDUF53	matrix	Q	
Nad7 ^m /49 kDa	AtMg00510	NUO7/ND7	Cre09.g405850	NDUF52	matrix	Q	
Nad1 ^m	AtMg00516, AtMg01120, AtMg01275	ND1 ^{m*}	AAB93446	ND1 ^m	mb	P _γ	
Nad2 ^m	AtMg00285, AtMg01320	ND2 ^{m*}	AAB93444	ND2 ^m	mb	P _γ	
Nad3 ^m	AtMg00990	ND3, NUO3	Cre08.g578900	ND3 ^m	mb	P _γ	
Nad4L ^m	AtMg00650	NUO11, ND4L*	Cre09.g402552	ND4L ^m	mb	P _γ	
Nad4 ^m	AtMg00580	ND4 ^{m*}	AAB93441	ND4 ^m	mb	P _β	
Nad5 ^m	AtMg00513, AtMg00601, AtMg00665	ND5 ^{m*}	AAB93442	ND5 ^m	mb	P _β	
Nad6 ^m	AtMg00270	ND6 ^{m*}	AAB93445	ND6 ^m	mb	P _γ	
Conserved non-core subunits							
18 kDa	At5g67590	NUO54	Cre03.g146247	NDUF54	matrix	N	
13 kDa	At3g03070	NUO56	Cre03.g178250	NDUF56	matrix	N	
MWFE	At3g08610	NUO41*	Cre10.g459750	NDUFA1	mb	P _γ	
B8	At5g47890	NUO88	Cre16.g679500	NDUFA2	matrix	N	
DAP13/17.2	At3g03100	NUO13	Cre11.g467767	NDUFA12	matrix	N	
SGDH	At1g67785	-	-	NDUF85	matrix	N	
B13	At5g52840	NUO813	Cre13.g568800	NDUFA5	matrix	Q	
B14.5a	At5g08060	Cre12.g484700*	Cre12.g484700*	NDUFA7	matrix	N/Q	
39 kDa	At2g20360	NUO49	Cre10.g434450	NDUFA9	matrix	Q	
ATDNK	At1g72040*	DNK1**	Cre02.g95350**	NDUFA10	?	Q/P _γ	
B9	At2g46540	Cre12.g537050*	Cre12.g537050*	NDUFA3	mb	P _γ	
B14	At3g12260	NUO814	Cre12.g555250	NDUFA6	mb	P _γ	
PGIV	At5g18890, At3g06310	NUO48*	Cre07.g333900	NDUFA8	mb peripheral	P _γ	
B14.7	At2g42210	TIM17/TIM22	Cre14.g617826	NDUFA11	mb	P _β	
B16.6/GRIM-19	At1g04610, At2g33220	NUO816	Cre16.g664600	NDUFA13	mb	P _γ	
20.9 kDa/MNLL	At4g16450	NUO21	Cre06.g267200	NDUF81	mb	P _β	
AGGG	At1g76290	-	-	NDUF82	mb	P _β	
B12	At2g02510, At1g14450	NUO812*	Cre05.g244850	NDUF83	mb	P _β	
NDUR/815	At2g31400	NUO84	Cre03.g204650	NDUF84	mb	P _β	
B18	At2g02050	NUO818	Cre06.g278188	NDUF87	mb	P _β	
ASH1	At5g47570	TEF29*	Cre01.g007850	NDUF88	mb	P _β	
B22	At4g34790	NUO822*	Cre11.g467668	NDUF89	mb	P _β	
POSW	At1g40140, At3g18410	NUO810	Cre12.g555150	NDUF810	mb peripheral	P _β	
NDU12/ESSS	At3g57785, At2g42310	NUO17	Cre05.g240800	NDUF811	mb	P _β	
NDU10/KF01	At4g00585	Cre17.g725400*	Cre17.g725400*	NDUFC1	mb peripheral	P _β	
NDUR/814.5b	At4g20150	NUOP1	Cre13.g571150	NDUFC2	mb	P _β	
15 kDa	At3g62790, At2g47690	NUO55*	Cre12.g511200	NDUF55	mb	P _β	
-	-	ACP1*	Cre16.g673109*	NDUF81	?	Q and P _γ	
Non-conserved non-core subunits							
CA1	At1g19580	-	-	-	mb peripheral		
CA2	At1g47260	-	Cre12.g516450,	-	mb peripheral		
CA3	At5g66510	CAG1, CAG2, CAG3	Cre06.g291850,	-	mb peripheral		
CAL1	At5g63310	-	Cre09.g415850	-	mb peripheral		
CAL2	At3g48680	-	-	-	mb peripheral		
P1/11 kDa	At1g67350	-	-	-	mb		
P2/16 kDa	At2g27710	-	-	-	mb		
TIM22	At1g18320	TIM22A**	Cre01.g021050**	-	mb		
At3g07480*	At3g07480*	NUOP3	Cre02.g100200	-	?		
-	-	NUOP4	Cre08.g578550	-	?		
-	-	NUOP5	Cre08.g578050	-	?		
Candidate plant-specific subunits							
P3	At5g14105	-	-	-	mb		
unknown protein	At1g68680	-	-	-	likely mb		
TIM22	At3g10110	TIM22A**	Cre01.g021050**	NP_037468.2**	?		
DUFS43	At1g72170	-	-	-	?		
unknown protein	At2g28430	-	-	-	?		
TIM23-2	At1g72750	TIM23**	Cre10.g434250**	-	?		

Single asterisk (*) indicate plant orthologs of mammalian subunits. Double asterisk (**) indicate reported candidate identified via similarity searches using BLASTs. Localization of subunits in the membrane or matrix arm of complex I: matrix; mb, membrane-associated; mb peripheral, membrane-associated, but lacking predicted trans-membrane domains. Column name: m indicates mitochondrially-encoded core subunits. The three functional modules are indicated as N for the NADH dehydrogenase module, Q for the quinone-binding module, and P for the proton-translocating module.

In Arabidopsis, the mitochondrial cI contains 14 conserved core units: seven in the membrane arm and seven in the peripheral arm (Figure 1.10) as well as 35 non-core subunits among which 9 non-conserved non-core subunits seem to be present just in plants (Table 1.1) (Subrahmanian et al., 2016).

2.2.1.1.2. cI impairment

The analysis of several mutants affected in cI subunits provided useful insights into the composition and assembly of the mitochondrial cI (Subrahmanian et al., 2016). Most of them show retarded growth (Lee et al., 2002; Perales et al., 2005; Meyer et al., 2009; Haïli et al., 2013; Colas des Francs-Small et al., 2014; Haïli et al., 2016) but, unlike in mammals, the lack of cI is not lethal in plants, which may be explained by the presence of alternative NADH dehydrogenases that bypass cI while still feeding electrons to the downstream complexes in the mETC (Kühn et al., 2015). In humans, cI impairments is related to neurodegenerative diseases like Parkinson's disease (Schapira, 1998). cI chemical inhibition was recently reported to prevent cancerous cells progression. However, the use of preventive doses of a cI inhibitor for cancer healing is not a solution for the moment because of its toxic side-effects including a marked bone atrophy (Wheaton et al., 2014; Heinz et al., 2017).

cI is one of the major sources of reactive oxygen species (ROS) production in the eukaryotic cell (Sousa et al., 2018). ROS are detoxified by the mitochondrial anti-oxidant system. During stress condition or in cI mutants, ROS production is increased and induces cellular and metabolic modifications to maintain plant growth and development (Lee et al., 2002; Juszczuk et al., 2012). cI activity can be chemically impaired and inhibitors may be classified according to their impact on ROS production: class A inhibitors (including Rotenone and Piericidin A) increase ROS production; Class B inhibitors (like Stigmatellin and Capsaicin) prevent ROS production, also in the presence of Class A inhibitors (Fato et al., 2009). In most cases, cI inhibitors block electrons transfer from the iron-sulfur clusters to the ubiquinone. Unlike class A, most of the class B compounds also inhibit mitochondrial cIII. (Esposti, 1998; Fato et al., 2009).

When the mitochondrial cI is impaired, cells adapt their metabolism to recover cellular homeostasis and ensure an optimal growth and development (Garmier et al., 2008; Meyer et al., 2009; Juszczuk et al., 2012; Kühn et al., 2015). Dysfunctions of cI increase the anti-oxidative detoxification and enhance stress tolerance (Juszczuk et al., 2012). Some

Arabidopsis cI mutants showed an enhanced stress resistance (Meyer et al., 2009) whereas others are more affected by specific stress, for example cold temperatures (Lee et al., 2002).

2.2.1.2. Complex II (cII)

Succinate dehydrogenase (cII) is part of the mETC but also of the citric acid cycle. It catalyzes the oxidation of succinate to fumarate and the reduction of ubiquinone to ubiquinol. The cII includes four core subunits: a flavo-protein, an iron-sulfur subunit, and two membrane anchor subunits (Millar et al., 2011; Schertl and Braun, 2014; Sousa et al., 2018).

2.2.1.3. Complex III (cIII)

Ubiquinol:cytochrome c oxidoreductase (cIII) transfers electrons from ubiquinol to the peripheral electron carrier cytochrome c and translocates four protons across the inner membrane through the process (Sousa et al., 2018). CIII is a symmetrical dimer made of 10 subunits with 3 conserved subunits across bacteria and mammals: cytochrome b (cyt b), cytochrome c1 (cyt c1), and the Rieske iron-sulfur protein (ISP) (Yang and Trumpower, 1986; Millar et al., 2011). This cIII is the second major producer of ROS among the mETC complexes (Dröse and Brandt, 2012).

2.2.1.4. Complex IV (cIV)

Cytochrome c oxidase (cIV) is the terminal enzyme of the mETC. It transfers four electrons from cytochrome c to molecular oxygen for its reduction into H₂O. This oxidation-reduction is coupled to the translocation of two protons across the inner membrane (Sousa et al., 2018). CIV contains 13 subunits forming a monomer. This complex can also form a dimer within the mitochondrial membrane (Dudkina et al., 2006).

2.2.2. The alternative pathway

The alternative respiratory pathway may be used to bypass the complexes I, III or IV. This pathway is mediated by type 2 NAD(P)H dehydrogenases (NADH₂s or NDs) and alternative oxidases (AOX) and is found in many organisms including animals, but not in mammals (McDonald and Gospodaryov, 2018).

2.2.2.1 Rotenone-insensitive Type 2 NAD(P)H dehydrogenases (NADH₂s)

To bypass mitochondrial cI, plants use alternative electron entries through internal (NDA1, NDA2 and NDC1) and external (NDB1-4) NAD(P)H dehydrogenases to reduce ubiquinone (Figure 1.9). Unlike cI, NADH₂s operate without the translocation of protons (Millar et al., 2011; Schertl and Braun, 2014).

2.2.2.2 Cyanide-insensitive alternative oxidase

Alternative oxidase (AOX) operates at the terminal step of the alternative pathway bypassing the cytochrome c chain (complexes III and IV) with a direct electron transfer from ubiquinol to the molecular oxygen. AOX dramatically reduces the ATP level because, on the one hand, it does not pump protons across the inner membrane and, on the other hand, it redirects electrons flow and thus bypasses the proton pumping complexes III and IV. AOX is part of the mitochondrial anti-oxidant machinery that reduces ROS levels. This quinol oxidase is encoded by several genes categorized as either *AOX1* or *AOX2* types. *AOX1* is expressed in stress conditions and is related to plant adaptation whereas *AOX2* expression is reported in normal developmental conditions (Juszczuk and Rychter, 2003; Millar et al., 2011; Vanlerberghe, 2013; Schertl and Braun, 2014).

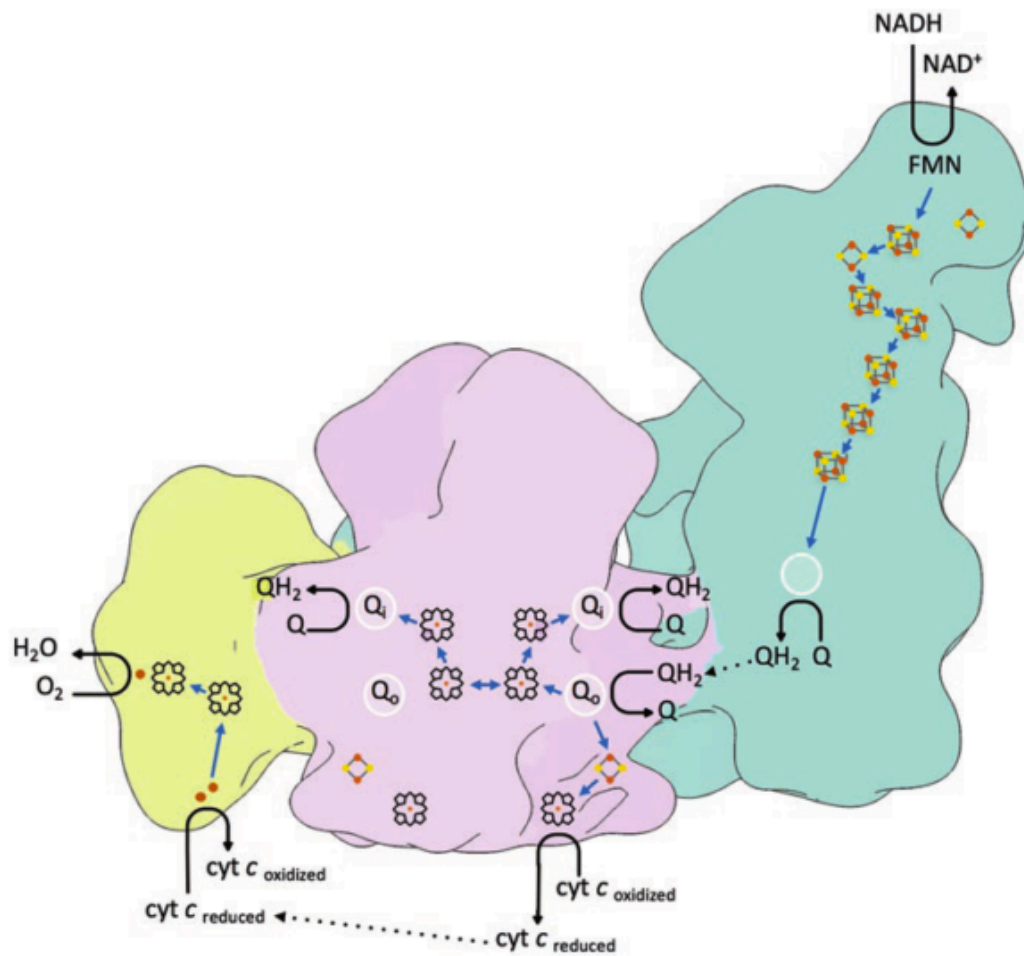


Figure 1.11: Schematic representation of electron and substrate transfer in the respirasome (Sousa et al., 2018). Rapid electron equilibration between b_L hemes allows quinone reduction in either monomer of cIII. Quinone oxidation occurs preferentially at the central monomer of cIII. CI, III and IV are depicted in green, pink and yellow, respectively. Quinone-binding sites are represented by circles. Blue arrows indicate transfer of electrons and dotted arrows diffusion of substrates. Reactions are indicated as black arrows.

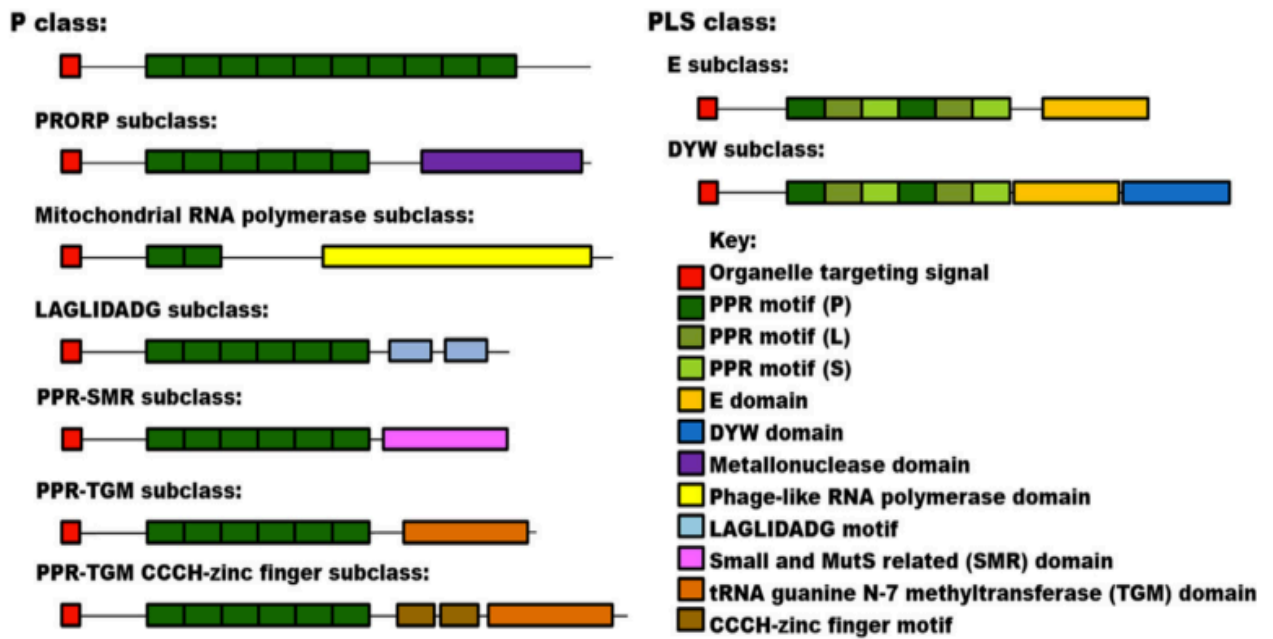
2.2.3. The respirasome

The respirasome is a super-complex conserved in all higher eukaryotes that includes mitochondrial electron transport complexes I, II and III. The arrangement of these respiratory complexes is identical in all respirasome structures: cIII lies on the inner side of the cI membrane arc, while cIV is located at the distal end of the cI membrane arm, adjacent to cIII. The complexes are connected by several direct protein-protein interactions. This compact arrangement reduces electron leakage, thus resulting in less ROS formed (Sousa et al., 2018) (Figure 1.11).

2.2.4. ATP synthase (complex V, cV)

Pushed by the electrochemical gradient across the inner membrane resulting from mETC-driven proton translocation, protons flow back into the matrix through the ATP synthase complex. The proton flow induces a mechanical rotation of the rotor, resulting in conformational changes that catalyze the conversion of ADP and phosphate into ATP in the matrix (Sousa et al., 2018).

A



B

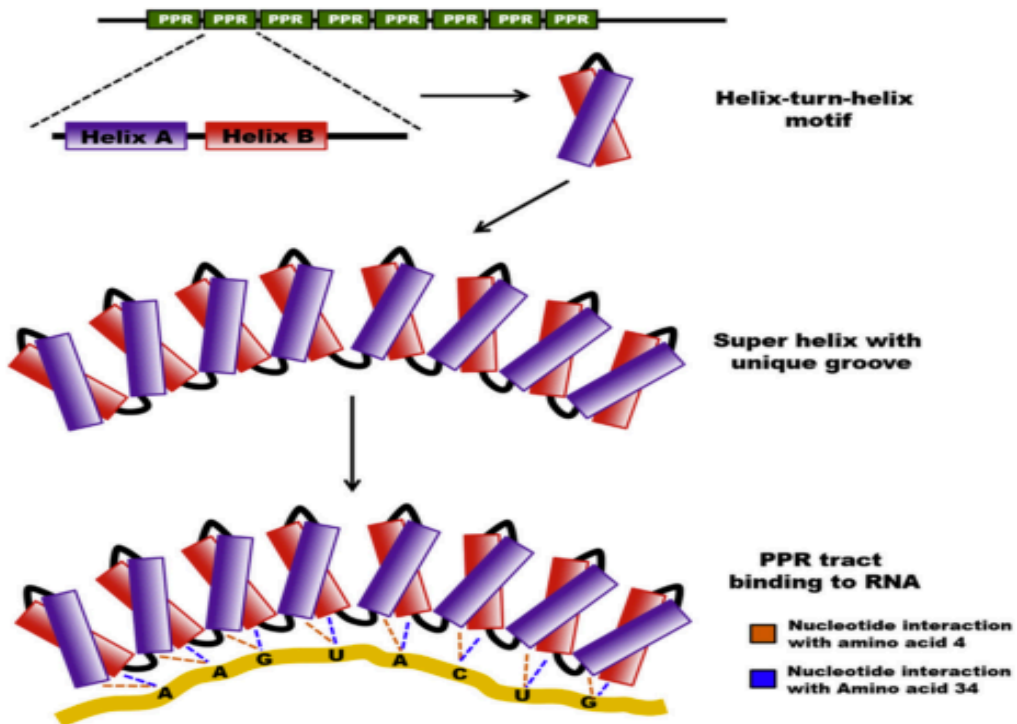


Figure 1.12: PPR proteins in eukaryotic cells (Manna, 2015). A, Overview representation of PPR subfamilies. Number of PPR motifs displayed in each protein is not characteristic of all members of that respective subfamily and schematics are not to scale. B, Schematic representation of PPR protein structure and the mechanism of ARN recognition. Each PPR motif forms two α -helices, which interact to form a helix turn helix motif. The series of helix turn helix motifs throughout the protein are stacked together to form a superhelix with an RNA binding groove. Modular recognition of transcripts is mediated by nucleotide interactions with the amino acids at positions 4 and 34 of each PPR motif.

2.3. Pentatricopeptide Repeat (PPR) proteins

2.3.1. PPR protein family

The nuclear-encoded PPR proteins are found in all eukaryotes and most of them are targeted into plastids and mitochondria where they regulate organellar gene expression. Through their affinity for RNA molecules, specific members of the family control different steps in transcription and translation, including RNA splicing, editing, cleavage and stabilization. Only a handful of PPR-encoding genes have been identified in most sequenced genomes. But a massive expansion of the PPR gene family occurred during plant evolution. With more than 450 members in *Arabidopsis*, the PPR protein family is thus one of the largest in land plants. PPR proteins are characterized by tandem repeats of a degenerate 35 amino acid motif (Lurin et al., 2004; O'Toole et al., 2008; Barkan and Small, 2014).

2.3.2. PPR protein structure

Based on variation in their tandem repeats, two types of PPR proteins have been defined: (1) P-class proteins, bearing the canonical 35 amino acid motif and (2) PLS-class proteins that contain PPR domains of varying lengths (P, 35 amino acids; L, long; S, short) (Figure 1.12 A) (Lurin et al., 2004; Schmitz-Linneweber and Small, 2008).

Each PPR repeat forms a pair of anti-parallel α -helices connected by a short loop that interact to form a helix-turn-helix structure. Together the PPR domain produces a super-helix with a central groove binding to specific RNA sequences. The PPR protein affinity for its cognate RNA substrate(s) is dictated by the amino acid residues at position 4 and 34 within each motif, one PPR motif recognizing one nucleotide (Figure 1.12 B) (Barkan and Small, 2014; Manna, 2015).

2.3.3. Arabidopsis PPR mutants affected in mitochondrial *ci* to study the link between respiration and development

PPR proteins are generally involved in the control of organellar genome expression and defects in PPR activity result in phenotypes associated with organellar dysfunction. The consequences of a *PPR* gene mutation thus depend on the organelle transcript(s) that the

corresponding PPR protein binds to and, indirectly, on the function(s) encoded in said transcript(s) (Barkan and Small, 2014; Manna, 2015). We have characterized Arabidopsis *ppr* mutants that prevent the expression of mitochondrial genes encoding different subunits of the mETC cI.

During the last decade, several studies have reported the biochemical and molecular consequences of *PPR* gene mutations affecting mitochondrial cI assembly and activity. During my PhD project, I characterized Arabidopsis *ppr* mutants that prevent the expression of mitochondrial genes encoding different subunits of the mETC cI. We investigated the impact of cI dysfunction on the growth and organogenesis observed in calli derived from protoplasts. For this purpose, we selected four mutants showing graded growth retardation and each of them carries a mutation in a different nuclear gene. These mutants are: *BSO-insensitive roots 6 (bir6)* (Koprivova et al., 2010), *mitochondrial stability factor 2 (mtsf2)* (Wang et al., 2017), *mitochondrial translation factor1 (mtl1)* (Haïli et al., 2016) and *mitochondrial stability factor 1 (mtsf1)* (Haïli et al., 2013).

mtsf2, *mtl1* and *mtsf1* were isolated from an Arabidopsis T-DNA mutant collection. Each mutated gene was predicted to encode a PPR protein directed to mitochondria. *mtsf2*, *mtl1* and *mtsf1* plants are characterized by retarded growth compared to the wild-type plants. *MTSF2* encodes a 20-PPR protein involved in the processing and stabilization of one among three *nad1* mRNA precursors resulting in the absence of the Nad1 subunit and, consequently, the absence of the cI from the inner membrane. *MTL1* encodes a 16-PPR protein involved in *nad7* mRNA splicing and translation. The lack of Nad7 subunit similarly prevents the cI assembly. The third gene, *MTSF1* encodes a 19-PPR protein involved in the stabilization of the mitochondrial *nad4* mRNA and, in parallel, in the splicing of the *nad2* mRNA. *mtsf1* has a reduced amount of truncated and non-functional cI (Haïli et al., 2013; Haïli et al., 2016; Wang et al., 2017). *bir6* was identified in a screen for buthionine sulfoximine (SBO) resistant mutants. SBO inhibits an enzyme required for glutathione synthesis and SBO insensitive mutants show sustained root growth in the presence of the inhibitor. *BIR6* encodes an 8-PPR protein involved in the splicing of the mitochondrial *nad7* intron 1. The *bir6* mutation results in a slightly reduced amount of a functional cI, hence *bir6* is less affected in its growth and development (Koprivova et al., 2010) compared to *mtsf2*, *mtl1* and *mtsf1*.

Table 1.2: Properties, reactivity and production site of the main reactive oxygen species (ROS) in plants (Mittler, 2017).

ROS	$t_{1/2}$	Migration distance	Mode of action	Production site
Superoxide ($O_2^{\cdot-}$)	1–4 μ s	30 nm	Reacts with Fe–S proteins Dismutates to H_2O_2	Apoplast (RBOHs), chloroplasts, mitochondria, peroxisomes, electron transfer chains
Hydroxyl radical ($OH\cdot$)	1 ns	1 nm	Extremely reactive with all biomolecules including DNA, RNA, lipids, and proteins	Iron and H_2O_2 (Fenton reaction)
Hydrogen peroxide (H_2O_2)	>1 ms	>1 μ m	Reacts with proteins by attacking cysteine and methionine residues. Reacts with heme proteins. Reacts with DNA.	Peroxisomes, chloroplasts, mitochondria, cytosol, apoplast
Singlet oxygen (1O_2)	1–4 μ s	30 nm	Oxidizes lipids, proteins (Trp, His, Tyr, Met, and Cys residues), and G residues of DNA	Membranes, chloroplasts, nuclei

Fenton reaction is the reaction of H_2O_2 (or dismutated $O_2^{\cdot-}$) with Fe^{2+} to form the hydroxyl radical ($HO\cdot$).

3. Redox signaling and plant development

In several biological processes involving energy transfer, reactive oxygen species (ROS) are generated as a by-product when escaping electrons or energy react with the molecular oxygen (O_2) present in the cells. ROS can also be generated as primary products that are perceived as signal molecules in stress-related conditions (Waszczak et al., 2018).

The ROS term refers to oxygen-containing compounds with a high chemical reactivity. They can be divided in two groups: oxygen radicals containing an impaired electron (superoxide anion, $O_2^{\cdot-}$; hydroxyl radical, HO^{\cdot} ; peroxy radical, RO^{\cdot} ; hydroperoxyl radical HO_2^{\cdot}) and non-radical oxidizing agents (hydrogen peroxide, H_2O_2 ; ozone, O_3 ; hypochlorous acid, $HOCl$) (Bayir, 2005). Different forms of ROS are found in plants, depending on the cellular compartments and the biological processes considered. The most common ROS molecules are singlet oxygen (1O_2), superoxide anion ($O_2^{\cdot-}$), hydrogen peroxide (H_2O_2), and hydroxyl radical (HO^{\cdot}) (Noctor et al., 2017; Waszczak et al., 2018). ROS are generated in several cell compartments and have different properties (Table 1.2).

ROS production is increased when cells are under stressful conditions (injury, starvation, pathogen attack, chemical treatments, etc.). In detrimental conditions, ROS accumulation overcomes the cell scavenging capacity and leads to an oxidative stress. Persistent ROS can then react with different cellular components and migrate to damage neighboring cells inducing an overall cell death (Gill and Tuteja, 2010; Mittler, 2017).

Cellular redox homeostasis is essential in all living organisms to avoid ROS-related damages. This homeostasis is ensured through a cell reducing environment mediated by anti-oxidant enzymes and compounds (Bayir, 2005; Noctor et al., 2017; Sies et al., 2017). Cellular redox state in a given organism depends on the cell type and its developmental stage. Thus, the redox state is different between cells within the same organism (Sies et al., 2017).

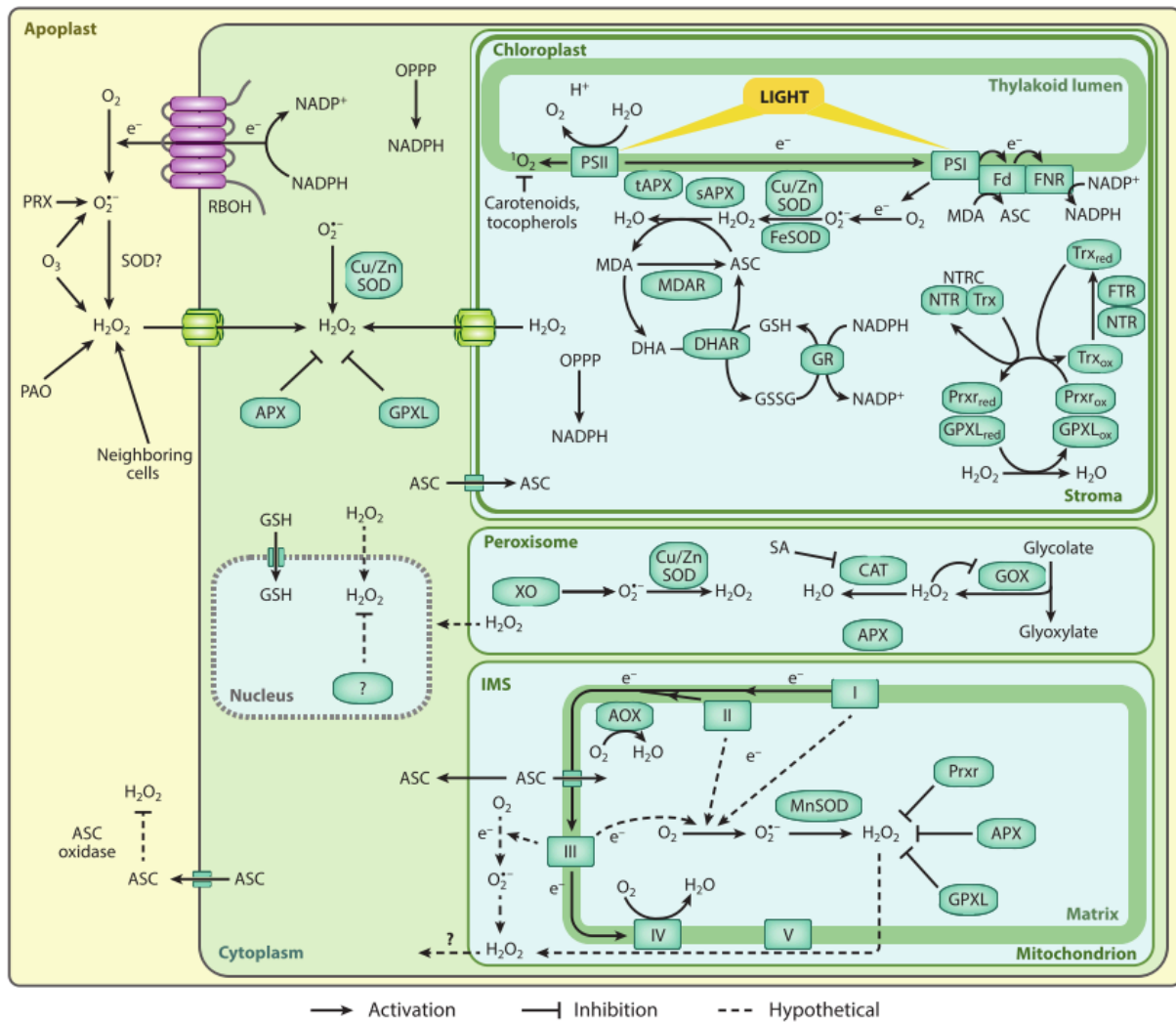


Figure 1.13: Overview of ROS production and scavenging in plants (Waszczak et al., 2018). Singlet oxygen ($^1\text{O}_2$) is formed in chloroplast through the energy transfer from PSII to the ground state triplet oxygen ($^3\text{O}_2$). Superoxide anions ($\text{O}_2^{\cdot-}$) are generated during electron leakage from mitochondrial and chloroplastic electron transport chains. Enzymatic and spontaneous dismutation of superoxide anions and glycolate oxidase activity (GOX) generate hydrogen peroxide (H_2O_2) that might cross cell membranes via aquaporins. In the different plant cell compartments, various non-enzymatic and enzymatic ROS scavengers maintain a basal ROS level to ensure the integrity of biological processes. Abbreviations: AOX, alternative oxidase; APX, ascorbate peroxidase; ASC, ascorbate; CAT, catalase; DHA, dehydro-ascorbate; DHAR, dehydro-ascorbate reductase; Fd, ferredoxin; FNR, ferredoxin-NADP⁺ reductase; FTR, ferredoxin-dependent thioredoxin reductase; GR, glutathione reductase; GPXL, glutathione peroxidase-like; IMS, intermembrane space; MDA, mono-dehydro-ascorbate; MDAR, mono-dehydro-ascorbate reductase; NTR, NADPH-dependent thioredoxin reductase; NTRC, NADPH-dependent thioredoxin reductase C; OPPP, oxidative pentose phosphate pathway; PAO, polyamine oxidase; PRX, peroxidase; Prxr, peroxiredoxin; PSI/II, photosystem I/II; RBOH, respiratory burst oxidase homolog; ROS, reactive oxygen species; SA, salicylic acid; SOD, superoxide dismutase; TRX, thioredoxin; XO, xanthine oxidase.

3.1. ROS production in plants

3.1.1. Singlet oxygen ($^1\text{O}_2$)

Singlet oxygen is mostly produced within the chloroplastic thylakoid membrane as a result of the energy leakage that is transferred from photosystem II (PSII) to the ground state molecular oxygen ($^3\text{O}_2$) (Figure 1.13) (Waszczak et al., 2018). $^1\text{O}_2$ mediated signaling was related with photo-oxidative stress adaptation (Ramel et al., 2012) and is also involved in ROS-induced cell death in leaves (Triantaphylides et al., 2008).

3.1.2. Hydroxyl radicals (OH^\cdot)

OH^\cdot is the most reactive form of ROS (Gill and Tuteja, 2010; Waszczak et al., 2018). This free radical is supposed to react with almost all cell constituents. It can be produced from O_2^\cdot or H_2O_2 in the presence of transition metals such as iron (Fe^{2+}) through the Fenton reaction: $\text{Fe}^{2+} + \text{H}_2\text{O}_2 \rightarrow \text{Fe}^{3+} + \text{OH}^\cdot + \text{OH}^\cdot$ (Gill and Tuteja, 2010).

3.1.3. Superoxide (O_2^\cdot)

The superoxide radical is produced by the reduction of molecular oxygen (O_2) with one single electron (Slesak et al., 2007). It is generated in the chloroplast through PSI activity, in peroxisome through xanthine oxidase activity, and finally in mitochondria through mETC (Waszczak et al., 2018). O_2^\cdot can dismutate into H_2O_2 , either spontaneously or enzymatically (Asada, 2006).

3.1.4. Hydrogen peroxide (H_2O_2)

Hydrogen peroxide is largely used as an antiseptic solution thanks to its cytotoxic activity (Slesak et al., 2007). Compared to the other oxidizing species, H_2O_2 is moderately reactive but it migrates more easily through cells (Table 1.2). It is considered as one of the major ROS and the more stable pro-oxidant compound (Bayir, 2005; Slesak et al., 2007; Gill and Tuteja, 2010; Waszczak et al., 2018). H_2O_2 is found in many cell compartments, including

chloroplast, mitochondria, peroxisome, but also in cytoplasm, plasma membrane and in the extracellular matrix (Slesak et al., 2007).

Hydrogen peroxide is mostly generated either through the direct disproportionation of superoxide radical: $2\text{O}_2^- + 2\text{H}^+ \rightarrow \text{H}_2\text{O}_2 + \text{O}_2$; or through anti-oxidant molecules like thiol-containing compounds: $2\text{O}_2^- + \text{H}^+ + \text{XH}_2 \rightarrow \text{H}_2\text{O}_2 + \text{XH}$, where X refers to a reducing compound (Slesak et al., 2007).

H_2O_2 scavenging is tightly connected to the scavenging of the other ROS. Cellular hydrogen peroxide level is finely managed and coordinated in all plant cell compartments to maintain a steady redox state (Slesak et al., 2007). It is scavenged by several anti-oxidant enzymes, including peroxidases and catalases, together with anti-oxidant metabolites such as flavonoids and thiol-containing compounds (Bayir, 2005; Gill and Tuteja, 2010; Racchi, 2013).

3.2. ROS scavenging

3.2.1. Anti-oxidant compounds

Anti-oxidants prevent the oxidation of other molecules thereby avoiding unwanted oxidative damages (Gill and Tuteja, 2010). Different anti-oxidant molecules are found in plant cells. They can be separated in two groups depending on their solubility: (1) hydrophilic molecules such ascorbic acid, glutathione and phenolic compounds and (2) lipid-soluble molecules such tocopherols and carotenoids (Racchi, 2013).

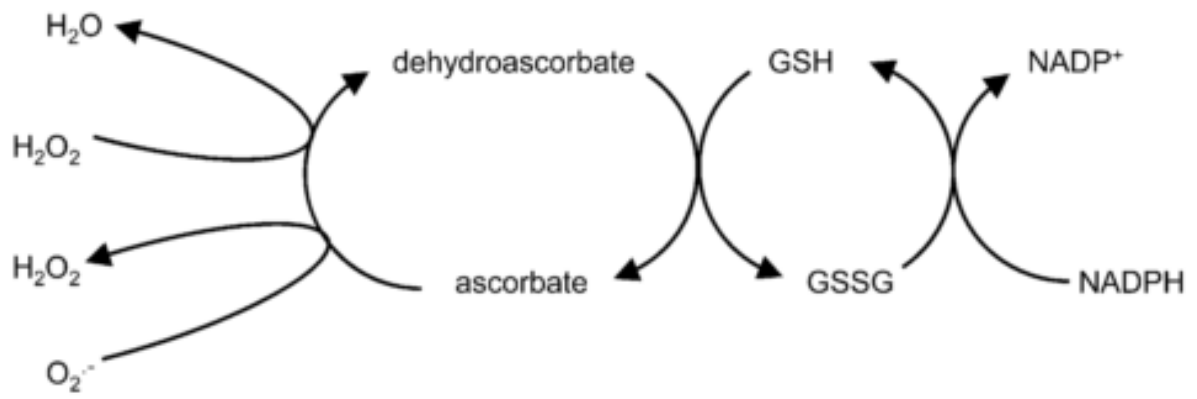


Figure 1.14: Foyer-Halliwell-Asada pathway for ROS scavenging (Foyer and Noctor, 2011).

3.2.1.1. Ascorbate-glutathione pathway

Also called the “Foyer-Halliwell-Asada” pathway (Figure 1.14), this ROS scavenging pathway is present in chloroplasts, mitochondria, peroxisomes and the cytoplasm. In this ROS detoxification system, ascorbate (ASC) scavenges ROS, and glutathione (GSH) regenerates the oxidized ascorbate (dehydroascorbate, DHA), either chemically or enzymatically (Foyer and Noctor, 2011).

3.2.1.1.1. Ascorbate (vitamin C)

Ascorbate (ascorbic acid) is considered the most powerful ROS scavenger in plants (Gill and Tuteja, 2010). It is synthesized in the mitochondria and transferred to the other cell compartments for ROS removal (Racchi, 2013). Mitochondria are also involved in the regeneration of ascorbate through the reduction of the oxidized ascorbate form, DHA, by the mETC (Szarka et al., 2007). Ascorbate detoxifies cells from H_2O_2 , $O_2^{\cdot-}$, HO^{\cdot} and lipid peroxides. Ascorbate can be used as a peroxidase co-factor for ROS scavenging or it can have a direct chemical activity on oxidative radicals (Noctor et al., 2017).

3.2.1.1.2. Glutathione (GSH)

GSH is a small thiol-containing molecule indispensable for plant growth and development. This anti-oxidant is used in the glutathione-ascorbate scavenging system to regenerate ASC through the reduction of DHA. Glutathione can also directly scavenge ROS. Reduced glutathione (GSH) is rapidly oxidized into GSSG (disulphide form) through several biochemical reactions. GSH is thus continuously regenerated from GSSG by the NADPH-dependent glutathione reductase (GR) (Noctor et al., 2012; Hasanuzzaman et al., 2017). Beside its crucial activity in ROS scavenging, glutathione is also involved in biosynthetic pathways, redox homeostasis, lipid peroxidation prevention and plasma membrane protection (Hasanuzzaman et al., 2017). GSH is crucial for embryo development as *Arabidopsis* mutants affected in the first step of GSH biosynthesis are embryo-lethal (Cairns et al., 2006).

3.2.1.2. Tocopherols (vitamin E) and carotenoids

Both α -tocopherol and β -carotene are scavengers of $^1\text{O}_2$ in the chloroplast (Asada, 2006; Waszczak et al., 2018). $^1\text{O}_2$ oxidizes α -tocopherol into α -tocopherol quinone (Asada, 2006) and β -carotene into β -cyclocitral and other by-products involved in the chloroplast retrograde signaling during photo-oxidative stress (Ramel et al., 2012).

3.2.2. Enzymatic ROS detoxification

3.2.2.1. Superoxide dismutase (SOD)

SODs are found in almost all cell compartments (Figure 1.1) to mediate the dismutation of $\text{O}_2^{\cdot-}$ into H_2O_2 and O_2 as follows: $2\text{O}_2^{\cdot-} + 2\text{H}^+ \rightarrow 2\text{H}_2\text{O}_2 + \text{O}_2$ (Gill and Tuteja, 2010). Different SODs exist in plant: iron-SODs (FeSODs) in chloroplasts; copper/zinc-SODs (Cu/ZnSODs) in chloroplasts, peroxisomes and cytoplasm; and manganese-SODs (MnSODs) in mitochondria (Waszczak et al., 2018).

3.2.2.2. Catalase (CAT)

CATs are considered among the most important H_2O_2 detoxifying enzymes (Noctor et al., 2016). Catalase enzymatic activity dismutates directly H_2O_2 into H_2O and O_2 with the following reaction: $2\text{H}_2\text{O}_2 \rightarrow 2\text{H}_2\text{O} + \text{O}_2$. CATs have an important role in H_2O_2 removal during stress conditions since one catalase molecule dismutates 6 millions of H_2O_2 per minute (Gill and Tuteja, 2010).

3.2.2.3. Ascorbate peroxidase (APX)

Ascorbate peroxidase reduces cellular H_2O_2 using the reduced ascorbate (ASC) as electron donor: $\text{H}_2\text{O}_2 + \text{ASC} \rightarrow 2\text{H}_2\text{O} + \text{DHA}$. This enzyme is part of the glutathione-ascorbate cycle and its affinity for H_2O_2 is higher than catalase (Gill and Tuteja, 2010).

3.2.2.4. Monodehydroascorbate reductase (MDHAR)

MDHAR is a flavin adenine dinucleotide (FAD) enzyme that reduces monodehydroascorbate (MDHA), an oxidant radical generated through ASC oxidation. The enzymatic activity of MDHAR is NAD(P)H-dependent: $\text{MDHA} + \text{NAD(P)H} \rightarrow \text{ASC} + \text{NAD(P)}^+$ (Gill and Tuteja, 2010). Recently, this protein, largely known as anti-oxidant enzyme, was related to a pro-oxidant activity in Arabidopsis during trinitrotoluene (TNT) induced oxidative stress (Johnston et al., 2015).

3.2.2.5. Dehydroascorbate reductase (DHAR)

DHAR is a glutathione *S*-transferase enzyme that uses reduced GSH for ascorbate regeneration in the ascorbate-glutathione pathway: $\text{DHA} + 2\text{GSH} \rightarrow \text{ASC} + \text{GSSG}$ (Gill and Tuteja, 2010; Foyer and Noctor, 2011).

3.2.2.6. Glutathione reductase (GR)

GR has an essential activity in the glutathione-ascorbate pathway. This enzyme ensures a continuous regeneration of the reduced form of glutathione (GSH) using the reducing power of NAD(P)H in the following reaction: $\text{GSSG} + \text{NAD(P)H} \rightarrow 2\text{GSH} + \text{NAD(P)}^+$ (Gill and Tuteja, 2010; Noctor et al., 2012).

3.2.2.7. Guaiacol peroxidase (GPOX)

GPOX is involved in H_2O_2 scavenging and uses guaiacol and pyragallol as electron donors. This enzyme takes part in the ROS-hormone cross-talks as it decomposes the plant hormone indole-3-acetic acid (IAA) (Gill and Tuteja, 2010).

3.2.2.8. Thioredoxins (Trx) and glutaredoxins (Grx)

Trx and Grx have thiol oxidoreductase activity. In plants, several compounds containing oxidized thiols are reduced by these enzymes (Meyer et al., 2012).

3.3. Mitochondrial ROS and anti-oxidant systems

In the dark and in non-green tissues, mitochondria seem to be the major site of ROS production (Rhoads et al., 2006; Racchi, 2013). During the mitochondrial respiration, ROS production is related to the activity of complexes I, II and III (Slesak et al., 2007). The prevalent ROS in mitochondria is the superoxide radical (O_2^-) which is produced at two sites: complexes I and II generate O_2^- in the mitochondrial matrix; whereas cIII generates the superoxide radical in the mitochondrial matrix and in the inter-membrane space (Waszczak et al., 2018).

Mitochondrial ROS are scavenged by the mitochondrial anti-oxidant machinery (Figure 1.13) to maintain a basal non-toxic ROS level. Superoxide radical is dismutated by the mitochondrial MnSOD into H_2O_2 in the matrix (Chew et al., 2003). The intermembrane O_2^- could be directly scavenged by ASC as the final biosynthesis step of this anti-oxidant compound occurs in the intermembrane space (Waszczak et al., 2018). The resultant hydrogen peroxide is then detoxified by the ascorbate-glutathione cycle (Chew et al., 2003).

When the mETC terminal oxidases are inhibited, the ubiquinone pool becomes over reduced leading to an important electron leakage that enhances ROS production (Møller, 2001) and the over-produced ROS can damage mitochondrial lipids, proteins and DNA. Thus, in stress conditions or when the mETC is impaired (in respiratory mutants or in plants treated with respiratory inhibitors), redox homeostasis is unbalanced and some ROS can escape from mitochondria into other cell compartments creating a mitochondrial oxidative signal (Rhoads et al., 2006).

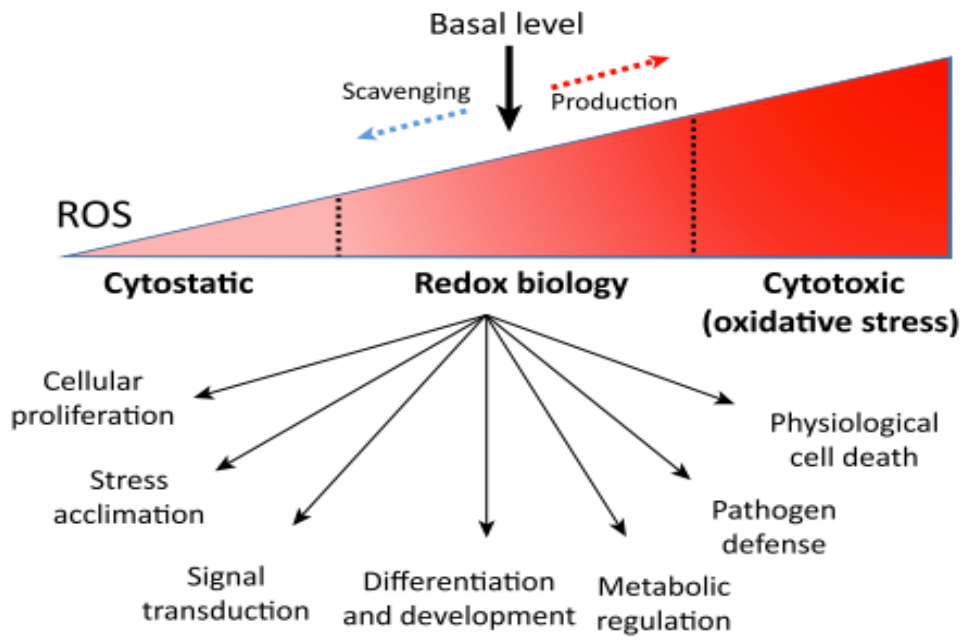


Figure 1.15: Cellular functions are conditioned by basal ROS level maintenance (Mittler, 2017). Redox balance is important to maintain a basal level of ROS to ensure biological processes. ROS exceeding this level leads to a cytotoxic oxidative stress. When ROS levels drop under a certain threshold, cells enter a cytostatic state.

3.4. Redox regulation of plant development

Redox balance is important for the sustainability of almost all biological processes. The maintenance of a basal ROS level is essential for optimal plant development (Figure 1.15) (Mittler, 2017). A decrease in anti-oxidants or an increase in ROS will shift the ROS/anti-oxidants balance to the ROS side. This un-balanced state results either in plant adaptation to stress or programmed cell death (PCD) depending on ROS level (Noctor et al., 2017).

3.4.1. ROS and plant growth

The best known example for ROS-mediated plant regulation is the programmed cell death (PCD) involving ROS interaction with the stress-related hormones salicylic acid (SA), jasmonic acid (GA) and ethylene (Overmyer et al., 2003).

ROS affect plant growth through hormonal regulations (Berkowitz et al., 2016). This could be through direct hormone oxidation or indirectly. For example, ROS-mediated plant growth modulation can be relayed through GA signaling. This interaction involves DELLA proteins that modulate ROS accumulation thereby enabling GA-related cell elongation (Achard et al., 2008).

Auxin signaling is also affected by redox homeostasis. When facing stress conditions, plants alter their growth as a stress adaptation strategy to ensure their survival. This strategy involves auxin catabolism through ROS-mediated auxin oxidation (Peer et al., 2013).

Mutation in anti-oxidants enzymes TRX and a glutathione biosynthesis enzyme results in an impaired auxin signaling affecting plant apical dominance and vascular defects (Bashandy et al., 2010). ROS are also able to modulate root meristem activity (Tsukagoshi et al., 2010). Furthermore, they can be involved in plant differentiation independently from auxin and cytokinin signaling. The transcription factor UPBEAT1 (UPB1) regulates the expression of peroxidases that control ROS-induced root development (Tsukagoshi et al., 2010).

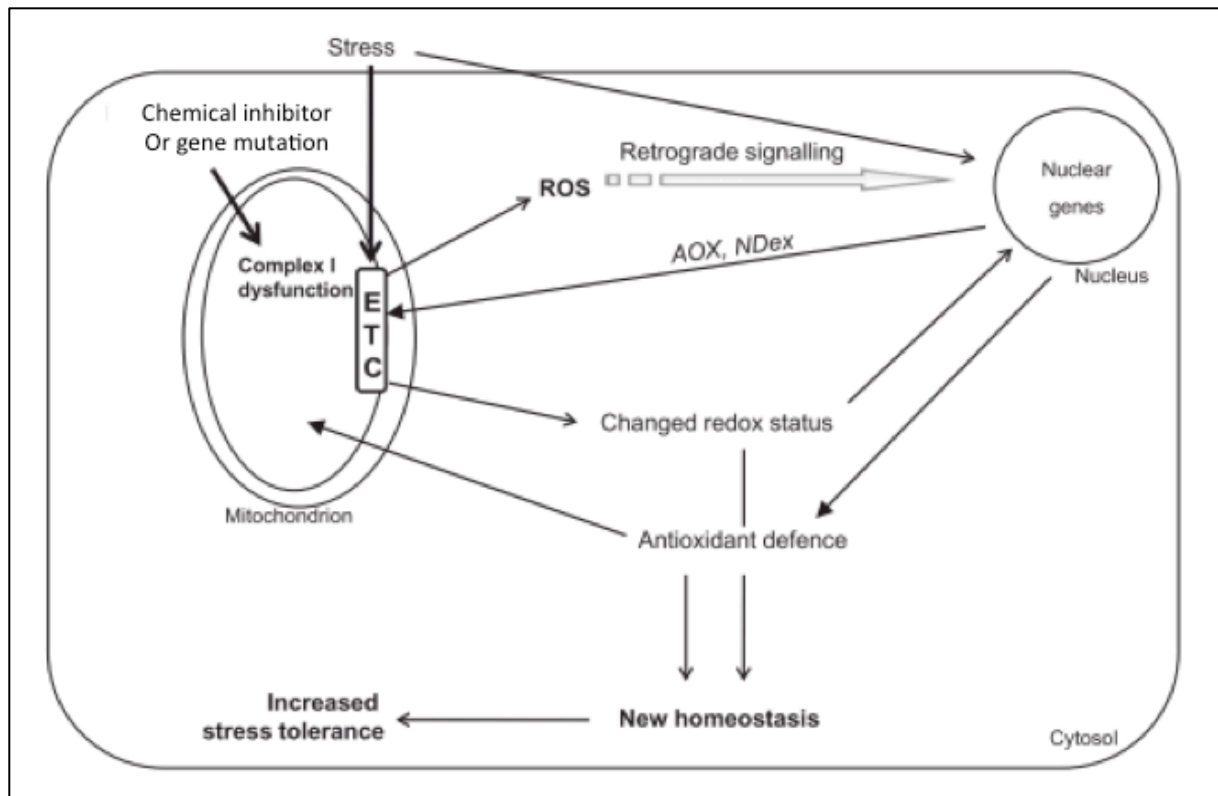


Figure 1.16: Hypothetical model for nucleus-mitochondrion cross-talk in response to CI dysfunction (Juszczuk et al., 2012). CI defect induces an increase of the mitochondrial reactive oxygen species (ROS) production that triggers mitochondrial retrograde signaling (MRS). In response to MRS, genes related to the anti-oxidant defense system are up-regulated together with the activation of the respiratory alternative pathway (alternative NAD(P)H dehydrogenase [NDex] and alternative oxidase [AOX]) to dampen the stress resulting from increased ROS levels. Eventually, in non-extreme scenarios, ROS production and anti-oxidant defense mechanisms reach a novel equilibrium compatible with plant growth and development, despite suboptimal conditions.

3.4.2. ROS and plant regeneration

Many pro-oxidant compounds, especially H₂O₂ and anti-oxidant molecules such as glutathione and ascorbate, have been used for decades to modulate organ regeneration in several species. Oxidative stress induction is also integrated in several protocols to induce somatic embryogenesis, for example for the regeneration of doubled haploids from microspore-derived calli.

Overexpression of the glutathione peroxidase gene PHGPx, coding for a peroxidase largely involved during oxidative stress induced by biotic and abiotic stresses, completely inhibited *in vitro* shoot regeneration in tobacco, potato and tomato explants (Faltin et al., 2010). The *in vitro* regeneration of forest trees also depends on redox homeostasis. Peroxidase and SOD activities are higher in calli derived from shoot explants compared to the shoot explants themselves (Arican et al., 2008). Plant de-differentiation was also reported as stress mediated mechanism (Grafi and Barak, 2015).

3.4.3. ROS and mitochondrial retrograde signals

Juszczuk and co-workers proposed a model that integrates plant mitochondrial CI dysfunction with the retrograde (from mitochondria to nucleus) and anterograde (from nucleus to mitochondria) signals (Figure 1.16) (Juszczuk et al., 2012). CI activity may be affected in mutants lacking one or more CI subunits or following the chemical inhibition of element(s) in the mETC. Such perturbations cause organellar and cellular redox disequilibrium eventually corrected in a renewed oxidation–reduction homeostasis. Thus, mitochondria use retrograde signaling to communicate with the nucleus about their functional status (Huang et al., 2016). However, mitochondrial retrograde signals are not yet well characterized (Berkowitz et al., 2016).

AOX activity has often been described as the favorite marker of the mitochondrial retrograde regulation (MRR) as it is induced in several stress conditions (Ho et al., 2008; Ng et al., 2014). The retrograde nuclear regulation of *AOX* gene expression is mediated by two transcription factors physically associated with the endoplasmic reticulum: ARABIDOPSIS NAC DOMAIN CONTAINING PROTEIN13 (ANAC013) and ANAC017 (De Clercq et al., 2013; Ng et al., 2013b). *AOX* genes belong to the MRR targets induced during mitochondrial dysfunction (MDS). The MDS genes, collectively called the MDS stimulon, are characterized

by a mitochondrial dysfunction motif (MDM) found in the upstream promoter region and responsible for their transcriptional activation following mitochondrial impairments (De Clercq et al., 2013). Some MDS genes (e.g. genes involved in PCD suppression) that are targeted by ANAC017 are also induced by chloroplast retrograde regulation mediated via phosphoadenosine phosphate (PAP). PAP is produced in chloroplasts in stressful conditions, for example as a response to high light stress, then migrates to the nucleus as a retrograde signal. Thus, ANAC017 and PAP represent a good example of the cross-talk between organelle (mitochondria and chloroplast) retrograde signaling (Aken and Pogson, 2017).

Although ROS-mediated hormonal regulations were largely analyzed, the mitochondrial-ROS interaction with hormonal signaling was recently investigated (Berkowitz et al., 2016). Recently, auxin was reported as a probable player in the cross-talk between MRR and hormonal growth regulation because the inhibition of the mETC by antimycin A (inhibiting cIII) transiently blocked auxin signaling, whereas auxin treatment repressed the antimycin A-mediated expression of the MRR marker *AOX1a* (Ivanova et al., 2014). Another study reported that a chemical screen for *AOX1a* regulators identified the nuclear cyclin-dependent kinase E1 (CDKE1) as an important component in MRR (Ng et al., 2013a). Finally, the important anti-oxidative machinery activated in most cI mutants has been linked with the advanced stress tolerance in these plants (Juszczuk et al., 2012).

Research outline

As presented in the previous Chapter I, *in vitro* regeneration relies on complex mechanisms that are controlled by multiple factors including various stresses. In this network, mitochondria play an important role as they participate to the integration of stress signals occurring during diverse environmental challenges and relay these cues to affect plant developmental processes. In the course of my PhD thesis, I investigated the effect of mitochondrial impairments on specific biological processes: the *in vitro* growth of de-differentiated cells (calli) and the *in vitro* shoot regeneration from protoplasts-derived calli.

The next Chapter II describes our analysis of four *Arabidopsis* mutants affected in the mitochondrial complex I, which is the first complex in the mitochondrial electron transport chain. These complex I mutants were chosen because they display graduated growth retardation phenotypes and with the aim to unravel a potential correlation between *in vitro* growth and shoot formation in calli.

Chapter III explains how we were able to phenocopy the complex I mutations with a potent chemical inhibitor of the mitochondrial complex I, rotenone. We applied the inhibitor at three different moments during the callus regeneration sequence and at different concentrations to find the application mode that most efficiently induced organogenesis. Processes involved in both callus growth and induced shoot regeneration were investigated with the application of this inhibitor. We also used a cytosolic redox biosensor to analyze the redox state of calli following rotenone treatment.

As detailed in Chapter IV, the results obtained in some of our experiments were marked by a persistent level of variability, especially for treatments with the rotenone concentrations most efficient in inducing shoot formation. We investigated the plausible cause(s) of this variability by searching for parameters possibly correlated with shoot regeneration efficiency in wild type untreated calli. We also studied whether callus size and growth rate were correlated with shoot regeneration rate. We closed this part of our research work by analyzing the effect of two additional respiratory inhibitors - targeting the mitochondrial complex IV and the alternative oxidase activity - on callus growth and shoot regeneration.

Finally, with the goal to better understand the link between organogenesis and complex I impairment, we characterized the molecular shifts occurring at key steps of the regeneration sequences through a thorough transcriptome microarray analysis presented in

Chapter V. This study is the basis for several working hypotheses explaining the observed enhanced regeneration phenotypes of complex I mutant calli and rotenone-treated calli, laid out in Chapter VI.

Chapter 2:

**Mitochondrial complex I genetic dysfunction
enhances shoot regeneration in *Arabidopsis*
thaliana protoplast-derived calli**

Introduction

Mitochondria carry out multiple functions ranging from the production of energy and metabolic intermediates to the biosynthesis and of numerous compounds. They also play a key role in retrograde signaling and programmed cell death (PCD) in response to abiotic and biotic stress^{1,2}. Mitochondria are the central power generator of most eukaryotic cells and the mitochondrial electron transport chain (mETC) is the main system for ATP production. It is composed of four protein respiratory complexes: the NADH:quinone oxido-reductase (complex I, cI), the succinate dehydrogenase (complex II, cII), the cytochrome c reductase (complex III, cIII) and the cytochrome c oxidase (complex IV, cIV)³. The plant mETC contains five other accessory enzymes not present in animal mitochondria: an alternative oxidase (AOX) and four NAD(P)H dehydrogenases⁴. The cI is the main port of entry of the electrons in the mETC. It oxidizes NADH and pumps protons across the mitochondrial inner membrane, thereby contributing to the maintenance of the proton gradient used by the complex V to generate ATP. With more than 40 subunits, cI is the largest complex of the mETC and, through its activity, the major producer of reactive oxygen species in the mitochondria⁵⁻⁷.

Strong mitochondrial defects are highly deleterious and result in compromised growth or cell death. In land plants for example, mitochondrial dysfunction can lead to male sterility due to the aborted development of pollen grains⁸. So-called cytoplasmic male sterility systems have been dissected down to the causal genes in various species because they have been of considerable value in facilitating efficient hybrid seed production in various crops. However, very little is known about the role mitochondria may have as general regulators of plant development.

Multiple reports have described the biochemical and molecular consequences of mitochondrial defects in plants⁸⁻¹³. This work investigates how cI dysfunction affects organogenesis in mutant plants. For this purpose, we have analyzed four *Arabidopsis thaliana* mutants that have an altered cI and show graded growth retardation: *mitochondrial stability factor 2 (mtsf2)*, *mitochondrial translation factor1 (mtl1)*, *mitochondrial stability factor 1 (mtsf1)* and *buthionine sulfoximine (BSO) insensitive roots 6 (bir6)*. Each of them carries a mutation in a different nuclear gene belonging to the Pentatricopeptide Repeat (PPR) family characterized by tandem repeats of degenerate 35 amino acid motifs^{3,14-17}.

PPR proteins constitute a large family of trans-factors that are imported into organelles and act through sequence-specific association with RNA molecules, thereby controlling their stability, splicing, editing or translation. The four genes listed above code for protein targeted to mitochondria and facilitate in various ways the production of specific cI subunits encoded in the mitochondrial genome. The *mtsf2*, *mtl1* and *mtsf1* mutants were isolated from Arabidopsis T-DNA collections, while *bir6* was identified in a genetic screen for resistance to buthionine sulfoximine (BSO), which is an inhibitor of glutathione synthesis. *MTSF2* is required for the processing and stabilization of one of the *nad1* mRNA precursors assembled through trans-splicing. The *mtsf2* plants do not produce any detectable level of cI¹⁸. *MTL1* is involved in the splicing and translation of the *nad7* mRNA. In the *mtl1* mutant, the absence of the Nad7 sub-unit prevents cI assembly¹⁹. *MTSF1* controls the stability of the *nad4* mRNA and the splicing of the *nad2* intron 1 and 2. *mtsf1* plants contain reduced amount of a truncated and non-functional cI²⁰. The *BIR6* gene participates to the splicing of the *nad7* intron 1. However, *bir6* mutants accumulate trace amount of cI²¹ and are thus less affected in their growth and development than *mtsf2*, *mtl1* and *mtsf1*.

For our study, we used a regeneration system in which protoplasts prepared from whole plants proliferate into calli that eventually produce *de novo* shoot meristems. By comparing regeneration rates between the different the cI mutants listed above and the wild type, we could reveal that respiratory impairment at the level of cI induce a dramatic increase of shoot meristem production in Arabidopsis. Additionally, although the growth of whole plants and *in vitro* calli was similarly ranked across the *ppr* mutant series compared to wild type, we observed that mutants with the strongest growth penalty have the highest rate of shoot initiation on protoplast-derived calli. Our findings demonstrate a positive correlation between growth retardation resulting from mitochondrial activity impairment and *in vitro* organogenesis that may be valuable to enhance the regeneration of transformed tissues or the vegetative multiplication of plant explants.

Methods

Plant materials and growth conditions

All cI mutants derive from the *Arabidopsis thaliana* Columbia ecotype (Col-0): *bir6* (*bir6-1*, N500310)²¹; *mtsfl* (*mtsfl-1*, N654650)²⁰; *mtl1* (*mtl1-1*, N539066)¹⁹; *mtsf2* (*mtsf2-1*, N654650)¹⁸. For protoplast preparation, seeds were surface sterilized as described by Chupeau *et al.* (2013) and sown on 70 mL germination medium in green-boxes (Kalys). The boxes were incubated for 2 days at 4°C for seeds stratification, then transferred in a growth chamber (Biolux tubes; light intensity $\sim 60 \mu\text{E m}^{-2} \text{s}^{-1}$) under 10 h light / 14 h dark cycle, 70% relative air humidity (RH), at 20 °C.

Protoplast culture, callus induction and shoot regeneration

Five hundred milligrams of three-week-old (wild type, *mtsf2*, *bir6*) and four-week-old (*mtsfl*, *mtl1*) sterile plantlets were finely cut in 10 mL of maceration medium (Supplementary Table 1) in a Petri dish as described by Chupeau and coworkers²² and summarized in Supplementary Fig. 1. Cell walls were enzymatically digested overnight with cellulolytic enzymes, in the dark, at 24 °C. Protoplasts were harvested in a glass tube containing 5 mL of washing solution (2.5% KCl, 0.2% CaCl₂), through a 80- μm mesh filter to discard debris. The protoplast suspension was centrifuged at 70 g for 6 minutes three times and the pellets were resuspended in 20 mL of washing solution after each spin. Protoplast density was estimated with a Malassez slide from an aliquot of the resuspended suspension before the last centrifugation and diluted to a final concentration of 4×10^6 protoplasts/mL. The protoplast suspension was incubated 1 h at 4 °C and 200 μL aliquots were mixed with 10 mL of protoplast-culture medium (PCM, Supplementary Table 1) dispensed in plastic round Petri dishes (9 cm in diameter) at a final density of 8×10^4 /mL (Protoplast preparation; P). Cell suspensions were incubated in the dark at 20 °C and 70 % RH. Eleven days after the start of the culture, the cell suspension was diluted two-fold by adding 11 mL of callus induction medium 1 (CIM1) to each Petri dish. The cell culture was homogenized by gently rocking the dish and 10 mL of the mix was pipetted into a second Petri dish. All dishes were incubated for an additional 3 weeks in the dark, at 20 °C and

70% RH (Dilution 1; D1). The cell cultures were then diluted three-fold by adding 6.6 mL of the callus induction medium 2 (CIM2) to 3.3 mL of suspension (Dilution 2; D2). Petri dishes were incubated as above under a 10 h/14 h light/dark cycle (Biolux coolwhite tube, light intensity $\sim 50 \mu\text{E m}^{-2} \text{ s}^{-1}$). One month later, about 20 calli per Petri dish were transferred to the gelled (Agar Kalys, 3.5 g/L) regeneration medium (shoot induction medium [SIM], Supplementary Table 1) to initiate shoot formation (Transfer; T). The phytohormones added to the media were as follows: Protoplast Preparation (P), 1 mg/L 2,4-dichlorophenoxyacetic acid (2,4-D), 0.2 mg/L thidiazuron (TDZ); Dilution 1 (D1) and Dilution 2 (D2), 0.2 mg/L TDZ; Transfer (T), 0.2 mg/L meta-topolin.

Growth analysis

To quantify *in vitro* tissue growth, Petri dishes were imaged with a flatbed scanner (Epson Perfection V800 Photo scanner) immediately after callus transfer (T_0) and 2 weeks later (T_2). Cell proliferation was measured with the ImageJ software (ImageJ64) as the differential growth ($T_2 - T_0$) of calli, calculated based on their 2D projection and averaged per condition ($n = 29$ to 40). To estimate organ growth, seeds were sterilized, stratified and sown on square plates containing germination medium. Plates were incubated vertically in the growth chamber for two weeks then scanned. The length of the primary root of each seedling was measured with ImageJ as the distance from the collet to the root tip with manual tracing of each root and averaged per genotype ($n = 14$ to 84).

Total RNA isolation and RT-qPCR

Total RNA was extracted with the RNeasy Plant mini kit (QIAGEN) including the DNase step (DNaseI kit) according to the manufacturer's instructions (QIAGEN). Samples were prepared from explants at two time points: just prior transfer (T_0) and 1 week after transfer (T_1). Calli in liquid medium contained in two CIM2 Petri dishes were pooled for the T_0 stage and twenty calli corresponding to one SIM Petri dish were pooled for each mutant at the T_{+1} stage. One μg of total RNA was reverse-transcribed with Superscript II (Invitrogen). Quantitative Real Time RTq-PCR was performed in 96-well plates, including three technical replicates, on a Bio-Rad CFX Connect Real-Time system (Bio-Rad) and SYBR Green Supermix (Bio-Rad). Each

experiment included two independent biological replicates. The reference housekeeping gene was AT5G13440. mRNA levels were estimated with the delta-delta CT ($2^{-\Delta\Delta CT}$) method²³. Wild type values were arbitrarily set at 100% to express normalized relative expression. RT-qPCR primers are listed in supplementary Table 2.

Results

CI genetic dysfunction results in smaller plants but does not prevent organogenesis

As previously reported¹⁵, we noted that *ppr* cI-deficient mutants have reduced fertility and that the germination rate of mutant seeds is lower and declines faster than for wild-type ones (data not shown). In the greenhouse, mutant plants grew smaller with somewhat shorter inflorescences for *bir6* and markedly fewer branches for *mtl1*, *mtsf1* and *mtsf2* (Fig. 1a). Mutant roots grown on vertical gelled medium showed similar retarded growth (Fig. 1b) and their ranking based on two-week-old primary root length (Fig. 1d) was consistent with that of aerial growth: wild type > *bir6* > *mtsf2* > *mtl1* > *mtsf1*.

Despite their growth defect, germinated cI-deficient mutant plants produced all the organs necessary to complete a full life cycle (Fig. 1a). Thus, their reduced aerial stature and shorter root length compared to the wild type are unlikely due to specific developmental failures but are rather the consequences of slower cell growth and proliferation, resulting in fewer and smaller organs.

CI deficiency reduces cell proliferation in mutant protoplast-derived calli

To compare wild-type and cI-mutant cell growth and division outside of an organ context, we measured the proliferation of tissue cultures derived from the analysed plant lines. Briefly, three-week-old (wt, *mtsf2*, *bir6*) and four-week-old (*mtl1*, *mtsf1*) sterile plantlets were finely cut, cell walls were digested with cellulolytic enzymes in isotonic medium, and the resulting protoplasts and calli were maintained in a still layer of liquid media (CIM1 then CIM2) for approximately 60 days, with two dilutions and the addition of exogenous auxin and cytokinin phytohormones (Supplementary Fig. 1; see Methods for details). To track the growth of individual objects in a fixed position, calli of approximately 1 mm and above were transferred on a gelled medium (SIM). The increase in callus size was calculated as the difference of their 2D surface area projection from the time of transfer (T_0) up to two weeks (T_{+2}), as measured from scanned images of the culture Petri dishes (Fig. 1c, e and f).

The average callus size of all genotypes grew significantly once transferred on SIM gelled medium (Fig. 1c). As expected, the growth defect of the cI mutants was also observed *in vitro*, in several ways. The mean size of callus populations maintained in liquid CIM2 medium and sampled at the time of transfer was smaller for the mutants and ranked as follows: wild type > *bir6* > *mtsf2* \approx *mtl1* > *mtsf1* (Fig. 1e; based on the Student's *t* test). The absolute increase in callus size on gelled SIM medium was also significantly larger for wild type (n=36), compared to *bir6* (n=29; p=2.0 x 10⁻¹⁵), *mtsf2* (n=37; p=4.0 x 10⁻²¹), *mtl1* (n=39; p=3.2 x 10⁻¹⁵) and *mtsf1* (n=36; p=5.6 x 10⁻²⁰). However, we noted a negative correlation between callus size and growth (Fig. 1f). In other words, small calli grew faster than larger ones. This relationship was strong for the wild type and the least affected mutants *bir6* and *mtsf2*, lesser for *mtl1*, and negligible for the slowest grower *mtsf1*. But the differential growth after transfer between genotypes was not simply the reflection of the initial callus size at transfer because calli in the same size classes proliferated at rates reminiscent of the growth rank observed in all other conditions.

CI mutant tissues produce more shoot meristems than wild type

Next, we measured morphogenesis occurring in wild-type and cI mutant tissues treated according to a regeneration sequence adapted for protoplast-derived calli²². In this protocol, the initiation of shoot meristems follows the transfer of calli from liquid CIM2 medium to gelled SIM medium, and the simultaneous replacement of thidiazuron by meta-topolin, with the first differentiated buds clearly identified at the surface of regenerative calli within 7 to 10 days.

Four weeks after the transfer of calli on regeneration medium, significantly more buds were observed on *mtl1* and *mtsf1* tissues compared to wt and *bir6* (Fig. 2a). Among the four cI mutants, *mtl1* and *mtsf1* had the best regeneration rate with an average shoot regeneration rate of 50.1% and 53.1% respectively, followed by *mtsf2* with 24.0%, then *bir6* with 9.3%, compared to the wild-type regeneration rate of 5.6% (Fig. 2b). Thus, cI mutants initiated up to 5 times more buds than the wild type and the ones with the strongest growth defect (*mtl1* and *mtsf1*) initiated more shoots than the others (*mtsf2* and *bir6*). According to the same striking trend, the genotypes ranked as follows for the number of buds per regenerative callus: wild type < *bir6* < *mtsf2* < *mtl1* \approx *mtsf1* (Fig. 2c), which is opposite to the order based on growth

(see above). Additionally, as illustrated with complete callus series, wild-type calli grew homogeneously while cI mutant calli had markedly heterogeneous sizes, some failing to grow at all after transfer, and produced various organ-like structures (Fig. 3).

Marker gene profiles indicate that cI mutants respond differently to tissue transfer than wild type

As a first step towards the characterisation of the physiological state in the wild-type and cI mutant explants, we analysed *via* RT-qPCR the profiles of selected transcripts coding for the alternative oxidase isoform 1a (*AOX1a*) which is a component of the alternative respiratory pathway, the homeobox transcription factor SHOOT MERISTEMLESS (*STM*) involved in the initiation and maintenance of the shoot meristem²⁴, and the cyclin B1;1 (*CYCB1;1*) which is a reliable indicator of cell division. Although profiles were variable between biological replicates, the trends described here below were observed in at least two independent experiments.

RNA was extracted from pooled calli of all genotypes at two time points: just before the transfer (T_0), and one week after transfer (T_{1w}). Gene expression was measured relative to a reference housekeeping gene (Fig. 4). The *AOX1a* transcripts were detected at higher levels in the strongest cI mutants compared to wild type before the transfer, and in all mutants after the transfer. The up-regulation of *AOX1a* in cI mutant tissues indicates the activation of the alternative respiratory pathway and is associated with oxidative stress. The larger differentials between cI mutants and wild type after transfer suggests that mutant tissues are much more responsive to a combination of stresses caused, on the one hand, by the manipulation of the explants, on the other hand, by the transfer to the regeneration medium. However, the cI mutants with the strongest developmental alterations are not those associated with the highest *AOX1a* expression after transfer, possibly indicating that slow growing mutant tissues are also better able to mitigate the stress resulting from the transfer.

The expression profiles of *CYCB1;1* and *STM* follow a similar pattern suggesting that mitotic activity and organogenesis are linked. Both marker genes show much higher expression levels in cI mutants compared to the wild type before transfer, indicating that prior to transfer they are in a physiological state that is consistent with an increased regenerative capacity.

However, *CYCBI;1* transcript levels cannot be simply correlated with the observed callus speed growth since they are often higher in cI mutant tissues that grow slower. Both marker genes show much higher expression levels in cI mutants compared to the wild type before transfer, indicating that prior to transfer they are in a physiological state that is consistent with an increased regenerative capacity. High *AOX1a* expression seems thus associated with lower level of *CYCBI;1* and *STM* transcripts which can be explained by the general antagonistic relationship between stress and growth. Nevertheless, the genotypes that show the highest level of *STM* transcripts 1 week after transfer (*mtl1* and *mtsfl*) are also those characterized by the highest rates of regeneration, confirming molecularly that shoot meristem induction is enhanced in cI mutants.

To conclude, our comparative analysis of the wild-type and cI mutant tissues based on selected marker genes confirms that genetic cI dysfunction significantly improves in different ways the response of explants in terms of cell proliferation and organogenesis.

Discussion

Mitochondrial genome expression depends largely on the control of PPR RNA-binding proteins²⁵. Plants bearing mutations in nuclear genes encoding PPR proteins have different phenotypes depending on the mitochondrial mRNA that is affected and thereby the respiratory complex subunit that is missing. To better understand, at the physiological level, the developmental alterations that are in place in plant respiratory mutants, we compared the *in vitro* growth and regeneration of four Arabidopsis cI mutants showing different growth retardation: *bir6*, *mtsf2*, *mtl1* and *mtsf1*. The underneath *ppr* mutations have distinct effects on cI production and activity, as they affect different CI subunits. The *bir6* mutant has a reduced amount of a functional cI²¹ and *mtsf1* mutant has a low amount of truncated cI²⁰. *mtsf2* and *mtl1* mutants lack detectable levels of fully-assembled cI^{18,19}.

The absence of functional cI is responsible for the growth decrease in cI mutants (Fig. 1). The lack of mitochondrial cI leads to a reduction of proteins involved in the photosynthesis, the Calvin cycle and photorespiration, contributing to the significant delay in growth and development of some cI mutants²⁶. Surprisingly, *ppr* mutants lacking cI (*mtsf2* and *mtl1*) or with non-functional cI (*mtsf1*) have the highest shoot regeneration rate (Fig. 2).

The link between cI defect and shoot regeneration or shoot apical meristem development was not described before our study. However, some recent publications reported a reduced root-meristem activity in *ppr* mutants affected in cI. Hsieh *et al.*¹⁷ analyzed the root meristem of *slow growth3 (slo3)*, a cI mutant affected in the splicing of *nad7* resulting in a dramatic reduction in cI activity. The *slo3* mutant plants are characterized by severe growth retardation and delayed development. These authors found that the size of *slo3* root apical meristem (RAM) is reduced and the number of root meristem cells is decreased. To explain this phenomenon, they suggested that defective mitochondria may interact with auxin signaling pathways to control the boundary of RAM. The hormonal disorder in cI mutants resulting in reduction of meristem activity was also described in another *ppr* mutant, aba overly sensitive mutant, *abo8-1*, which is affected in the splicing of *NAD4* intron 3. *abo8-1* has a reduced root meristem activity and a reduced auxin accumulation/signaling. The mutation also leads to higher level of reactive oxygen species (ROS) in root tips. In Arabidopsis *abo8-1* mutant, ABA-induced ROS production in the mitochondria of root tips plays a key role in root meristem activity by controlling auxin accumulation/signaling

and *PLETHORA* (*PLT1* and *PLT2*) expression. In general, *PLT* gene expression is related to developing tissues in roots and shoots, and controls growth of organ primordia^{27,28}. In contrast to RAM inhibition, our results therefore show that mitochondrial respiratory alteration enhances the production of shoot meristems.

Mitochondria produce retrograde signals directed to the nucleus that modulate nuclear gene expression, in turn modulating the organelle and cellular activity to external stimuli. While mitochondrial perturbations are known to affect nuclear gene expression, mitochondrial retrograde signaling (MRS) has only been partially characterised^{1,29}. Over the last decade, several studies described the implication of ROS in MRS induced by chemical treatments or in mitochondrial mutants^{30,12,31}. In animals and plants, ROS play an important role in mitochondrial retrograde signaling, yet the mode of action of ROS signal(s) in gene expression activation is still not fully understood³². Superoxide ($O_2^{\cdot-}$) and hydrogen peroxide (H_2O_2) have been described as ROS candidate oxidative signals in plant mitochondria with a role in mitochondrial regulation³³. The respiratory cI is a major site of superoxide production in normal mETC activity and this production is enhanced by respiratory chain dysfunction^{4,33}.

Recent studies have demonstrated the role of alternative oxidase (AOX) in preventing the over-reduction of mETC that leads to single electron leak causing superoxide formation³⁴. AOX is part of the alternative respiratory pathway that is induced when the mETC is impaired to help the Cytochrome C oxidase (cIV) to reduce O_2 into H_2O removing by this way the excess of reducing power and lowering the eventual cellular redox poise³⁴⁻³⁶. AOX induction is widely used as a model for MRS³⁷. In our experimental system, the expression of the retrograde marker gene *AOX1a*³³ is expressed at higher levels in the cI mutants that also have a higher regeneration rate than wild type (Fig. 4), suggesting the implication of the mitochondrial retrograde signal in the observed shoot regeneration boost.

Ng *et al.*³² identified a transcription factor acting as a positive regulator of *AOX1a* (RAO2), which is also known as the Arabidopsis NAC domain-containing protein17 (ANAC017). This factor migrates from the endoplasmic reticulum to the nucleus where it activates *AOX1a* as a consequence of mitochondrial dysfunction. RAO2/ANAC017 is also implicated in primary response to cytosolic H_2O_2 under stress treatments. These results demonstrate that ANAC017 is a key regulator of ROS responses related with mitochondrial retrograde signals. ANAC017-dependent retrograde signaling has recently been shown to

improve plant performance under impaired mitochondrial activity (Van Aken et al, 2016). It would be interesting to see if key genes for shoot meristem induction counts among the targets of ANAC017. We could observe that *STM* shows very high expression levels in cI mutants, and could therefore represent one of such targets.

Ivanova *et al.*³⁵ used regulators of *AOX1a* (ROA) to study the links between mitochondrial signaling and auxin signaling. The MRS induced by a chemical inhibition of mETC caused a transient suppression of auxin signaling and, on the other hand, auxin treatment repressed *AOX1a* induction, thereby highlighting the inter-regulation between mitochondrial retrograde signaling and auxin signaling. The growth retardation of cI mutants (Fig. 1 and 2) may be explained by the negative effect of MRS on auxin-induced growth. This hypothesis is supported by the studies showing that mitochondrial defects reduce auxin responses. Since auxin stimulates growth in non-stress conditions, mitochondria defects causing an oxidative stress transduced by the MRS may cause a growth reduction due to a potential oxidative-degradation of auxin and resulting in a negative regulation of growth to ensure plant survival during stress conditions^{33,38}.

Shoot regeneration is a complex phenomenon involving an intricate auxin-cytokinin crosstalk. Unlike auxin, the interaction between cytokinin (CK) and MRS is much less investigated. CK and auxin behave antagonistically to control several aspects of plant growth and development. How MRS and auxin-cytokinin interactions are coordinated is not yet clear. TCP (TEOSINTE BRANCHED 1, CYCLOIDEA AND PCF FAMILY) transcription factors represent an interesting connection between these two processes. TCP transcription factors regulate nuclear genes encoding mitochondrial proteins by binding site II elements in their promoter. Two TCPs (TCP14 and TCP15) have been described as inducers of CK-mediated cell proliferation and transcriptional responses, including CK-mediated induction of *CYCB1;1* and may represent a crosstalk point between CK, auxin and MRS³⁸.

In plants lacking a functional cI, cells must reorganize their metabolic processes not only in mitochondria but also in plastids, peroxisomes, and other cellular compartments, all changes that may impact growth and development²⁶.

In conclusion, our findings reveal a positive correlation between cI dysfunction and organogenesis. We thus show that the impairment of respiratory activity, at least at the level of cI, triggers beneficial physiological conditions for shoot meristem induction that are either

memorized or maintained to sufficient levels in the long run on shoot regeneration medium to significantly increase shoot production in plants.

Figures

Figure 1 | Growth defects of *ppr* cI-deficient mutants. **a**, Aerial growth defect. Plants were germinated and grown in the greenhouse. **b**, Root growth defect. Plants were germinated and grown for 14 days on vertical gelled medium. **c**, Primary root length. For each genotype, growth is measured as the average length of the manually traced primary roots, from collet to tip, of two-week plantlets illustrated in (b). All genotypes are statistically different from each other (Student's *t* test; $p < 0.001$; $n_{wt} = 79$, $n_{bir6} = 14$, $n_{mtsf2} = 14$, $n_{mll1} = 25$). **d**, Average callus growth. The projected area of each callus was measured with ImageJ just after transfer on gelled medium (T_0) and two weeks after transfer (T_{+2}). **e**, Relationship between individual callus size and growth. Relative growth (y axis) is expressed as the increase in callus area projection ($T_{+2} - T_0$) relative to the callus area at transfer (T_0). The few calli that died out of 40 transferred for each genotype are represented as open dots at the bottom of the graph with the same color code and were not taken into consideration for growth calculation. **f**, Illustration of callus growth. Bars in graphs represent standard errors. Bar: 5 mm (panel a and f).

Figure 2 | Shoot regeneration efficiency in cI mutants. **a**, Representative plates illustrating the *in vitro* response of calli four weeks after transfer on regeneration medium. White arrows indicate regenerating calli. Bar: 5 mm. **b**, Shoot regeneration rates of wt and cI mutants. Bars represent average rate (mean \pm SE; at least two biological repeats for each genotype, $n=9-175$ calli/genotype/biological repetition). Asterisks mark mutant significantly different from wt (Student's *t* test; $p < 0.05$). **c**, Pie chart representation of regenerative classes according to the number of buds per callus.

Figure 3 | Callus *in vitro* response. Explants were imaged individually 8 weeks after transfer on gelled regeneration medium. Wild type (Col-0), top; *mtsf1*, bottom. Bar: 1 mm.

Figure 4 | Gene expression profiles in wild-type and cI mutant calli. Relative expression in the indicated genotypes was measured for genes encoding an isoform of the AOX alternative oxidase (*AOX1a*), a cyclin B1 (*CYCB1;1*), and the homeobox protein STM. For transcript level quantification, RNA was prepared from calli pooled from two Petri dishes for the time just prior

transfer (T_0) and one Petri dish for the time point 1 week after transfer (T_{+1w}). Transcript levels were calculated as a ratio of transcript abundance for the studied gene to that of the At5g13440 reference gene, and expressed relative to the wild-type ratio arbitrarily set at 100. Similar results were obtained in another independent experiment. The data from one experiment are shown here.

References

1. Welchen, E., García, L., Mansilla, N. & Gonzalez, D. H. Coordination of plant mitochondrial biogenesis: keeping pace with cellular requirements. *Front. Plant Sci.* **4**, 551 (2014).
2. Rao, R. S. P. *et al.* The proteome of higher plant mitochondria. *Mitochondrion* **33**, 22–37 (2017).
3. Braun, H.-P. *et al.* The life of plant mitochondrial complex I. *Mitochondrion* **19**, 295–313 (2014).
4. Møller, I. M. PLANT MITOCHONDRIA AND OXIDATIVE STRESS : Electron Transport, NADPH Turnover, and Metabolism of Reactive Oxygen Species. *Annu. Rev. Plant Physiol. Plant Mol. Biol.* **52**, 561–591 (2001).
5. Brandt, U. Energy Converting NADH: Quinone Oxidoreductase (Complex I). *Annu. Rev. Biochem.* **75**, 69–92 (2006).
6. Dröse, S. & Brandt, U. Molecular Mechanisms of Superoxide Production by the Mitochondrial Respiratory Chain In Mitochondrial Oxidative Phosphorylation. **748**, 145–169 (2012).
7. Hirst, J. Mitochondrial Complex I. *Annu. Rev. Biochem.* **82**, 551–575 (2013).
8. Pétriacq, P. *et al.* Photoperiod Affects the Phenotype of Mitochondrial Complex I Mutants. *Plant Physiol.* **173**, 434–455 (2017).
9. Kühn, K. *et al.* Complete Mitochondrial Complex I Deficiency Induces an Up-Regulation of Respiratory Fluxes That Is Abolished by Traces of Functional Complex I. *Plant Physiol.* **168**, 1537–1549 (2015).
10. Dahan, J. *et al.* Disruption of the *CYTOCHROME C OXIDASE DEFICIENT 1* gene leads to cytochrome c oxidase depletion and reorchestrated respiratory metabolism in *Arabidopsis thaliana*. *Plant physiology* (2014). doi:10.1104/pp.114.248526
11. Garmier, M. *et al.* Complex I Dysfunction Redirects Cellular and Mitochondrial Metabolism in Arabidopsis. *Plant Physiol.* **148**, 1324–1341 (2008).
12. Meyer, E. H. *et al.* Remodeled Respiration in *ndufs4* with Low Phosphorylation Efficiency Suppresses Arabidopsis Germination and Growth and Alters Control of Metabolism at Night. *Plant Physiol.* **151**, 603–619 (2009).
13. Juszczuk, I. M., Szal, B. & Rychter, A. M. Oxidation-reduction and reactive oxygen species homeostasis in mutant plants with respiratory chain complex I dysfunction. *Plant, Cell Environ.* **35**, 296–307 (2012).
14. O’Toole, N. *et al.* On the expansion of the pentatricopeptide repeat gene family in plants. *Mol. Biol. Evol.* **25**, 1120–1128 (2008).
15. Barkan, A. & Small, I. Pentatricopeptide Repeat Proteins in Plants. *Annu. Rev. Plant Biol.* **65**, 415–442 (2014).
16. Sazanov, L. A. A giant molecular proton pump: structure and mechanism of respiratory complex I. *Nat. Rev. Mol. Cell Biol.* **16**, 375–388 (2015).
17. Hsieh, W.-Y., Liao, J.-C. & Hsieh, M.-H. Dysfunctional mitochondria regulate the size of

- root apical meristem and leaf development in Arabidopsis. *Plant Signal. Behav.* **10**, e1071002 (2015).
18. Wang, C. *et al.* The pentatricopeptide repeat protein MTSF2 stabilizes a nad1 precursor transcript and defines the 3' end of its 5'-half intron. *Nucleic Acids Res.* **45**, 6119–6134 (2017).
 19. Haïli, N. *et al.* The MTL1 Pentatricopeptide Repeat Protein Is Required for Both Translation and Splicing of the Mitochondrial NADH DEHYDROGENASE SUBUNIT7 mRNA in Arabidopsis. *Plant Physiol.* **170**, 354–366 (2016).
 20. Haïli, N. *et al.* The pentatricopeptide repeat MTSF1 protein stabilizes the nad4 mRNA in Arabidopsis mitochondria. *Nucleic Acids Res.* **41**, 6650–6663 (2013).
 21. Koprivova, A. *et al.* Identification of a pentatricopeptide repeat protein implicated in splicing of intron 1 of mitochondrial nad7 transcripts. *J. Biol. Chem.* **285**, 32192–32199 (2010).
 22. Chupeau, M.-C. *et al.* Characterization of the Early Events Leading to Totipotency in an Arabidopsis Protoplast Liquid Culture by Temporal Transcript Profiling. *Plant Cell* **25**, 2444–2463 (2013).
 23. Winer, J., Jung, C. K. S., Shackel, I. & Williams, P. M. Development and Validation of Real-Time Quantitative Reverse Transcriptase–Polymerase Chain Reaction for Monitoring Gene Expression in Cardiac Myocytes in Vitro. *Anal. Biochem.* **270**, 41–49 (1999).
 24. Motte, H., Verecke, D., Geelen, D. & Werbrouck, S. The molecular path to in vitro shoot regeneration. *Biotechnol. Adv.* **32**, 107–21 (2014).
 25. Manna, S. An overview of pentatricopeptide repeat proteins and their applications. *Biochimie* **113**, 93–99 (2015).
 26. Fromm, S., Senkler, J., Eubel, H., Peterhansel, C. & Braun, H. P. Life without complex I: Proteome analyses of an Arabidopsis mutant lacking the mitochondrial NADH dehydrogenase complex. *J. Exp. Bot.* **67**, 3079–3093 (2016).
 27. Santuari, L. *et al.* The PLETHORA gene regulatory network guides growth and cell differentiation in Arabidopsis roots. *Plant Cell* **28**, tpc.00656.2016 (2016).
 28. Yang, L. *et al.* ABA-Mediated ROS in Mitochondria Regulate Root Meristem Activity by Controlling PLETHORA Expression in Arabidopsis. *PLoS Genet.* **10**, (2014).
 29. Sechet, J. *et al.* The ABA-deficiency suppressor locus HAS2 encodes the PPR protein LOI1/MEF11 involved in mitochondrial RNA editing. *Mol. Plant* **8**, 644–656 (2015).
 30. Van Aken, O. *et al.* Mitochondrial type-I prohibitins of Arabidopsis thaliana are required for supporting proficient meristem development. *Plant J.* **52**, 850–864 (2007).
 31. Van Aken, O. & Whelan, J. Comparison of transcriptional changes to chloroplast and mitochondrial perturbations reveals common and specific responses in Arabidopsis. *Front. Plant Sci.* **3**, 281 (2012).
 32. Ng, S. *et al.* A membrane-bound NAC transcription factor, ANAC017, mediates mitochondrial retrograde signaling in Arabidopsis. *Plant Cell* **25**, 3450–3471 (2013).
 33. Huang, S., Van Aken, O., Schwarzländer, M., Belt, K. & Millar, A. H. The Roles of Mitochondrial Reactive Oxygen Species in Cellular Signaling and Stress Response in

- Plants. *Plant Physiol.* **171**, 1551–1559 (2016).
34. Vanlerberghe, G. C. Alternative oxidase: A mitochondrial respiratory pathway to maintain metabolic and signaling homeostasis during abiotic and biotic stress in plants. *Int. J. Mol. Sci.* **14**, 6805–6847 (2013).
 35. Ivanova, A. *et al.* A Functional Antagonistic Relationship between Auxin and Mitochondrial Retrograde Signaling Regulates Alternative Oxidase1a Expression in Arabidopsis. *Plant Physiol.* **165**, 1233–1254 (2014).
 36. Rasmusson, A. G., Soole, K. L. & Elthon, T. E. Alternative Nad(P)H Dehydrogenases of Plant Mitochondria. *Annu. Rev. Plant Biol.* **55**, 23–39 (2004).
 37. Millar, A. H., Whelan, J., Soole, K. L. & Day, D. A. Organization and Regulation of Mitochondrial Respiration in Plants. *Annu. Rev. Plant Biol.* **62**, 79–104 (2011).
 38. Berkowitz, O., De Clercq, I., Van Breusegem, F. & Whelan, J. Interaction between hormonal and mitochondrial signalling during growth, development and in plant defence responses. *Plant, Cell Environ.* **39**, 1127–1139 (2016).

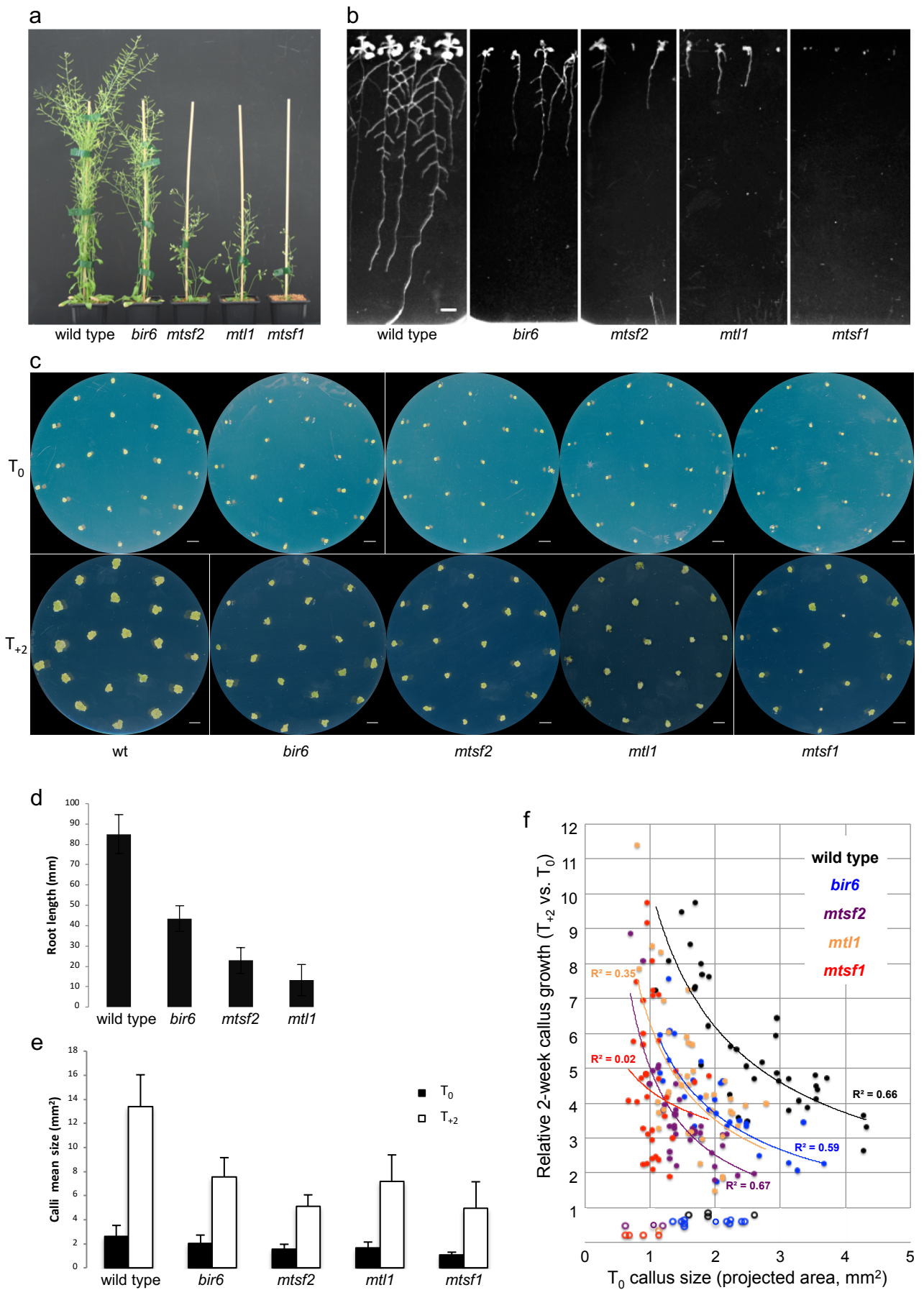


Figure 1

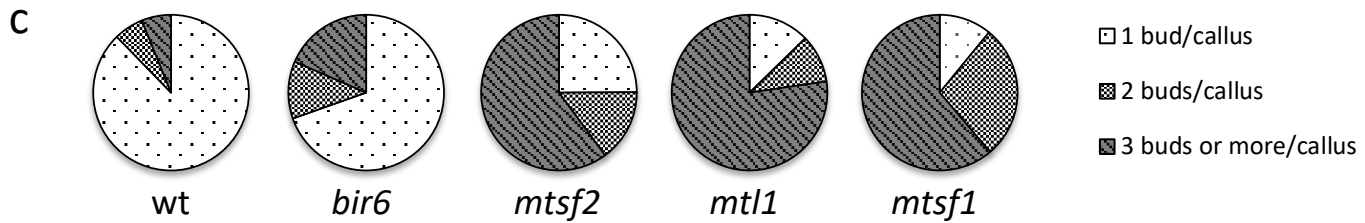
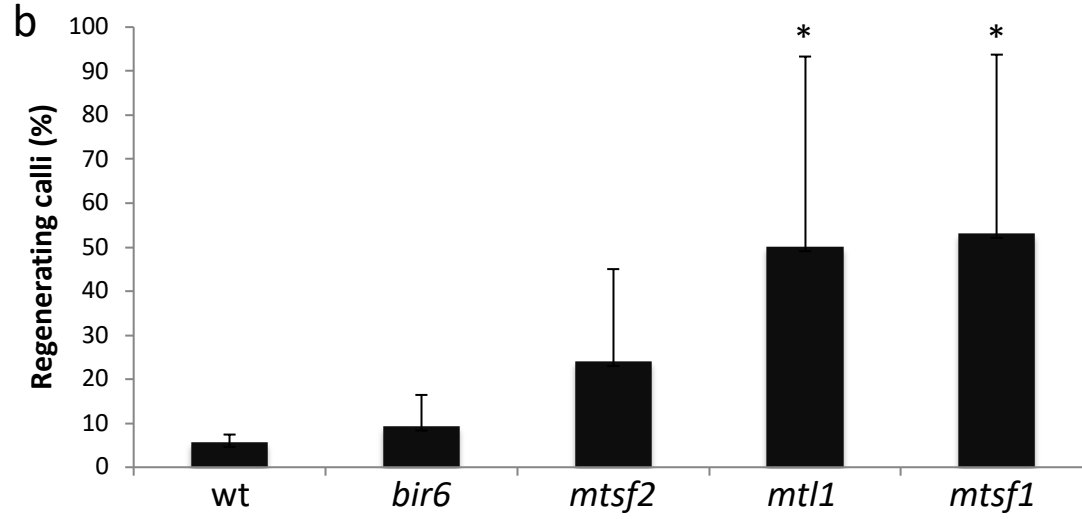
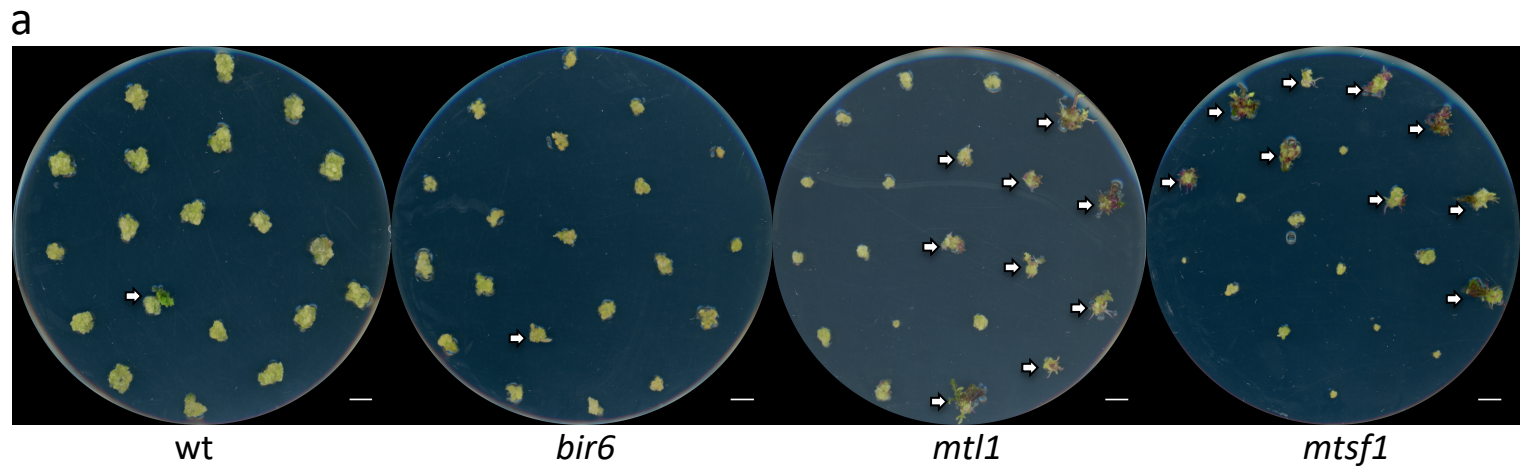


Figure 2

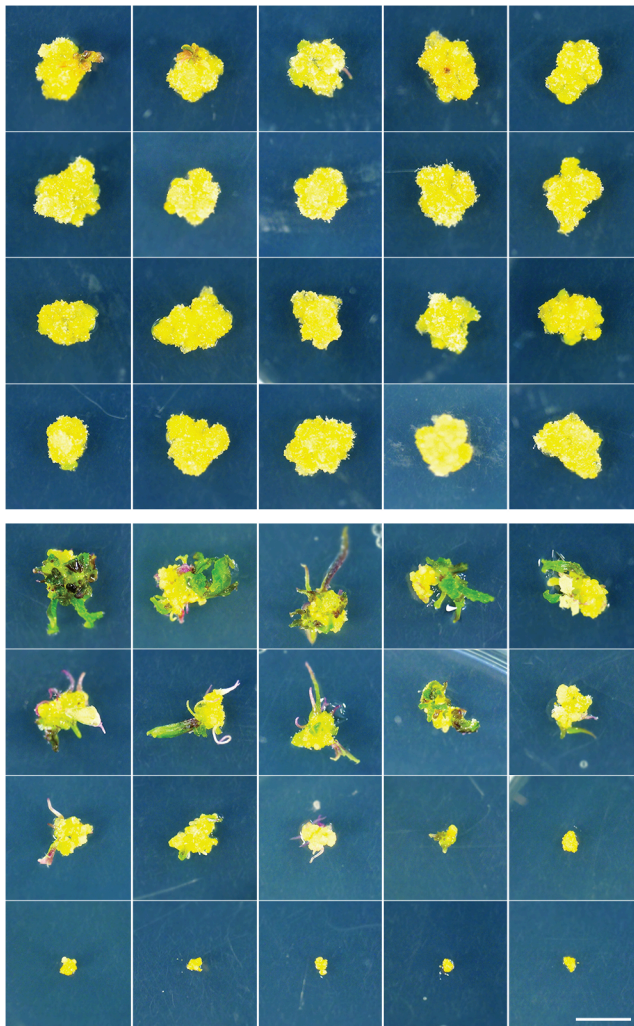


Figure 3

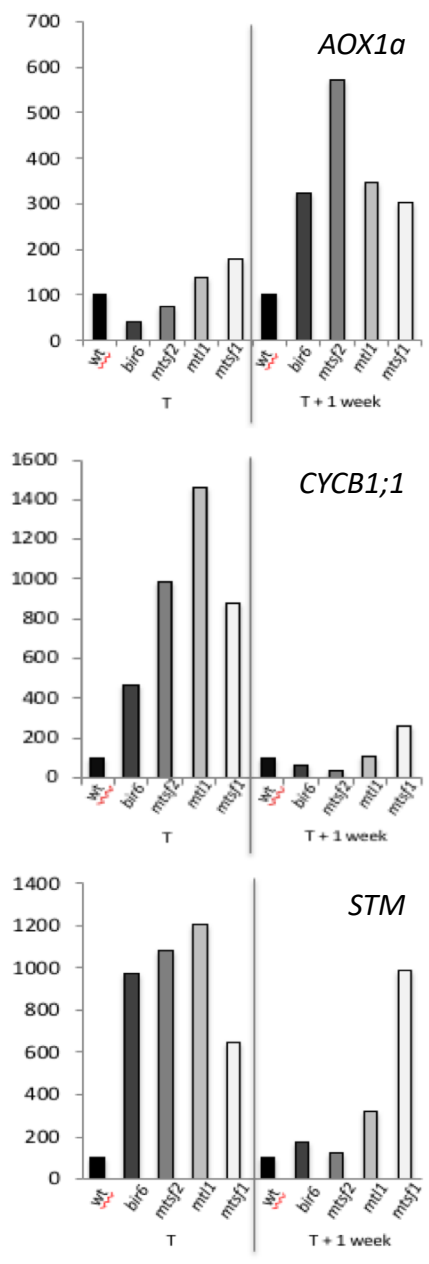
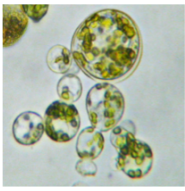
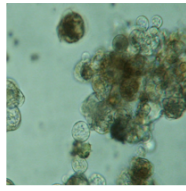


Figure 4



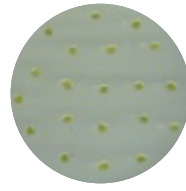
protoplasts



micro-colonies



micro-calli



shoot induction



regenerating calli

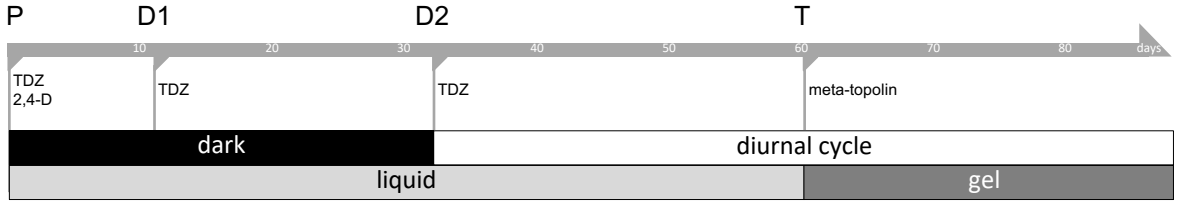


Table S1

	Germination medium	Maceration medium	Protoplast culture medium	Callus induction medium 1	Callus induction medium 2	Shoot induction medium
Macro-salts						
KNO ₃	950	250	505	505	1010	1010
NH ₄ NO ₃	825		160	400	800	0
CaCl ₂ , 2H ₂ O	220	15	440	440	440	220
MgSO ₄ , 7H ₂ O	185	25	370	370	185	185
KH ₂ PO ₄	85		170	170	170	85
(NH ₄) ₂ SO ₄		13.4				
NaH ₂ PO ₄		15				
Micro-elements						
Fe Citrate NH ₄	50		30	30	30	50
KI	0.4	0.75	0.01	0.01	0.01	0.8
H ₃ BO ₃	1.5	3	1	1	1	3
MnCl ₂ , 4H ₂ O	15					30
MnSO ₄ , 4H ₂ O		10	0.1	0.1	0.1	
ZnSO ₄ , 7H ₂ O	6	2	1	1	1	12
Na ₂ MoO ₄ , 2H ₂ O	0.45	0.25				0.9
CuSO ₄ , 5H ₂ O	0.045	0.025	0.03	0.03	0.03	0.09
CoCl ₂ , 6H ₂ O	0.045	0.025				0.09
AlCl ₃			0.03	0.03	0.03	
NiCl ₂ , 6H ₂ O			0.03	0.03	0.03	
Vitamines						
Inositol	100	100	100	100	100	100
Panhotenate Ca	1	1	1	1	1	1
Biotin	0.01	0.01	0.01	0.01	0.01	0.01
Niacin	1	1	1	1	1	1
Pyridoxin	1	1	1	1	1	1
Thiamin	1	1	1	1	1	1
Folic Acid			0.2			
Other components						
Glucose		45000	40000	0		
Sucrose	10000		0	30000	20000	20000
Mannitol			60000	70000	60000	40000
Glycine		25000				
2,4-D			1	0	0	0
Thidiazuron (TDZ)			0.2	0.2	0.2	
Meta-topolin						0.2
MES	700	700	700	700	700	700
Bromocresol purple (BCP)	8	8	8	8	8	8
Agar Kalys	7000					7000
Onozuka R10		1000				
Macerozyme		300				
Driselase		400				
pH	5.7	5.7	5.7	5.7	5.7	5.7

Table S2

Gene name	Forward primer	Reverse primer
AT5G13440	ACAAGCCAATTTTGGCTGAGC	ACAACAGTCCGAGTGTCATGGT
AOX1A	GTTTCGTCTCACGAGGCTTAT	GGTGGATTCGTTCTCTGTTTC
NDB2	TCCTTCTCTACCAGGATTCTC	AGTTCAACAACAGCACCACCATT
STM	CCAAGATCATGGCTCATCCT	CCTGTTGGTCCCATAGATGC
CYCB2	GGATACGAGGATTGGAGCAA	TTGTGATGCAAACCAACCAT

Chapter 3:

**The chemical inhibition of the
mitochondrial electron transport chain
enhances *de novo* shoot regeneration in
Arabidopsis protoplast-derived calli and
results in cytosolic oxidative stress**

Introduction

Plant *in vitro* regeneration is largely used in industry for the production of plantlets through micro-propagation and in fundamental research to study organogenesis. Still, this process is not well characterized at the molecular level (Ikeuchi et al., 2016; Zhang et al., 2017). Since the discovery, by Skoog and his collaborators (Skoog and Miller, 1957), that different hormonal balances steer plant explants in varying developmental paths, a large body of literature has emerged describing tissue culture protocols to induce *in vitro* shoot regeneration.

In the last decades, multiple inhibitors have been shown to boost morphogenesis when added to regeneration media, including for example molecules affecting ethylene production (Mohiuddin et al., 1997; Lei et al., 2014), auxin transport and signaling (Singhi and Syamal, 2000; Lall et al., 2005; Hu et al., 2017) and cytokinin catabolism (Motte et al., 2013). However, the precise mechanisms by which they enhance organogenesis often remain unclear. With converging evidence implying redox regulations in several developmental processes (Del Río, 2015; del Pozo, 2016; Foyer et al., 2017; Mittler, 2017; Noctor et al., 2017; Waszczak et al., 2018), independent groups resumed experiments initiated decades ago to test whether the addition of compounds with pro- or anti-oxidant power in plant culture media affects shoot organogenesis or somatic embryogenesis (Earnshaw and Johnson, 1987; Joy IV et al., 1988; Benson, 2000; Gupta and Datta, 2003; Tian et al., 2003; Gupta, 2011).

So far, no general conclusion has been drawn from the literature as the reported effect of redox modulating compounds on *in vitro* regeneration depends on its oxidative properties in combination with the species and the explants on which it is applied. On the same species, the treatment with oxidant and anti-oxidant compounds may have an opposite effect on morphogenesis depending whether it is induced through somatic embryogenesis or shoot organogenesis. For example, in gladiolus leaf explants, the addition of exogenous hydrogen peroxide (H_2O_2) in the medium increased the somatic embryogenesis rate but decreased the shoot regeneration rate. Reversely, the treatment of the same explants with anti-oxidants as glutathione (GSH) decreased somatic embryogenesis and increased the caulogenesis rate (Gupta and Datta, 2003). However, the addition of H_2O_2 has a positive effect on shoot regeneration in others species, for example when applied on strawberry calli to induce bud formation (Tian et al., 2003).

De novo shoot regeneration can be induced in many different types of explants. As explained in Chapter 2, we chose to study the induction of shoot meristems in *in vitro*

cultured calli derived from protoplasts. As in other systems, calli are formed after tissue dedifferentiation in media (CIM1 and CIM2) characterized by a high auxin/cytokinin ratio to induce callogenesis (callus formation). The calli are then transferred to a regeneration medium containing a low auxin to cytokinin ratio (or just cytokinin) to promote caulogenesis (SIM).

We previously described four *Arabidopsis* mutants in which the activity of the complex I (cI) in the mitochondrial electron transport chain (mETC) was affected and that have a reduced growth compared to the wild type. Through the analysis of the mutant *in vitro* caulogenesis, we found a positive correlation between growth retardation and shoot regeneration rate. In the present work, we phenocopied cI dysfunction with the chemical inhibition of the mETC by rotenone and showed that, as in cI mutants, it resulted in growth retardation and enhanced *in vitro* response. With selected marker genes, we confirmed that rotenone treatments further decreased the cell proliferation and amplified the oxidative stress occurring as the calli are transferred from the liquid callogenesis medium onto the gelled regeneration medium. Finally, we showed with a redox biosensor that rotenone cI inhibition, presumably causing ROS production in the mitochondria, resulted in an increasingly oxidative cytosolic state. These results suggest that chemical inhibition of the mitochondrial cI may promote shoot regeneration through retrograde oxidative signaling.

Materials and methods

Plant material

Seeds were surface sterilized as described by Chupeau *et al.* (2013) and sown on 70 mL gelled germination medium in green-boxes (Kalys). The boxes were kept 2 days at 4°C for stratification then transferred in a growth chamber (Biolux neon tubes with light intensity around 60 $\mu\text{Es m}^{-2} \text{s}^{-1}$) under a 10 h light / 14 h dark cycle, 70% relative air humidity (RH), at 20 °C.

Protoplast isolation, callus induction and shoot regeneration

Protoplasting, callus culture and shoot regeneration were conducted as described in Chapter II. Briefly, protoplasts were obtained after an enzymatic digestion of three-week-old plantlets then maintained in liquid culture with auxin (2,4-D; 1 mg/l) and cytokinin (TDZ; 0.2 mg/l) (CIM1) during approximately two months to induce callus formation. During the liquid culture, the medium was diluted twice with fresh medium containing exogenous cytokinin (TDZ; 0.2 mg/l) (CIM2): 11 days after protoplasts isolation and 4 weeks later on. Twenty calli of approximately 2 mm in diameter were transferred from liquid to gelled regeneration-medium containing the cytokinin meta-topolin (0.2 mg/l) to induce caulogenesis (SIM) (see Chapter 2 for additional details). Shoot regeneration rate was estimated 4 weeks after the transfer by counting the number of regenerating calli and the number of buds per callus.

Rotenone treatment

The cI inhibitor rotenone (Sigma-Aldrich) was freshly prepared before each experiment in dimethyl sulfoxide (DMSO) at 10 mM. Diluted rotenone solutions were then added to the medium at the indicated final concentration (1.25, 2.5, 5 or 10 μM) according to three distinct application schemes explained below and illustrated in Figure 2A. When applied in liquid medium (one week before the transfer), rotenone was added directly in the callus culture. In the regeneration medium, rotenone was added before the solidification of the medium and calli were transferred on the gelled regeneration medium shortly thereafter. In all cases, the final concentration of DMSO was identical (0.5 %).

Cell growth quantification

To measure the effect of rotenone on calli growth, Petri dishes were imaged with a flatbed scanner (Epson Perfection V800 Photo scanner) immediately after the transfer on regeneration medium and two weeks later. The size of each callus was quantified based on the 2D projected area with the ImageJ64 software.

Total RNA isolation and qRT-PCR

The total RNA was extracted with RNeasy Plant mini kits including a DNase step (QIAGEN) according to the manufacturer's instructions. Rotenone was added one week before the transfer to rotenone free-regeneration medium (Ap 1) and total RNA was extracted from pooled calli picked from two Petri dishes at the indicated time points. For each sample, 1 µg of total RNA was reverse-transcribed with Superscript II (Invitrogen). Quantitative Real Time PCR (qRT-PCR) was performed in 96-well plates including three technical replicates, on a Bio-Rad CFX Connect Real-Time system (Bio-Rad) and with SYBR Green Supermix (Bio-Rad). The experiment was repeated in two independent biological replicates. The reference house-keeping gene was AT5G13440 and the quantification of mRNA levels was based on the delta-delta CT ($2^{-\Delta\Delta CT}$) method (Winer et al., 1999). Relative expression levels were normalized against the wild-type reference values arbitrarily set at 100%. Primers for qRT-PCR are listed in Supplemental Table 1.

Redox state measurement

To monitor real-time *in vivo* redox changes, protoplast-derived calli were obtained from *Arabidopsis thaliana* plantlets expressing the cytosolic Grx1-roGFP2 fusion protein. This biosensor-protein is targeted to the cytosol and dynamically reports the glutathione redox potential (Gutscher et al., 2008; Schwarzländer et al., 2008). The Grx1-roGFP2 line (Col-0) was provided by Marcus Schwarzländer. Redox measurements were performed on protoplasts (just after protoplasting of three-week-old Grx1-roGFP2 transgenic plantlets) for technical validation and on protoplasts-derived calli one week before transfer to the regeneration medium (according to Ap 1). For protoplasts redox measurement, several images were taken before and after the addition of H₂O₂ directly in the microscopic chamber. For redox state measurements after rotenone treatment of calli, the explants were positioned in a home-made

container (Supplemental Figure 2) maintaining their position as oxidizing or reducing agents were injected in the culture medium. Images were collected with a laser confocal microscope (Leica SP5). Grx1-roGFP2 was excited at 405 nm and 488 nm and emitted fluorescence was collected with a band-pass filter of 501 to 534 nm. Autofluorescence was measured following excitation at 488 nm with a band-pass filter of 614 to 781 nm. The ratiometric calculations were performed as described in (Gutscher et al., 2008) with the Fiji software.

Results

Inhibitory effect of rotenone on *Arabidopsis* callus growth

Arabidopsis mutants affected in the mETC cI have a retarded growth compared to the wild type (see Chapter 2). To study the impact of a mitochondrial perturbation on *in vitro* plant development, we phenocopied the genetic cI defect with a specific cI inhibitor called rotenone. First, we investigate the effect of rotenone on calli growth. Calli with a projected 2D area of approximately 2 mm² were transferred individually from liquid culture to gelled shoot induction medium (SIM) containing rotenone at a final concentration of 1.25, 2.5, 5, or 10 μM, in addition to a mock control (0 μM). Callus initial size and growth after two weeks of culture were estimated through the analysis of scanned Petri dish images. As shown in Figure 1, rotenone gradually reduced growth at concentrations up to 10 μM. At 10 μM, the cI inhibitor strongly reduced growth and callus mean size was not significantly different between the beginning and the end of the growth period (Figure 1 A). The difference in size between calli treated with 10 μM of rotenone and mock-treated calli was visible with the naked eye (Figure 1 B). Calli transferred on regeneration medium containing rotenone concentrations higher than 10 μM stopped growing altogether and died (data not shown).

Rotenone promotes organogenesis when applied at specific stages

To test the effect of chemical cI inhibition on shoot initiation, rotenone was applied, at concentration partially inhibiting growth, according to three application (Ap) schemes: Ap 1, addition of rotenone in the liquid medium, one week before the transfer to the regeneration medium; Ap 2, addition of rotenone in the liquid medium one week before transfer and, at the same concentration, in the gelled regeneration medium to maintain the mETC inhibition throughout shoot induction; Ap 3, addition of rotenone only in the regeneration medium (see schematic representation in Figure 2 A).

Shoot formation was quantified four weeks after the callus transfer on the regeneration medium (Figure 2). A fraction of regenerating calli was observed in all mock samples and in samples treated at the lowest rotenone concentrations tested. When calli were exposed to rotenone for prolonged treatments (Ap 2 and Ap 3) at medium or high rotenone concentration, they produced fewer or no buds compared to mock samples. However, organogenesis was markedly enhanced by rotenone in calli treated for only one week, before transfer on

rotenone-free regeneration medium (Ap 1). This rotenone positive effect was measured as the percentage of regenerating calli (Figure 2 B) and also as the number of buds per regenerating callus (Figure 2 C). In two biological replicates, the rotenone concentration that yielded the highest enhancement (Ap 1) was either 5 μ M or 10 μ M, although these two conditions also correspond to the most variable response (Supplemental Figure 1). Thus, calli exposed to non-lethal doses of a cI inhibitor produce more shoot meristems than controls, thereby confirming the link between mETC dysfunction and organ initiation.

Rotenone inhibits cell proliferation and induces an oxidative stress in cultured calli

To characterize the molecular response of calli subjected to rotenone in the scheme resulting in the best organogenesis enhancement (Ap 1), we compared the expression of marker genes in treated and untreated explants. The tested rotenone concentrations were 5 and 10 μ M, yielding the highest observed regeneration rates (Figure 3). Calli were sampled at successive time points: just prior treatment (one week before transfer on regeneration medium) (0D); 12 h (0.5D) and 48 h (2D) after rotenone addition in the liquid medium to analyze early and late rotenone response, respectively; 7 days after addition, just prior transfer to regeneration medium (7D); 12 h later to analyze early response to transfer (7.5D); and two weeks after transfer when shoots are well developed on regenerating calli (21D).

First, we tracked the steady state levels of the *cyclin BI;1* encoding transcript which provides a reliable transcriptional readout of cell proliferation (Ferreira et al., 1994) (Figure 3 A). Shortly after rotenone addition, *CYCBI;1* mRNA levels decline compared to the mock control but are still easily detectable, indicating that the cI inhibitor at 5 or 10 μ M reduces but does not stop mitotic activity (0.5D and 2D), in agreement with our quantification of callus growth (Figure 1). After 5 more days, *CYCBI;1* mRNA transcripts rise in treated samples to reach levels comparable to that of mock controls (Figure 3 A, 7D). This recovery may be explained by the habituation of the tissues to the inhibitor or by the relative instability of rotenone in aqueous solutions exposed to light. In contrast, the collapse of *CYCBI;1* transcripts 12 h after the transfer of the calli from liquid medium to gelled regeneration medium (7.5D) implies that all explants arrest growth, rapidly and temporarily, whether previously exposed to rotenone or not.

Next, we investigated the expression pattern of two genes associated with mitochondrial dysfunction and oxidative stress. AOX1a is a plant-specific alternative oxidase, encoded in the nuclear genome, that transfers electrons from the mitochondrial ubiquinone

pool to oxygen, without energy conservation. It prevents the accumulation of damaging ROS when the OXPHOS pathway is inhibited, for example when cI activity is impaired. *AOX1a* transcription is induced with the activation of the alternative respiratory pathway and is a reporter of oxidative stress (Vanlerberghe, 2013). *AOX1a* transcripts were detected in all analyzed samples indicating that some oxidative stress is inherent to *in vitro* culture conditions (Figure 3 B). Furthermore, *AOX1a* transcript levels spiked 2- to 4-fold 12h after rotenone application according to a dose-dependent profile. A similar *AOX1a* transcriptional response was induced after transfer, but only in calli that were previously exposed to rotenone, even though the regeneration medium on which the calli were placed did not contain rotenone, suggesting that the inhibitor in some way sensitized the explants to the stress caused by the transfer. Finally, the *OXII* transcripts, coding for a kinase relaying oxidative stress signaling (Rentel et al., 2004), were also present in all tissues analyzed, and markedly induced upon rotenone application at 10 μ M, but not following callus transfer.

In summary, based on transcriptional signatures, we have measured varying levels of oxidative stress in protoplast-derived calli growing *in vitro*. Non-lethal rotenone-mediated cI inhibition resulted in the rapid activation of the mitochondrial alternative oxidase and increased level of oxidative stress, paired with a reduction of cell proliferation. The transfer of calli from callogenesis to shoot induction medium caused a transient growth arrest and a renewed transcriptional activation of *AOX1a* that was enhanced in tissues previously exposed to rotenone. However, the molecular events triggered by rotenone addition and explant transfer were different since *OXII* transcript levels did not increase in the later transition.

Mitochondrial cI rotenone inhibition is rapidly relayed as an oxidative cytosolic signal and the redox shift patterns are cell-dependent

To further study the intracellular redox state of protoplast-derived calli, we measured fluorescence in cells expressing a cytosolic biosensor multipartite protein. In this assembly, the human glutaredoxin Grx1 controls the redox-sensitive green fluorescent protein roGFP2 that carries two cysteine residues locked or not in a disulfide bond, depending on the redox state of their environment (Schwarzlander et al., 2008; Schwarzlander et al., 2016). The reduced and oxidized forms of the Grx1-roGFP2 fusion protein have distinct excitation maxima and their relative amount, reflecting a redox state, can be measured in real time and in live cells as the ratio of fluorescence emitted after the simultaneous excitation at 405 nm and 488 nm (Meyer et al., 2007; Gutscher et al., 2008; Schwarzlander et al., 2009).

To verify that the ratiometric analysis of cytosolic Grx1-roGFP2 was compatible with our *in vitro* regeneration system, we first analyzed the response of isolated protoplasts to an oxidant molecule. Protoplast were collected after an overnight maceration of transgenic plantlets constitutively expressing the biosensor protein and challenged with exogenous hydrogen peroxide (H₂O₂). The Grx1-roGFP2 signal was heterogeneous within each cell, reflecting the uneven distribution of the protein, in part due to the arrangement of the subcellular compartments (Figure 4). The 405 and 488 nm patterns were essentially overlapping and matched plausible cytosolic areas. The ratiometric signal differed between cells, as expected in a population derived from multiple tissue types, in which each entity has a specific history, and considering that redox states evolve over time. Nevertheless, the addition of H₂O₂ in the protoplast culture increased the portion of oxidized Grx1-roGFP2 molecules (Figure 4 A and B) and the average ratio across multiple cells is significantly different before and after treatment (Figure 4 C; $p < 0.001$, Student's t-test), indicating that the biosensor properly reports redox cytosolic shifts in our experimental system.

To investigate the early response to rotenone, we tracked redox fluctuation in Grx1-roGFP2 calli, at a stage corresponding to explants in which organogenesis rates were enhanced after transient treatment with the cI inhibitor, i.e. one week before transfer to gelled shoot induction medium (SIM). As was observed across isolated protoplasts, the redox state of neighboring cells within the same callus were heterogeneous (Figure 5 A). Nevertheless, when stationary calli were exposed to stepwise increase in rotenone concentration (5, 10, 20 and 40 μ M), the treated tissues displayed transient cytosolic Grx1-roGFP2 oxidation within seconds after the change in rotenone concentration over a period of over an hour (Figure 5 B).

All the cells tracked, across multiple areas of independent calli, displayed an oxidative cytosolic shift. However, the profiles of their individual response were markedly different. In some cells, an oxidative transient peak was observed after each rotenone addition (Figure 5 A, frames 2 and 4). In others, an initial rotenone treatment triggered a shift with a large amplitude (5 or 10 μ M) but the ratiometric signal then plateaued during subsequent rotenone additions (Figure 5 A, frame 3). Yet other cells displayed a slow oxidative response, that was not induced at the lowest rotenone concentration, but that kept raising with further rotenone addition without notable negative feedback within the studied time frame (Figure 5 A, frame 1). All cells remained responsive and physiologically active throughout the analysis because their integrity did not appear to be affected and the addition of the molecule dithiothreitol in the medium resulted in a reductive shift as expected, before and after the rotenone treatment (Figure 5B and all frames).

To conclude, the chemical inhibition of the mitochondrial cI, that presumably leads to an increased production of ROS within the mETC, is rapidly translated in the cytosol as a change of redox state towards a more oxidative environment. But the response is complex and the patterns of the redox shifts vary across the tissues.

Discussion

We previously analyzed the *in vitro* regeneration of four Arabidopsis mutants affected in the cI of the mitochondrial electron transport chain (mETC) and found that cI mutants showing a drastic growth retardation have also the highest regeneration rate. Based on these findings, we tested the effect of a cI chemical inhibitor on growth and shoot regeneration rate in protoplast-derived calli.

We first search for an effective rotenone concentration by testing the effect of cI inhibition on calli growth in the SIM medium. The application of rotenone in the gelled medium enabled the quantification of callus size at the time of transfer (T_0) and two weeks later (T_2). Chemical inhibition of the mitochondrial cI gradually inhibited callus growth with increasing rotenone concentrations (Figure 1). Calli treated with 10 μM showed no significant growth between T_0 and T_2 (Figure 1 A). These results are consistent with our previous findings showing that cI deficient mutants had a retarded *in vitro* growth (Chapter 2).

To test the effect of the cI inhibition on shoot regeneration, the same rotenone concentrations that reduced growth were applied on protoplast-derived calli in 3 different ways (Figure 2 A). In the application 1 (Ap 1) scheme, rotenone was added in the liquid medium one week before the transfer of calli to rotenone-free gelled regeneration medium. The second callus treatment (Ap 2) also included treatment one week before transfer but the inhibition was maintained through the addition of rotenone in the gelled regeneration medium on which treated calli were transferred. The third application (Ap 3) was restricted to the gelled regeneration. The chemical inhibition of the cI with rotenone enhanced the shoot regeneration rate when applied during the week before callus transfer to the regeneration medium (Figure 2). Although the best regeneration rate was obtained with the application 1 (Ap 1) (Figure 2 A and B), the rotenone concentration inducing the highest caulogenesis rate varied from an experiment to another between 5 and 10 μM (Supplemental Figure 1). This variation could be explained by the reactivity of explants to rotenone: in some experiments 5 μM was enough to enhance the regeneration but in others a higher concentration is needed.

To investigate the molecular changes after cI inhibition with rotenone, we analyzed the relative expression of specific marker genes: *CYCLIN B1;1* (*CYCBI;1*), a marker of cell division; *ALTERNATIVE OXIDASE 1a* (*AOX1a*) a marker of the alternative respiratory pathway, also described as stress marker; and *OXIDATIVE SIGNAL INDUCIBLE 1* (*OXII*), an oxidative stress marker. *CYCBI;1* relative expression dramatically decreased after

rotenone treatment of calli, and its expression was arrested after transfer to the regeneration medium in all treated and non-treated calli (Figure 3 A). Another type of stress, wounding caused by explant excision or section, is known to trigger regeneration in many tissues (Ikeuchi et al., 2016). The transfer of calli from liquid to gelled medium may play a similar role as we noticed the high induction of the stress marker *AOX1a* after transfer of rotenone-treated calli (Figure 3 B). This transfer-related stress had also a molecular impact on control calli as we noticed the inhibition of cell division indicated by *CYCB1;1* downregulation after transfer for both treated and untreated calli (Figure 3 A). This temporary arrest of mitotic activity could be explained not only by the shift from liquid to gelled medium, but by the cytokinin switch (from TDZ in CIM2 to meta-topolin in the SIM regeneration medium). *OXII* relative expression was enhanced after callus treatment with rotenone, again suggesting a rotenone-induced oxidative stress in treated calli (Figure 3 C).

Multiple recent studies pointed a close link between redox status and regeneration (Gupta and Datta, 2003; Tian et al., 2003; Gong et al., 2005; Matakias and Kintzios, 2005; Stasolla, 2010; Gupta, 2011; Zhang et al., 2017). On the other hand, mutants affected in the mitochondrial cI have been described to accumulate more ROS (Yang et al., 2014). Our present work further suggests that there may be a causal link between ROS induced by cI impairment and shoot regeneration.

The diversity of *in vitro* responses in explants treated with oxidant or reductive compounds is probably a reflection of the intricate regulatory mechanisms that integrate redox changes and signals. The cellular response towards ROS depends on the ROS type, where it is produced and at what time (Wrzaczek et al., 2013). With rotenone cI inhibition, ROS are induced in the mitochondria and the initial oxidative signal is transduced to the cytosol as we showed with the cytosolic redox biosensor expressed in calli (Figure 5).

A link between ROS homeostasis in mitochondria and shoot regeneration capacity was recently reported in an *Arabidopsis* mutant affected in a mitochondrial thioredoxin named DCC1 (Zhang et al., 2017). Thioredoxins (Trx) are proteins acting as redox regulators by modulating the structure and activity of targeted proteins (Geigenberger et al., 2017). The biological functions of the mitochondrial Trx is not well understood compared to other Trxs (Meyer et al., 2012). Zhang and collaborators demonstrated the function of the mitochondrial Trx DCC1 as a redox regulator of CA2, a subunit of the cI of the mitochondrial electron transport chain (mETC). The reduction of CA2 by DCC1 directly impacts the cI activity. Therefore, the cI activity is reduced in the *dcc1* mutant. The absence of the thioredoxin reductive power in *dcc1* results in a high ROS level but, in that mutant, it correlates with a

decrease in shoot regeneration rate compared to the wild type (Zhang et al., 2017). Thus, according to this study, a mitochondrial redox regulator is required for productive shoot regeneration.

In the *de novo* shoot regeneration system described by Zhang et al., the regeneration rate of wild-type Col-0 root-derived calli is very high, reaching 100% in some conditions. Our experimental system, based on protoplast-derived calli of the same Arabidopsis accession, yields lower shoot regeneration rates (Figure 2). Although the comparison of the two studies is limited because the same mutants have not been characterized, it suggests that the shoot regeneration rate of Arabidopsis calli in which the mitochondrial cI is affected may depend on the type of explants. In the root-derived calli, the regeneration rate of the wild type was high and the ROS induced by cI defect reduced the regeneration capacity in the mutant (Zhang et al., 2017), whereas in the protoplast-derived calli, the regeneration of the wild type is lower and the ROS produced by the cI inhibition enhanced shoot regeneration (Figure 2).

Figures

Figure 1: Effect of rotenone on callus growth. (A) Callus mean size. Calli derived from protoplasts were transferred on regeneration medium containing the indicated rotenone concentrations. The projected area of each callus was measured immediately after transfer (T_0) and two weeks later (T_2) with the ImageJ software. Asterisks show that values are significantly different with p -value < 0.05 as analysed with student t-test. $n = 94-117$ calli/rotenone concentration from three independent experiments. ns: non significant. (B) Illustration of calli treated with $10 \mu\text{M}$ of rotenone and the control ($0\mu\text{M}$) just after transfer (first line, T_0) and two weeks after (second line, T_2). Bars = 3 mm.

Figure 2: Enhancement of shoot initiation by transient rotenone treatment. (A) Schematic representation of rotenone application during protoplast-derived callus culture. Ap 1, application of rotenone one week before the transfer of calli on rotenone-free SIM medium; Ap 2, application of rotenone one week before transfer and in gelled SIM medium; Ap 3, application of rotenone only in gelled SIM medium. (B) Fraction of regenerating calli following rotenone treatment. The regeneration frequency was calculated four weeks after callus transfer as the percentage of calli with at least one regenerated shoot. Values are mean \pm SE of two biological repetitions. (C) Callus classes depending on the number of initiated shoots. The number of buds was quantified for each regenerating callus four weeks after transfer. (D) Illustration of regenerating calli four weeks after the transfer to SIM. Calli were treated with $5 \mu\text{M}$ and $10 \mu\text{M}$ of rotenone one week before the transfer (Ap 1). Bars = 5 mm.

Figure 3: Marker gene expression upon rotenone treatment. Relative transcript level of *CYCB1;1*, a cell division marker (A), *AOX1a*, an alternative pathway and oxidative stress marker (B), and *OXII*, an oxidative stress marker (C). Rotenone was applied in callus liquid culture (CIM2) one week before the callus transfer on rotenone-free regeneration medium (SIM). Fold induction in transcript levels was calculated as the ratio of the indicated transcript abundance with that of the housekeeping gene *At5g13440*. The reference time point (0 day, 0D) is arbitrarily set at 100. Graphs show data from one experiment. Identical trends were observed in at least one independent repetition. Time line (X axis) is not to scale.

Figure 4. Redox biosensor reporting H_2O_2 -induced oxidative shift in the protoplasts cytosol. (A) Signal in Grx1-roGFP2 protoplasts. Protoplasts were harvested from 3-week-old transgenic plantlets and imaged after excitation at the indicated wavelength, following no treatment (left panels) or exposure to $0.33 \mu\text{M}$ of hydrogen peroxide (H_2O_2) for 5 minutes

after addition in the callus induction liquid medium (CIM1) (right panels). The bottom panels illustrate in false colors the ratio calculated by dividing for each pixel the 405-nm signal by the 488-nm signal. TL, transmitted light. Bar size, 30 μm . (B) Ratiometric view of individual protoplasts. Left panel, cell before treatment; right panel, cell after H_2O_2 treatment. The frames correspond to the insets in the ratiometric image in (A) and have the same ratio color code. Bar size, 7 μm . (C) Ratiometric analysis of protoplast populations. Cell ratios were calculated as the mean ratio values associated to pixels in the circular area corresponding to individual protoplasts, either before ($n=150$) or after H_2O_2 addition ($n=177$). Student's t-test, $p < 0.001$.

Figure 5: Cytosolic oxidative response induced by rotenone in calli. (A) Ratiometric image of a callus portion before rotenone addition. Redox measurements were conducted in calli constitutively expressing the Grx1-roGFP2 protein in the cytosol, one week before transfer to the shoot inducing medium (SIM; Ap 1). The ratio was calculated as in Figure 4. Bar size, 30 μm . (B) Ratiometric analysis of calli treated with rotenone. To detect rotenone-induced redox fluctuation, calli stabilized in a microscopic flow cell (see Supplemental Figure 2) were initially treated with exogenous DTT (2 mM) as a reducing agent, followed by increasing concentrations of freshly prepared rotenone (5, 10, 20 and 40 μM), and finally with DTT (2 mM) after the last rotenone addition. Pixel intensity values were calculated from confocal microscope images processed with the Fiji software. Left Y axis, fluorescence signal emitted following excitation at 405 nm (blue line) or 488 nm (red line) expressed in arbitrary units. Right Y axis, average ratio between the 405 nm and 488 nm intensity calculated per pixel for the entire field represented in (A). To highlight differences in cellular response, the average ratios characterizing subframes containing one or two cells [red rectangles in (A)] are illustrated in the graphs below (Frames 1 to 4), along with snapshots illustrating the evolving redox state of the cells as recorded with the fluorescence signal after excitation at 405 or 488 nm, and with the deduced ratiometric image [see scale in (A)]. The corresponding time-lapse movies are available in Supplemental data.

Supplemental Figure 1: Shoot regeneration variability observed following rotenone treatment. Graphic representation of the percentage of regenerating calli after treatment (Ap 1, see Figure 2) with a range of rotenone concentrations.

Supplemental Figure 2: Schematic representation of the used installation to measure redox stat during rotenone application.

Acknowledgments

We thank Marcus Schwarzländer for Grx1-roGFP2 line.

References

- Benson EE** (2000) Special symposium: In vitro plant recalcitrance do free radicals have a role in plant tissue culture recalcitrance? *Vitr Cell Dev Biol - Plant* **36**: 163–170
- Earnshaw BA, Johnson MA** (1987) Control of Wild Carrot Somatic Embryo Development by Antioxidants. *Plant Physiol* **85**: 66–77
- Ferreira PCG, Hemerly AS, de Almeida Engler J, Van Montagu M, Engler G, Inzé D** (1994) Developmental expression of the Arabidopsis cyclin gene *cyc1At*. *Plant Cell* **6**: 1763–1774
- Foyer CH, Ruban A V., Noctor G** (2017) Viewing oxidative stress through the lens of oxidative signalling rather than damage. *Biochem J* **474**: 877–883
- Geigenberger P, Thormählen I, Daloso DM, Fernie AR** (2017) The Unprecedented Versatility of the Plant Thioredoxin System. *Trends Plant Sci* **22**: 249–262
- Gong H, Jiao Y, Hu WW, Pua EC** (2005) Expression of glutathione-S-transferase and its role in plant growth and development in vivo and shoot morphogenesis in vitro. *Plant Mol Biol* **57**: 53–66
- Gupta SD** (2011) Role of free radicals and antioxidants in in vitro morphogenesis. *React Oxyg Species Antioxidants High Plants* 229–247
- Gupta SD, Datta S** (2003) Antioxidant enzyme activities during in vitro morphogenesis of gladiolus and effect on application of antioxidants on plant regeneration. *Biol Plant* **47**: 179–183
- Gutscher M, Pauleau A-L, Marty L, Brach T, Wabnitz GH, Samstag Y, Meyer AJ, Dick TP, Goi A, Trapido M, et al** (2008) Real-time imaging of the intracellular glutathione redox potential. *Nat Methods* **5**: 553–559
- Hu Y, Depaepe T, Smet D, Hoyerova K, Klíma P, Cuypers A, Cutler S, Buyst D, Morreel K, Boerjan W, et al** (2017) ACCERBATIN, a small molecule at the intersection of auxin and reactive oxygen species homeostasis with herbicidal properties. *J Exp Bot.* doi: 10.1093/jxb/erx242
- Ikeuchi M, Ogawa Y, Iwase A, Sugimoto K** (2016) Plant regeneration: cellular origins and molecular mechanisms. *Development* **143**: 1442–1451

- Joy IV RW, Patel KR, Thorpe TA** (1988) Ascorbic acid enhancement of organogenesis in tobacco callus. *Plant Cell Tissue Organ Cult* **13**: 219–228
- Lall S, Mandegaran Z, Roberts A V.** (2005) Shoot multiplication in cultures of mature *Alnus glutinosa*. *Plant Cell Tissue Organ Cult* **83**: 347–350
- Lei C, Wang H, Liu B, Ye H** (2014) Effects of silver nitrate on shoot regeneration of *Artemisia annua* L. *Plant Biotechnol* **31**: 71–75
- Matakiadis T, Kintzios S** (2005) The effect of ATP on cucumber (*Cucumis sativus* L.) regeneration from nodal explants: Association with ??-tocopherol, H₂O₂ and size of culture vessel. *Plant Growth Regul* **45**: 127–137
- Meyer AJ, Brach T, Marty L, Kreye S, Rouhier N, Jacquot JP, Hell R** (2007) Redox-sensitive GFP in *Arabidopsis thaliana* is a quantitative biosensor for the redox potential of the cellular glutathione redox buffer. *Plant J* **52**: 973–986
- Meyer Y, Belin C, Delorme-Hinoux V, Reichheld J, Riondet C** (2012) Thioredoxin and Glutaredoxin Systems in Plants: Molecular Mechanisms, Crosstalks, and Functional Significance. *Antioxid Redox Signal* **17**: 1124–1160
- Mittler R** (2017) ROS Are Good. *Trends Plant Sci* **22**: 11–19
- Mohiuddin AKM, Chowdhury MKU, Abdullah ZC, Napis S** (1997) Influence of silver nitrate (ethylene inhibitor) on cucumber in vitro shoot regeneration. *Plant Cell Tissue Organ Cult* **51**: 75–78
- Motte H, Galuszka P, Spichal L, Tarkowski P, Plihal O, Smehilova M, Jaworek P, Vereecke D, Werbrouck S, Geelen D** (2013) Phenyl-Adenine, Identified in a LIGHT-DEPENDENT SHORT HYPOCOTYLS4-Assisted Chemical Screen, Is a Potent Compound for Shoot Regeneration through the Inhibition of CYTOKININ OXIDASE/DEHYDROGENASE Activity. *Plant Physiol* **161**: 1229–1241
- Noctor G, Reichheld JP, Foyer CH** (2017) ROS-related redox regulation and signaling in plants. *Semin Cell Dev Biol*. doi: 10.1016/j.semcdb.2017.07.013
- del Pozo JC** (2016) Reactive Oxygen Species: From Harmful Molecules to Fine-Tuning Regulators of Stem Cell Niche Maintenance. *PLoS Genet* **12**: 4–7
- Rentel MC, Lecourieux D, Ouaked F, Usher SL, Petersen L, Okamoto H, Knight H, Peck SC, Grierson CS, Hirt H, et al** (2004) OXI1 kinase is necessary for oxidative burst-mediated signalling in *Arabidopsis*. *Nature* **427**: 858–861
- Del Río LA** (2015) ROS and RNS in plant physiology: An overview. *J Exp Bot* **66**: 2827–2837
- Schwarzländer M, Fricker M, Müller C, Marty L, Brach T, Novak J, Sweetlove L, Hell**

- R, Meyer A** (2008) Confocal imaging of glutathione redox potential in living plant cells. *J Microsc* **231**: 299–316
- Schwarzländer M, Fricker MD, Sweetlove LJ** (2009) Monitoring the in vivo redox state of plant mitochondria: Effect of respiratory inhibitors, abiotic stress and assessment of recovery from oxidative challenge. *Biochim Biophys Acta - Bioenerg* **1787**: 468–475
- Schwarzländer M, Tobias DP, Meyer AJ, Morgan B** (2016) Dissecting Redox Biology using Fluorescent Protein Sensors. *Antioxid Redox Signal* **24**: 680–712
- Singhi SK, Syamal MM** (2000) Anti-auxin enhance *Rosa hybrida* L. micropropagation. *Biol Plant* **43**: 279–281
- Skoog F, Miller CO** (1957) Chemical regulation of growth and organ formation in plant tissues cultured in vitro. *Symp Soc Exp Biol* **11**: 118–131
- Stasolla C** (2010) Glutathione redox regulation of in vitro embryogenesis. *Plant Physiol Biochem* **48**: 319–327
- Tian M, Gu Q, Zhu M** (2003) The involvement of hydrogen peroxide and antioxidant enzymes in the process of shoot organogenesis of strawberry callus. *Plant Sci* **165**: 701–707
- Vanlerberghe GC** (2013) Alternative oxidase: A mitochondrial respiratory pathway to maintain metabolic and signaling homeostasis during abiotic and biotic stress in plants. *Int J Mol Sci* **14**: 6805–6847
- Waszczak C, Carmody M, Kangasjarvi J** (2018) Reactive Oxygen Species in Plant Signaling. *Annu Rev Plant Biol* **69**: 1–28
- Winer J, Jung CKS, Shackel I, Williams PM** (1999) Development and Validation of Real-Time Quantitative Reverse Transcriptase–Polymerase Chain Reaction for Monitoring Gene Expression in Cardiac Myocytes in Vitro. *Anal Biochem* **270**: 41–49
- Wrzaczek M, Brosché M, Kangasjärvi J** (2013) ROS signaling loops - production, perception, regulation. *Curr Opin Plant Biol* **16**: 575–582
- Yang L, Zhang J, He J, Qin Y, Hua D, Duan Y, Chen Z, Gong Z** (2014) ABA-Mediated ROS in Mitochondria Regulate Root Meristem Activity by Controlling PLETHORA Expression in Arabidopsis. *PLoS Genet*. doi: 10.1371/journal.pgen.1004791
- Zhang H, Zhang TT, Liu H, Shi DY, Wang M, Bie XM, Li XG, Zhang XS** (2017) Thioredoxin-mediated ROS Homeostasis Explains Natural Variation in Plant Regeneration. *Plant Physiol*. doi: 10.1104/pp.17.00633

Figure 1

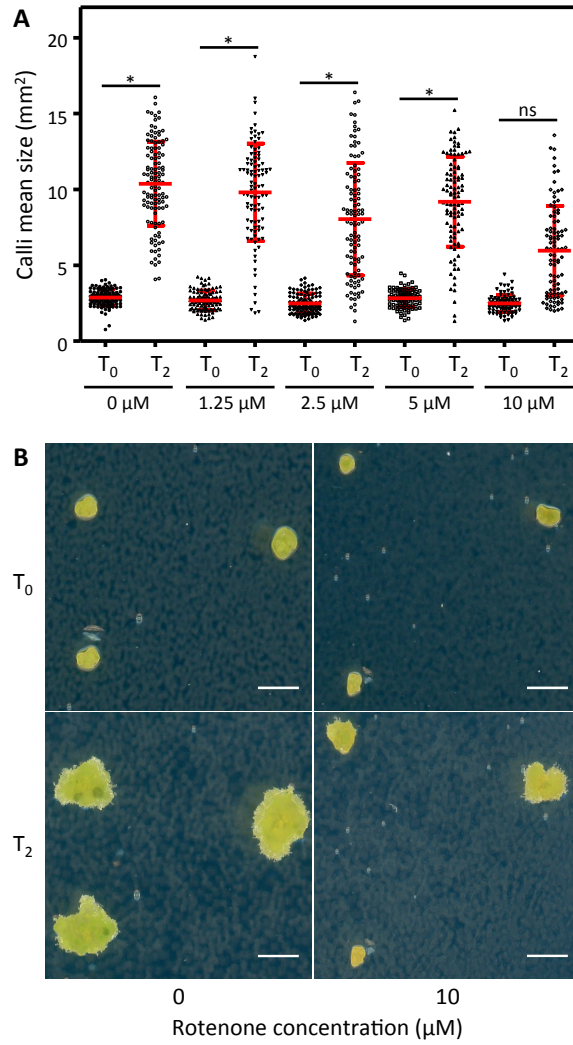


Figure 2

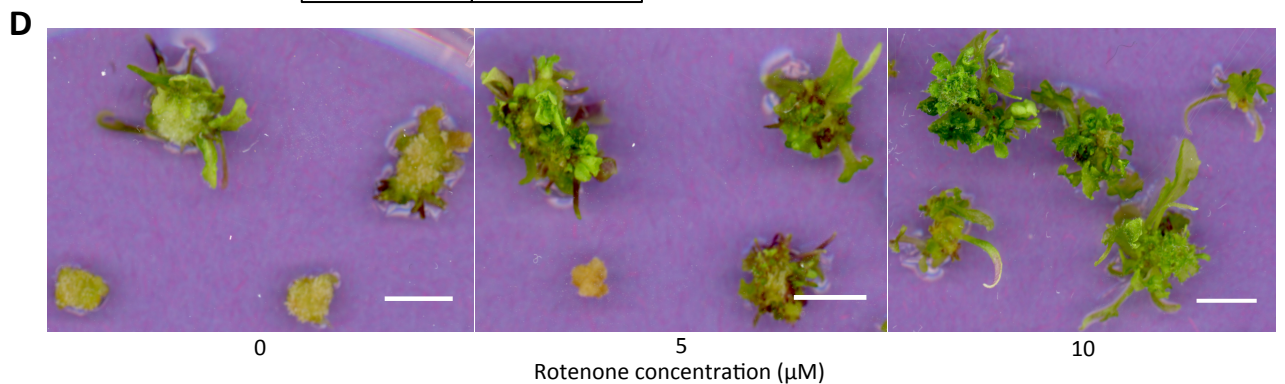
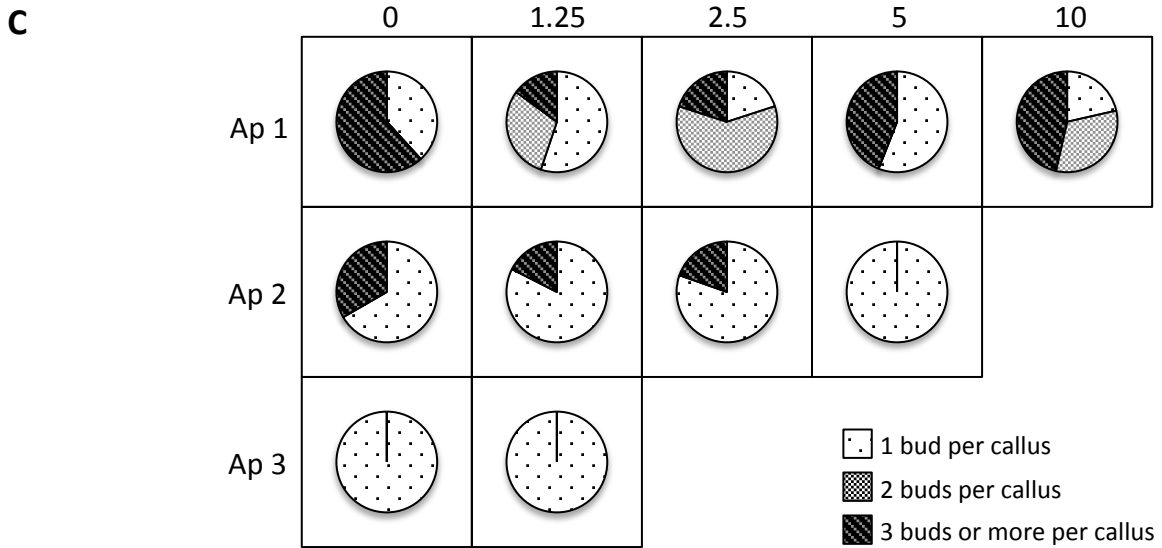
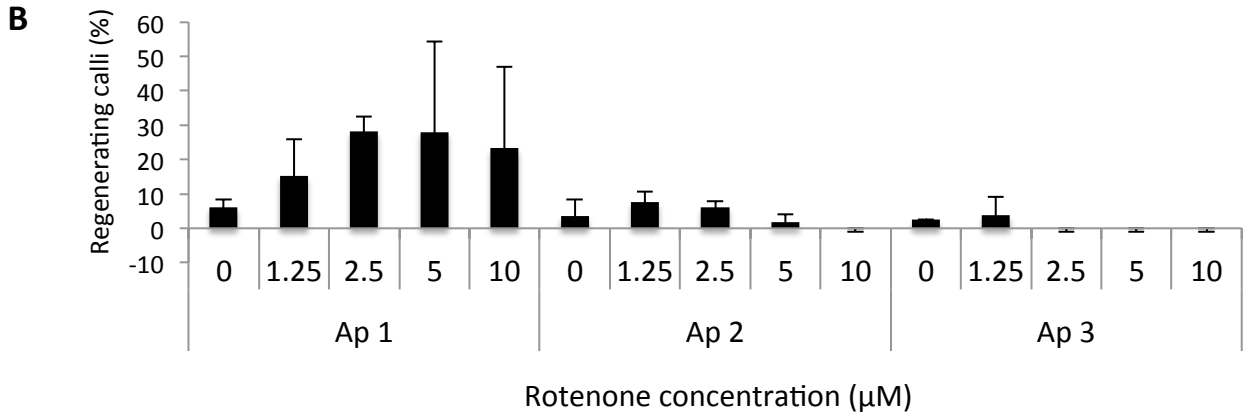
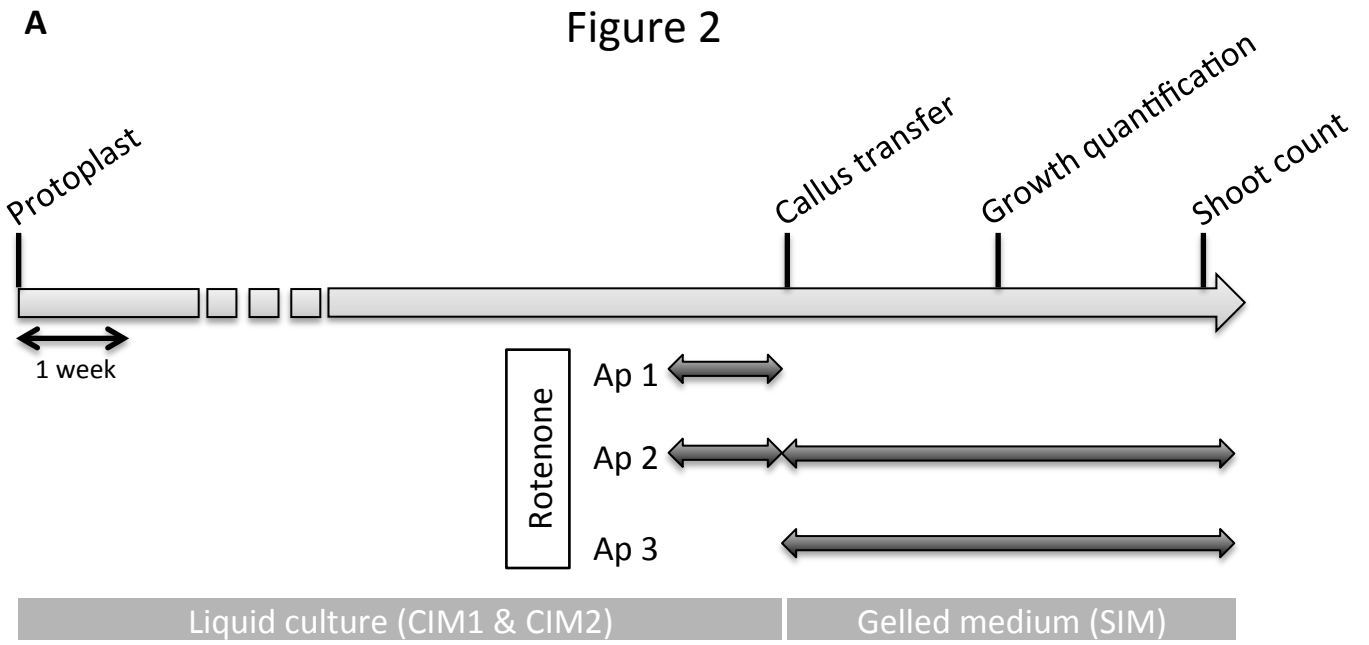


Figure 3

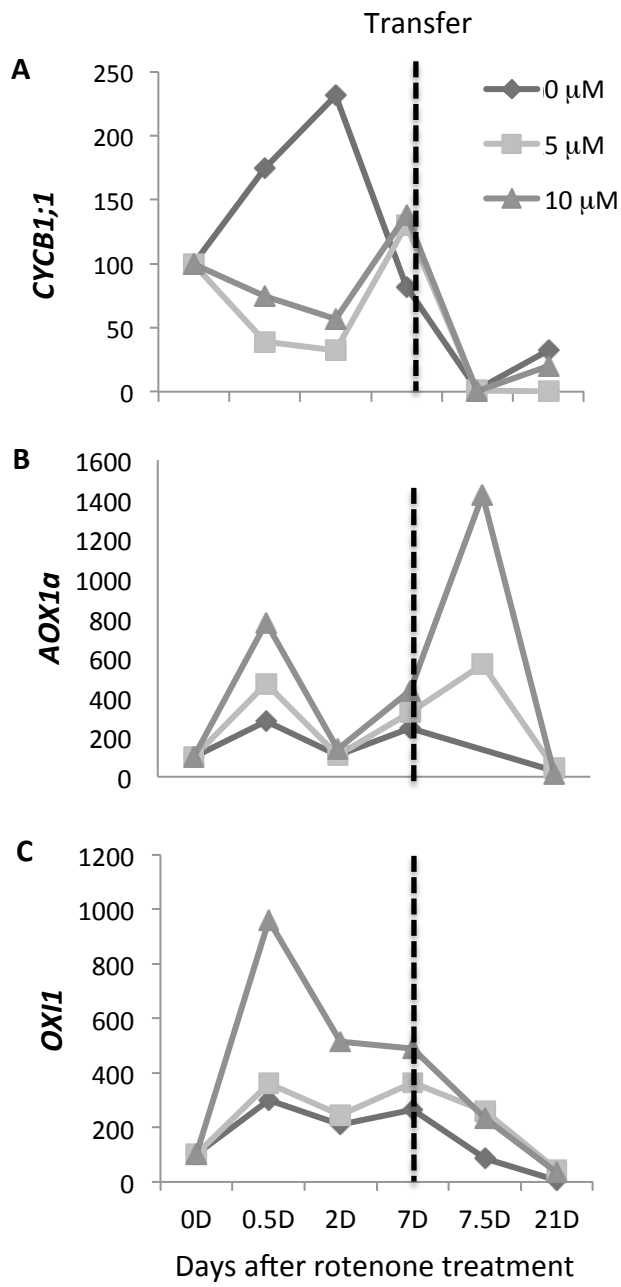


Figure 4

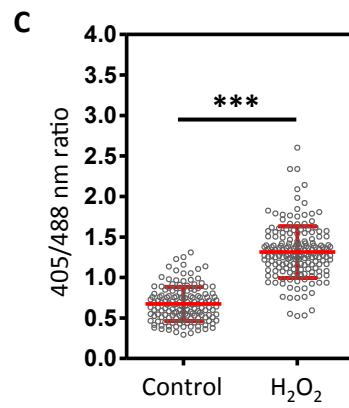
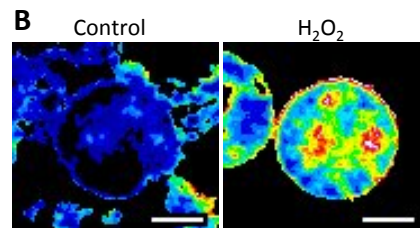
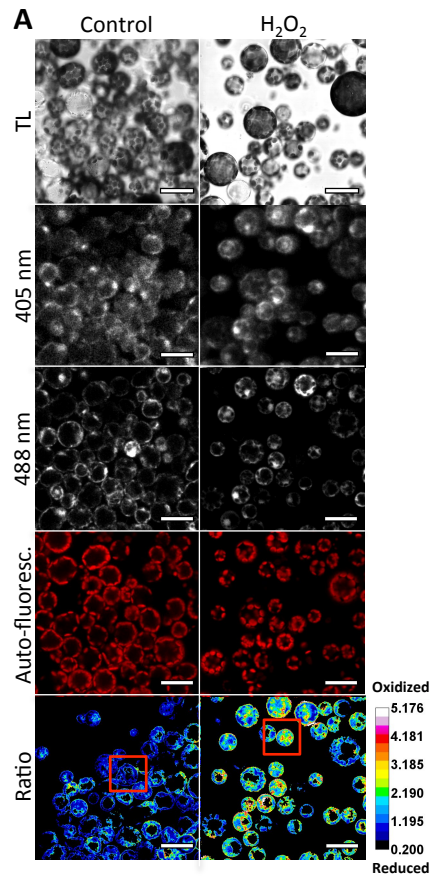
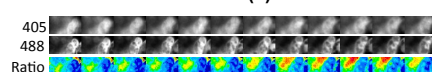
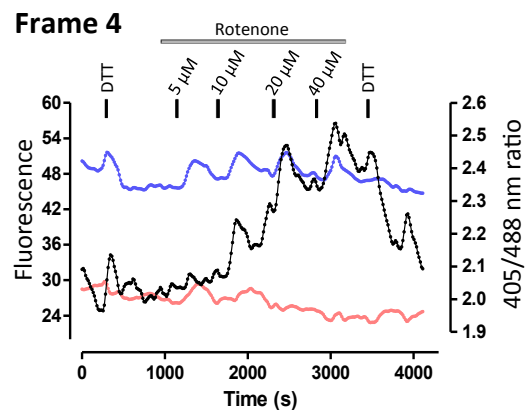
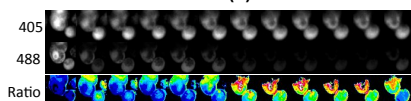
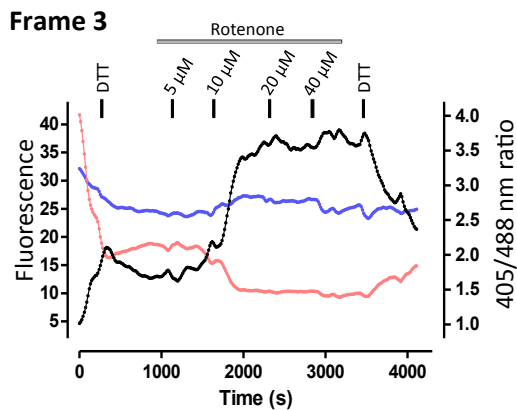
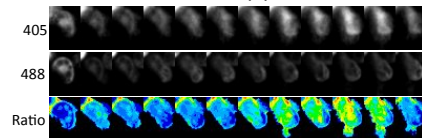
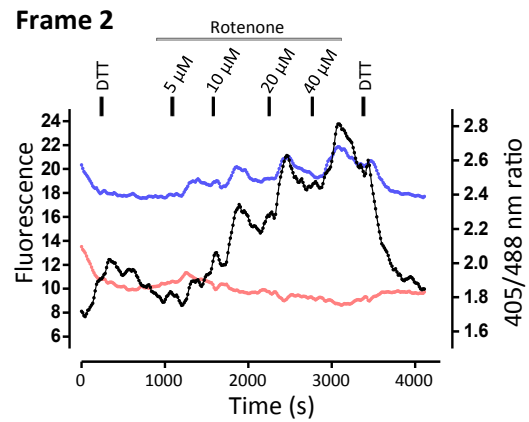
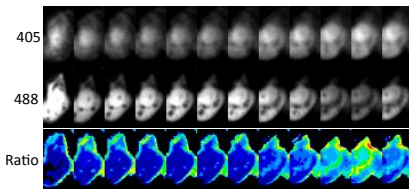
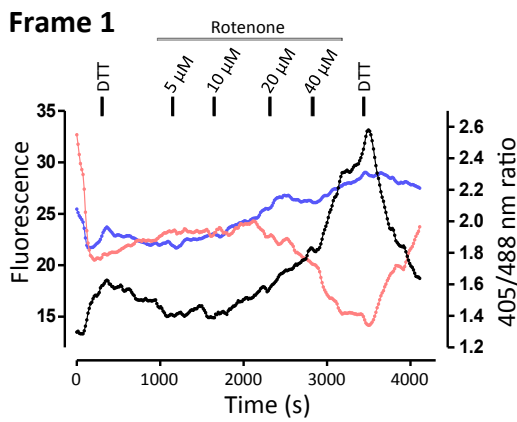
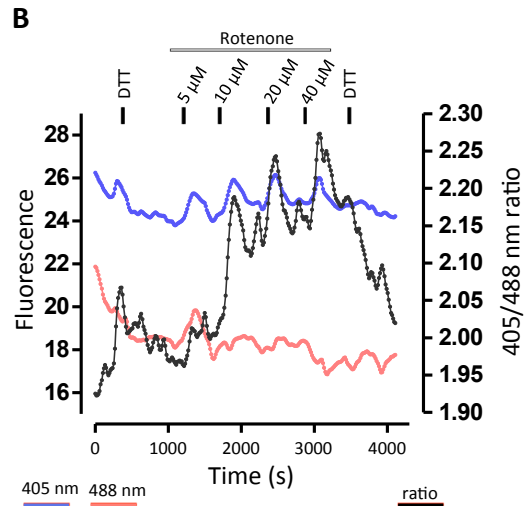
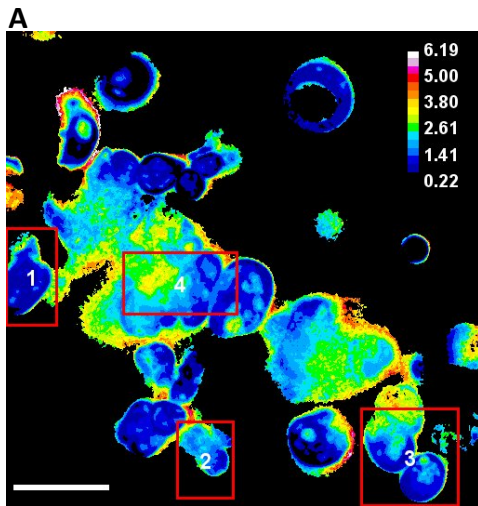
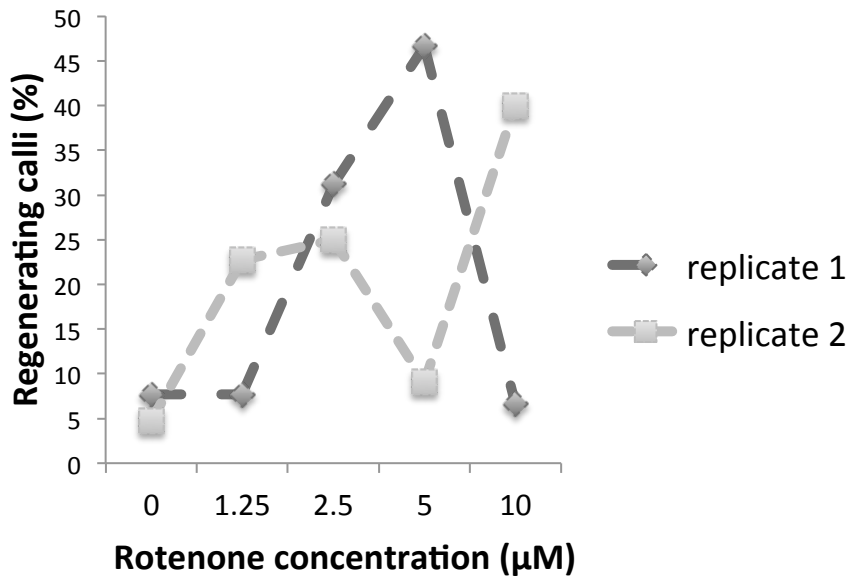


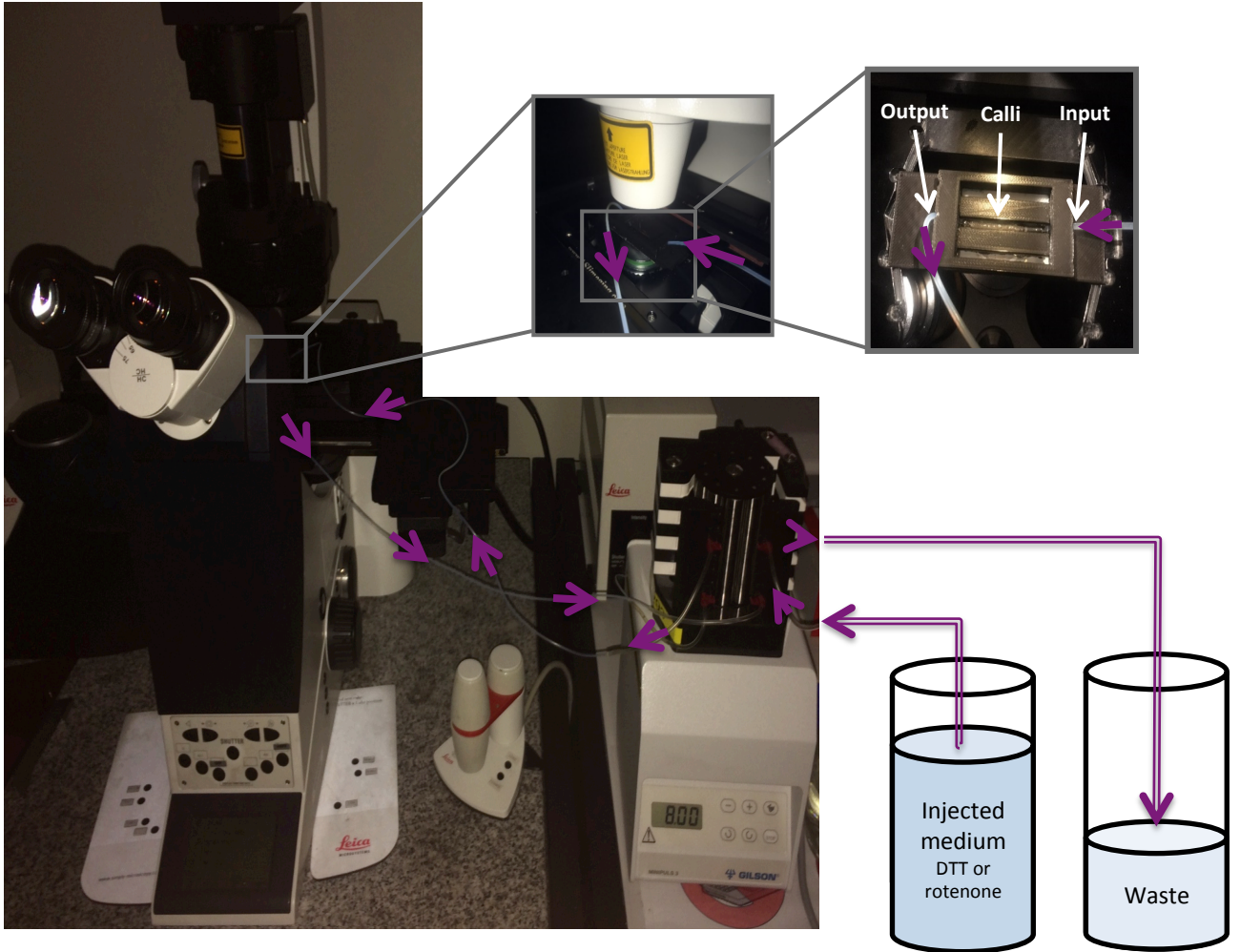
Figure 5



Supplemental Figure 1



Supplemental Figure 2



Chapter 4:
Variability hampers the functional analysis
of bioactive molecules on *in vitro*
development

Introduction

It is well known that tissue culture response can be significantly different between closely linked species or even among ecotypes in the same species (Sugiyama, 2015). In some studies, this genotype dependency was exploited to identify genes associated with regeneration capacity. For example, two *Arabidopsis* accessions with contrasted regeneration phenotypes were used for QTL analysis by association mapping combined with linkage analysis by Motte and collaborators, leading to the identification of the gene coding for RECEPTOR-LIKE PROTEIN KINASE1 (RPK1), a kinase involved in abscisic acid (ABA) signaling and, thereby, playing a role in *de novo* shoot regeneration (Motte et al., 2014).

But, beside genetic variations, *in vitro* culture conditions also influence explants growth and development. For example, the light spectrum has a direct effect on *in vitro* plant regeneration of the medicinal plant *coastal hogfennel*, both in callus proliferation and somatic embryo induction (Chen et al., 2016). The temperature is another important factor determining the efficiency of plant regeneration. For example, the pre-treatment of barley calli at 35 °C for just 6 hours enhanced *in vitro* plant regeneration up to 2-fold compared to the control.

In Chapter III, we demonstrated the effect of complex I (cI) inhibition on callus growth and shoot regeneration. These results confirmed the observations that we reported in the previous Chapter II describing the positive effect on shoot regeneration in mutants affected in the mitochondrial cI activity. In the present chapter, the effect of two additional inhibitors of the mETC will be discussed together with the variability inherent to *in vitro* tissue culture. The inhibitors are cyanide that inhibits the mitochondrial complex IV and salicylhydroxamic acid (SHAM) that inhibits the alternative oxidase AOX.

As mentioned in Chapter II, mutants affected in the assembly and activity of the mitochondrial cI yield calli of a reduced size in our regeneration protocol that are on the other hand characterized with higher regeneration rate compared to wild type. For this reason, we further investigated a potential link between callus size at transfer and the shoot regeneration rate observed in the weeks following the transfer.

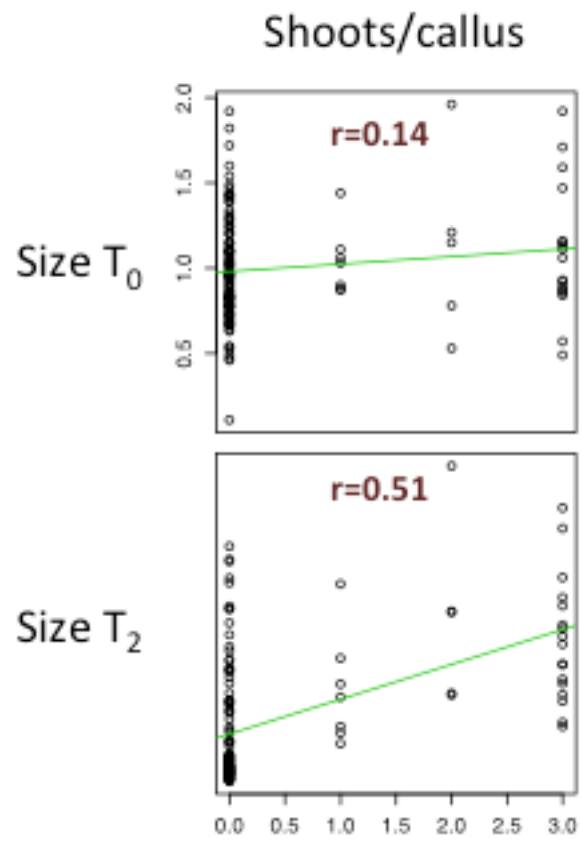
Results

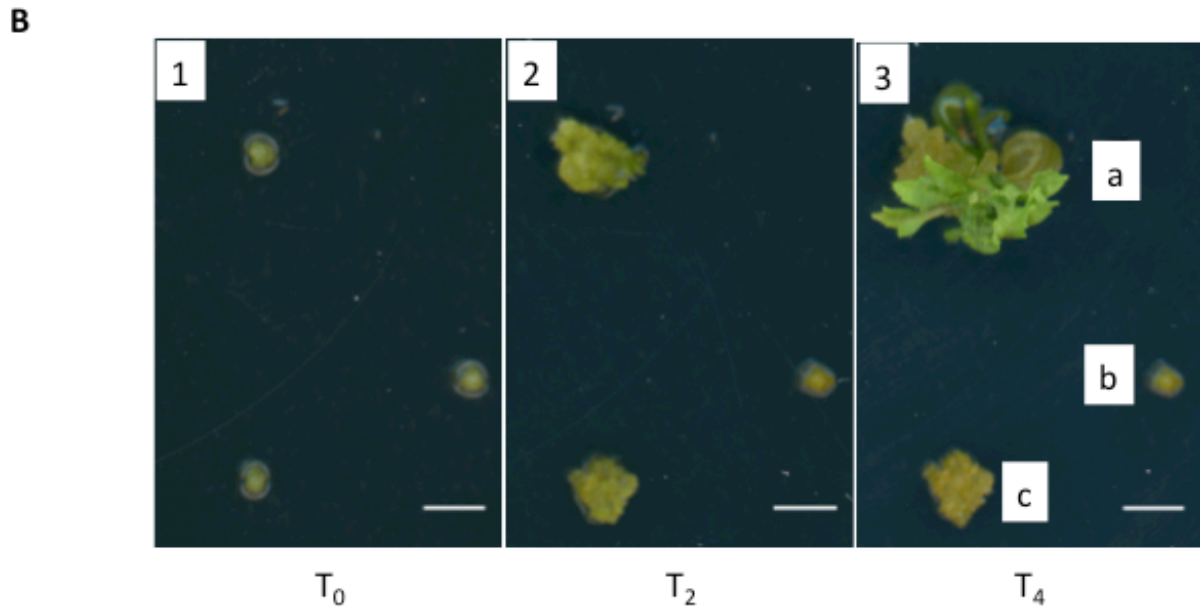
1. Beyond viability, callus size is not a good predictor of *in vitro* organogenesis

Calli derived from mutants affected in the mitochondrial cI and presenting a high regeneration frequency were on average smaller than the wild type at a given time point (Chapter 2). To investigate a potential link between callus size at transfer and regeneration frequency, calli with variable sizes were transferred to the regeneration medium. For each individual callus, we measured its size at transfer (T_0), two weeks after transfer (T_2) and we measured the number of regenerated shoots growing on each of them.

Callus size at transfer (T_0) was not correlated with shoot regeneration (correlation coefficient $r = 0.14$; Pearson test $P\text{-value} > 0.05$) as shown in Figure 4.1 A. To illustrate this result, three calli included in the analysis were imaged across the regeneration sequence (calli a, b and c, Figure 4.1, B and C) that were transferred side by side and had almost an identical size when transferred to the regeneration medium (0.93, 0.96 and 0.71 mm², respectively). Nevertheless, callus a succeeded to grow and regenerate shoots, whereas callus b died early without any noticeable growth and callus c grew but did not produce any shoot (Figure 4.1, B and C).

A





C

	Callus size (mm ²)		Shoot regeneration (T ₄)
	T ₀	T ₂	
Callus a	0.93	9.5	+
Callus b	0.96	1.96	-
Callus c	0.71	6.6	-

Figure 4.1: Shoot regeneration is not correlated with callus size at the transfer to the regeneration medium. (A) Correlation matrix between shoot regeneration and callus size. The size of each callus was measured at transfer (T₀) and two weeks afterwards (T₂). Shoot regeneration is reported as the number of shoots per callus (shoots/callus) four weeks after transfer. The indicated correlation coefficients (r) were obtained with the Pearson correlation test, n = 137. (B) Illustrations of callus variability in growth and regeneration. Panel 1, calli just after the transfer to the regeneration medium (T₀); Panel 2, calli two weeks after the transfer (T₂); Panel 3, calli four weeks after the transfer (T₄). a, callus with regenerated shoots; b, dead callus; c, growing callus with no regenerated shoot. Scale bar = 3mm. (C) Individual callus size and regeneration phenotype. Values represent callus size at the transfer (T₀) and two weeks later (T₂). Plus (+) represent the presence of regenerated shoots and minus (-) the absence of shoots.

2. The effect of complex IV and AOX inhibitors on callus growth and regeneration

The inhibition of the mitochondrial complex I through the addition of rotenone to the callus medium (CIM2) one week before their transfer to the shoot induction medium (SIM) enhanced regeneration frequency (Chapter III). To investigate whether the inhibition of other mitochondrial complexes may have a similar effect on shoot regeneration, we first tested different concentrations of additional specific inhibitors on callus growth with the goal to identify bioactive yet non-lethal concentrations. Calli were transferred to the regeneration medium containing a range of concentrations of cyanide and SHAM (Figure 4.2 A). The callus mean size was measured at the time of transfer and two weeks afterwards with the ImageJ software. Some of the tested concentrations enabled callus growth after the transfer. However, at some concentrations, SHAM induced the browning of a fraction of the transferred calli while others had a normal aspect and sustained growth (Figure 4.2 B).

Non-lethal inhibitor concentrations were then applied in the callus liquid culture (CIM2) one week before the callus transfer to an inhibitor-free regeneration medium (SIM). Four weeks after the transfer, the regeneration rate was estimated by counting the percentage of regenerating calli, i.e. producing at least one shoot (Figure 4.2 C). In the "replicate 1" experiment, the callus treatment with cyanide at a concentration of 200 μM or 400 μM led to an enhanced regeneration rate (50 % and 66 %, respectively) compared to the control (24%). However, in the "replicate 2" experiment, the shoot regeneration enhancement was observed only in calli treated with 200 μM cyanide (50%), but not in calli treated with 400 μM (12%), compared to the control (15%). AOX inhibition with SHAM also enhanced shoot regeneration rate, especially at 12.5 μM in both replicates (except in calli treated with 25 μM of SHAM in replicate 1). However, we noticed a high variability in the regeneration rate of calli in the mock control (0 μM) between the two replicates: 26 % of regenerating calli in replicate 1 and 2.5 % in replicate 2. The variability in the response to inhibitors may be due to the inherent variability between independent replicates.

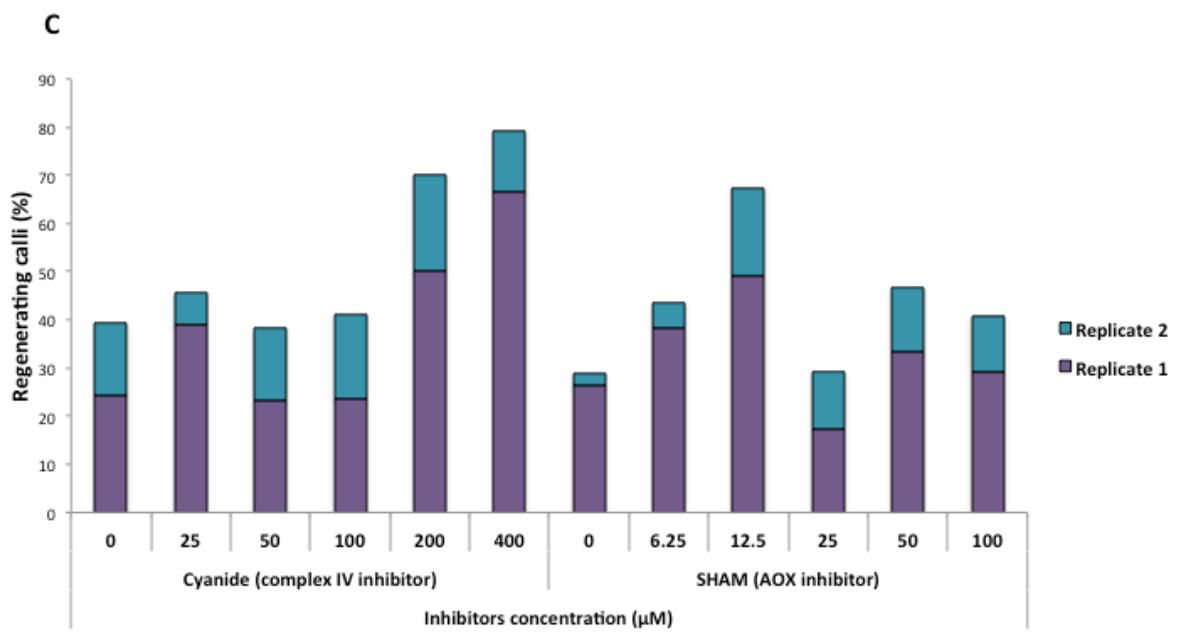
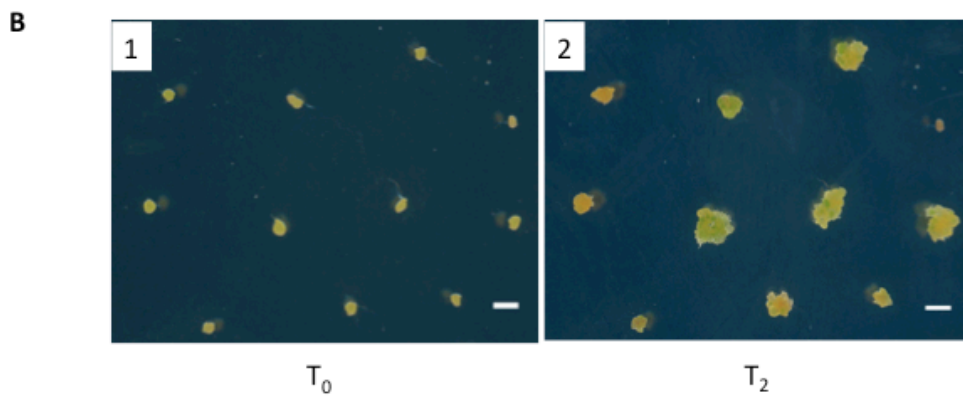
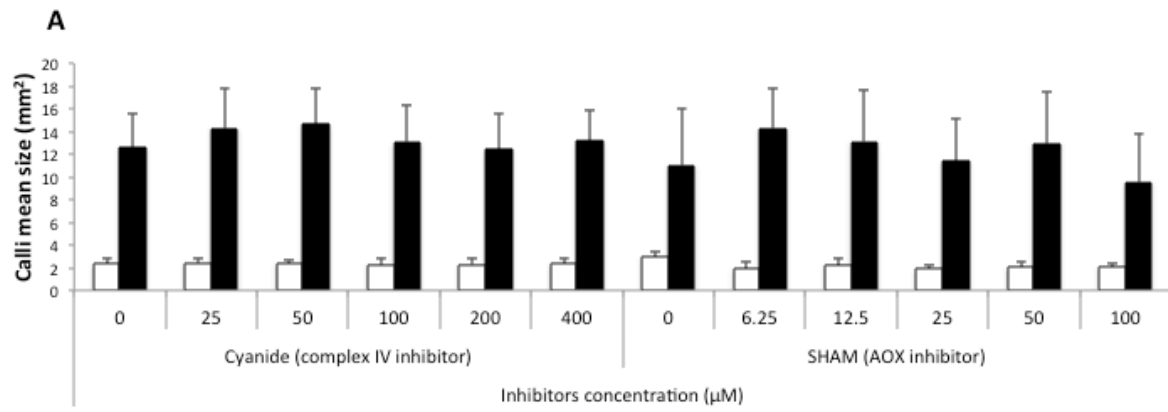


Figure 4.2: Calli growth and regeneration after inhibition of the mitochondrial complex IV with cyanide and of AOX with SHAM. A, Calli mean size after transfer on regeneration medium containing a range of cyanide and SHAM concentrations. White bars, calli mean size at transfer; black bars, calli mean size two weeks after transfer. n= 26-40 calli for each concentration. B, Illustration of calli after complex VI inhibition with 100 μ M of SHAM. Panel 1, calli just after transfer (T_0) on the regeneration medium containing 100 μ M of SHAM; Panel 2, calli two weeks afterwards (T_2) with some turned brown. Scale bar = 3 mm. C, Shoot regeneration rates after complex IV and AOX inhibition in two biological replicates. Inhibitors (cyanide and SHAM) were added to the callus medium (CIM2) one week before their transfer to the shoot induction medium (SIM). Regeneration frequency was estimated four weeks after the callus transfer as the percentage of calli with at least one regenerated shoot.

3. Sources of variability

As shown previously, shoot regeneration frequency varies from an experiment to another for both the inhibitor-treated calli and the mock-control calli. Two experiments were conducted with the aim to explain this variability. First, we analyzed the variability related to the mock control within the same biological repetition but with two independent wild-type (Col-0) seed batches (wt 1 and wt 2). Calli were treated as two types of controls (DMSO mock treatment and water addition), one week before the transfer to the regeneration medium (SIM). Six hours after addition, mock-treated calli and non-treated calli were collected. Callus total ARN was extracted for RT qPCR analysis to measure the level of two transcripts used as oxidative stress markers: *OXII* and *AOX1a*.

In the same culture conditions, calli derived from the two distinct pools of mother plants, but of the same ecotype (Col-0), have a different *in vitro* response (Figure 4.3). When either controls (DMSO and water) were added to the callus liquid medium, explants from wt 1 and wt 2 had a different response: *AOX1a* relative expression was lower in wt 1 but higher in wt 2, compared to the relative expression in the non-treated calli (Figure 4.3 A). The difference in the response of the mock calli is more apparent when we compare *OXII* relative expression in wt 1 and wt 2. In non-treated calli that eventually yield a higher regeneration rate, the controls (DMSO or water) showed an enhanced oxidative signals as we noticed the induction of *OXII* in wt 1 calli, associated with a high regeneration rate (50%) but not wt 2 calli with a lower regeneration rate (18%) (Figure 4.3 B and C).

In the second experiment, we assessed the variability in shoot regeneration rate across independent biological replicates. For this purpose, calli were collected from three experiments one week before the transfer to the regeneration medium and total ARN was extracted for RT qPCR analysis of the same oxidative stress markers: *OXII* and *AOX1a*. Their respective relative transcript level seems to be different between the biological repetitions (Figure 4.4 A and B). Compared to the replicate 1, *AOX1a* mRNA level is higher in replicate 2 and lower in replicate 3 (Figure 4.4 A). For the three biological replicates, the trends are the same between *AOX1a* relative expression and the shoot regeneration rate (Figure 4.4 A and C). We also noticed that *OXII* relative expression is not correlated with *AOX1A* relative expression among the three replicates: both *AOX1A* and *OXII* relative expression are higher in replicate 2 (with highest regeneration rate) compared to replicate 1 whereas in replicate 3

(lowest regeneration rate) *AOX1A* relative expression is lower and *OXII* relative expression is higher compared to replicate 1 (Figure 4.4 A and B).

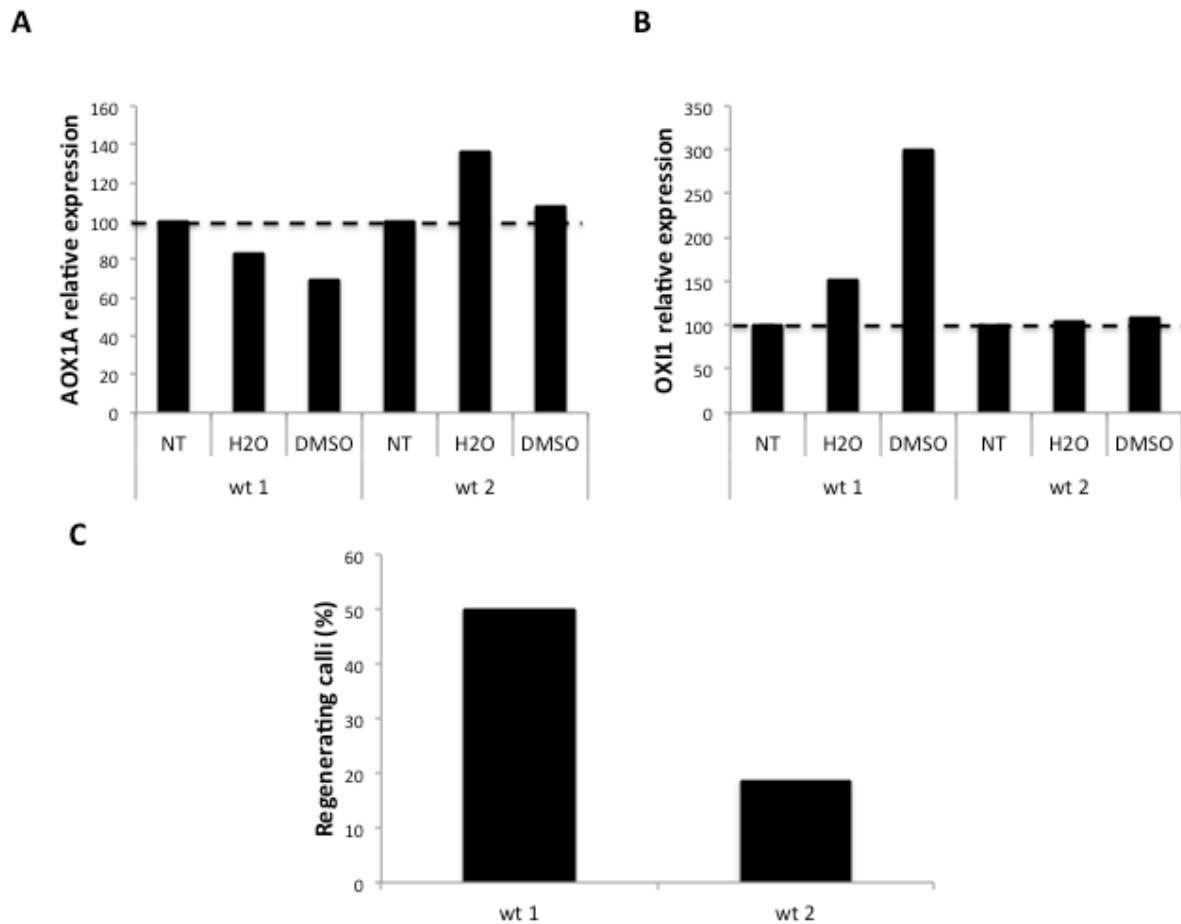


Figure 4.3: *In vitro* induced variations among calli derived from two pools of mother plants (wt 1 and wt 2) of the same ecotype (Col-0). A and B, *AOX1a* and *OXII* relative transcript level 6 hours after the addition of DMSO (mock) or water. DMSO or water was added to the callus liquid culture medium (CIM2) one week before their transfer to the shoot induction medium (SIM). NT: non-treated. C, Shoot regeneration rate of wt 1 and wt 2 non-treated calli. The *in vitro* response was estimated four weeks after transfer to the regeneration medium by calculating the percentage of calli with at least one regenerated shoot. wt: wild type.

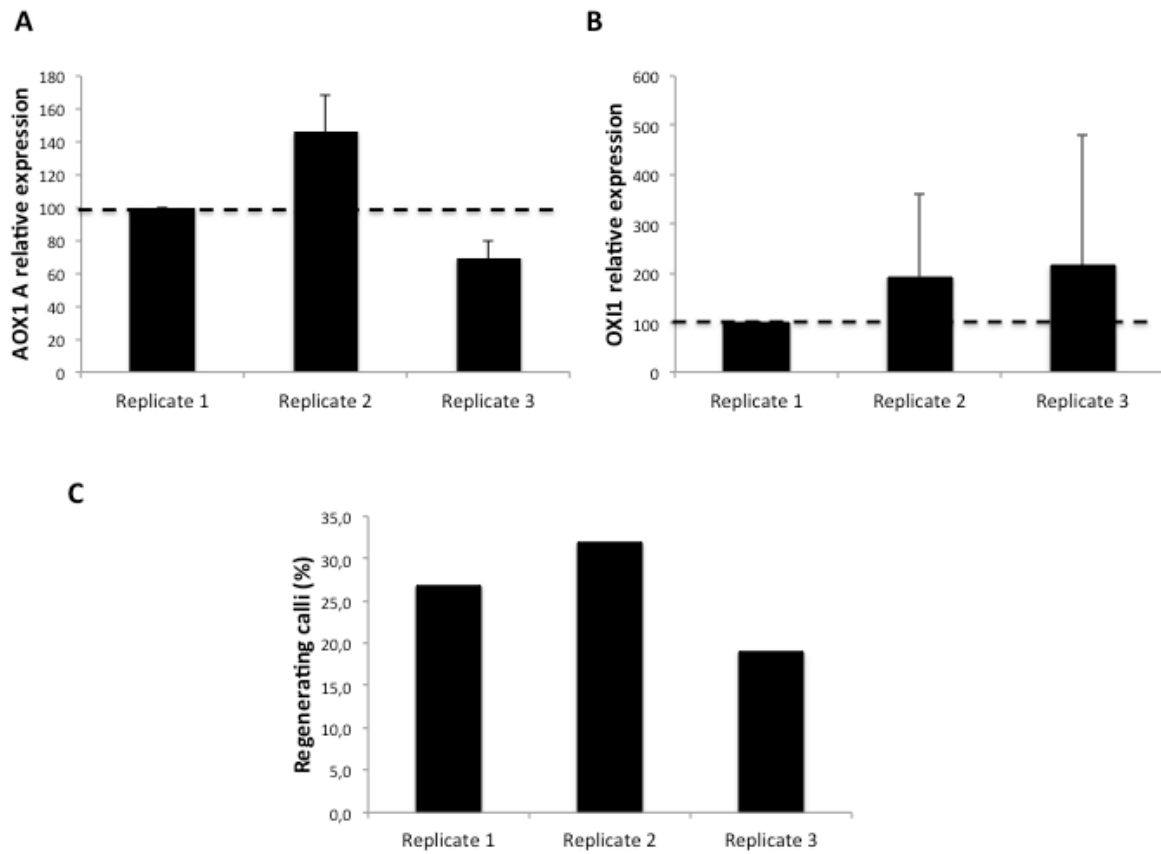


Figure 4.4: *In vitro* induced variation between three biological replicates. A and B, *AOX1a* and *OX11* relative transcript level one week before their transfer to the shoot induction medium (SIM). C, Shoot regeneration frequency four weeks after callus transfer to the regeneration medium. Values represent the percentage of calli with at least one regenerated shoot.

Discussion

The chemical inhibition of the mitochondrial cI one week before the callus transfer to the regeneration medium enhanced *in vitro* shoot regeneration (see Chapter III). To analyze the effect of other mETC inhibitors on *de novo* shoot regeneration, protoplast-derived calli were treated one week before the transfer to the regeneration medium with several concentrations of two specific inhibitors: cyanide to inhibit the mitochondrial complex IV, and SHAM to inhibit the AOX. These concentrations were chosen because they had an impact on callus growth but were not unambiguously lethal (Figure 4.2 B). mETC inhibition with cyanide and SHAM enhanced shoot regeneration rate in certain experiments and at given concentrations. However, the resulting *in vitro* response varied from one biological replicate to another (Figure 4.2 C). Inhibition of the complex IV with cyanide or of AOX with SHAM does induce ROS production (Schwarzländer et al., 2009). The observed shoot regeneration enhancement may thus be due to the induced oxidative stress after callus treatment with the inhibitors. The implication of AOX in another aspect of shoot development was previously reported in *Arabidopsis* seedlings as *AOX1a* seemed to have a potential role in the acclimation of shoots to low temperature (Fiorani et al., 2005).

During my PhD project, we observed variability in callus *in vitro* response between experiments for the same accession (Columbia O), either in the shoot regeneration rate of controls and in calli treated with inhibitors. As an attempt to explain this variability, we analyzed the expression of two markers of oxidative stress in calli sampled 6 hours after the addition of two controls (water and DMSO) to the liquid medium. Calli were derived from two pools of mother plants and cultivated side by side in the same conditions. We did not succeed to find a clear relationship between the factors analyzed (*AOX1a* and *OXII* transcript levels versus regeneration rate) that could point to the potential source of the observed variability, for example as an indirect indicator of the physiological state of the explants when additions were made to the liquid culture medium. However, we cannot exclude that the cellular redox state of the callus cell populations, that we have shown is quite heterogeneous even within a single callus, may be one of the decisive factors in the explant *in vitro* response that eventually leads to shoot regeneration.

We suppose that the observed variability in shoot regeneration after calli treatment with respiratory inhibitors depends on the callus redox state. Based on our observations, we propose that the optimal rotenone concentration leading to the best regeneration rate should

induce a moderate oxidative stress, sufficient to boost regeneration but not too high and thereby avoiding cytotoxicity that would affect cell viability (Figure 4.5).

We reported in Chapter II that tissues derived from cI mutants, that produce on average smaller calli, are characterized by a high regeneration frequency than wild type tissues. This observation led us to analyze the potential effect of callus size at the time of transfer to the regeneration medium on the regeneration frequency. To investigate a potential relationship, calli with different sizes were tracked across the regeneration sequence and our analysis revealed that there is no significant correlation between callus size at transfer and shoot regeneration rate observed four weeks after transfer. However, the effect of callus size on plant regeneration was reported in another study relative to regeneration through somatic embryogenesis of several rice cultivars. In this case, small callus pieces regenerated better than bigger ones (Peterson and Smith, 1990). Thus, the effect of callus size on regeneration rate may be variable depending on species, regeneration mode, or experimental setup.

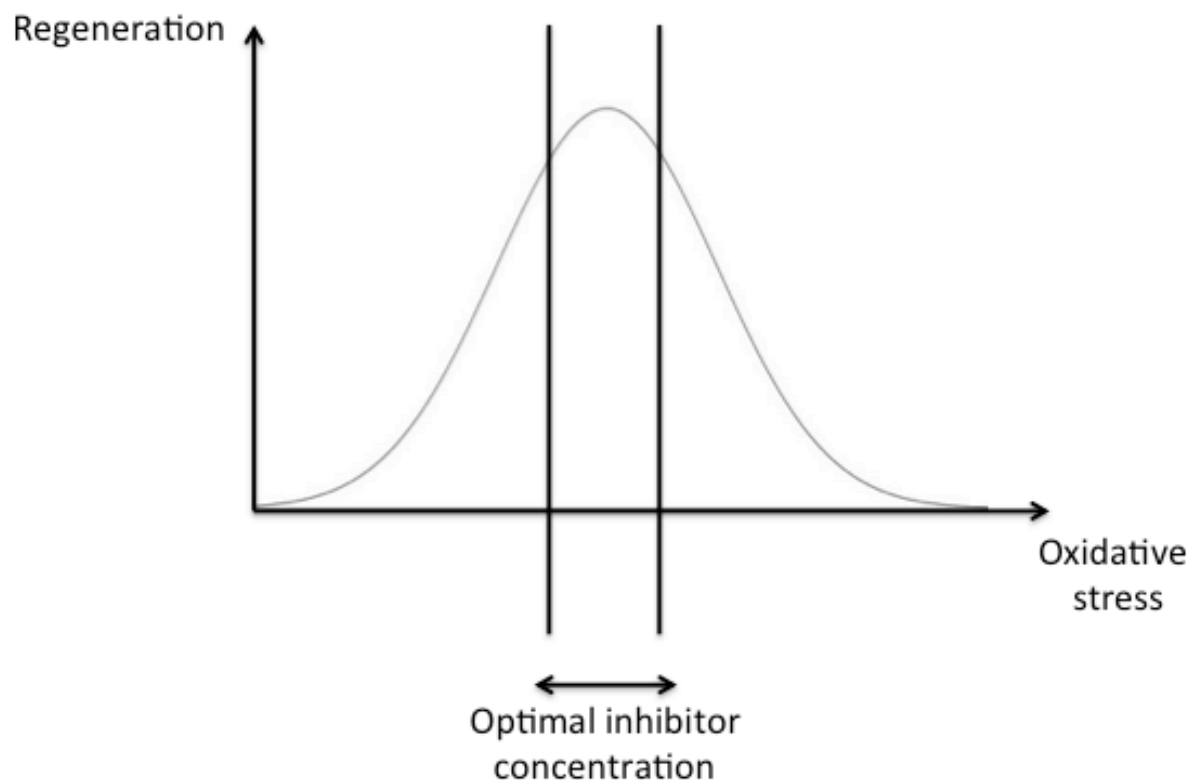


Figure 4.5: Hypothetical relationship between inhibitor-mediated oxidative stress and *in vitro* shoot regeneration.

Materials and methods

Plant material

Seeds were surface sterilized as described previously and sown on 70 ml of germination medium in green-boxes (Kalys). After 2 days at 4 °C, boxes were transferred in a growth chamber (Biolux tubes, light intensity $\sim 60 \mu\text{Es/s}^{-1}.\text{m}^2$) under a 10 h light / 14 h dark cycle, 70% relative air humidity (RH), at 20 °C.

Protoplast preparation, callus induction and shoot regeneration

Protoplast isolation, callus culture and shoot regeneration were conducted as described in Chapters II and III.

Inhibitors preparation and application

Cyanide was used to inhibit the mitochondrial complex IV and salicylhydroxamic acid (SHAM) to inhibit the alternative oxidase (AOX). Inhibitors were freshly prepared before addition in the callus liquid medium (CIM2). The cyanide powder was dissolved and diluted in water and the SHAM powder in dimethyl sulfoxide (DMSO). Diluted solutions were then added to the cell culture medium at a final concentration of 25, 50, 100, 200 and 400 μM for cyanide and 6.25, 12.5, 25, 50 and 100 μM for SHAM. Inhibitors were either added to the regeneration medium before it gelled or applied in the liquid callus medium one week before the callus transfer to the inhibitor-free regeneration medium.

Cell growth quantification

For callus growth analysis, explant size was measured just after the transfer on the regeneration medium and two weeks afterwards. The callus projected area was measured on images of the Petri dishes obtained with a flatbed scanner (Epson Perfection V800 Photo scanner) with the ImageJ64 software.

Total RNA isolation and RT qPCR analysis

The total RNA was extracted with an RNeasy Plant mini kit (QIAGEN), including the DNase step using the DNaseI kit according to the manufacturer's instructions (QIAGEN). For each sample, total RNA was prepared from pooled calli collected from one Petri dish one week before the transfer to the regeneration medium to investigate the variability between biological replicates and the mock-induced variability. One microgram of total RNA was reverse-transcribed with Superscript II (Invitrogen). Quantitative Real Time RT qPCR was performed in 96-well plates, including three technical replicates, on a Bio-Rad CFX Connect Real-Time system (Bio-Rad) and with the SYBR Green Supermix (Bio-Rad). AT5G13440 was used as house-keeping reference gene and the delta-delta CT ($2^{-\Delta\Delta CT}$) method was used for the quantification of mRNA levels. The non-treated calli and the replicate 1 were arbitrarily chosen as the 100% reference for the normalization of the marker's relative expression. Primers for RT qPCR are listed in Supplemental Table 1.

References

- Chen CC, Agrawal DC, Lee MR, Lee RJ, Kuo CL, Wu CR, Tsay HS, Chang HC (2016)** Influence of LED light spectra on in vitro somatic embryogenesis and LC-MS analysis of chlorogenic acid and rutin in *Peucedanum japonicum* Thunb.: A medicinal herb. *Bot Stud.* doi: 10.1186/s40529-016-0124-z
- Fiorani F, Umbach AL, Siedow JN (2005)** The Alternative Oxidase of Plant Mitochondria Is Involved in the Acclimation of Shoot Growth at Low Temperature. A Study of *Arabidopsis* AOX1a Transgenic Plants. *Plant Physiol* **139**: 1795–1805
- Motte H, Vercauteren A, Depuydt S, Landschoot S, Geelen D, Werbrouck S, Goormachtig S, Vuylsteke M, Vereecke D (2014)** Combining linkage and association mapping identifies RECEPTOR-LIKE PROTEIN KINASE1 as an essential *Arabidopsis* shoot regeneration gene. *Proc Natl Acad Sci* **111**: 8305–8310
- Peterson G, Smith R (1990)** Effect of abscisic acid and callus size on regeneration of american and international rice varieties. *Plant Cell Rep* **10**: 35–38
- Schwarzländer M, Fricker MD, Sweetlove LJ (2009)** Monitoring the in vivo redox state of plant mitochondria: Effect of respiratory inhibitors, abiotic stress and assessment of recovery from oxidative challenge. *Biochim Biophys Acta - Bioenerg* **1787**: 468–475
- Sugiyama M (2015)** Historical review of research on plant cell dedifferentiation. *J Plant Res* **128**: 349–359

Chapter 5:
Transcriptional landscape of
***in vitro* caulogenesis**

Introduction

Before the emergence of *Arabidopsis thaliana* as a model plant in the 80s, genetic resources to study the molecular mechanisms underlying plant regeneration were scarce (Sugiyama, 2013). In another shift, many studies have been published in the last decades describing developmental processes with microarrays and RNAseq approaches.

In our framework, several studies analyzed gene expression profiles after chemical inhibition of mETC in *Arabidopsis* (Clifton et al., 2005; Garmier et al., 2008; Ho et al., 2008). Rotenone, the most common cI inhibitor, was used by Garmier and collaborators (Garmier et al., 2008) to study plant cell adaptation following cI inhibition in *Arabidopsis* cell suspension. The chemical inhibition of cI induced the activation of the plant alternative respiratory pathway and reduced cell growth. To complement the transcriptomic results, a metabolomic and proteomic analysis revealed an alteration in glycolytic activities and tricarboxylic acid cycle after rotenone treatment (Garmier et al., 2008).

A comparative meta-analysis of 11 microarray datasets was performed by Schwarzländer and co-workers (Schwarzländer et al., 2012) to unravel mitochondrial signaling during respiratory impairment in *Arabidopsis* cell culture, rosettes, leaves and flowers. In this study, mitochondrial perturbations concerned respiratory pathway complexes inhibition by rotenone (complex I, cI), antimycin A (complex III, cIII) and oligomycin (ATP-synthase), as well as mutants affected in mitochondrial functions including mitochondrial ROS scavenger MnSOD mutant (*msd1*), cI mutants (*ndufa1*, *ndufs4*), ATP synthase mutants (AP3-uATP9, AP9-uATP9) and an alternative oxidase mutant (*aox1a*). This analysis revealed the co-regulation of three main biological modules: photosynthesis, plant-pathogen interactions and proteins synthesis (Schwarzländer et al., 2012).

With the goal to explain how cI dysfunction promotes shoot meristem initiation, we characterized the transcriptional response associated with the transfer on SIM medium following cI inhibition by rotenone and in two mitochondrial cI mutants. Even though previous studies analyzed the effect of cI mutations and rotenone applications in plant tissues, we repeated this analysis in our experimental system and confirmed that the overall consequences of cI impairment, caused either genetically or chemically, are conserved in protoplast-derived calli. We also compared the physiological state of plant tissues cultured *in vitro* in which cI activity is constantly compromised (in the mutants) to tissues in which cI activity is transiently inhibited (following rotenone treatment). Finally, we characterized the initial transcriptional response of calli transferred to shoot inducing medium and observed that

this step of the regeneration protocol causes a massive genetic reprogramming in all conditions examined. Rotenone pretreatments did affect to a certain extent the following transfer response. But the cI mutant tissue response to the transfer was markedly different, suggesting that cI constitutive impairment may better shield the explants from the shock inherent to transfer between media.

Materials and methods

Plant material and growth conditions

CI mutants *mtsfl* (*mtsfl-1*, N654650) (Haïli et al., 2013) and *mtl1* (*mtl1-1*, N539066) (Haïli et al., 2016) derive from the *Arabidopsis thaliana* Columbia accession (Col-0). Seeds were surface sterilized as described by Chupeau *et al.* (2013) and sown on 70 ml of germination medium in green-boxes. After two days of seed stratification at 4°C, green-boxes were transferred to a growth chamber with Biolux tubes displaying light intensity around 60 $\mu\text{Es/s}^{-1}.\text{m}^2$, with a 10 h light / 14 h dark cycle, 70% relative air humidity (RH) and 20 °C.

Protoplasting and callus culture were conducted as described in Chapter 2.

Rotenone application

Based on the results obtained in chapter 3, we used two rotenone concentrations to inhibit the mitochondrial cI: 5 μM and 10 μM . To avoid *in vitro* variability, 6 independent experiments were conducted using both concentrations and two independent experiments (biological duplicates) were selected for this study because they yielded a high rotenone-induced caulogenesis rate. Rotenone was freshly prepared before each experiment in Dimethyl sulfoxide (DMSO) at 10 mM. Diluted rotenone solutions were then added to the callus culture medium (CIM2) one week before callus transfer to the regeneration medium (SIM).

Total RNA isolation and microarray analysis

The total RNA was extracted with an RNeasy Plant mini kit (QIAGEN) including a DNase step using DNaseI kit according to the manufacturer's instructions (QIAGEN). For the transcriptomic analysis of cI mutants (*mtl1*, *mtsfl*) and wild-type calli, total RNA was isolated at two time points: just before transfer (*mtl1*_{7D}, *mtsfl*_{7D} and *wt*_{7D}) and 12 hours afterwards (*mtl1*_{7.5D}, *mtsfl*_{7.5D} and *wt*_{7.5D}). For cI chemical inhibition, rotenone was added one week before transfer to the regeneration medium and the callus total RNA was isolated for treated calli (T) and a DMSO control (C) at the following time-points: C₀, just before addition of rotenone; T_{12H}, 12 hours after rotenone treatment; before transfer corresponding to 7 days

after rotenone treatment for treated calli (T_{7D}) and control calli (C_{7D}) and finally 12h after the transfer on rotenone-free regeneration medium (T_{7.5D} and C_{7.5D} for treated and control calli respectively) (Figure 1).

RNA integrity was analyzed with the Agilent Bioanalyzer. Microarray analysis was conducted in collaboration with the IPS2 (Institute of Plant Sciences 2) POPS transcriptomic platform using CATMAv7 AGILENT arrays (Crow et al., 2003; Hilson et al., 2004). For both the treatment and genotype comparison subsets, transcript profiles were compared from two biological repetitions. In addition, each pair-wise comparison was performed as a technical dye-swap duplicate. Differential gene expression values were normalized and statistically validated with Bonferroni correction and Benjamini–Hochberg procedure and expressed as log₂-transformed ratios. Differentially expressed genes (DEGs) were listed with their normalized mean ratio and P-value ($P < 0.05$) for each gene.

Gene ontology (GO) enrichment analysis

DEGs with Bonferroni P-value < 0.05 were classified based on their associated biological process with the enrichment analysis tool of the gene ontology consortium (GOC) <http://www.geneontology.org/page/go-enrichment-analysis>. The enrichment analysis identifies GO terms that are either over-represented or under-represented among the up-regulated (or down-regulated) DEGs. GOC is connected to the PANTHER Classification System that provides up to date GO annotations (Mi et al., 2013; Mi et al., 2017). The graphical overview of functional classifications (biological process, molecular function and cellular component) was generated with the BAR classification SuperViewer (http://bar.utoronto.ca/ntools/cgi-bin/ntools_classification_superviewer.cgi) (Provar and Tong, 2003) based on Arabidopsis GO Classification from TAIR (ATH_GO_GOSLIM.20120925.txt).

MapMan analysis

Trends according to biological processes were visualized with the MapMan software (v10) based on the provided pathway and bin representation (Thimm et al., 2004).

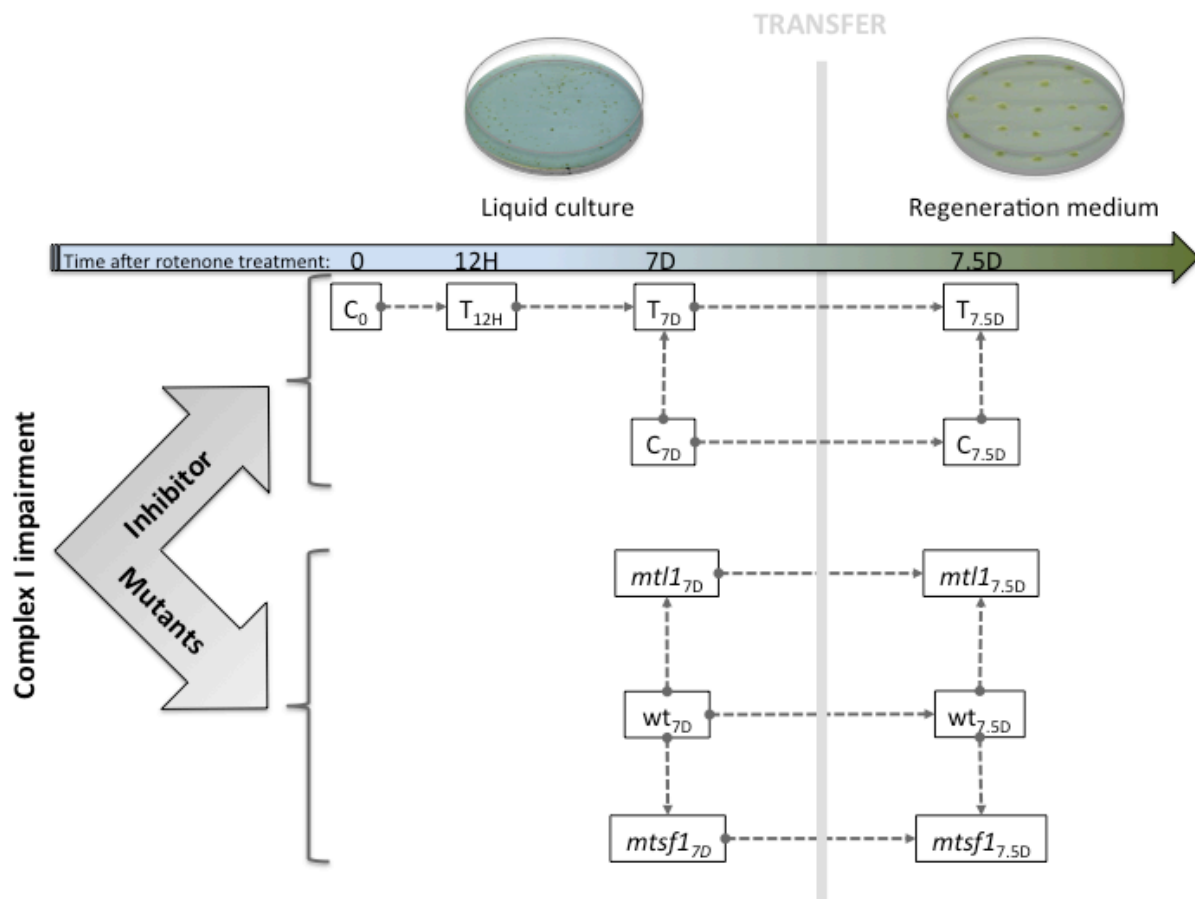


Figure 5.1: Representation of the experimental setup showing treatments, genotypes and time points characterized through microarray transcriptome analysis. Rotenone treatments, T; DMSO mock control, C; cI mutant calli, *mtsfl* and *mtsfl*, respectively; wild type, wt. Six samples were prepared for callus response analysis following rotenone addition to the liquid culture medium (CIM1): C₀, control before rotenone treatment; T_{12H}, 12 hours after treatment with rotenone; T_{7D}, 7 days after rotenone treatment and before transfer; C_{7D}, DMSO control before transfer; T_{7.5D}, 12 hours after transfer of rotenone-treated calli on regeneration medium (SIM); C_{7.5D}, 12 hours after transfer of control calli. Six samples were prepared for analysis for the cI mutants *mtsfl* and *mtsfl*: before transfer (*mtsfl*_{7D} and *mtsfl*_{7D}); 12 hours after transfer (*mtI1*_{7.5D} and *mtI1*_{7.5D}) and the wild type calli (wt_{7D}, prior to transfer; wt_{7.5D}, 12h after the transfer). Dotted arrows represent the direction of pair-wise comparisons.

Results and discussion

Experimental set up

Rotenone treatment

First, we analyzed with CATMA v7 microarrays which biological processes were affected after cI chemical inhibition by comparing the over-represented biological processes among differentially expressed genes (DEGs) between either rotenone-treated calli (T) and DMSO mock control (C), as well as treated calli at successive time points in the regeneration series (Figure 5.1). In this context, "7 days after rotenone treatment" corresponds to the moment before callus transfer to the regeneration medium (SIM) and "7.5 days" corresponds to 12 hours after transfer and provides information about the early response to the transfer. To harmonize data point names across all experiments, the time-point denominations were as follows: the 7D suffix indicates samples before transfer and the "7.5D" suffix indicates 12 hours after transfer.

Six pairwise comparisons were conducted to study the effect of rotenone in our callus regeneration system:

- three comparisons before the callus transfer to the regeneration medium, i.e. when calli were in liquid culture (CIM2): control calli before treatment versus calli 12 hours after rotenone-treatment (C_0 vs T_{12H}), providing information about the early response to rotenone; calli 12 hours after treatment versus calli 7 days after treatment (T_{12H} vs T_{7D}), to compare the early response to rotenone and the state of the calli after a long exposure to the inhibitor; and calli 7 days after the treatment versus control calli at 7 days (T_{7D} vs C_{7D}), to compare untreated tissues to tissues after a long exposure to the inhibitor;
- two comparisons involving the transfer: calli 7 days after rotenone-treatment versus 7.5 days after the treatment (T_{7D} vs $T_{7.5D}$) and control calli at 7 days versus control calli at 7.5 days (C_{7D} vs $C_{7.5D}$), to investigate how a prior rotenone treatment affects gene expression changes induced by the transfer;
- finally, one comparison 12 hours after transfer: calli 7.5 days after rotenone treatment versus control calli at 7.5 days ($T_{7.5D}$ vs $C_{7.5D}$), to complement the analysis of the transfer-induced changes performed in rotenone-treated and untreated calli separately.

Mutants

In addition, we compared the over-represented biological processes among DEGs between two cI mutants (*mtsfl* and *mtl1*) and wild type (wt), before and after callus transfer to the regeneration medium. These two mutants were selected because shoot initiation was markedly promoted in calli derived from either genotype, although *mtsfl* displayed a stronger growth defect.

Seven pairwise comparisons were conducted between cI mutants and wild type:

- two before transfer: *mtl1* calli versus wild type calli (*mtl1*_{7D} vs wt_{7D}) and *mtsfl* calli versus wild type calli (*mtsfl*_{7D} vs wt_{7D}), to compare the state of proliferating calli according to their genotype;
- three comparisons during the transfer: *mtl1*_{7D} vs *mtl1*_{7.5D}, *mtsfl*_{7D} vs *mtsfl*_{7.5D} and wt_{7D} vs wt_{7.5D}; to investigate how a genetic cI dysfunction affects gene expression changes induced by the transfer;
- finally, two comparisons 12 hours after transfer: *mtl1*_{7.5D} vs wt_{7.5D} and *mtsfl*_{7.5D} vs wt_{7.5D}, to complement the analysis of the transfer-induced changes performed in the separate genotypes.

Table 5.1: Number of differentially expressed genes (DEGs) for each pair-wise comparison.

Rotenone treatments	C ₀ vs T _{12H}	C _{7D} vs T _{7D}	T _{12H} vs T _{7D}	C _{7D} vs C _{7.5D}	T _{7D} vs T _{7.5D}	C _{7.5D} vs T _{7.5D}
Down-regulated	223	89	214	2419	2273	54
Up-regulated	220	195	302	2285	2137	20
Total de-regulated	443	284	516	4704	4410	74

Complex I mutants	wt _{7D} vs mtl _{17D}	wt _{7D} vs mtsf _{17D}	wt _{7D} vs wt _{7.5D}	mtl _{17D} vs mtl _{17.5D}	mtsf _{17D} vs mtsf _{17.5D}	wt _{7.5D} vs mtl _{17.5D}	wt _{7.5D} vs mtsf _{17.5D}
Down-regulated	642	738	1674	1020	659	541	283
Up-regulated	671	690	1773	848	607	474	247
Total de-regulated	1313	1428	3447	1868	1266	1015	530

See Figure 5.1 for the orientation of the pair-wise comparison.

CI rotenone inhibition reduces the mitotic activity of proliferating protoplast-derived calli and induces genes associated with stress and hormone signaling

Twelve hours after cI inhibition by rotenone (C₀ vs T_{12H}), 443 genes were differentially expressed between the control and treated calli (223 down-regulated and 220 up-regulated) (Table 5.1). Seven days after rotenone treatment, 284 genes were differentially expressed between treated calli and the control (T_{7D} vs C_{7D}) (89 down, 195 up), whereas 516 genes were differentially expressed between treated calli at 7 days after treatment and treated calli 12 hours after treatment (T_{12H} vs T_{7D}) (214 down, 302 up). Thus, calli evolve after the initial exposure to rotenone as classically observed following non-lethal perturbations.

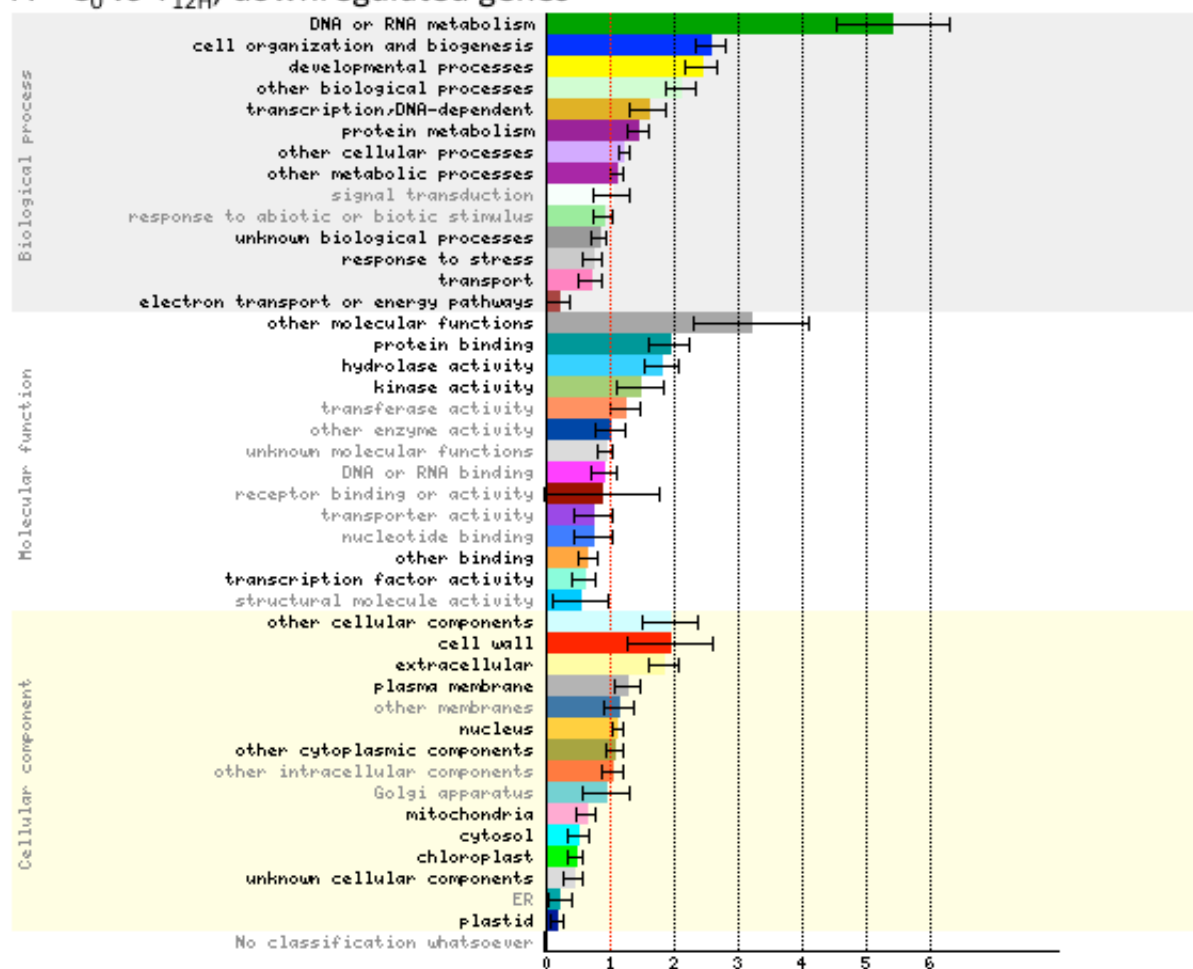
To investigate the early (12 hours after rotenone treatment) and late (7 days after rotenone treatment) responses to cI inhibition, we searched for GO term enrichment in either down- or up-regulated DEGs in each pair-wise comparisons. Twelve hours after rotenone treatment, repressed genes pointed to the shutdown of DNA and RNA metabolism (P-value= $7.955 \cdot 10^{-16}$), cell organization and biogenesis (P-value= $4.033 \cdot 10^{-14}$) and developmental processes (P-value= $3.41010 \cdot 10^{-13}$) (Figure 5.2 A). Three genes in particular were found in these biological process categories: cyclin A1.1 (*CYCA1.1*), cyclin-dependent kinase B1.1 (*CDKB1.1*) and cyclin-dependent kinase B2.2 (*CDKB2.2*). *CYCA1* is related to the regulation of DNA replication (GO:0006275), histone phosphorylation (GO:0016572) and cell proliferation (GO:0008283). *CDKB1.1* is related to DNA endo-reduplication (GO:0042023) and uni-dimensional cell growth (GO:0009826). Finally, *CDKB2.2* is related to cell

proliferation (GO:0008283), DNA endo-reduplication (GO:0042023), regulation of DNA replication (GO:0006275), regulation of DNA replication (GO:0006275) and nuclear division (GO:0000280) (Figure 5.2 B). The down-regulation of these genes indicates a repressive effect of rotenone on cell division.

DEGs up-regulated 12 hours after rotenone treatment point to response to stress (P-value= $5.091 \cdot 10^{-26}$) and to abiotic or biotic stimulus (P-value= $1.522 \cdot 10^{-22}$) (Figure 5.2 C). Common genes in these two classes are related to: oxidative stress (regulation of hydrogen peroxide metabolic process, GO:0010310), e.g. cytochrome P450 (*CYP71A13*); detoxification (toxin catabolic process, GO:0009407), e.g. glutathione S-transferase F3 (*GSTF3*); and hormone signaling (response to gibberellin, GO:0009739; response to jasmonic acid, GO:0009753; response to ethylene, GO:0009723; response to abscisic acid, GO:0009737; response to auxin, GO:0009733 and salicylic acid mediated signaling pathway, GO:0009862) (Figure 5.2 D).

After one week of rotenone treatment, 205 genes were exclusively down-regulated as identified in T_{7D} vs T_{12H} (Figure 5.2 E). These genes are related to response to stimuli and response to stress (GO:0006950) with highly significant P-Value ($2.37 \cdot 10^{-23}$ and $3.24 \cdot 10^{-18}$, respectively). We noticed that the most induced biological processes in the early rotenone response (12 hours after treatment) were repressed 7 days later (Figure 5.2 G and H), for example response to stimuli and response to stress, suggesting again an adaptation of calli to cI inhibition.

A C_0 vs T_{12H} downregulated genes



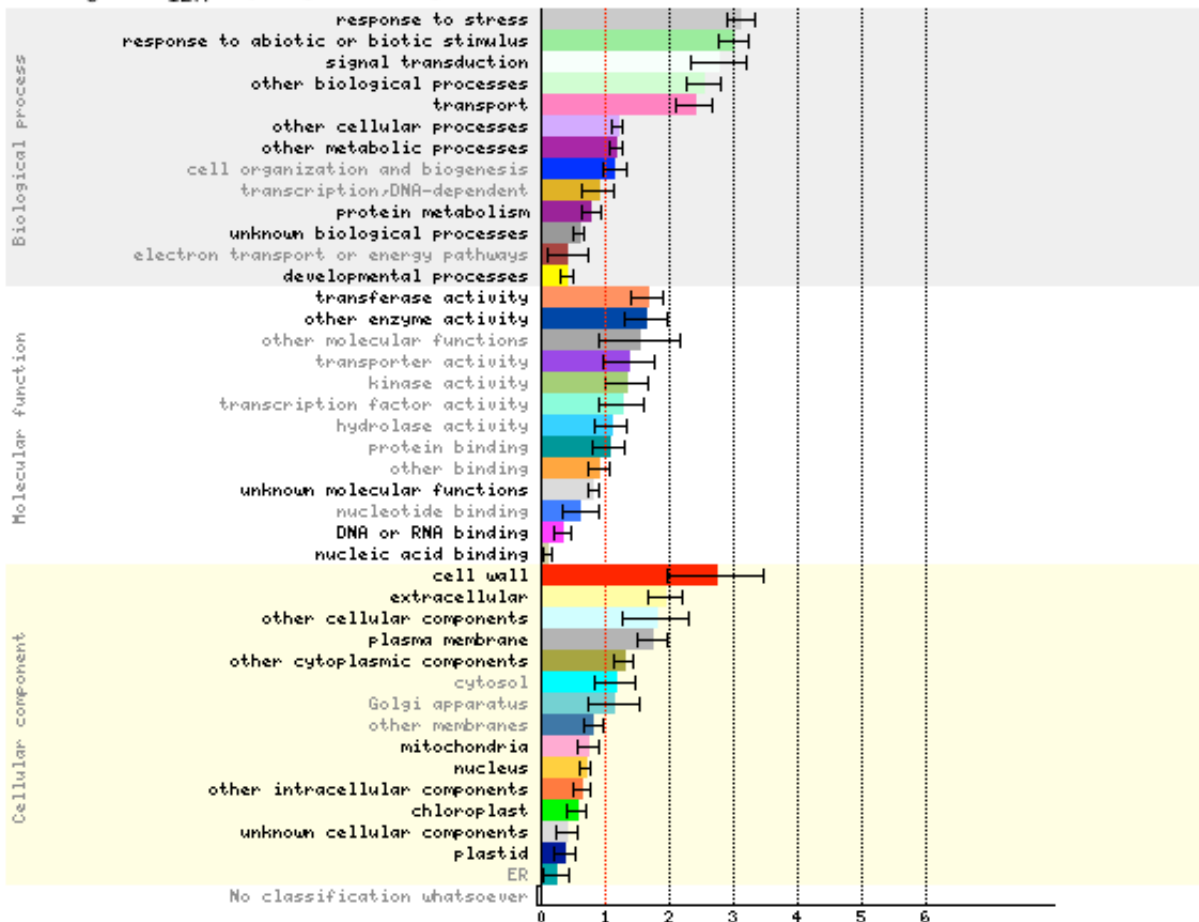
B

Gene ID	Biological processes	Annotation	Class and subcategory
At1g44110		CYCA1;1 (Cyclin A1;1)	[GO:0006275] regulation of DNA replication [GO:0016572] histone phosphorylation [GO:0008283] cell proliferation
At3g54180		CDKB1;1 (Cyclin-dependent kinase B1;1)	[GO:0042023] DNA endoreduplication [GO:0009826] unidimensional cell growth [GO:0008283] cell proliferation
At1g20930		CDKB2;2 (cyclin-dependent kinase B2;2)	[GO:0042023] DNA endoreduplication [GO:0006275] regulation of DNA replication [GO:0000280] nuclear division

Figure 5.2: Early and late responses to cI rotenone inhibition.

A, gene ontology (GO) enrichment in biological processes, molecular function and cellular components of down-regulated DEGs 12 hours after rotenone treatment as identified in C_0 vs T_{12H} comparison (early response). A ranking score is calculated for each functional class. The annotations in bold have $P < 0.05$. Bars indicate standard deviation from 100 bootstraps. Red dotted line indicates score of 1; values over 1 show over-representation and values under 1 show under-representation. B, Cell division is repressed 12 hours after rotenone inhibition of the mitochondrial cI. Colour key for biological processes is as in A. Results were obtained with the BAR classification SuperViewer.

C C₀ vs T_{12H} upregulated genes



D

Gene ID	Class and subcategory	Annotation
At2g25735	[GO:0006979] response to oxidative stress	
At1g17860, At1g17870	[GO:0042542] response to hydrogen peroxide	
At2g30770	[GO:0010310] regulation of hydrogen peroxide metabolic process	CYP71A13 (cytochrome P450, family 71, subfamily A, polypeptide)
At2g02930	[GO:0009407] toxin catabolic process	ATGSTF3 (glutathione S-transferase F3)
At1g72900	[GO:0009862] systemic acquired resistance, salicylic acid mediated signaling pathway	Toll-Interleukin-Resistance (TIR) domain-containing protein
At2g30250		ATWRKY25 (WRKY DNA-binding protein 25)
At2g40750		ATWRKY54 (WRKY DNA-binding protein 54)
At5g66880, At5g66890	[GO:0009739] response to gibberellin	
At1g71697, At1g71700	[GO:0009753] response to jasmonic acid	
At2g43000	[GO:0009723] response to ethylene	NAC042 (NAC domain containing protein 42)
At3g50260	[GO:0009737] response to abscisic acid	CEJ1 (cooperatively regulated by ethylene and jasmonate 1)
At5g54500	[GO:0009733] response to auxin	FQR1 (flavodoxin-like quinone reductase 1)

Figure 5.2: Early and late responses to complex I rotenone inhibition. [continued]

C, gene ontology (GO) enrichment in biological processes, molecular function and cellular components of up-regulated DEGs 12 hours after rotenone treatment as identified in C₀ vs T_{12H} comparison (early response). A ranking score is calculated for each functional class. The annotations in bold have P<0.05. Bars indicate standard deviation from 100 bootstraps after class score normalization. Red dotted line indicates score of 1; values over 1 show over-representation and values under 1 show under-representation. D, cI inhibition induces an oxidative stress and diverse hormonal responses. Results were obtained with the BAR classification SuperViewer.

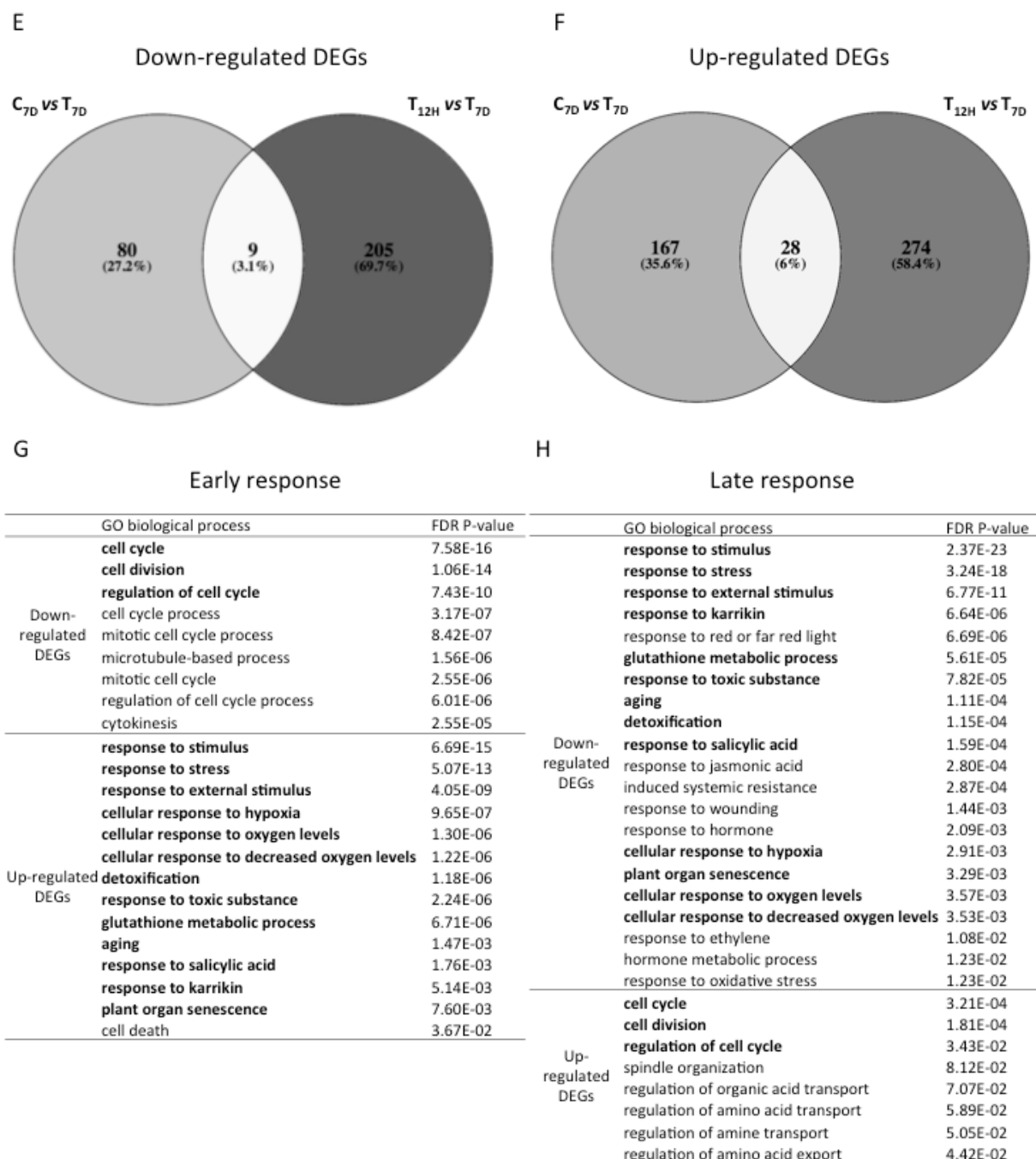


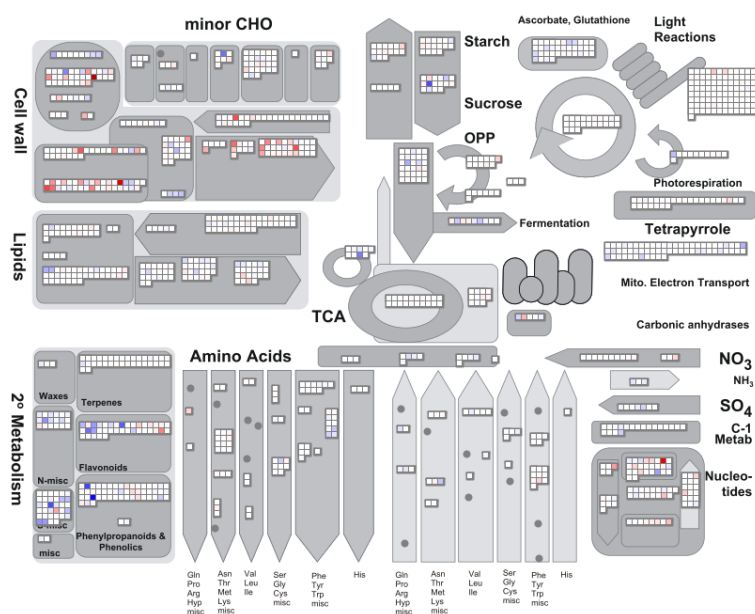
Figure 5.2: Early and late responses to complex I rotenone inhibition. [continued]

E and F, analysis of late response to cI inhibition; E, Venn diagram showing overlap between down-regulated genes identified in the C_{7D} vs T_{7D} and T_{12H} vs T_{7D} comparisons. F, Venn diagram showing overlap between up-regulated genes identified in the C_{7D} vs T_{7D} and T_{12H} vs T_{7D} comparisons. G, over-represented biological processes of up- and down-regulated DEGs identified in C_0 vs T_{12H} comparison (early response). H, over-represented biological processes of up- and down-regulated DEGs identified exclusively in T_{12H} vs T_{7D} comparison (late response) extracted from E (205 down-regulated DEGs) and F (274 up-regulated DEGs). Common biological processes are in bold. DEGs were classified using Panther classification system for biological process. Represented lists are not exhaustive. C_0 , control before

treatment; T_{12H}, 12 hours after rotenone treatment; T_{7D}, 7 days after rotenone treatment; C_{7D}, DMSO control after 7 days.

Similar trends can be visualized when mapping gene expression changes corresponding to early or late rotenone response on MapMan overview drawings. Rotenone treatments result in changes in genes involved in metabolism with notably rapid down-regulation in cell wall processes and later up-regulation in tetrapyrrole biosynthesis (Figure 5.3). Rotenone also deregulates genes associated with cell responses, with different early and late patterns (Figure 5.4).

Early rotenone response



Late rotenone response

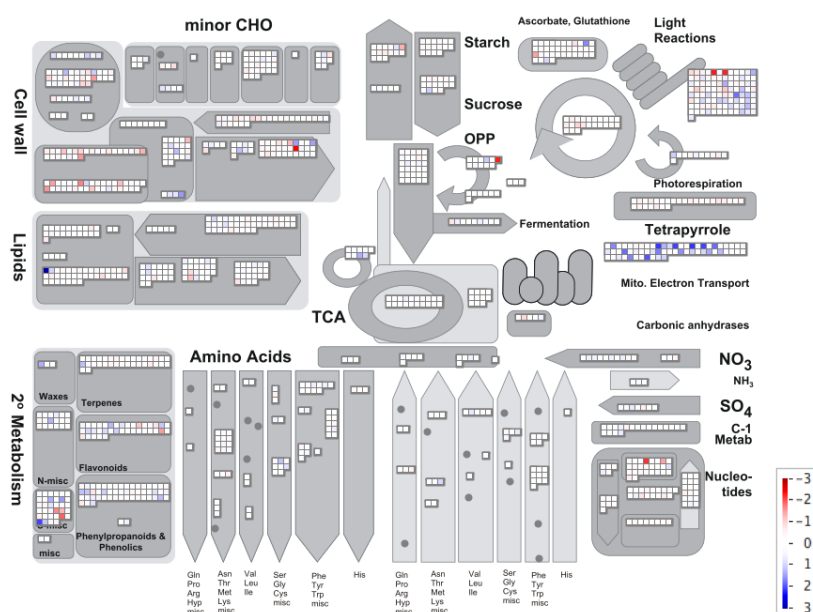


Figure 5.3: Transcriptional signature of metabolism genes in rotenone treated calli. Callus response 12 hours or 7 days after rotenone addition to the liquid medium (CIM2). Blue, upregulated genes, red downregulated genes. The direction of pair-wise comparisons are as indicated in Figure 5.1.

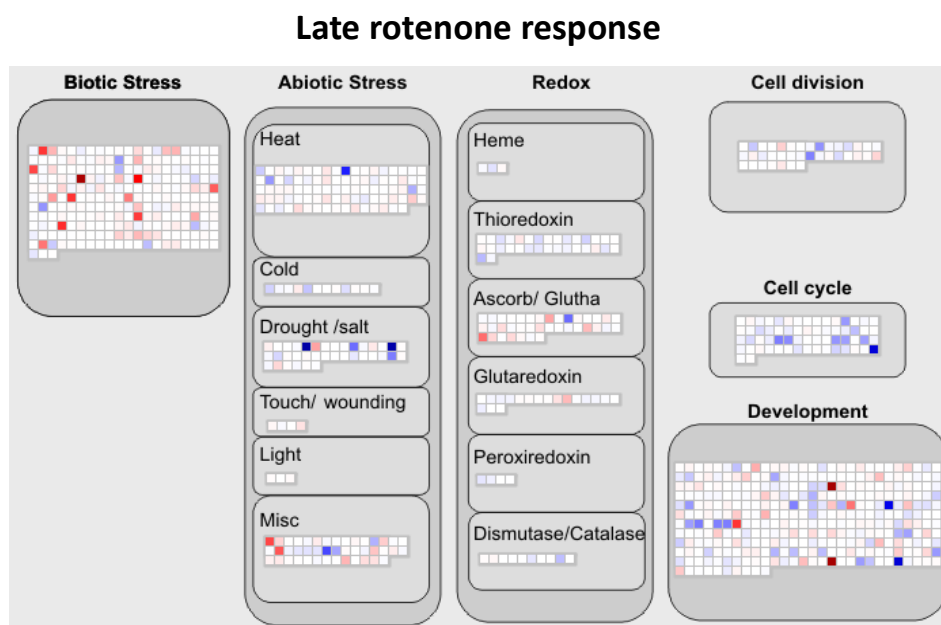
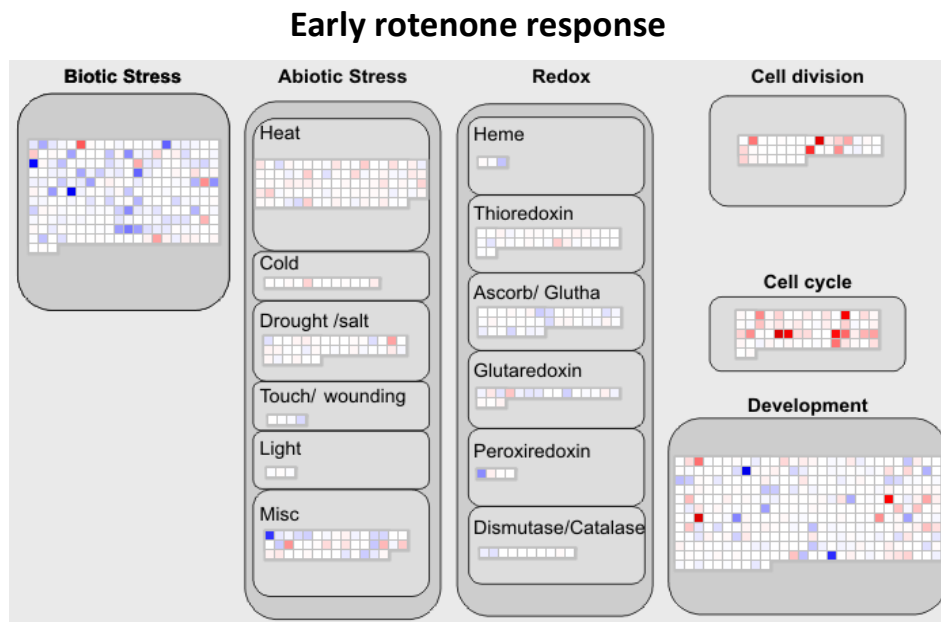


Figure 5.4. Transcriptional signature of cell response genes in rotenone treated calli. Callus response 12 hours or 7 days after rotenone addition to the liquid medium (CIM2). Blue, upregulated genes, red downregulated genes. The direction of pair-wise comparisons are as indicated in Figure 5.1.

Proliferating cI mutant calli *mtl1* and *mtsfl* are affected in photosynthesis, oxidative stress and hormonal responses

When comparing cI mutant calli growing in liquid culture (CIM2) to wild type, 1313 genes were identified as differentially expressed in *mtl1* (*mtl1*_{7D} vs *wt*_{7D}) (642 down, 671 up) and some more genes were differentially expressed (1428) in *mtsfl* (*mtsfl*_{7D} vs *wt*_{7D}) (738 down, 690 up) (Table 5.1). Although DEG numbers are not vastly different between the two pair-wise comparisons, the slightly larger differential observed between *mtsfl* and wild type may reflect the stronger growth impairment phenotype of *mtsfl* compared to *mtl1*.

Considering overlapping DEGs, 510 genes were down regulated in both cI mutants (*mtl1*_{7D} and *mtsfl*_{7D}) compared to the wild type (*wt*_{7D}); 132 were exclusively down-regulated in *wt*_{7D} vs *mtl1*_{7D}; and 228 DEGs were exclusively down-regulated in *wt*_{7D} vs *mtsfl*_{7D} (Figure 5.5 A). 545 DEGs were down-regulated in common between *wt*_{7D} vs *mtl1*_{7D} and *wt*_{7D} vs *mtsfl*_{7D} comparisons, 126 exclusively down-regulated in *wt*_{7D} vs *mtl1*_{7D} comparison and 145 exclusively down-regulated in *wt*_{7D} vs *mtsfl*_{7D} comparison (Figure 5.5 B).

Compared to wild type, the most significantly over-represented biological processes found in common between *mtl1*_{7D} and *mtsfl*_{7D} down-regulated DEGs were: response to abiotic stimulus ($2.31 \cdot 10^{-7}$), photosynthesis ($2.13 \cdot 10^{-7}$) and response to stimulus ($6.33 \cdot 10^{-6}$). From a total of 46 over-represented biological processes, we also found those related to hormones (response to hormone $1.24 \cdot 10^{-3}$ and response to cytokinin $4.75 \cdot 10^{-2}$) and oxidative stress (cellular response to oxidative stress, $6.61 \cdot 10^{-3}$; response to oxidative stress $6.91 \cdot 10^{-3}$; response to reactive oxygen species, $1.21 \cdot 10^{-2}$ and reactive oxygen species metabolic process $2.68 \cdot 10^{-2}$) (Figure 5.5 C).

The more significant over-represented biological processes identified from DEGs exclusively down-regulated in *wt*_{7D} vs *mtl1*_{7D} comparison were related to auxin-signaling (auxin-activated signaling pathway, $3.22 \cdot 10^{-3}$; cellular response to auxin stimulus, $3.36 \cdot 10^{-3}$ and response to auxin, $5.68 \cdot 10^{-3}$) and organogenesis (anatomical structure formation involved in morphogenesis, $9.66 \cdot 10^{-3}$; anatomical structure morphogenesis, $1.05 \cdot 10^{-2}$; plant organ development, $2.46 \cdot 10^{-2}$ and cotyledon development, $2.38 \cdot 10^{-2}$). Biological processes related to hormones were also over-represented in DEGs exclusively down-regulated in *wt*_{7D} vs *mtsfl*_{7D} comparison (response to jasmonic acid, $2.14 \cdot 10^{-2}$ and response to hormone $2.99 \cdot 10^{-2}$) (Figure 5.5 C).

Stress related processes were the most significantly over-represented in up-regulated DEGs in common between *wt*_{7D} vs *mtl1*_{7D} and *wt*_{7D} vs *mtsfl*_{7D} (response to external stimulus,

7.60 10^{-12} ; response to stimulus, 6.73 10^{-12} and response to stress, 1.73 10^{-11}) followed by processes related to hypoxia (cellular response to hypoxia, 2.89 10^{-9} ; cellular response to oxygen levels, 5.06 10^{-9} cellular response to decreased oxygen levels, 4.67 10^{-9} ; response to decreased oxygen levels, 1.12 10^{-5} and response to oxygen levels, 1.22 10^{-5}). Among the other over-represented processes (63 in total), we found those related to hormones (hormone metabolic process, 4.56 10^{-3} ; induced systemic resistance, 1.49 10^{-2} ; regulation of hormone levels, 1.64 10^{-2} ; salicylic acid metabolic process, 2.18 10^{-2} ; response to hormone, 2.29 10^{-2}) and detoxification (glutathione metabolic process, 3.27 10^{-5} ; detoxification, 7.68 10^{-5}). No over-represented process was found among DEGs up-regulated exclusively in *wt*_{7D} vs *mtl1*_{7D} and just two were over-represented in DEGs up-regulated exclusively in *wt*_{7D} vs *mtsfl*_{7D} (response to stimulus, 9.91 10^{-3} and regulation of biological process, 4.85 10^{-02}) (Figure 5.5 D).

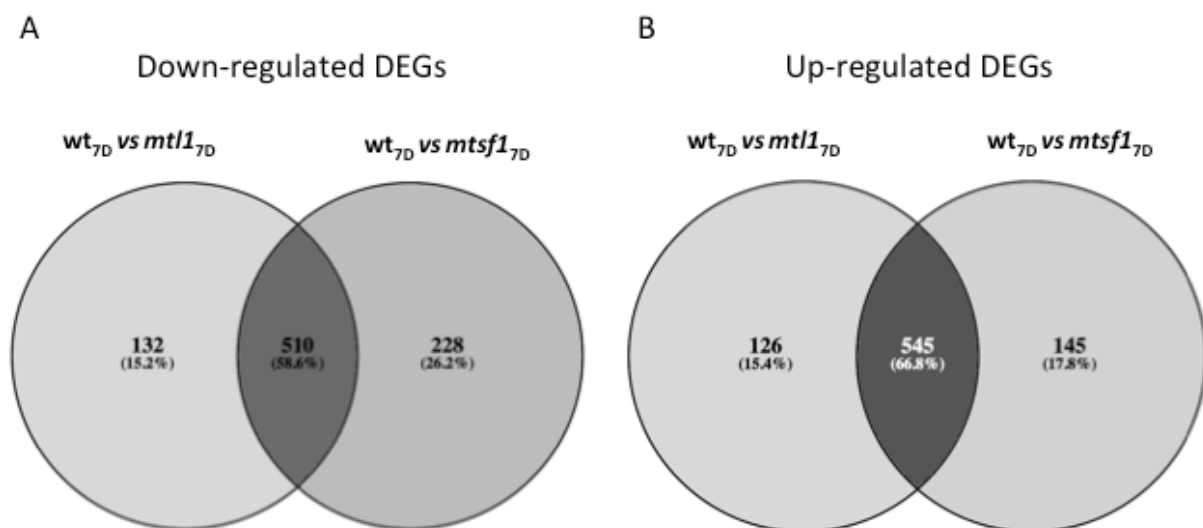


Figure 5.5: Comparison between two cI mutants (*mtl1*, *mtsfl*) and wild type in liquid culture. A, Venn diagram showing overlap between down-regulated DEGs identified in the *wt*_{7D} vs *mtl1*_{7D} and *wt*_{7D} vs *mtsfl*_{7D} comparisons. B, Venn diagram showing overlap between up-regulated DEGs identified in the *wt*_{7D} vs *mtl1*_{7D} and *wt*_{7D} vs *mtsfl*_{7D} comparisons.

C

Down-regulated DEGs in <i>wt_{7D}</i> vs <i>mtl1_{7D}</i> and <i>wt_{7D}</i> vs <i>mtsfl1_{7D}</i> (510)		Down-regulated DEGs exclusively in <i>wt_{7D}</i> vs <i>mtl1_{7D}</i> (132)		Down-regulated DEGs exclusively in <i>wt_{7D}</i> vs <i>mtsfl1_{7D}</i> (228)	
GO biological process (12 out of 46 total BP)	FDR P-value	GO biological process (13 out of 25 total BP)	FDR P-value	GO biological process (5 out of 8 total BP)	FDR P-value
response to abiotic stimulus	2.31E-07	auxin-activated signaling pathway	3.22E-03	response to oxygen-containing compound	1.44E-02
photosynthesis	2.13E-07	cellular response to auxin stimulus	3.36E-03	response to stimulus	1.63E-02
response to stimulus	6.33E-06	response to auxin	5.68E-03	response to jasmonic acid	2.14E-02
response to hormone	1.24E-03	anatomical structure formation	9.66E-03	response to hormone	2.99E-02
cellular response to oxidative stress	6.61E-03	involved in morphogenesis			
response to oxidative stress	6.91E-03	anatomical structure morphogenesis	1.05E-02		
response to stress	7.96E-03	plant organ development	2.46E-02		
response to reactive oxygen species	1.21E-02	cotyledon development	2.38E-02		
reactive oxygen species metabolic process	2.68E-02	post-embryonic plant morphogenesis	2.40E-02		
response to cytokinin	4.75E-02	response to hormone	2.40E-02		
		plant organ morphogenesis	3.46E-02		
		hormone-mediated signaling pathway	4.52E-02		
		regulation of cell cycle	4.80E-02		

D

Up-regulated DEGs in <i>wt_{7D}</i> vs <i>mtl1_{7D}</i> and <i>wt_{7D}</i> vs <i>mtsfl1_{7D}</i> (545)		Up-regulated DEGs exclusively in <i>wt_{7D}</i> vs <i>mtl1_{7D}</i> (126)		Up-regulated DEGs exclusively in <i>wt_{7D}</i> vs <i>mtsfl1_{7D}</i> (145)	
GO biological process (16 out of 63 total BP)	FDR P- value	No GO biological process		GO biological process (2 out of 2 total BP)	FDR P- value
response to external stimulus	7.60E-12			response to stimulus	9.91E-03
response to stimulus	6.73E-12			regulation of biological process	4.85E-02
response to stress	1.73E-11				
cellular response to hypoxia	2.89E-09				
cellular response to oxygen levels	5.06E-09				
cellular response to decreased oxygen levels	4.67E-09				
response to decreased oxygen levels	1.12E-05				
response to oxygen levels	1.22E-05				
glutathione metabolic process	3.27E-05				
detoxification	7.68E-05				
cellular response to stress	2.75E-03				
hormone metabolic process	4.56E-03				
induced systemic resistance	1.49E-02				
regulation of hormone levels	1.64E-02				
salicylic acid metabolic process	2.18E-02				
response to hormone	2.29E-02				

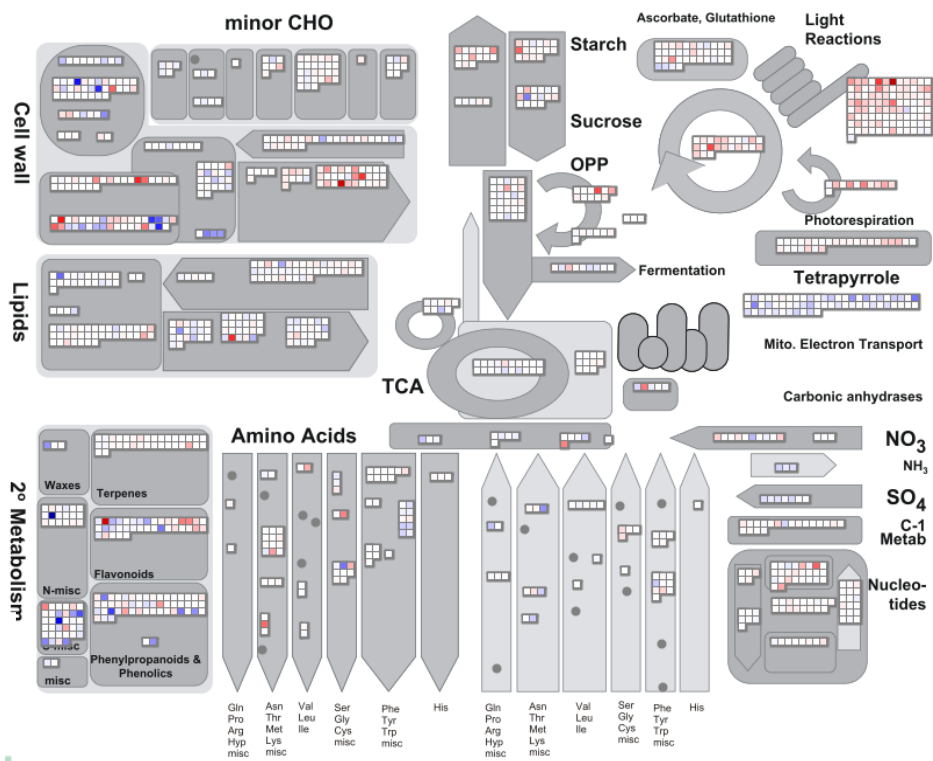
Figure 5.5: Comparison between two *cl* mutants (*mtl1*, *mtsfl1*) and wild type in liquid culture. [continued]

C, over-represented biological processes (BP) of down-regulated DEGs; left, in common between *wt_{7D}* vs *mtl1_{7D}* and *wt_{7D}* vs *mtsfl1_{7D}* comparisons; middle, exclusively in *wt_{7D}* vs *mtl1_{7D}* comparison and on the right, exclusively in *wt_{7D}* vs *mtsfl1_{7D}*. D, over-represented biological processes of up-regulated DEGs; left, in common between *wt_{7D}* vs *mtl1_{7D}* and *wt_{7D}* vs *mtsfl1_{7D}* comparisons; middle, exclusively in *wt_{7D}* vs *mtl1_{7D}* comparison and on the right, exclusively in *wt_{7D}* vs *mtsfl1_{7D}*. The two first biological processes with the highest FDR P-value are in bold. Represented lists are not exhaustive. *wt_{7D}*, wild type prior to transfer; *mtl1_{7D}*, *mtl1* prior to transfer; *mtsfl1_{7D}*, *mtsfl1* prior to transfer; *wt_{7.5D}*, 12 hours after the transfer of wild type calli; *mtl1_{7.5D}*, 12 hours after the transfer of *mtl1* calli; *mtsfl1_{7.5D}*, 12 hours after the transfer of *mtsfl1* calli.

The MapMan metabolism gene expression overview also shows that overall trends are similar in the mutants compared to the wild type, with peculiar shifts in cell wall and secondary metabolism processes, an overall up-regulation of tetrapyrrole biosynthesis, and the overall down-regulation of genes associated with photosynthesis (Figure 5.6). Cellular response genes follow similar patterns in either mutant, with an overall down-regulation trend for genes associated with cell division and cell cycle (Figure 5.7).

Complex I Mutants state before transfer

mtl1 versus wild type



mtsf1 versus wild type

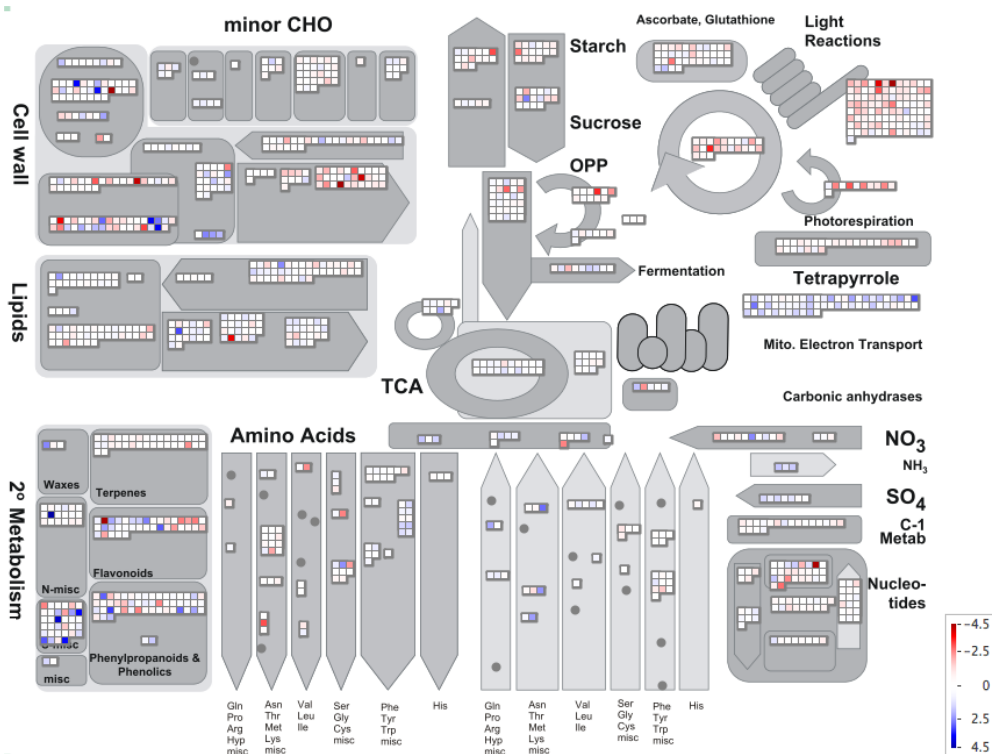
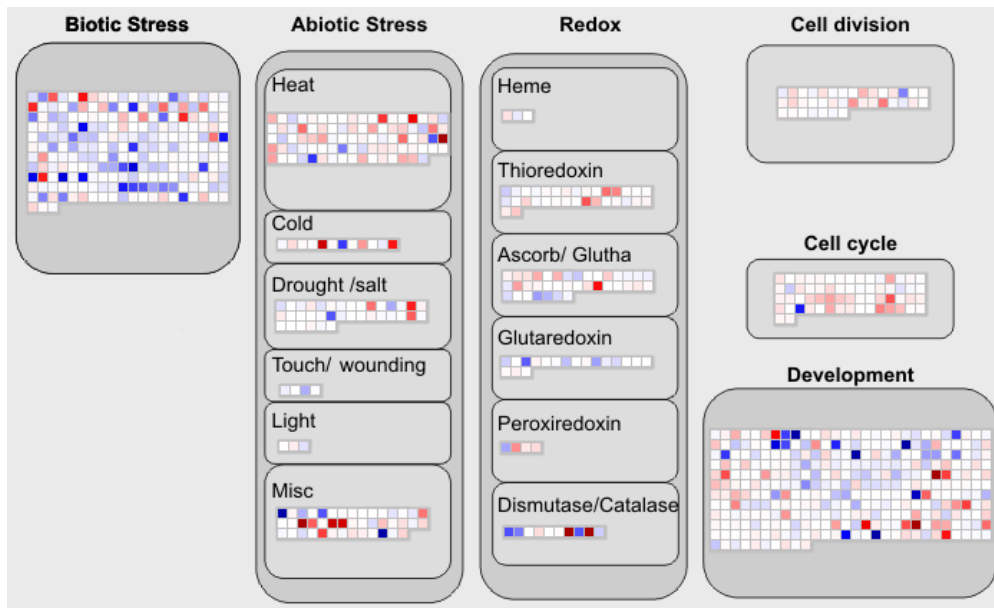


Figure 5.6: Transcriptional signature of metabolism in cI mutant calli. Blue, upregulated genes, red downregulated genes. The direction of pair-wise comparisons are as indicated in Figure 5.1.

Complex I Mutants state before transfer

mtl1 versus wild type



mts1 versus wild type

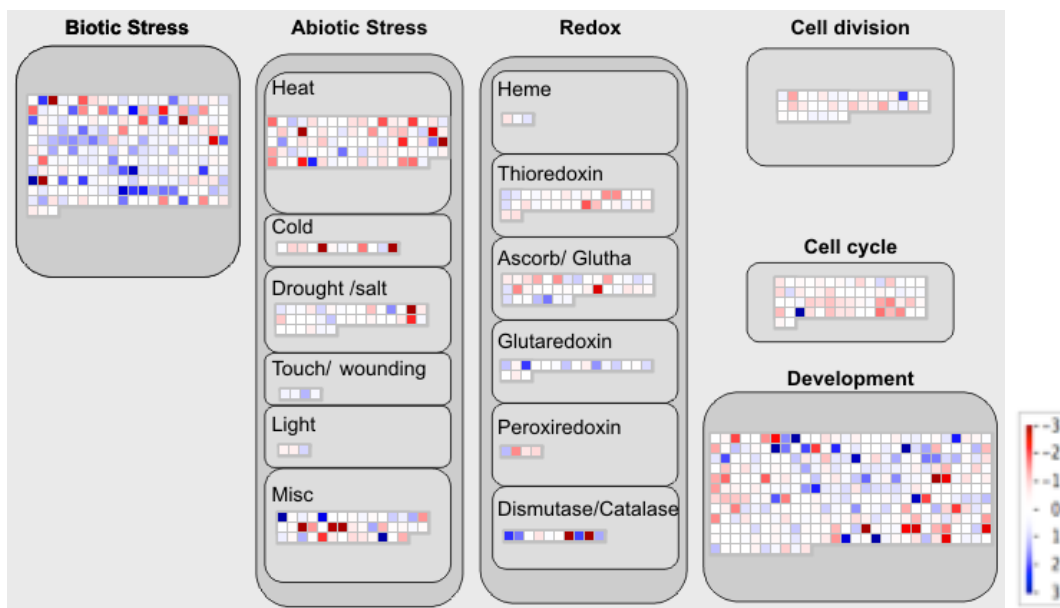


Figure 5.7: Transcriptional signature of cell response genes in cI mutant calli. Blue, upregulated genes, red downregulated genes. The direction of pair-wise comparisons are as indicated in Figure 5.1.

The difference between a constant genetic defect and a transient chemical defect

To analyze the difference between the two cI mutant calli and rotenone-treated calli, we compared DEGs of cI mutants versus wild type (wt_{7D} vs $mtll_{7D}$ and wt_{7D} vs $mtsfl_{7D}$) to DEGs of short-term (C_0 vs T_{12H}) and long-term (C_{7D} vs T_{7D}) cI inhibition (Figure 5.8). Among down-regulated DEGs, 59 were in common between cI mutants calli and short-term rotenone treated calli and less in common with long-term rotenone treated calli (10 DEGs); 450 DEGs were exclusively down-regulated in cI mutants when compared to short-term rotenone treated calli and 499 when compared to long-term treated calli. Compared to cI mutants, 384 DEGs were exclusively down-regulated in short-term rotenone treated calli and 204 DEGs exclusively down-regulated in long-term treated calli (Figure 5.8 A and B).

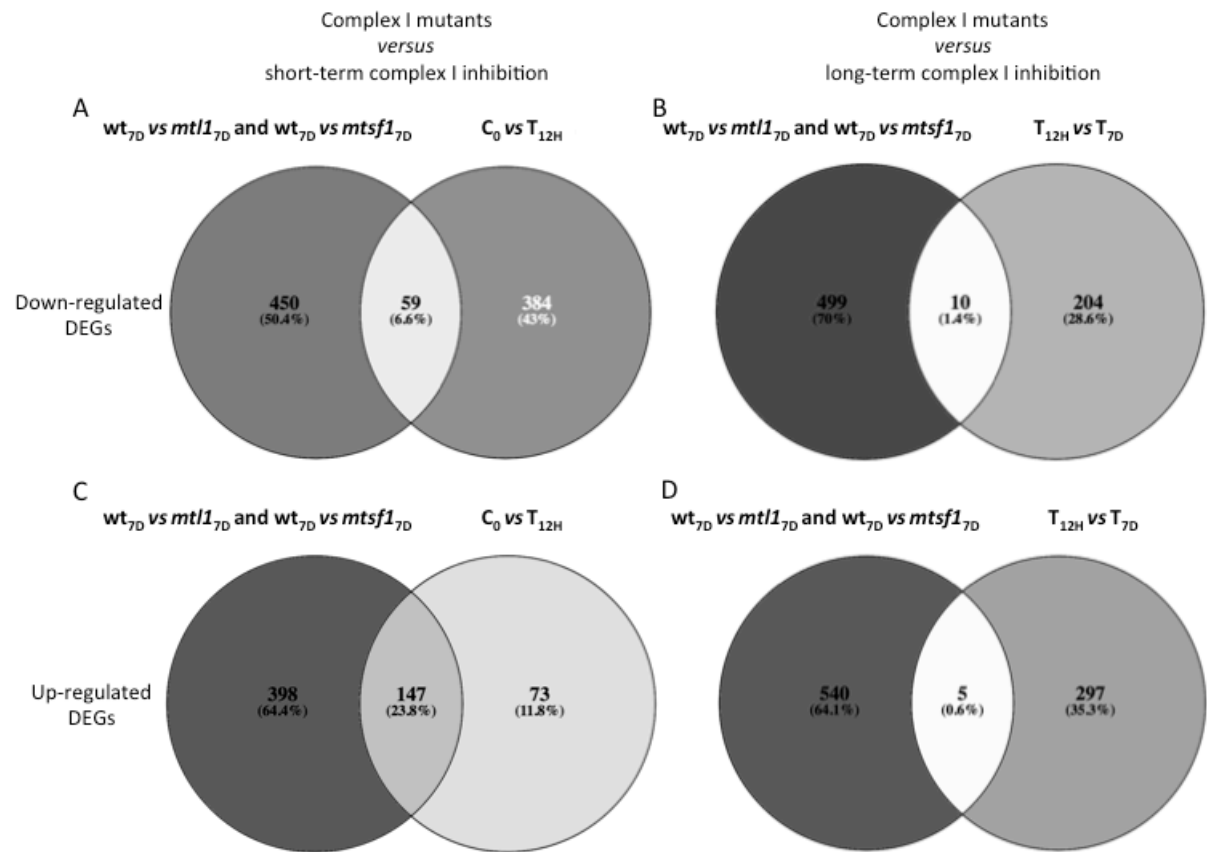
Regarding up-regulated DEGs, 147 were in common between cI mutants and short-term rotenone treatment and just 5 in common with long-term treatment. 398 DEGs were exclusively up-regulated in cI mutants against 73 exclusively up-regulated in short-term treated calli whereas 297 DEGs were exclusively up-regulated in long-term treated calli against 540 in cI mutants (Figure 5.8 C and D).

We did not find over-represented biological processes in common down-regulated DEGs between cI mutants and short-term rotenone treated calli. Among DEGs exclusively down-regulated in cI mutants compared to short term rotenone treatment, the most significantly over-represented biological processes are related photosynthesis ($3.63 \cdot 10^{-8}$), response to abiotic stress ($3.16 \cdot 10^{-7}$) and response to oxidative stress ($6.15 \cdot 10^{-3}$) whereas the major over-represented biological processes exclusively present in short-term treatment response are related to cell cycle ($1.81 \cdot 10^{-9}$), cell division ($1.61 \cdot 10^{-8}$) and cellular response to hypoxia ($4.13 \cdot 10^{-5}$) (Figure 5.8 E). Among the over-represented biological processes in up-regulated DEGs in common between cI mutants and short-term rotenone treated, we found response to stress ($1.75 \cdot 10^{-6}$), cellular response to hypoxia ($6.75 \cdot 10^{-8}$) and cellular response to oxygen levels ($9.66 \cdot 10^{-8}$). The biological processes response to external stimuli ($1.02 \cdot 10^{-3}$), response to stimuli ($2.89 \cdot 10^{-3}$) and response to stress ($1.62 \cdot 10^{-2}$) were exclusively over-represented in cI mutants against just one biological process that was exclusively over-represented in short-term rotenone treated calli and is related to response to stimulus ($5.80 \cdot 10^{-3}$) (Figure 5.8 F).

Unlike short-term rotenone treatment, six biological processes are over-represented in common down-regulated DEGs between long-term treatment and cI mutants. These biological processes are for the most related to photosynthesis (photosynthesis, light

harvesting in photosystem I, $3.47 \cdot 10^{-4}$; photosynthesis, light harvesting, $1.15 \cdot 10^{-3}$; photosynthesis, light reaction $1.32 \cdot 10^{-2}$; photosynthesis, $3.72 \cdot 10^{-2}$). The most significant biological process in DEGs exclusively down-regulated in cI mutants compared to long-term treatment is also related to photosynthesis ($1.99 \cdot 10^{-6}$) followed by other shared biological processes with those exclusively down-regulated in cI mutants compared to short-term treatment like response to abiotic stimulus ($2.35 \cdot 10^{-6}$) and response to oxidative stress ($7.15 \cdot 10^{-3}$). Among over-represented biological processes found exclusively in down-regulated DEGs of long-term treated calli we found several biological processes related to hormone signaling (response to jasmonic acid, $2.93 \cdot 10^{-4}$; response to salicylic acid, $1.02 \cdot 10^{-3}$; response to hormone, $2.21 \cdot 10^{-3}$; response to abscisic acid, $4.88 \cdot 10^{-2}$) (Figure 5.8 G).

From the 5 common up-regulated DEGs in cI mutants and long-term treatment we did not find an over-represented biological process whereas 62 biological processes were over-represented exclusively in cI mutants up-regulated DEGs like response to stress ($1.19 \cdot 10^{-11}$), detoxification ($7.21 \cdot 10^{-5}$), response to hormone ($2.15 \cdot 10^{-02}$) and regulation of hormone levels ($3.75 \cdot 10^{-2}$). After a long-term cI inhibition, rotenone-treated calli resume cell division as we noticed the over-representation of the two biological processes cell division ($9.62 \cdot 10^{-4}$) and cell cycle ($4.98 \cdot 10^{-4}$) in DEGs up-regulated exclusively in long-term rotenone treated calli (figure 5.8 H).



E

Down-regulated DEGs in complex I mutants vs wt and <i>C</i> ₀ vs <i>T</i> _{12H} (59)	Down-regulated DEGs exclusively in complex I mutants vs wt (450)		Down-regulated DEGs exclusively in <i>C</i> ₀ vs <i>T</i> _{12H} (384)	
No GO biological process	GO biological process (7 out of 33 total BP)	FDR P-value	GO biological process (11 out of 54 total BP)	FDR P-value
	photosynthesis	3.63E-08	cell cycle	1.81E-09
	response to abiotic stimulus	3.16E-07	cell division	1.61E-08
	response to oxidative stress	6.15E-03	cellular response to hypoxia	4.13E-05
	cellular response to oxidative stress	1.64E-02	response to stress	4.61E-05
	reactive oxygen species metabolic process	1.98E-02	cellular response to decreased oxygen levels	5.10E-05
	response to reactive oxygen species	2.54E-02	detoxification	1.15E-04
	<u>response to hormone</u>	<u>3.43E-02</u>	microtubule-based process	1.23E-04
			cytokinesis	1.25E-04
			mitotic cell cycle	2.73E-04
			regulation of cell cycle	5.43E-04
			<u>response to salicylic acid</u>	<u>1.80E-02</u>

F

Up-regulated DEGs in complex I mutants vs wt and <i>C</i> ₀ vs <i>T</i> _{12H} (147)	Up-regulated DEGs exclusively in complex I mutants vs wt (398)		Up-regulated DEGs exclusively in <i>C</i> ₀ vs <i>T</i> _{12H} (73)		
GO biological process (9 out of 53 total BP)	FDR P-value	GO biological process (3 out of 22 total BP)	FDR P-value	GO biological process (1 out of 1 total BP)	FDR P-value
response to stress	1.75E-10	response to external stimulus	1.02E-03	response to stimulus	5.80E-03
cellular response to hypoxia	6.75E-08	response to stimulus	2.89E-03		
cellular response to oxygen levels	9.66E-08	<u>response to stress</u>	<u>1.62E-02</u>		
cellular response to decreased oxygen levels	8.92E-08				
detoxification	1.68E-05				
salicylic acid metabolic process	1.15E-02				
cellular response to stress	1.25E-02				
response to salicylic acid	3.73E-02				
<u>induced systemic resistance</u>	<u>4.03E-02</u>				

G

Down-regulated DEGs in complex I mutants vs wt and T _{12H} vs T _{7D} (10)		Down-regulated DEGs exclusively in complex I mutants vs wt (499)		Down-regulated DEGs exclusively in T _{12H} vs T _{7D} (204)	
GO biological process (5 out of 6 total BP)	FDR P-value	GO biological process (8 out of 32 total BP)	FDR P-value	GO biological process (15 out of 152 total BP)	FDR P-value
photosynthesis, light harvesting in photosystem I	3.47E-04	photosynthesis	1.99E-06	response to stimulus	1.20E-22
photosynthesis, light harvesting	1.15E-03	response to abiotic stimulus	2.35E-06	response to stress	7.29E-17
photosynthesis, light reaction	1.32E-02	response to stimulus	2.87E-05	response to abiotic stimulus	3.83E-14
response to abiotic stimulus	1.25E-02	cellular response to oxidative stress	6.57E-03	glutathione metabolic process	5.93E-05
photosynthesis	3.72E-02	response to oxidative stress	7.15E-03	detoxification	1.15E-04
		response to reactive oxygen species	1.31E-02	response to jasmonic acid	2.93E-04
		reactive oxygen species metabolic process	3.16E-02	response to salicylic acid	1.02E-03
		response to stress	3.22E-02	response to hormone	2.21E-03
				cellular response to hypoxia	3.02E-03
				cellular response to oxygen levels	3.83E-03
				cellular response to decreased oxygen levels	3.78E-03
				hormone metabolic process	1.20E-02
				response to oxidative stress	1.21E-02
				abscisic acid metabolic process	2.73E-02
				response to abscisic acid	4.88E-02

H

Up-regulated DEGs in complex I mutants vs wt and T _{12H} vs T _{7D} (5)		Up-regulated DEGs exclusively in complex I mutants vs wt (540)		Up-regulated DEGs exclusively in T _{12H} vs T _{7D} (297)	
GO biological process	FDR P-value	GO biological process (11 out of 62 total BP)	FDR P-value	GO biological process (2 out of 2 total BP)	FDR P-value
No GO biological process		response to external stimulus	5.28E-12	cell division	9.62E-04
		response to stimulus	3.20E-12	cell cycle	4.98E-04
		response to stress	1.19E-11		
		cellular response to hypoxia	2.69E-09		
		cellular response to oxygen levels	4.70E-09		
		cellular response to decreased oxygen levels	4.33E-09		
		glutathione metabolic process	2.95E-05		
		detoxification	7.21E-05		
		hormone metabolic process	1.49E-02		
		response to hormone	2.15E-02		
		regulation of hormone levels	3.75E-02		

Figure 5.8: Comparison between cI genetic defect (*mtl1*, *mtsfl*) and cI rotenone inhibition. A, Venn diagram showing overlap between down-regulated DEGs identified in cI mutants (*wt*_{7D} vs *mtl1*_{7D} and *wt*_{7D} vs *mtsfl*_{7D}) versus short-term inhibition of cI (*C*₀ vs T_{12H}). B, Venn diagram showing overlap between down-regulated DEGs identified in cI mutants (*wt*_{7D} vs *mtl1*_{7D} and *wt*_{7D} vs *mtsfl*_{7D}) versus long-term inhibition of cI (T_{12H} vs T_{7D}). C, Venn diagram showing overlap between up-regulated DEGs identified in cI mutants (*wt*_{7D} vs *mtl1*_{7D} and *wt*_{7D} vs *mtsfl*_{7D}) versus short-term inhibition of cI (*C*₀ vs T_{12H}). D, Venn diagram showing overlap between up-regulated DEGs identified in cI mutants (*wt*_{7D} vs *mtl1*_{7D} and *wt*_{7D} vs *mtsfl*_{7D}) versus long-term inhibition of cI (T_{12H} vs T_{7D}). E, over-represented biological processes (BP) of down-regulated DEGs; left, in common between cI mutants and short-term cI inhibition; middle, exclusively in cI mutants and on the right, exclusively in short-term cI inhibition. F, over-represented biological processes of up-regulated DEGs; left, in common cI mutants and short-term cI inhibition; middle, exclusively in cI mutants and on the right, exclusively in short-term cI inhibition. G, over-represented biological processes (BP) of down-regulated DEGs; left, in common between cI mutants and long-term cI inhibition; middle, exclusively in cI mutants and on the right, exclusively in long-term cI inhibition. H, over-represented biological processes of up-regulated DEGs; left, in common cI mutants and long-term cI inhibition; middle, exclusively in cI mutants and on the right, exclusively in long-term cI inhibition. Represented lists are not exhaustive. *wt*_{7D}, wild type prior to transfer; *mtl1*_{7D}, *mtl1* prior to transfer; *mtsfl*_{7D}, *mtsfl* prior

to transfer; C₀, control before treatment; T_{12H}, 12 hours after rotenone treatment (short-term); T_{7D}, 7 days after rotenone treatment (long-term).

The transfer of calli from callogenesis liquid medium to regeneration gelled medium prompts a major gene expression reprogramming, but cl genetic defects dampen the shock

All comparisons including the callus transfer step yielded a very large number of DEGs (Table 5.1). In control untreated calli (C_{7D} vs C_{7.5D}) and rotenone-treated calli (T_{7D} vs T_{7.5D}), a similar number of genes were differentially deregulated through the transfer (control: 4704 [2419 down, 2285 up]; treated: 4410 [2273 down, 2137 up]).

But the amplitude of the transcriptional response prompted by the transfer across genotypes pointed to another trend. They ranked as follows: the larger DEG number was observed in the wild type (wt_{7D} vs wt_{7.5D}; 3447 DEGs; 1674 down, 1773 up), reminiscent of the shift observed in wild-type control and rotenone -treated explants; in *mtl1* tissues (*mtl1*_{7D} vs *mtl1*_{7.5D}), 1868 DEGs were detected (1020 down, 848 up); in *mtsfl* tissues (*mtsfl*_{7D} vs *mtsfl*_{7.5D}) 1266 DEGs were detected (659 down, 607 up) (Table 5.1). This order is a hint that the mutants may be less affected by callus transfer than the wild type, especially considering that *mtsfl*, which is the most affected genotype in terms of callus growth, is also the genotype with the smallest number of genes de-regulated by the transfer.

In agreement with a potentially larger dampening effect of the *mtsfl* mutation against the perturbations resulting from callus transfer, the number of DEGs between *mtl1* and wild type (*mtl1*_{7.5D} vs wt_{7.5D}) 12 hours after transfer (1015; 541 down, 474 up) was almost twice the number of DEGs between *mtsfl* and wild type (*mtsfl*_{7.5D} vs wt_{7.5D}) (530; 283 down, 247 up) (Table 5.1).

Impact of rotenone on the callus transfer response

As illustrated in Figures 5.9, 5.10 and 5.11, the control (C_{7D} vs C_{7.5D}) and rotenone-pretreated (T_{7D} vs T_{7.5D}) calli underwent major gene expression shifts during transfer, often with large fold changes. However, the overlap in up- or down-regulated genes between the two conditions only represented a minority of genes (Figure 5.9 A and B). Furthermore, the GO term biases detected in the up- or down-regulated DEGs - either in common, exclusively in control calli, or exclusively in rotenone-pretreated calli - were essentially pointing to the

same upper classes of biological processes: responses to chemicals, including hormones and ROS, and responses to various stresses (Figure 5.9 C and D), thus making it difficult to discern anything else but the very large shock sustained by the tissues upon transfer.

The same molecular upheaval is shown, for example, in the MapMan overviews displaying the metabolism and cell response gene expression signatures of rotenone-pretreated calli after transfer (T_{7D} vs $T_{7.5D}$) (Figure 5.10 A and B, respectively).

Strikingly, the direct comparison of control and rotenone-pretreated samples 12 hours after transfer ($T_{7.5D}$ vs $C_{7.5D}$) only identified 74 DEGs (54 down, 20 up) (Table 5.1), out of which no statistically significant GO biological process term enrichment was detected. We explain this observation in two ways. First, the variability across biological replicates - that is increased because of the amplitude of the transfer shock - reduces the number of genes that are statistically differentially expressed. Second, the callus transfer is such an overwhelming event that it erases subtle differences that were induced by the prior rotenone pretreatment.

The similarity between the control and rotenone-treated samples after transfer ($T_{7.5D}$ vs $C_{7.5D}$) is also apparent in the MapMan metabolism and cell response overviews (Figure 5.11 A and B), in which almost no gene boxes are brightly colored. However, it is possible to reveal in the $T_{7.5D}$ vs $C_{7.5D}$ comparison some of the patterns specific to the late rotenone response (e.g. the tetrapyrrole biosynthesis genes) when enhancing lower fold changes with a narrower log ratio scale (Figure 10 B; compare metabolism overview panels with the [-2 to 2] and [-4.5 to 4.5] scales). Also, note that lower fold changes are also associated with the repression of the genes associated with photosynthesis in rotenone-pretreated samples as this portion of metabolism will be addressed later.

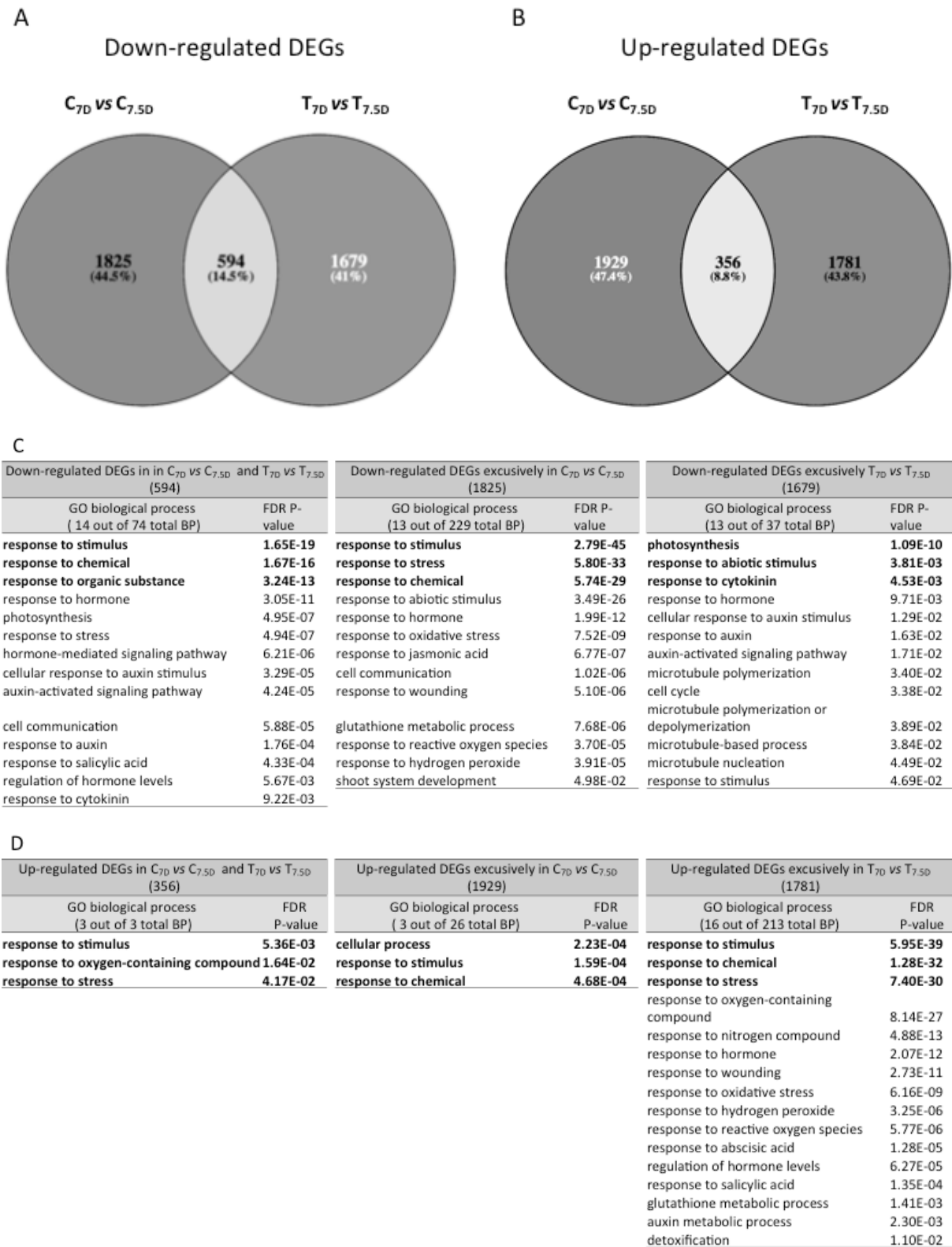


Figure 5.9: Comparison between response to the transfer in rotenone-treated calli and control calli. A, Venn diagram showing overlap between down-regulated DEGs identified in the C_{7D} vs $C_{7.5D}$ and T_{7D} vs $T_{7.5D}$ comparisons. B, Venn diagram showing overlap between up-regulated DEGs identified in the C_{7D} vs $C_{7.5D}$ and T_{7D} vs $T_{7.5D}$ comparisons. C, over-

represented biological processes (BP) of down-regulated DEGs; left, in common between C_{7D} vs $C_{7.5D}$ and T_{7D} vs $T_{7.5D}$ comparisons; middle, exclusively in C_{7D} vs $C_{7.5D}$ comparison and on the right, exclusively in T_{7D} vs $T_{7.5D}$. D, over-represented biological processes of up-regulated DEGs; left, in common between C_{7D} vs $C_{7.5D}$ and T_{7D} vs $T_{7.5D}$ comparisons; middle, exclusively in C_{7D} vs $C_{7.5D}$ comparison and on the right, exclusively in T_{7D} vs $T_{7.5D}$. The three first biological processes with the highest FDR P-value are in bold. Represented lists are not exhaustive. T_{7D} , 7 days after rotenone treatment and prior to transfer; C_{7D} , DMSO control after 7 days and prior to transfer; $T_{7.5D}$, 12 hours after the transfer of rotenone treated calli; $C_{7.5D}$, 12 hours after the transfer of control calli.

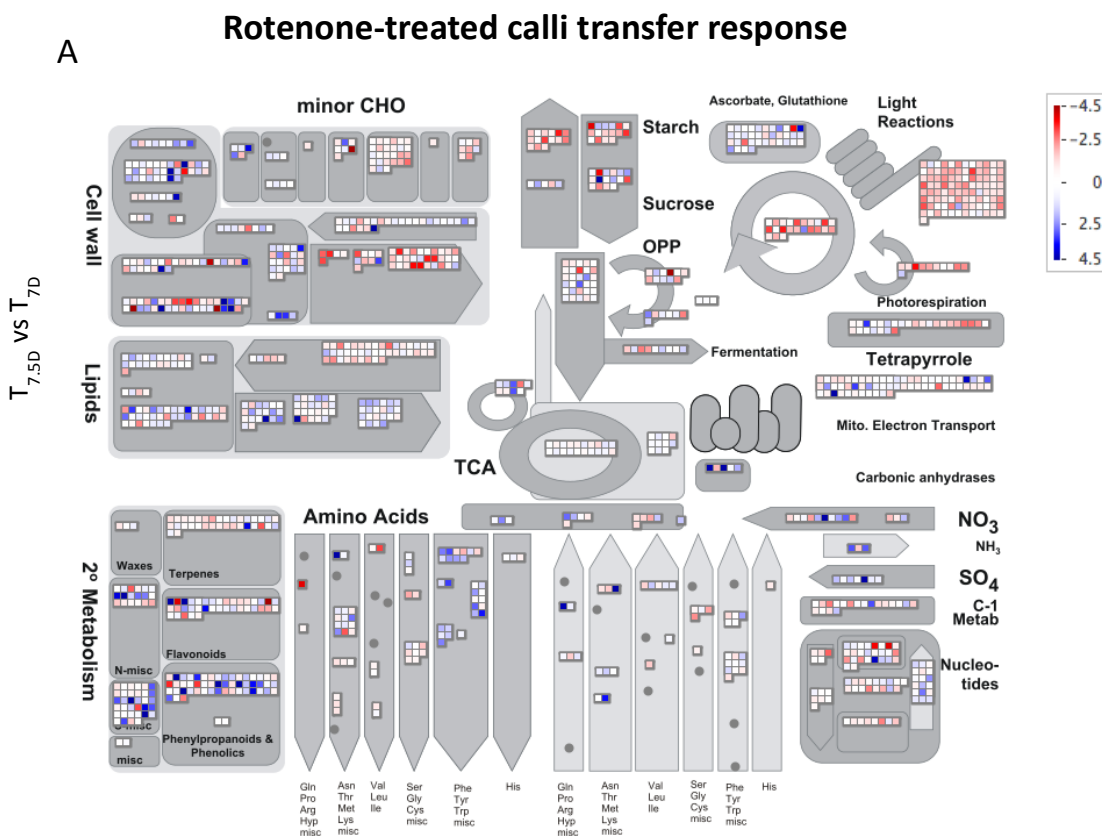


Figure 5.10: Transcriptional signature of metabolism genes induced by callus transfer and depending on rotenone treatment. A. Gene expression changes induced 12 hours after transfer on shoot induction medium in rotenone-treated calli.

B Impact of rotenone on transfer response

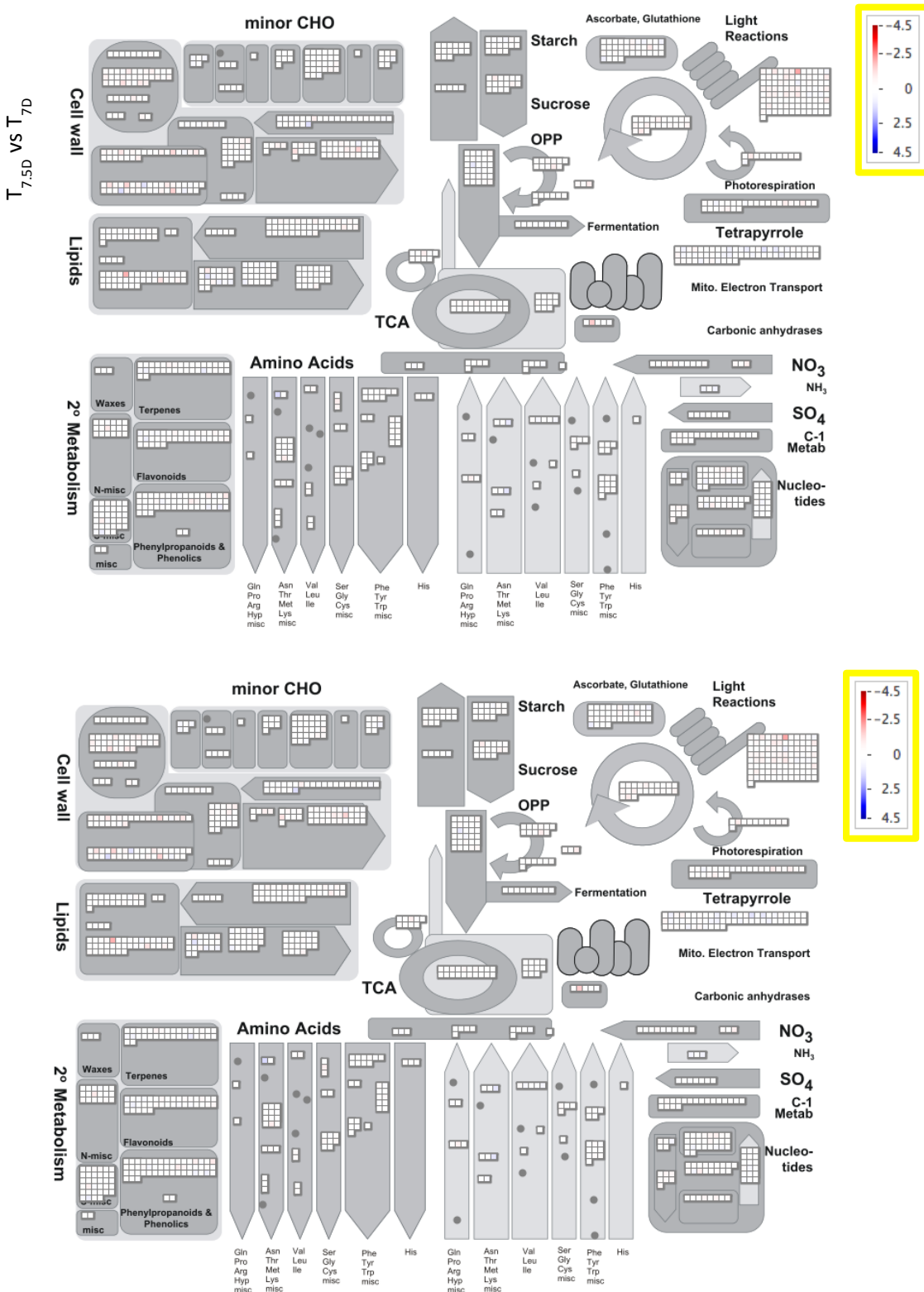
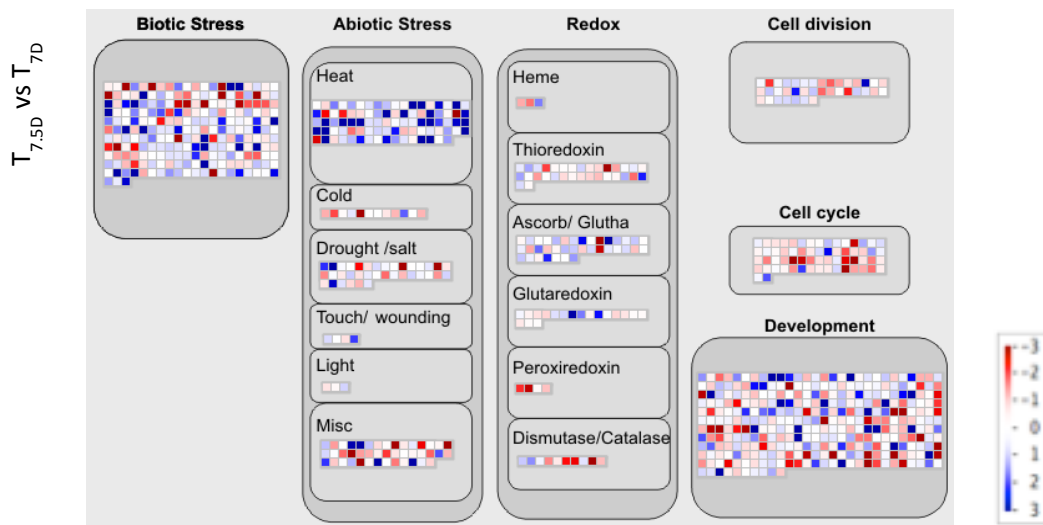


Figure 5.10: Transcriptional signature of metabolism genes induced by callus transfer and depending on rotenone treatment [continued]. B. Difference between treated (T) and control (C) calli after transfer. Top and bottom panels are identical except for the log ratio scales highlighted with a yellow outline. Blue, upregulated genes, red downregulated genes. The direction of pair-wise comparisons are as indicated in Figure 5.1.

A

Rotenone-treated calli transfer response



B

Impact of rotenone on transfer response

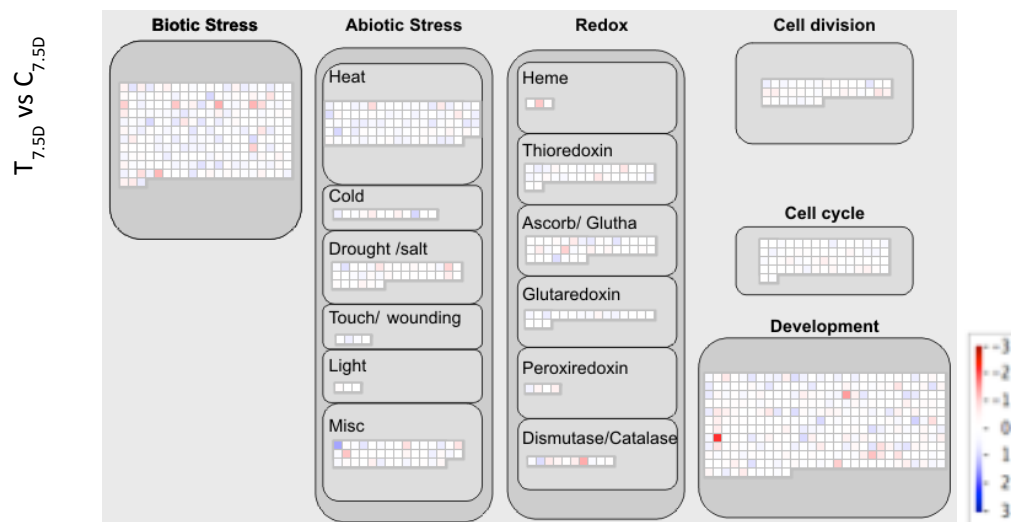


Figure 5.11: Transcriptional signature of cell response genes induced by callus transfer and depending on rotenone treatment. A. Gene expression changes induced 12 hours after transfer on shoot induction medium in rotenone-treated calli. B. Difference between treated (T) and control (C) calli after transfer. Blue, upregulated genes, red downregulated genes. The direction of pair-wise comparisons are as indicated in Figure 5.1.

Impact of cI genetic defects on the transcriptional response to the transfer

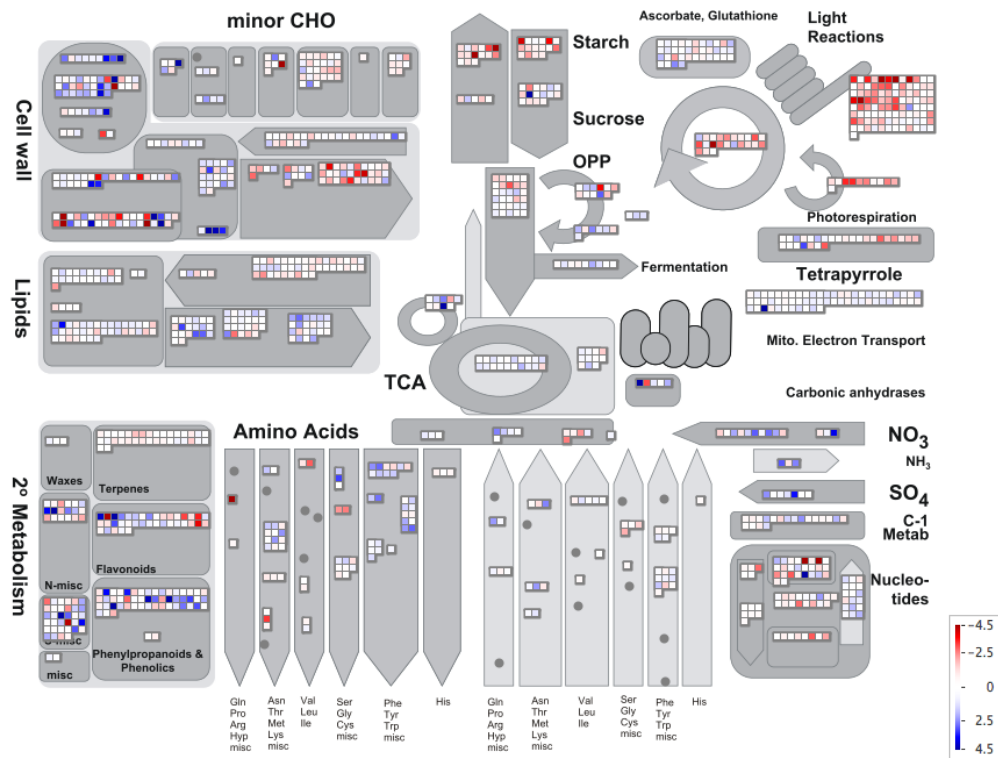
As mentioned above, the callus transfer from liquid callogenesis medium (CIM2) to shoot induction medium (SIM) induces a large genetic reprogramming in wild-type tissues (wt_{7D} vs wt_{7.5D}). This is for example illustrated in the metabolism gene expression overview (Figure 5.12, also Figure 5.10 A). Furthermore, as already suggested by the mere count of DEGs in the three analyzed genotypes, gene expression changes have in general a smaller amplitude in transferred cI mutant calli (*mtl1*_{7D} vs *mtl1*_{7.5D}; *mtsf1*_{7D} vs *mtsf1*_{7.5D}) (Figure 5.12). The cell response gene overview outlines the same overall picture (Figure 5.13).

We noted that some of the functional modules affected in the cI mutant tissues prior to callus transfer were also among those most affected by the transfer in wild type explants. For example, among genes involved in cell wall processes (Figure 5.14 A), both mutants were characterized by induced pectin synthesis, overall down-regulation of pectate lyases and polygalacturonases, and peculiar expression profiles of genes coding for cell wall proteins, pectin esterases and other enzymes modifying cell wall components (Figure 5.14 B). In addition, the gene profiles induced by the transfer of wild-type calli bear similarities with those characterizing the cI mutants prior transfer (compare panels in Figure 5.14 B with top panel [wild type transfer response] in Figure 5.14 C). Logically, the gene shifts occurring upon callus transfer in mutant tissues do not resemble those observed in the wild type (e.g. no further induction of pectin synthesis genes or repression of pectate lyases and polygalacturonases) since these processes were already activated or deactivated in the mutants before transfer.

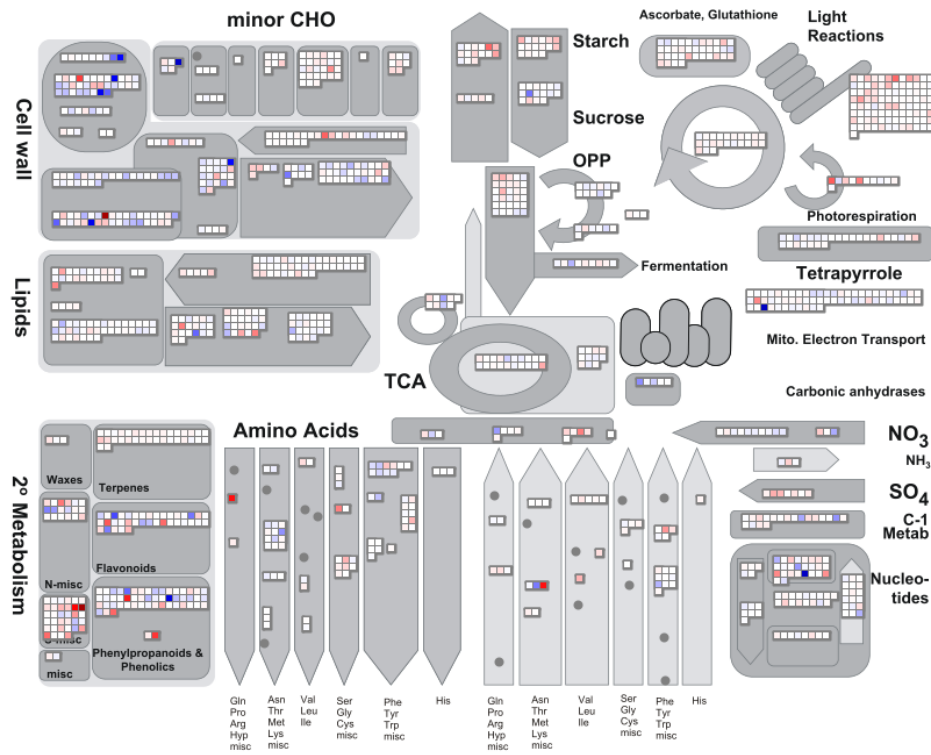
The same conclusion may be drawn when considering that, compared to wild type, the down-regulation of photosynthesis genes is already established in cI mutants before callus transfer (Figure 5.15 A), and that the same genes are repressed in the wild type following callus transfer (Figure 5.15 B).

An outcome of these assumptions is that the impact of cI mutations on the physiological state of the protoplast-derived calli is very similar to - at least some of - the changes induced by the transfer of the explants from the callogenesis medium to the shoot induction medium.

wild type transfer (wt_{7D} vs $wt_{7.5D}$)



mtl1 transfer response ($mtl1_{7D}$ vs $mtl1_{7.5D}$)



mtsfl transfer response (*mtsfl*_{7D} vs *mtsfl*_{7.5D})

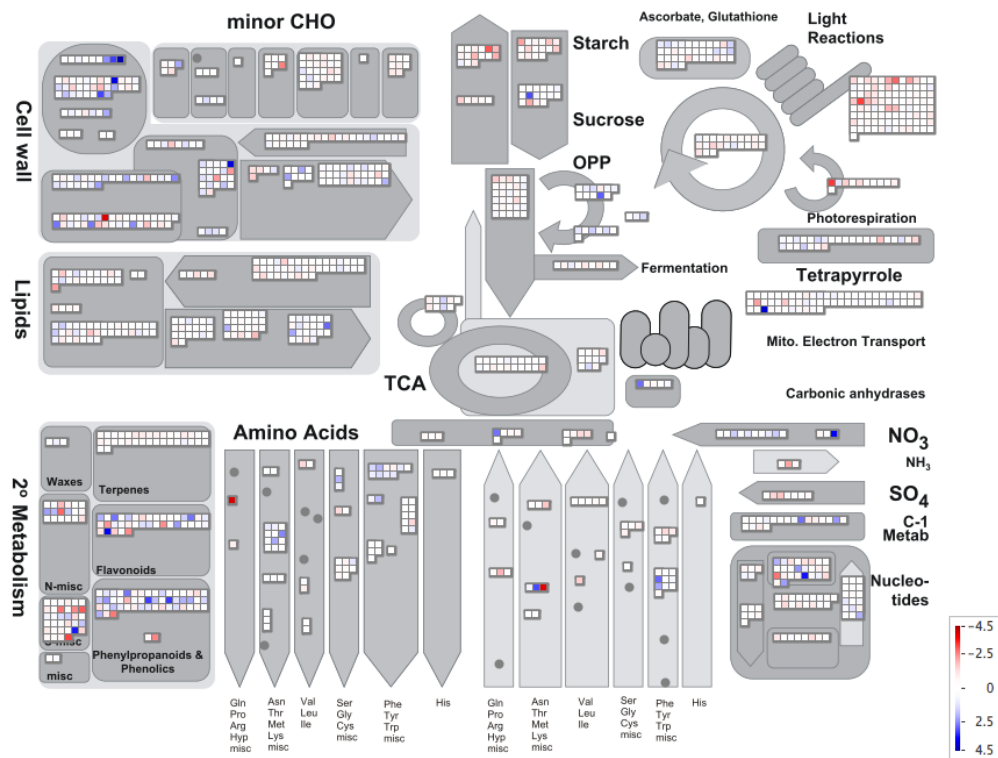
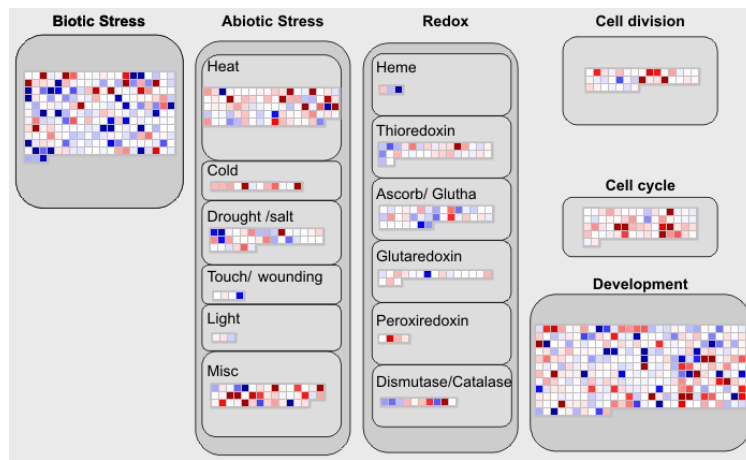


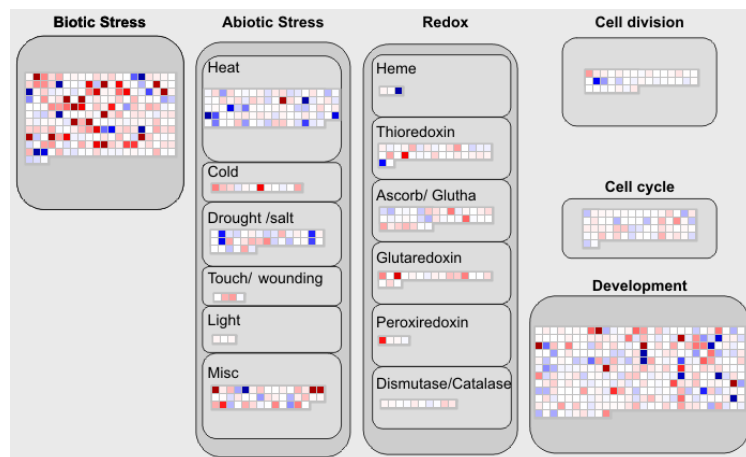
Figure 5.12: Transcriptional signature of metabolism genes induced by callus transfer in wild type and *cl* mutant calli. Gene expression changes induced 12 hours after transfer on shoot induction medium in wild type, *mtl1* and *mtsfl* calli. Blue, upregulated genes, red downregulated genes. The direction of pair-wise comparisons are as indicated in Figure 5.1.

A **Transfer response per genotype**

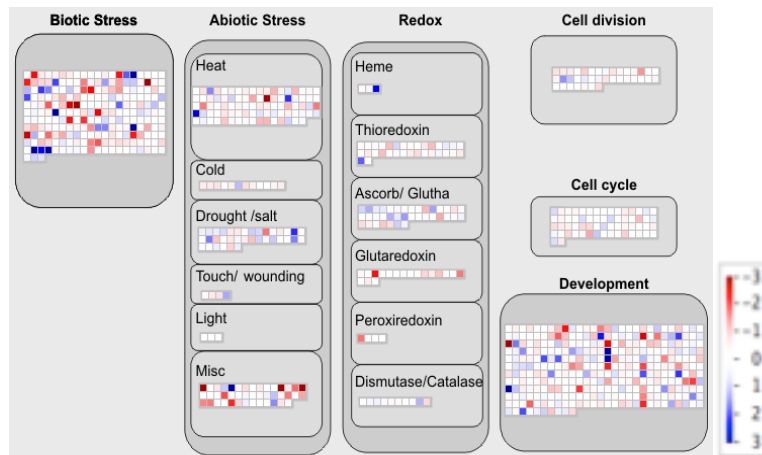
$wt_{7.5D}$ vs wt_{7D}



$mtl1_{7.5D}$ vs $mtl1_{7D}$



$mtsfl_{7.5D}$ vs $mtsfl_{7D}$



B Transfer response: mutant vs wild type

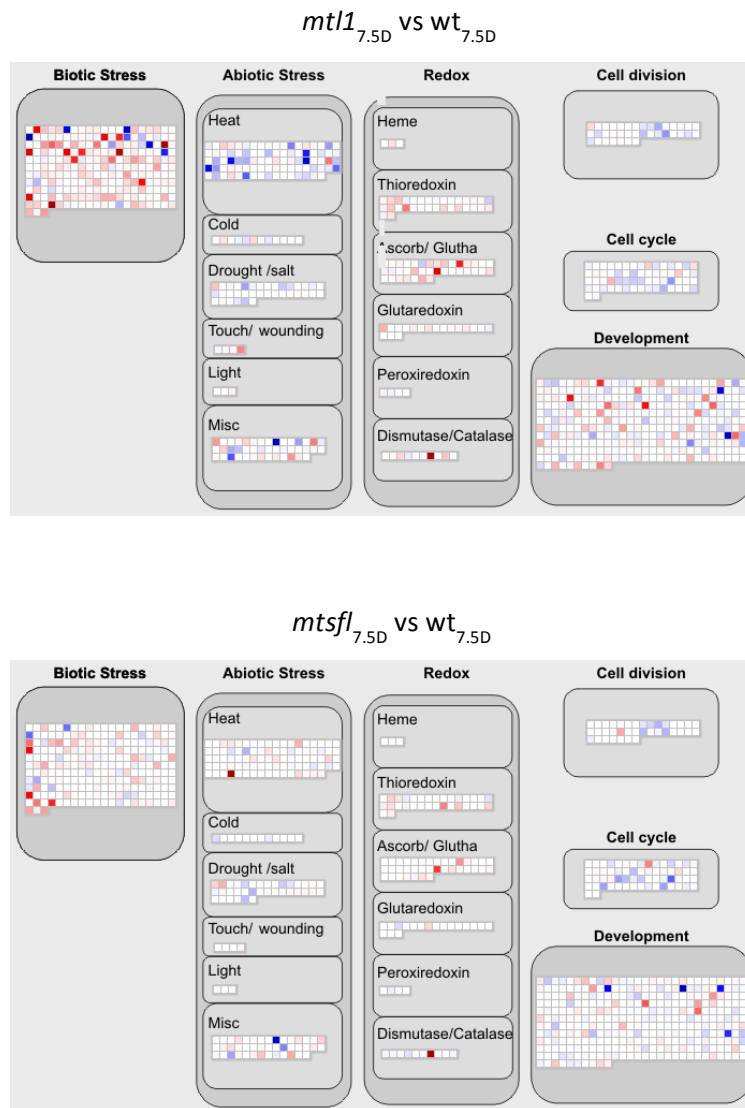
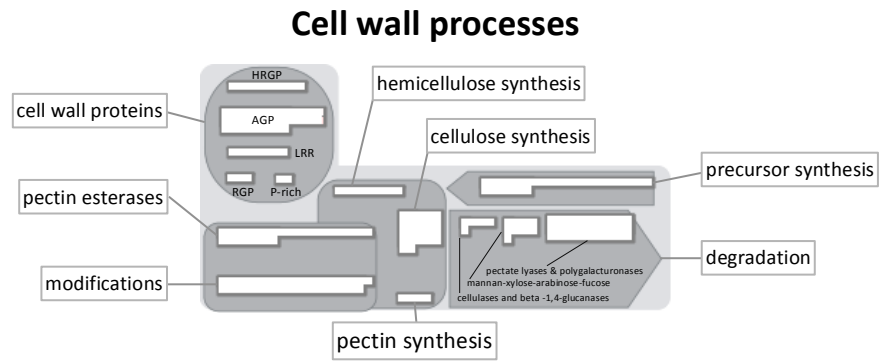


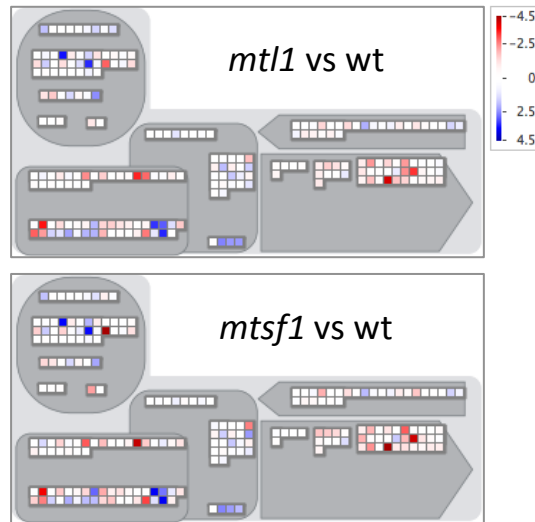
Figure 5.13: Transcriptional signature of cell response genes induced by callus transfer in wild type and *cl* mutant calli. Gene expression changes induced 12 hours after transfer on shoot induction medium in wild type, *mtl1* and *mtsfl* calli. A. Changes induced 12 hours after transfer of each genotype. B. Difference between wild type and *cl* mutant tissues after transfer. Blue, upregulated genes, red downregulated genes. The direction of pair-wise comparisons are as indicated in Figure 5.1.

A



B

Mutant state before transfer



C

Mutant transfer response

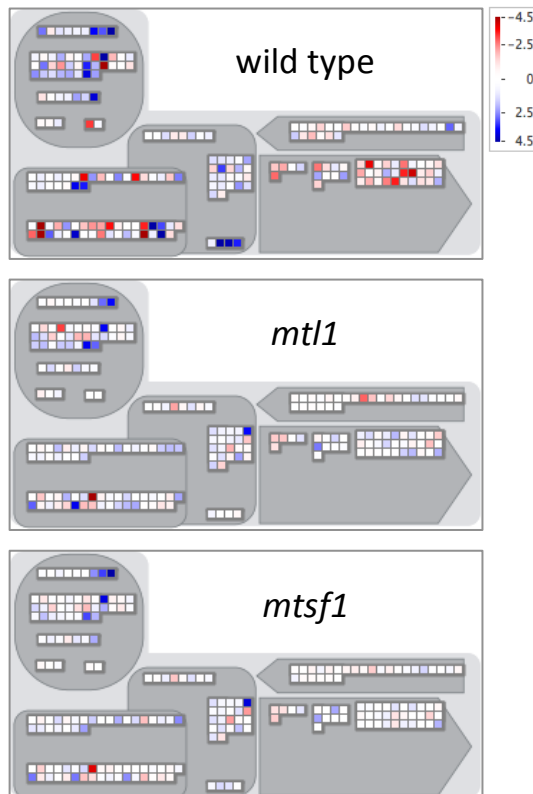


Figure 5.14: Impact of *ci* genetic defects on the cell wall related genes. A. Annotation of the “Cell wall” in the MapMan metabolism overview. B. Callus state before transfer to shoot inducing medium. C. Gene expression changes induced by transfer to shoot inducing medium. Blue, upregulated genes, red downregulated genes. The direction of pair-wise comparisons are as indicated in Figure 5.1.

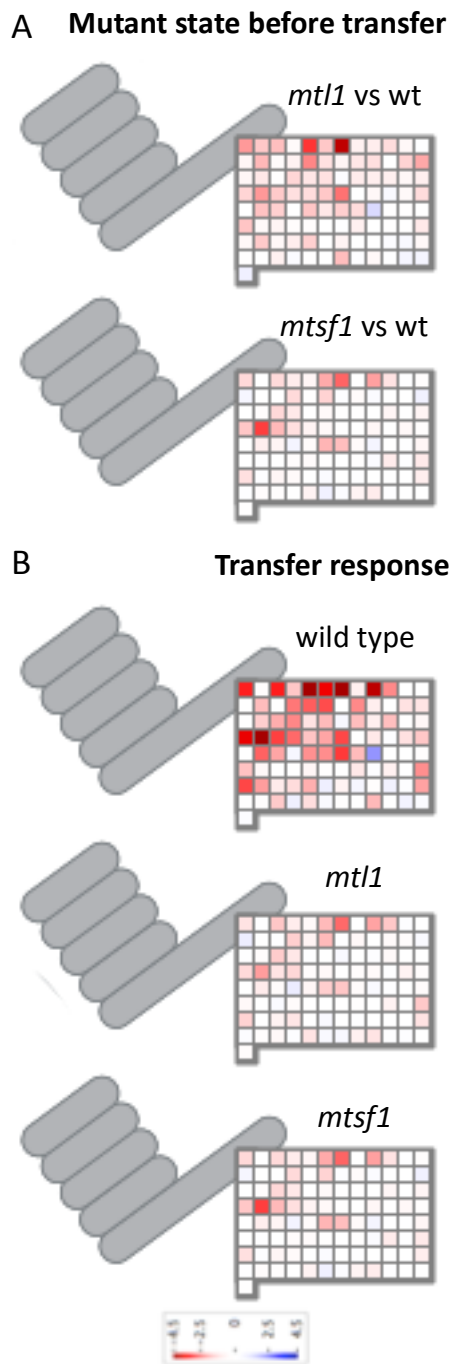


Figure 5.15: Impact of *ci* genetic defects on photosynthesis related genes. A. Callus state before transfer to shoot induction medium. B. Gene expression changes induced by transfer to shoot induction medium. Blue, upregulated genes, red downregulated genes. The direction of pair-wise comparisons are as indicated in Figure 5.

Cell cycle transcriptional signatures indirectly report the dynamics of callus proliferation

The arrest of cell division after callus transfer to the regeneration medium has been described in other *in vitro* culture systems. When explants are cultured on a callus induction medium then transferred on a shoot induction medium, cell proliferation is first arrested then resumes in localized regions where buds generally appear (Sugiyama, 2013).

To assess indirectly the overall mitotic activity of the tissue samples we analyzed, and as a complement to the trends already documented with GO term enrichment analysis and MapMan overviews, we plotted the expression profiles of cell cycle related genes (Vandepoele et al., 2002) across the treatment and genotype experiments (Figure 5.16). The majority of cyclins (CYC) and cyclin-dependent kinases (CDK) were down-regulated in all comparisons except T_{12H} vs T_{7D} , $C_{7.5D}$ vs $T_{7.5D}$, $wt_{7.5D}$ vs $mtl1_{7.5D}$ and $wt_{7.5D}$ vs $mtsfl_{7.5D}$.

In T_{12H} vs T_{7D} , the up-regulation of most cyclin and CDK genes indicates that the tissues were able to recover from the stress induced by the initial rotenone addition, confirming results presented in Chapter 3.

In $C_{7.5D}$ vs $T_{7.5D}$, the absence of significant expression differential for any of the analyzed cell cycle genes confirms, again, that the rotenone pretreatment has little overall effect on the general state of the cultured cells, and no detectable effect on their proliferation, shortly after their transfer to the regeneration medium.

Interestingly, the patterns emerging from the cI mutant vs wild type comparisons, corresponding to the early response of the calli after transfer ($wt_{7.5D}$ vs $mtl1_{7.5D}$, $wt_{7.5D}$ vs $mtsfl_{7.5D}$), indicate that cell cycle genes classically associated with active cell division are transcribed at higher levels in the mutants. This observation is in agreement with the dampened transcriptional response of the mutants following callus transfer and suggests that mutant calli are able to resume proliferation earlier and at a higher pace than the wild-type explants.

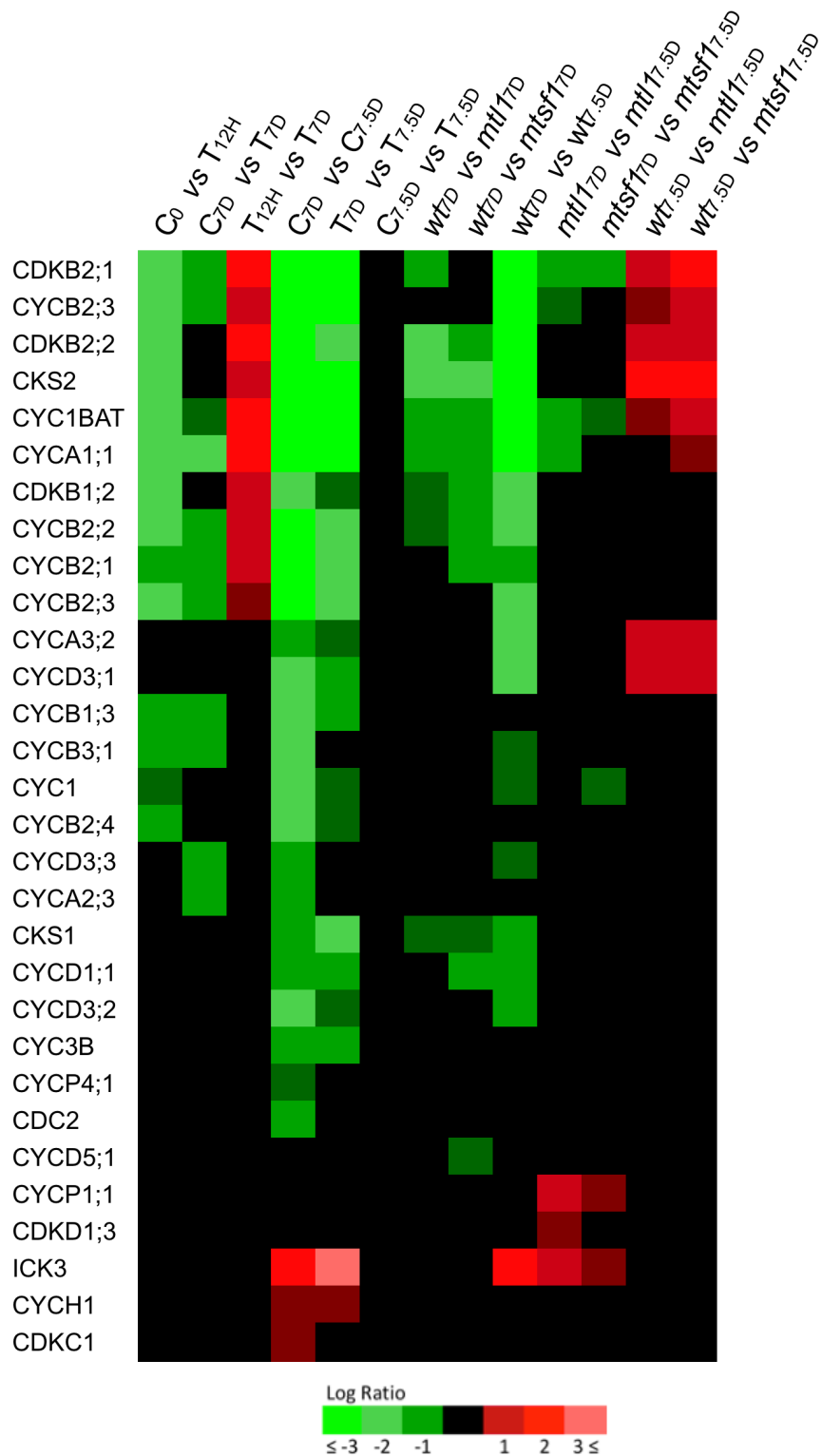


Figure 5.16: Expression patterns of cell cycle related genes. Red, upregulated genes, green, downregulated genes. The direction of pair-wise comparisons are as indicated in Figure 5.1.

Phytohormones metabolism and signaling

As is also the case in the regeneration sequence implemented in this study, auxin-rich media are classically used to promote cell proliferation, while cytokinin-rich media are generally used to promote morphogenesis. However, the initiation and maintenance of shoot meristems are less a direct reflection of overall hormone tissue content than the results of complex network actions involving signaling pathways triggered by different hormones, cross-talks between them, and feedback loops controlling hormone synthesis, conjugation and degradation. Nevertheless, we plotted the expression patterns of genes associated with cytokinin and auxin metabolism and signaling with the aim to identify potential molecular links with cI activity and mitochondrial functions. Some peculiar patterns are highlighted here below.

Molecules belonging to the cytokinin class have a major role in inducing proliferation and organogenesis in *planta* and during *in vitro* regeneration (Figure 5.17 A). The cytokinin oxidase/dehydrogenases (CKXs) catalyze the irreversible degradation of cytokinins and the overexpression of the CKX coding genes is associated with lower cytokinin levels in plant tissues (Schmülling et al., 2003). *CKX1*, *CKX3* and *CKX6* were the most variable genes in the family. All three were up-regulated in both cI mutants compared with wild type after the transfer (*wt*_{7.5D} vs *mtl1*_{7.5D} and *wt*_{7.5D} vs *mtsfl*_{7.5D}), but otherwise unregulated or down-regulated in following rotenone treatment or callus transfer. Other *CKX* genes showed some regulation in rotenone-treated and untreated calli upon transfer, but with no obvious trends. It is difficult to deduce any pattern from the modulation of *CKX* genes in these experiments.

The type-A Arabidopsis Response Regulators ARR3, ARR4, ARR5, ARR6, ARR8, and ARR9 have been described as negative regulator of cytokinin signaling (To et al., 2004). In addition, type-A *ARR7* and *ARR15* overexpression was shown to repress callus proliferation and shoot regeneration (Buechel et al., 2010). *ARR15* was down-regulated in all calli 12h after transfer (*C*_{7D} vs *C*_{7.5D}, *T*_{7D} vs *T*_{7.5D}, *wt*_{7D} vs *wt*_{7.5D}, *mtl1*_{7D} vs *mtl1*_{7.5D}, *mtsfl*_{7D} vs *mtsfl*_{7.5D}) which may accompany the onset of organogenesis.

Cytokinin Response Factors (CRFs) are AP2/ERF transcription factors induced by cytokinin (Rashotte et al., 2006). As expected because the regeneration medium (SIM) contains meta-topolin, two cytokinin response factors (*CRF3* and *CRF2*) were up-regulated 12h after transfer in all comparisons (*C*_{7D} vs *C*_{7.5D}, *T*_{7D} vs *T*_{7.5D}, *wt*_{7D} vs *wt*_{7.5D}, *mtl1*_{7D} vs *mtl1*_{7.5D} and *mtsfl*_{7D} vs *mtsfl*_{7.5D}). Furthermore, *CRF6* is reported to be induced during mitochondrial retrograde regulation (MRR) as a result of mitochondrial dysfunction (De

Clercq et al., 2013). It is also implicated in cross-talk between cytokinin signaling and oxidative stress (Zwack et al., 2016). Interestingly, *CRF6* was up-regulated after transfer in control, treated calli and wilt type (C_{7D} vs $C_{7.5D}$, T_{7D} vs $T_{7.5D}$, wt_{7D} vs $wt_{7.5D}$). It is also up-regulated in both cI mutant tissues before transfer (wt_{7D} vs $mtl1_{7D}$ and wt_{7D} vs $mtsfl_{7D}$), which is possibly why no further induction was detected upon transfer in the mutant calli ($mtl1_{7D}$ vs $mtl1_{7.5D}$, $mtsfl_{7D}$ vs $mtsfl_{7.5D}$).

Several *AUXIN RESPONSE FACTOR (ARFs)* were down-regulated after transfer of control and rotenone-treated calli (C_{7D} vs $C_{7.5D}$, wt_{7D} vs $wt_{7.5D}$, T_{7D} vs $T_{7.5D}$). ARFs are transcription factors implicated in the activation or repression of the auxin response genes (Guilfoyle and Hagen, 2007). *ARFs* expression was less impacted by the transfer in cI mutants calli (Figure 5.17 B). We noticed that *YADOKARI 1 (YDK1)* expression profile is nearly the same in rotenone-treated calli and cI mutants calli. This gene is up-regulated in calli after rotenone treatment (C_0 vs T_{12H} , C_{7D} vs T_{7D}) and also in cI mutants before transfer (wt_{7D} vs $mtl1_{7D}$, wt_{7D} vs $mtsfl_{7D}$); and down-regulated after calli transfer in control (C_{7D} vs $C_{7.5D}$), rotenone treated (T_{7D} vs $T_{7.5D}$) and cI mutants calli ($mtl1_{7D}$ vs $mtl1_{7.5D}$, $mtsfl_{7D}$ vs $mtsfl_{7.5D}$) (Figure 5.17 B). This gene, also known as *GH3.2*, is described as a negative regulator of auxin signaling because the encoded protein catalyzes the synthesis of auxin-amino acid conjugates (Takase et al., 2004; Staswick et al., 2005).

A

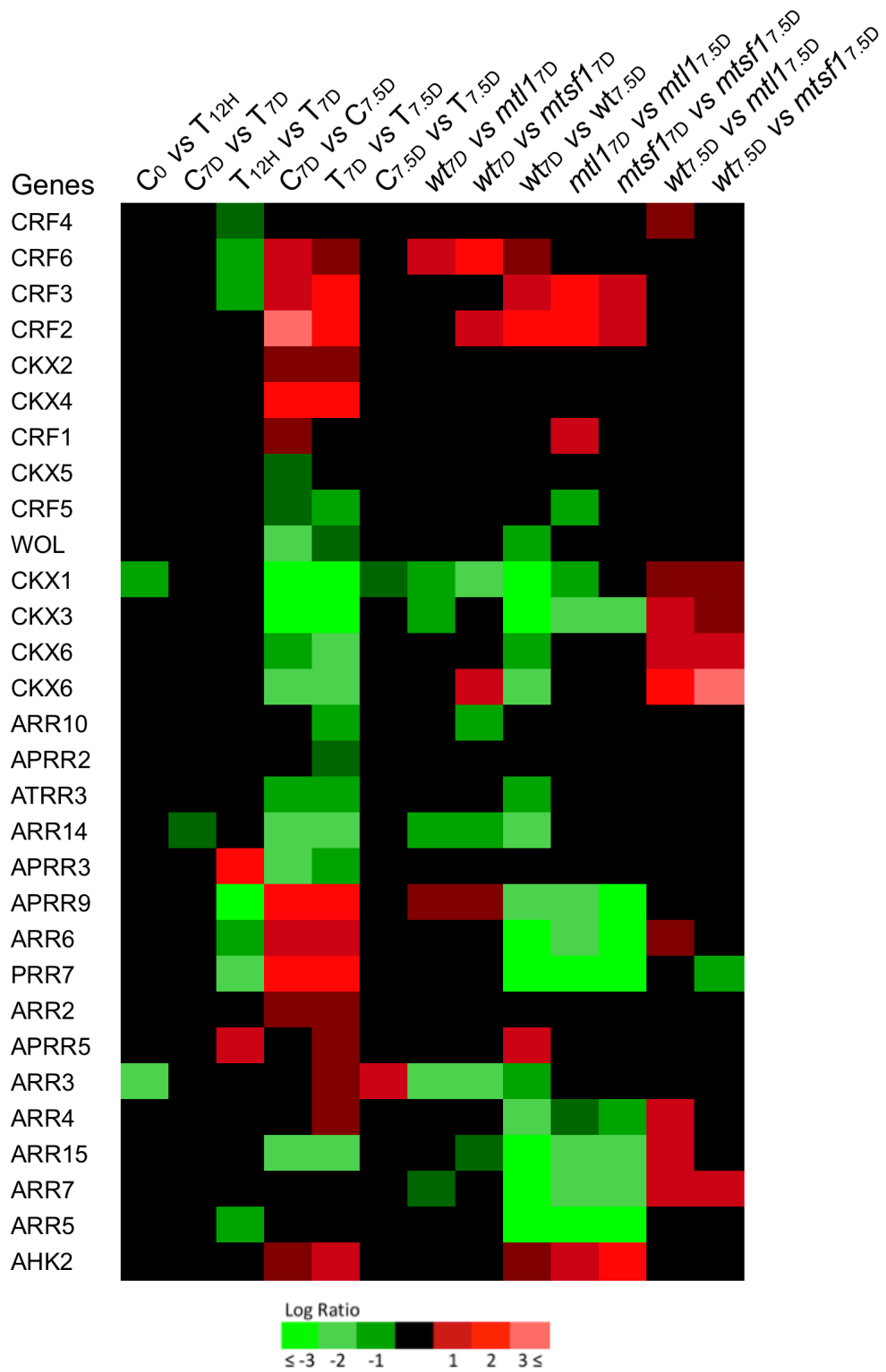


Figure 5.17: Expression patterns of cytokinin and auxin related genes. A, auxin related. Red, upregulated genes, green, downregulated genes. The direction of pair-wise comparisons are as indicated in Figure 5.1.

B

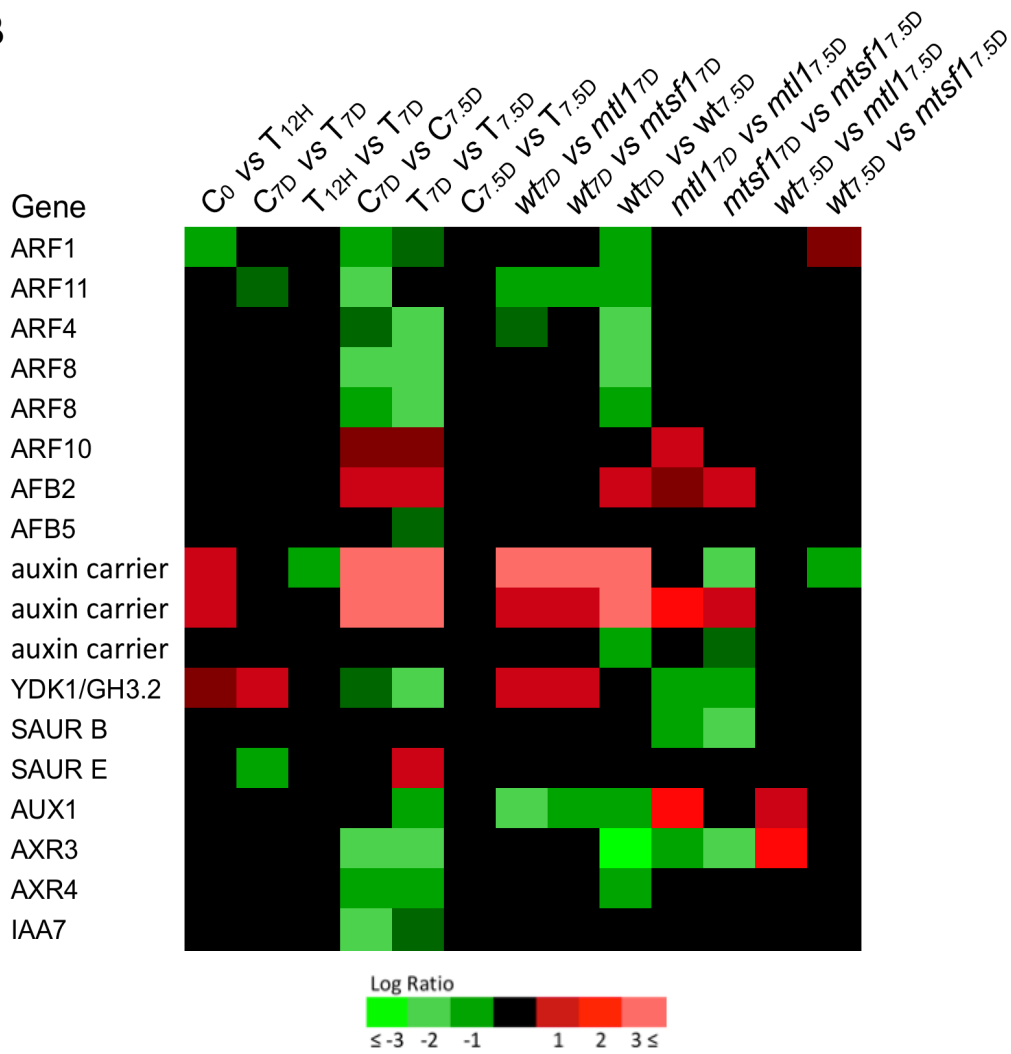


Figure 5.17: Expression patterns of cytokinin and auxin related genes [continued]. B, cytokinin related. Red, upregulated genes, green, downregulated genes. The direction of pairwise comparisons are as indicated in Figure 5.1.

Induction of the alternative respiratory pathway

Through the analysis of a few selected gene expression profiles, we have previously shown that *in vitro* tissue culture and callus transfer resulted in the activation of the alternative pathway (Chapter 3) and that the pathway seemed further induced in cI mutants (Chapter 2). We explored the full transcriptome dataset for confirmation of this previous observation (Figure 5.18).

The genes coding for the alternative oxidases *AOX1a* and *AOX1d*, as well as the NAD(P)H dehydrogenases *NDB2* and *NDB4*, were all up-regulated in cI mutants compared to wild type before transfer (*wt*_{7D} vs *mtll*_{7D}, *wt*_{7D} vs *mtsfl*_{7D}). Twelve hours after transfer, these four genes were also up-regulated in rotenone-treated calli and control calli (*C*_{7D} vs *C*_{7.5D}, *T*_{7D} vs *T*_{7.5D}). However, *AOX1d* was down-regulated just in cI mutants after transfer (*mtll*_{7D} vs *mtll*_{7.5D}, *mtsfl*_{7D} vs *mtsfl*_{7.5D}). *NDB4* was also up-regulated in the *mtll* cI mutant after transfer (*mtll*_{7D} vs *mtll*_{7.5D}) and in the wild type, and the gene was expressed at higher level in both cI mutants compared to wild type after transfer (*wt*_{7.5D} vs *mtll*_{7.5D}, *wt*_{7.5D} vs *mtsfl*_{7.5D}). *AOX1a* was up-regulated 12h after rotenone treatment compared to control calli (*C*₀ vs *T*_{12H}) and it was induced in control and treated calli after transfer (*T*_{7D} vs *T*_{7.5D}, *C*_{7D} vs *C*_{7.5D}).

In summary, at least four genes (*AOX1a*, *AOX1d*, *NDB2*, *NDB4*) known to be induced following oxidative stress or cI dysfunction were up-regulated by callus transfer, reinforcing the overlap between oxidative stress and explant manipulation. Furthermore, all four genes were also up-regulated in the better regenerating cI mutants.

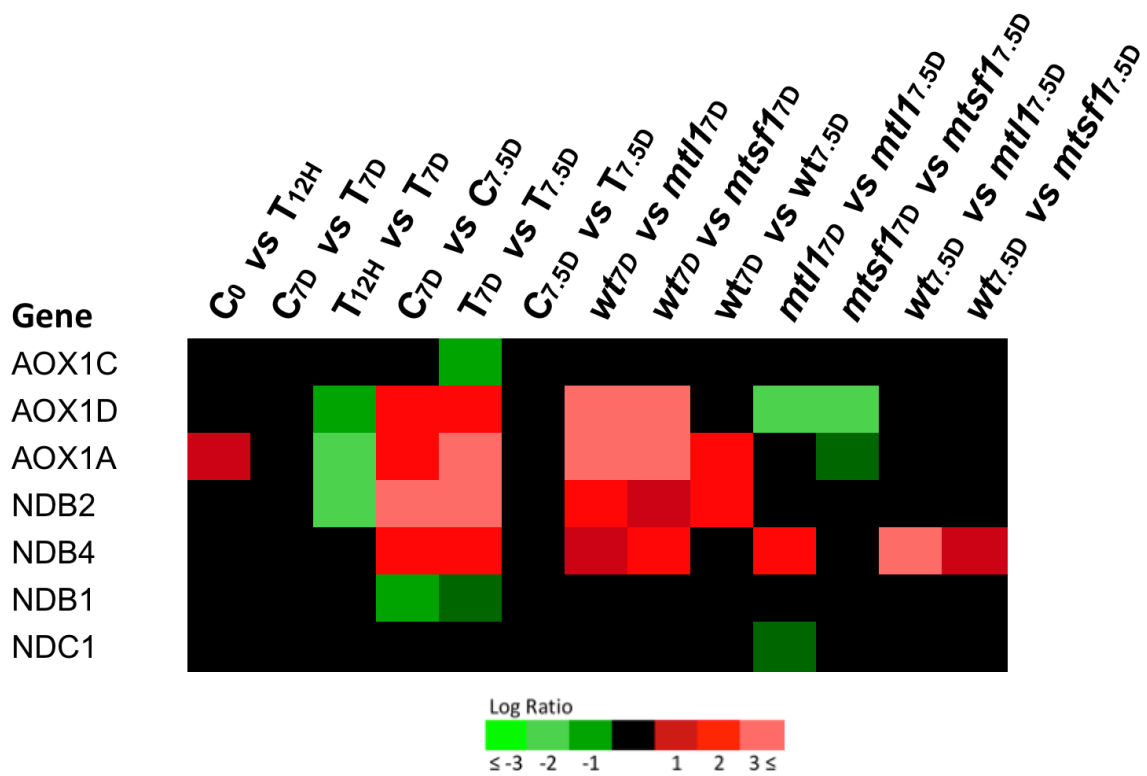


Figure 5.18: Expression patterns of alternative pathway genes. Red, upregulated genes, green, downregulated genes. The direction of pair-wise comparisons are as indicated in Figure 5.1.

Comparison with previous reports investigating transcriptional responses to various mitochondrial dysfunctions

Schwarzländer and co-workers compared 11 microarray datasets prepared from both mutants and chemical treatments that induce mitochondrial dysfunction. From this meta-analysis, they made a list of marker genes of mitochondrial dysfunctions (Schwarzländer et al., 2012). Among mitochondrial dysfunctions, the two cI mutants used in this comparative analysis *ndufs4* (NADH dehydrogenase [ubiquinone] fragment S subunit 4) and *ndufa1* are also characterised by growth retardation (Meyer et al., 2009) (as cI mutants in our study, see chapter 2). *ndufs4* lacks cI just like *mtl1* whereas *ndufa1* has a highly reduced cI level and activity. Another dataset used in this comparative analysis concerned rotenone treatment applied on Landsberg *erecta* cell culture and the analysis was done 4h after the cI inhibition (Clifton et al., 2005). When we compared the expression profile of these genes with our data, we noticed a significant difference in some gene expression profiles (Figure 5.19). The difference in transcript levels could be explained by the plant material used for microarrays analysis: cI mutants *ndufs4* and *ndufa1* were characterized with leaves samples (Meyer et al., 2009) and rotenone treatments in cell cultures of the Landsberg *erecta* genotype (Clifton et al., 2005) (our work is based on Columbia accession) and the reported rotenone treatment was shorter (4h versus 12h in our study).

Van Aken and collaborators (2009) analysed the mitochondrial retrograde signalling resulting from stress-inducing conditions like treatments with oxidant compounds (H₂O₂) or cI inhibition (rotenone). For this purpose, they analysed 16 microarrays data where several stresses were applied and found out 26 nuclear encoded genes that they defined as MRR markers since these genes are differentially expressed after stress-induced treatments and their encoded proteins are directed to the mitochondria (Van Aken et al., 2009). The expression profile of only three genes from this list are differentially expressed in our data: up-regulation of *AOX1a* and *UPOX* (universal marker of oxidative stress) and down-regulation of the heat shock protein *HSP23.6* (Figure 5.19).

Finally, Ho and co-workers (Ho et al., 2008) established a list of 10 candidate genes that share cis-acting regulatory elements (CAREs) in their promoter region. These CAREs are related to the response to stress induced by rotenone and H₂O₂. Four genes from this list that are up-regulated by rotenone are also up regulated in rotenone treated-calli and cI mutants in our data (*AOX1a*, *UPOX*, *WRKY15* and an unknown protein) (Figure 5.19).

Mitochondrial dysfunction marker genes		This work			Schwarzländer <i>et al.</i> (2012)		
AGI	Gene	rotenone	<i>mtl1</i>	<i>mts1l</i>	rotenone	<i>ndufs4</i>	<i>ndufa1</i>
AT3G22370	AOX1a	Red	Red	Red	Red	Red	Red
AT2G41730	unknown protein	Red	Red	Red	Red	Red	Red
AT4G37370	CYP81D8	Red	Red	Red	Red	Red	Red
AT1G32870	ANAC013	Red	Red	Red	Red	Red	Red
AT5G40690	unknown protein	Red	Red	Red	Red	Red	Red
AT5G59220	PP2C	Red	Red	Red	Red	Red	Red
AT1G24090	RNase H domain-containing protein	Red	Red	Red	Red	Red	Red
AT2G41380	embryo-abundant protein-related	Red	Red	Red	Red	Red	Red
AT1G68840	RAV2	Red	Red	Red	Red	Red	Red
AT2G25200	unknown protein	Red	Red	Red	Red	Red	Red
AT4G17340	TIP2;2	Red	Red	Red	Red	Red	Red
AT5G62900	unknown protein	Red	Red	Red	Red	Red	Red
AT1G63840	C3HC4-type RING finger	Red	Red	Red	Red	Red	Red
AT4G01700	chitinase, putative	Red	Red	Red	Red	Red	Red
AT5G54130	calcium-binding	Red	Red	Red	Red	Red	Red

Mitochondrially targeted stress-response genes (MRR-related)		This work			Van Aken <i>et al.</i> (2009)
AGI	Gene	rotenone	<i>mtl1</i>	<i>mts1l</i>	rotenone
AT3G22370	AOX1a	Red	Red	Red	Red
AT4G05020	NDB2	Red	Red	Red	Red
AT2G21640	UPOX	Red	Red	Red	Red
AT2G41380	embryo-abundant protein-related	Red	Red	Red	Red
AT4G25200	HSP23.6	Green	Red	Red	Red
AT5G51440	HSP23.5	Red	Red	Red	Red
AT1G32350	AOX1d	Red	Red	Red	Red
AT3G48850	PiC	Red	Red	Red	Red
AT3G50930	BCS1	Red	Red	Red	Red
AT1G20350	TIM17-1	Red	Red	Red	Red
AT2G41380	embryo abundant	Red	Red	Red	Red
AT5G38710	proline oxidase	Red	Red	Red	Red
AT5G16200	50S RibP	Red	Red	Red	Red
AT5G25450	QCR7	Red	Red	Red	Red
AT4G27940	MTM1	Red	Red	Red	Red
AT4G30490	AFG1-like	Red	Red	Red	Red
AT4G28390	AAC3	Red	Red	Red	Red
AT4G36580	AAA ATPase	Red	Red	Red	Red
AT5G09590	HSC70-5	Red	Red	Red	Red
AT5G55200	GrpE	Red	Red	Red	Red
AT1G21400	2-oxoisovalerate DH	Red	Red	Red	Red
AT5G61810	mitochondrial carrier	Red	Red	Red	Red

Stress induced genes with similar CAREs in their promoters		This work			Ho <i>et al.</i> (2008)
AGI	Gene	rotenone	<i>mtl1</i>	<i>mts1l</i>	rotenone
AT3G22370	AOX1a	Red	Red	Red	Red
AT4G05020	NDB2	Red	Red	Red	Red
AT2G21640	UPOX	Red	Red	Red	Red
AT1G13990	Unknown Predicted to Chloroplast	Red	Red	Red	Red
AT1G70420	unknown	Red	Red	Red	Red
AT1G75730	Unknown Predicted to Mitochondria	Red	Red	Red	Red
AT2G01630	glycosyl hydrolase	Red	Red	Red	Red
AT2G17850	Senescence Associated Protein	Red	Red	Red	Red
AT2G23320	WRKY15	Red	Red	Red	Red
AT4G28240	wound-responsive protein-related	Red	Red	Red	Red

Figure 5.19: Expression profile of genes related with complex I impairment. Red, up-regulated genes (log ratio > 1); green, down-regulated genes (log ratio < -1) and black, genes with log ratio between -1 and 1. CYP81D8, cytochrome P450, family 81, subfamily D, polypeptide 8; ANAC013, Arabidopsis NAC domain containing protein 13; PP2C, protein phosphatase 2C; RAV2, REGULATOR OF THE ATPASE OF THE VACUOLAR MEMBRANE; TIP2;2, tonoplast intrinsic protein 2;2; UPOX, up-regulated during oxidative stress; HSP23.6, 23.6 kDa small heat shock protein; HSP23.5, SMALL HEAT SHOCK PROTEIN; PiC, mitochondrial phosphate transporter; BCS1, AAA-type ATPase family protein; TIM17-1, mitochondrial inner membrane translocase; PRO2, proline oxidase,

osmotic stress-responsive proline dehydrogenase; 50S RibP, 50S ribosomal protein-related; QCR7, ubiquinol-cytochrome C reductase complex (Complex III); MTM1, mitochondrial substrate carrier family protein; AFG1-like, mitochondrial substrate carrier family protein; AAC3, mitochondrial substrate carrier family protein; HSC70-5, HEAT SHOCK PROTEIN; GrpE, co-chaperone grpE protein; 2-oxoisovalerate DH, 2-oxoisovalerate dehydrogenase.

Induction of genes expressed in the shoot meristem

The observation of the regenerating calli following their transfer on the gelled shoot induction medium indicated that the first shoot meristems were visible 7 to 10 days after transfer with a binocular microscope. In almost all cases, the meristems formed at sites were a few purple cells - likely accumulating anthocyanes - were visible 3 or 4 days earlier (data not shown). Considering that an Arabidopsis shoot meristem develops within 4 to 5 days (Rosspopoff et al., 2017), we looked for early signs of organogenesis in the transcriptome dataset (Figure 5.20).

None of the genes analyzed varied much across rotenone treatments or transfer of wild-type tissues, except for *WUSCHEL* (*WUS*) that codes for a homeodomain transcription factor that positively regulates the fate and proliferation of stem cells. *WUS* was consistently down-regulated immediately after rotenone addition (C_0 vs T_{12H}) and upon transfer of wild-type tissues (C_{7D} vs $C_{7.5D}$, T_{7D} vs $T_{7.5D}$, wt_{7D} vs $wt_{7.5D}$) on shoot induction medium. However, in agreement with the enhanced initiation of buds after transfer in the cI mutant calli, *STM*, *CUC2* and *CLV1* were already up-regulated in the mutants compared to the wild type before transfer (wt_{7D} vs $mtl1_{7D}$, wt_{7D} vs $mtsfl_{7D}$). Furthermore, *WUS*, *STM*, *CUC2*, *ESR1* and *CLV1* were all up-regulated in at least one cI mutant compared to wild type after the transfer ($wt_{7.5D}$ vs $mtl1_{7.5D}$, $wt_{7.5D}$ vs $mtsfl_{7.5D}$).

Thus, even though our analysis is limited to the early response following the transfer of the calli to the shoot induction medium (12 hours), multiple genes associated with shoot meristem development are expressed at higher level in the better regenerating cI mutants.

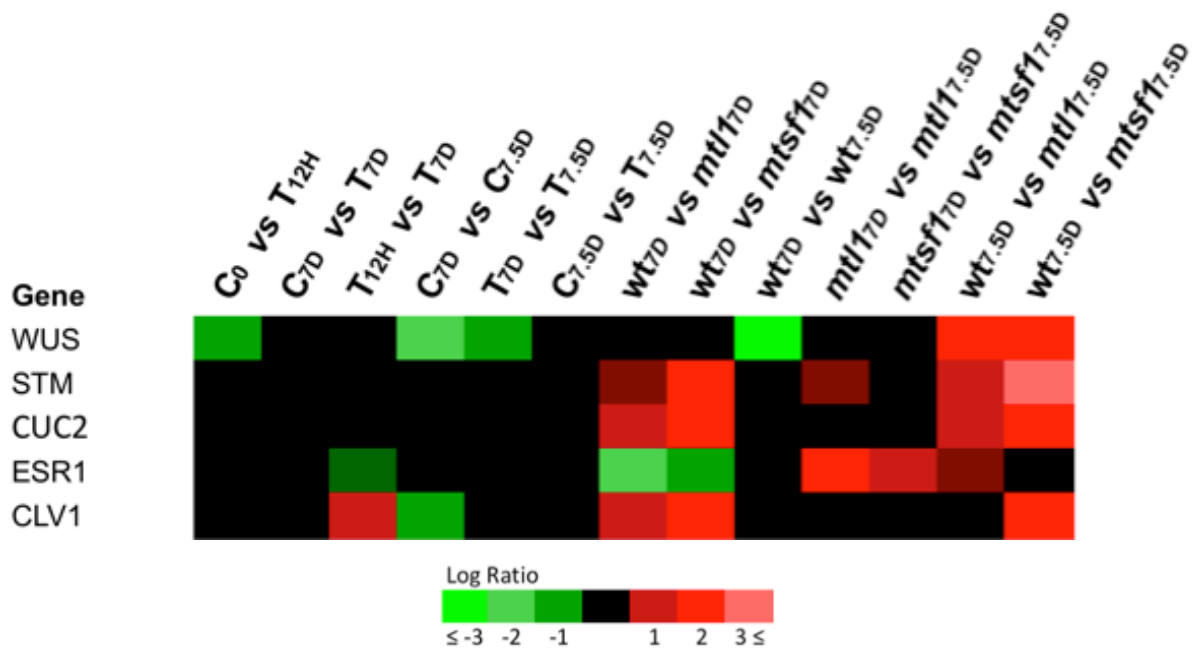


Figure 5.18: Expression patterns of alternative pathway genes. Red, upregulated genes, green, downregulated genes. The direction of pair-wise comparisons are as indicated in Figure 5.1.

Cautionary remarks

While our transcriptome profile analysis is informative, we do know that these results must be carefully interpreted for several reasons. The RNA used in this study were all prepared from pooled calli. Thus, patterns may be blurred if their response is not synchronous. More importantly, organogenesis occurs when neighboring cells adopt different fates and only a minor portion of any given callus undergoes morphogenesis. It is therefore not possible to track precisely successive stages of development with our experimental setup.

Furthermore, the profiles generated in this study highlight the complexity of the cell responses induced in the course of a regeneration sequence. In all pair-wise comparisons, we detected changes simultaneously resulting in up- and down-regulation of genes associated with the same general classes of response. Similarly, when considering large gene families, opposite changes were almost always observed.

Nevertheless, the transcriptome signatures we obtained enable us to formulate informed hypotheses to explain how the modulation cI activity affects the propensity of *in vitro* cultured tissues to undergo morphogenesis as detailed in the next chapter.

References

- Van Aken O, Zhang B, Carrie C, Uggalla V, Paynter E, Giraud E, Whelan J (2009)**
Defining the mitochondrial stress response in *Arabidopsis thaliana*. *Mol Plant* **2**: 1310–1324
- Buechel S, Leibfried A, To JPC, Zhao Z, Andersen SU, Kieber JJ, Lohmann JU (2010)**
Role of A-type *Arabidopsis* Response Regulators in meristem maintenance and regeneration. *Eur J Cell Biol* **89**: 279–284
- De Clercq I, Vermeirssen V, Van Aken O, Vandepoele K, Murcha MW, Law SR, Inze A, Ng S, Ivanova A, Rombaut D, et al (2013)** The Membrane-Bound NAC Transcription Factor ANAC013 Functions in Mitochondrial Retrograde Regulation of the Oxidative Stress Response in *Arabidopsis*. *Plant Cell* **25**: 3472–3490
- Clifton R, Lister R, Parker KL, Sappl PG, Elhafez D, Millar AH, Day DA, Whelan J (2005)** Stress-induced co-expression of alternative respiratory chain components in *Arabidopsis thaliana*. *Plant Mol Biol* **58**: 193–212
- Crow ML, Serizet C, Thareau V, Aubourg S, Rouzé P, Hilson P, Beynon J, Weisbeek P, van Hummelen P, Reymond P, et al (2003)** CATMA: A complete *Arabidopsis* GST database. *Nucleic Acids Res* **31**: 156–158
- Garmier M, Carroll AJ, Delannoy E, Vallet C, Day DA, Small ID, Millar AH (2008)**
Complex I Dysfunction Redirects Cellular and Mitochondrial Metabolism in *Arabidopsis*. *Plant Physiol* **148**: 1324–1341
- Guilfoyle TJ, Hagen G (2007)** Auxin response factors. *Curr Opin Plant Biol* **10**: 453–460
- Haïli N, Arnal N, Quadrado M, Amiar S, Tcherkez G, Dahan J, Briozzo P, Colas des Francs-Small C, Vrielynck N, Mireau H (2013)** The pentatricopeptide repeat MTSF1 protein stabilizes the *nad4* mRNA in *Arabidopsis* mitochondria. *Nucleic Acids Res* **41**: 6650–6663
- Haïli N, Planchard N, Arnal N, Quadrado M, Vrielynck N, Dahan J, Francs-Small CC des, Mireau H (2016)** The MTL1 Pentatricopeptide Repeat Protein Is Required for Both Translation and Splicing of the Mitochondrial NADH DEHYDROGENASE SUBUNIT7 mRNA in *Arabidopsis*. *Plant Physiol* **170**: 354–366
- Hilson P, Allemeersch J, Altmann T, Aubourg S, Avon A, Beynon J, Bhalerao RP, Bitton F, Caboche M, Cannoot B, et al (2004)** Versatile Gene-Specific Sequence Tags for *Arabidopsis* Functional Genomics : Transcript Profiling and Reverse Genetics Applications Versatile Gene-Specific Sequence Tags for *Arabidopsis* Functional

- Genomics : Transcript Profiling and Reverse Genetics Applic. *Genome Res* 2176–2189
- Ho LHM, Giraud E, Uggalla V, Lister R, Clifton R, Glen A, Thirkettle-watts D, Aken O Van, Whelan J** (2008) Identification of Regulatory Pathways Controlling Gene Expression of Stress-Responsive Mitochondrial Proteins. *Plant Physiol* **147**: 1858–1873
- Meyer EH, Tomaz T, Carroll AJ, Estavillo G, Delannoy E, Tanz SK, Small ID, Pogson BJ, Millar AH** (2009) Remodeled Respiration in *ndufs4* with Low Phosphorylation Efficiency Suppresses Arabidopsis Germination and Growth and Alters Control of Metabolism at Night. *Plant Physiol* **151**: 603–619
- Mi H, Huang X, Muruganujan A, Tang H, Mills C, Kang D, Thomas PD** (2017) PANTHER version 11: Expanded annotation data from Gene Ontology and Reactome pathways, and data analysis tool enhancements. *Nucleic Acids Res* **45**: 183–189
- Mi H, Muruganujan A, Casagrande JT, Thomas PD** (2013) Large-scale gene function analysis with the panther classification system. *Nat Protoc* **8**: 1551–1566
- Provart N, Tong Z** (2003) A Browser-based Functional Classification SuperViewer for Arabidopsis Genomics. *Curr Comput Mol Biol* 271–272
- Rashotte AM, Mason MG, Hutchison CE, Ferreira FJ, Schaller GE, Kieber JJ** (2006) A subset of Arabidopsis AP2 transcription factors mediates cytokinin responses in concert with a two-component pathway. *Proc Natl Acad Sci* **103**: 11081–11085
- Rosspopoff O, Chelysheva L, Saffar J, Lecorgne L, Gey D, Caillieux E, Colot V, Roudier F, Hilson P, Berthomé R, et al** (2017) Direct conversion of root primordium into shoot meristem relies on timing of stem cell niche development. *Development* **144**: 1187–1200
- Schmülling T, Werner T, Riefler M, Krupková E, Bartrina Y, Manns I** (2003) Structure and function of cytokinin oxidase/dehydrogenase genes of maize, rice, Arabidopsis and other species. *J Plant Res* **116**: 241–252
- Schwarzländer M, König AC, Sweetlove LJ, Finkemeier I** (2012) The impact of impaired mitochondrial function on retrograde signalling: A meta-analysis of transcriptomic responses. *J Exp Bot* **63**: 1735–1750
- Staswick PE, Serban B, Rowe M, Tiryaki I, Maldonado MT, Maldonado MC, Suza W** (2005) Characterization of an Arabidopsis Enzyme Family That Conjugates Amino Acids to Indole-3-Acetic Acid. *Plant Cell* **17**: 616–627
- Sugiyama M** (2013) Molecular genetic analysis of organogenesis in vitro with temperature-sensitive mutants. *Plant Biotechnol Rep.* doi: 10.1007/s11816-013-0292-1
- Takase T, Nakazawa M, Ishikawa A, Kawashima M, Ichikawa T, Takahashi N, Shimada H, Manabe K, Matsui M** (2004) *ydk1-D*, an auxin-responsive GH3 mutant

that is involved in hypocotyl and root elongation. *Plant J* **37**: 471–483

Thimm O, Bla O, Gibon Y, Nagel A, Meyer S, Kru P, Selbig J, Mu LA, Rhee SY, Stitt M (2004) MAPMAN : a user-driven tool to display genomics data sets onto diagrams of metabolic pathways and other biological processes. *Plant J* **37**: 914–939

To JPC, Haberer G, Ferreira FJ, Deruère J, Mason MG, Schaller GE, Alonso JM, Ecker JR, Kieber JJ (2004) Type-A Arabidopsis response regulators are partially redundant negative regulators of cytokinin signaling. *Plant Cell* **16**: 658–671

Vandepoele K, Raes J, De Veylder L, Rouze P, Rombauts S, Inze D (2002) Genome-wide analysis of core cell cycle genes in Arabidopsis. *Plant Cell* **14**: 903–916

Zwack PJ, De Clercq I, Howton TC, Hallmark HT, Hurny A, Keshishian EA, Parish AM, Benkova E, Mukhtar MS, Van Breusegem F, et al (2016) Cytokinin Response Factor 6 Represses Cytokinin-Associated Genes during Oxidative Stress. *Plant Physiol* **172**: pp.00415.2016

Chapter 6:

General discussion and perspectives

With the development of *in vitro* tissue culture, different plant regeneration systems have been developed in multiple species based either on *de novo* organogenesis (shoot regeneration and root regeneration) or somatic embryogenesis. Since the beginning of this era, the regeneration rate has always been largely dependent on the species and protocols developed, and these were not interchangeable.

Within a species, the regeneration frequency also depends on the cultivars or ecotypes from which explants are prepared. For example, the *Arabidopsis thaliana* accession Columbia, which is the wild-type genotype in our assays, has been shown to produce far fewer buds than Wassilewskija in a protoplast-based regeneration system (Chupeau et al., 2013). The seminal observation that a Columbia well-characterized mutation markedly improves *in vitro* organogenesis response in this context thus offered a unique opportunity to investigate the cause(s) of recalcitrance and could possibly lead to original ways to alleviate this lingering bottleneck in plant biotechnology (Altpeter et al., 2016).

During my PhD thesis, I analysed the impact of mitochondrial impairments on *in vitro* callus growth and shoot regeneration in the Arabidopsis model. First we characterized the *in vitro* development phenotypes of four cI mutants known to display graded plant growth retardation. The protoplast-derived calli prepared from cI mutant plants also have a gradual growth defect reminiscent of whole plant phenotypes. However, the two cI mutants most affected in callus growth yielded the highest shoot formation frequency (chapter II).

To confirm the link between cI impairment and the observed regeneration boost, we chemically inhibited the mitochondrial cI with rotenone in the *in vitro* cultured tissues. When applied transiently on wild-type calli at high but non-lethal concentrations, the inhibitor phenocopied the growth defect observed in cI mutant calli while simultaneously enhancing the regeneration rate (chapter III).

Furthermore, we showed that this improved *in vitro* response is linked specifically to cI dysfunction and cannot be simply explained by the reduction of callus size in mutant tissue cultures as, in wild-type, callus size is not correlated with regeneration rate (chapter IV).

Several studies investigated the molecular and metabolic adaptations in respiratory mutant plants and in plant or cell culture subjected to different chemical treatments to impair the mETC. The major objective of these analyses was to understand the implication of mitochondria and especially mitochondrial signalling in plant development. Our work described the effect of mitochondrial perturbations on *in vitro* callus growth and regeneration. To understand how molecular adaptation in respiratory mutants or in rotenone-treated tissues

may explain the observed shoot enhancement with cI dysfunction, we completed the transcriptomic analysis of the corresponding derived calli (chapter 5).

The rearrangement of cellular metabolism in plants subjected to mitochondrial impairments results in altered or enhanced tolerance to various stresses (Lee et al., 2002; Meyer et al., 2009; Juszczuk et al., 2012). *In vitro* cell culture has itself an effect on mitochondrial mutants compared to the wt. An Arabidopsis mutant with reduced complex I amount showed a normal growth and development in soil but cell culture tissues derived from this mutant had a marked growth retardation (Perales et al., 2005). In fact, we suspect that in most cases the manipulation of *in vitro* cultured explants results in major stresses that impact *in vitro* tissue response, whether it is recognized or not, and triggering many signals and metabolic perturbations inherent to these stresses.

Among the striking features of *in vitro* manipulations, we can cite the rapid and dramatic drop in *CYCB1;1* transcripts suggesting that explants undergo a strong stress when moved from one medium to another. The arrest of cell division in an explant following its transfer to a regeneration medium has been described in other *in vitro* culture systems. The shift of calli from a callus induction medium (CIM) to a shoot induction medium (SIM) was shown to stop cell proliferation that is only reactivated in localized regions where buds generally appear (Sugiyama, 2013). We have observed a similar phenomenon in root segments bearing lateral root (LR) primordia. When transferred from an auxin to a cytokinin medium, actively dividing LR primordia cease mitotic activity for about 24 hours and then resume cell division, some of them immediately converting into shoot meristems (Rosspopoff et al., 2017). Thus, in our *in vitro* system, cell division arrest observed after the transfer to the regeneration medium could be an important step for calli to launch shoot regeneration programme.

We also noticed the induction of wound-responsive genes after the transfer to the regeneration medium. One wound responsive gene (*WIND1*) was already found to be induced after organ wounding, where callus and future organs are formed (Iwase et al., 2015). Wounded tissues are even able to regenerate organs naturally without exogenous hormones (Xu and Huang, 2014). The impact of the transfer on wound-responsive genes expression was slightly different between complex I mutants calli and the wild type. The up-regulation of wound-responsive genes when calli are transferred to the regeneration medium could be among the first steps of shoots induction.

We suppose that the *in vitro* regeneration boost observed in our cI mutants and in rotenone-treated calli is caused by a stress-related response, especially an oxidative stress

response, induced by the mitochondrial impairments. Still, the oxidative stress induced by rotenone must be balanced since it is either productive or cytotoxic, presumptively depending on oxidative stress generated within the callus cells, itself correlated with the final rotenone concentration in the culture media and the length of the exposure to the inhibitor.

In accordance with this hypothesis, the redox biosensor (grx-roGFP2) reports a remarkable heterogeneity in redox state among the callus cells, both before and after rotenone treatment. Thus, the observed diversity in caulogenesis rate during our experiments may be explained by the heterogeneity of the cells and of their response to the rotenone-induced oxidative stress. Furthermore, the boundaries between productive stress and irreparable damage may be wide or narrow, and may themselves vary between experiments. In the latter case, small variation and slight heterogeneity in growth conditions may explain the variability we observed measuring *in vitro* response at the level of the explant, the dish and the culture chamber.

The redox biosensor included in our experiments was designed to visualize ROS action in the cytosol, in our case after rotenone treatment. To confirm the hypothesis that a rotenone-induced ROS signal acts as a mitochondrial retrograde signal transduced from the mitochondria to the nucleus going through the cytosol, multiple redox biosensors could be combined, for example cytosolic and mitochondrial targeted grx-roGFP2, to show that rotenone inhibition of complex I first induces a redox state change in mitochondria and then in the cytosol.

Zeng and collaborators described ROS regulation of shoot differentiation as a balance between superoxide ($O_2^{\cdot-}$) and hydrogen peroxide (H_2O_2). $O_2^{\cdot-}$ production in shoot stem cells seems to control *WUS* expression and, thereby, plant stem cell maintenance, whereas H_2O_2 promotes differentiation. Thus, the balance between these two ROS might control the shoot stem cell fate (Zeng et al., 2017). The enhancement of shoot organogenesis in cI mutants and rotenone-treated calli could be related to an unbalanced $O_2^{\cdot-}/H_2O_2$ ratio caused by mitochondrial dysfunctions.

In another perspective, we can assume that cI impairments may lead to the upregulation of mechanisms shielding the cells from excessive ROS levels, thereby mitigating the detrimental effects of ROS inevitably produced at critical steps of the regeneration sequence, and indirectly increasing the number of sites in which primed cells eventually initiate the formation of self-structuring shoot meristems.

Hence, the opposite *in vitro* response observed by (Zhang et al., 2017), i.e. the reduction of the organogenetic response in an Arabidopsis mutant with higher ROS levels

caused by mETC dysfunction, may have a simple explanation. According to this hypothesis, it is the indirect enhancement of ROS levels occurring in cI mutants that results in better protection. The *dcc1* mutant studied by Zhang and collaborators is characterized by a defect in a thioredoxin (*trx*), an anti-oxidant protein, targeted to mitochondria. They showed that *dcc1* defects included higher ROS levels and disturbed cI activity, reminiscent of the cI mutant phenotypes. But *ddc1* calli showed reduced regeneration rates. We speculate that this negative effect may simply be a direct consequence of the diminished ability of the *dcc1* explants to protect themselves from ROS damage.

It is important to note that the specific type of oxidative stress is important. In our case, it is the result of a mitochondrial defect. However, the addition of an oxidant compound like H₂O₂ (the most used ROS) directly in the culture medium does not have the same effect as the treatment with a specific inhibitor of the respiratory pathway resulting in a mitochondrial ROS. In fact, H₂O₂ and rotenone induce distinct signalling pathways (Ho et al., 2008).

However, the observed regeneration boost results probably from a combination of factors related to plant adaptation after cI impairment. In addition to the induced oxidative stress observed when mETC is impaired, the energy state could be another important factor that affect shoot regeneration. The alternative pathway (NADH₂s and AOX) are induced when mETC is impaired as a stress response to reduce the mitochondrial ROS. But this non-phosphorylating pathway also alters ATP level in the cell. Thus, the energy disequilibrium in cI mutants (Meyer et al., 2009) could be another important factor that determines the callus faith during the regeneration process. It would be interesting to measure ATP levels in the cI mutants used in our study and also in calli after complex I inhibition.

The mETC is also implicated in the production of nitric oxide (NO) (Gupta and Kaiser, 2010). NO belongs to reactive nitrogen species (RNS). As for ROS, RNS are also implicated in plant response to stress-related conditions. NO is considered a key signalling factor during several biological processes [for review see (Del Río, 2015)]. Thus, we cannot exclude that RNS may also be involved in the callus response to mitochondrial impairments. To verify this hypothesis, NO measurement using specific probes could be conducted on calli after rotenone treatment and in cI mutant calli.

In humans, cI activity is enhanced during cell division to increase mitochondrial ATP production. This enhancement is mediated by the cell cycle proteins CyclinB1/Cdk1 that phosphorylate cI to upregulate its activity (Wang et al., 2014). CyclinB1/Cdk1 are also implicated in the mitochondrial MnSOD phosphorylation resulting in free radicals

detoxification during cellular resistance to abiotic stress (Candas et al., 2013). In our microarrays data, we noticed an up-regulation of *CyclinB1;1* transcripts during callus adaptation to rotenone-induced stress (T_{12H} vs T_{7D}). This up-regulation was also observed in cI mutants after transfer compared to wt (wt_{7.5D} vs *mtsfl*_{7.5D} and wt_{7.5D} vs *mtll*_{7.5D}).

In mammals this rotenone-induced cell proliferation arrest was related to an inhibitory effect on microtubule assembly. This second inhibitory effect on microtubule-destabilising activity seems to be dissociated from the ROS-related cI inhibition (Srivastava and Panda, 2007; Passmore et al., 2017). In our microarrays data, we also noticed down regulation of biological processes related to microtubules in rotenone-treated calli. To investigate the potential implication of this activity in the observed shoot regeneration, we could test other microtubule assembly inhibitors (with no known action on the mETC) in our regeneration system.

To summarize, genetic or chemical impairments affecting the mitochondria have a considerable effect on plant growth and plant *in vitro* regeneration. In protoplasts-derived calli, mitochondrial dysfunction results in growth decrease and *de novo* organogenesis enhancement. Both chemical inhibition of mETC and genetic defect of mitochondrial complex I mutants enhanced shoot regeneration rate. However, regeneration enhancement observed in complex I mutants calli was higher than in calli treated with inhibitors. The molecular response signature to chemical inhibition of mETC and in two complex I mutants is not identical demonstrating that there is a difference in long term adaptation and transient adaptation to mitochondrial impairment. For example, mechanisms protecting against ROS burst, shown to occur following transfer, are constitutively on in the mutants but only transiently triggered in tissues exposed to the inhibitor.

As a first step towards the implementation of alternative protocols to enhance regeneration response, our findings have been recently transferred to *in vitro* regeneration of two major crops: tomato (*Solanum lycopersicum*) and maize (*Zea mays*). The treatment of tomato cotyledon-explants with 5 μ M of rotenone significantly enhanced shoot regeneration rate of rotenone-treated explants compared to mock-treated explants (F. Delmas and M. Hernould; unpublished results).

In maize, mutation in a nuclear PPR gene encoding the PPR2263 protein results in reduced cell division with an overall reduced plant growth. In *ppr2263* plants, cells are affected in both complex I and complex III of the mETC (Sosso 2012). Recently, immature embryos collected from this mitochondrial-defective mutant were tested in a regeneration assay for the formation of secondary somatic embryos. In this experiment, the wild-type genotype was recalcitrant for somatic embryos regeneration. As expected, the wild-type embryo explants did not regenerate plantlets, whereas *ppr2263* embryo explants regenerated up to 9.27 % plantlets from calli derived from the immature mutant embryos (G. Gendrot and P. Rogowsky; unpublished results).

Altogether, these results confirm the link between a mitochondrial defect and *in vitro* plant regeneration and pave the way towards agronomic applications using mitochondrial dysfunction either by chemical treatment of explants or inducing transient mitochondrial mutations to regenerate recalcitrant crops and elite genotypes.

References

- Achard P, Renou J, Berthome R, Harberd NP, Genschik P** (2008) Report Plant DELLAs Restrain Growth and Promote Survival of Adversity by Reducing the Levels of Reactive Oxygen Species. *Curr Biol* **18**: 656–660
- Van Aken O, Pečenková T, Van De Cotte B, De Rycke R, Eeckhout D, Fromm H, De Jaeger G, Witters E, Beemster GTS, Inzé D, et al** (2007) Mitochondrial type-I prohibitins of *Arabidopsis thaliana* are required for supporting proficient meristem development. *Plant J* **52**: 850–864
- Aken O Van, Pogson BJ** (2017) Convergence of mitochondrial and chloroplastic ANAC017 / PAP-dependent retrograde signalling pathways and suppression of programmed cell death. *Cell Death Differ* **24**: 955–960
- Van Aken O, Whelan J** (2012) Comparison of transcriptional changes to chloroplast and mitochondrial perturbations reveals common and specific responses in *Arabidopsis*. *Front Plant Sci* **3**: 281
- Van Aken O, Zhang B, Carrie C, Uggalla V, Paynter E, Giraud E, Whelan J** (2009) Defining the mitochondrial stress response in *Arabidopsis thaliana*. *Mol Plant* **2**: 1310–1324
- Altpeter F, Springer NM, Bartley LE, Blechl A, Brutnell TP, Citovsky V, Conrad L, Gelvin SB, Jackson D, Kausch AP, et al** (2016) Advancing Crop Transformation in the Era of Genome Editing. *Plant Cell* **28**: 1510–1520
- Arican E, Albayrak G, Gozukirmizi N** (2008) Calli cultures from *Abies equi-trojani* (Aschers et Sinten) and changes in antioxidant defense system enzymes. *J Environ Biol* **29**: 841–844
- Asada K** (2006) Production and Scavenging of Reactive Oxygen Species in Chloroplasts and Their Functions. *Plant Physiol* **141**: 391–396
- Avivi Y, Morad V, Ben-meir H, Zhao J, Kashkush K, Tzfira T, Citovsky V, Grafi G** (2004) Reorganization of Specific Chromosomal Domains and Activation of Silent Genes in Plant Cells Acquiring Pluripotentiality. *Dev Dyn* **230**: 12–22
- Bai B, Su YH, Yuan J, Zhang XS** (2013) Induction of somatic embryos in *Arabidopsis* requires local YUCCA expression mediated by the down-regulation of ethylene biosynthesis. *Mol Plant* **6**: 1247–1260
- Baradaran R, Berrisford JM, Minhas GS, Sazanov LA** (2013) Crystal structure of the entire respiratory complex I. *Nature* **494**: 443–448
- Barkan A, Small I** (2014) Pentatricopeptide Repeat Proteins in Plants. *Annu Rev Plant Biol* **65**: 415–442

- Bartoli CG, Pastori GM, Foyer CH** (2000) Ascorbate Biosynthesis in Mitochondria Is Linked to the Electron Transport Chain between Complexes III and IV. *Plant Physiol* **123**: 335–344
- Bashandy T, Guillemintot J, Vernoux T, Caparros-ruiz D, Ljung K, Meyer Y, Reichheld J** (2010) Interplay between the NADP-Linked Thioredoxin and Glutathione Systems in Arabidopsis Auxin Signaling. *Plant Cell* **22**: 376–391
- Bayir H** (2005) Reactive oxygen species. *Crit Care Med.* doi: 10.1097/01.CCM.0000186787.64500.12
- Benson EE** (2000) Special symposium: In vitro plant recalcitrance do free radicals have a role in plant tissue culture recalcitrance? *Vitr Cell Dev Biol - Plant* **36**: 163–170
- Berkowitz O, De Clercq I, Van Breusegem F, Whelan J** (2016) Interaction between hormonal and mitochondrial signalling during growth, development and in plant defence responses. *Plant, Cell Environ* **39**: 1127–1139
- Bloch R** (1941) Wound Healing in Higher Plants. *Bot Rev* **7**: 110–146
- Bloch R** (1952) Wound Healing in Higher Plants II. *Bot Rev* **18**: 655–679
- Brandt U** (2006) Energy Converting NADH: Quinone Oxidoreductase (Complex I). *Annu Rev Biochem* **75**: 69–92
- Braun H-P, Binder S, Brennicke A, Eubel H, Fernie AR, Finkemeier I, Klodmann J, König A-C, Kühn K, Meyer E, et al** (2014) The life of plant mitochondrial complex I. *Mitochondrion* **19**: 295–313
- Braybrook SA, Stone SL, Park S, Bui AQ, Le BH, Fischer RL, Goldberg RB, Harada JJ** (2006) Genes directly regulated by LEAFY COTYLEDON2 provide insight into the control of embryo maturation and somatic embryogenesis. *Proc Natl Acad Sci* **103**: 3468–3473
- Buechel S, Leibfried A, To JPC, Zhao Z, Andersen SU, Kieber JJ, Lohmann JU** (2010) Role of A-type Arabidopsis Response Regulators in meristem maintenance and regeneration. *Eur J Cell Biol* **89**: 279–284
- Cairns NG, Pasternak M, Wachter A, Cobbett CS, Meyer AJ** (2006) Maturation of Arabidopsis Seeds Is Dependent on Glutathione Biosynthesis within the Embryo 1 [C]. *Plant Physiol* **141**: 446–455
- Candas D, Fan M, Nantajit D, Vaughan AT, Murley JS, Woloschak GE, Grdina DJ, Li JJ** (2013) CyclinB1/Cdk1 phosphorylates mitochondrial antioxidant MnSOD in cell adaptive response to radiation stress. *J Mol Cell Biol* **5**: 166–175
- Catterou M, Dubois F, Smets R, Vaniet S, Kichey T, Onckelen H Van, Sangwann-**

- Norreel BS, Sangwan RS** (2002) *hoc*: an Arabidopsis mutant overproducing cytokinins and expressing high in vitro organogenic capacity. *Plant J* **30**: 273–287
- Chanvivattana Y, Bishopp A, Schubert D, Stock C, Moon Y, Sung ZR, Goodrich J** (2004) Interaction of Polycomb-group proteins controlling flowering in Arabidopsis. *Development* **131**: 5263–5276
- Che P, Gingerich DJ, Lall S, Howell SH** (2002) Global and Hormone-Induced Gene Expression Changes during Shoot Development in Arabidopsis. *Plant Cell* **14**: 2771–2785
- Chen CC, Agrawal DC, Lee MR, Lee RJ, Kuo CL, Wu CR, Tsay HS, Chang HC** (2016) Influence of LED light spectra on in vitro somatic embryogenesis and LC-MS analysis of chlorogenic acid and rutin in *Peucedanum japonicum* Thunb.: A medicinal herb. *Bot Stud.* doi: 10.1186/s40529-016-0124-z
- Cheng ZJ, Wang L, Sun W, Zhang Y, Zhou C, Su YH, Li W, Sun TT, Zhao XY, Li XG, et al** (2013) Pattern of Auxin and Cytokinin Responses for Shoot Meristem Induction Results from the Regulation of Cytokinin Biosynthesis by AUXIN RESPONSE FACTOR3. *Plant Physiol* **161**: 240–251
- Chew O, Whelan J, Millar AH** (2003) Molecular Definition of the Ascorbate-Glutathione Cycle in Arabidopsis Mitochondria Reveals Dual Targeting of Antioxidant Defenses in Plants. *J Biol Chem* **278**: 46869–46877
- Chi G, Barfield DG, Sim G, Pua E** (1990) Effect of AgNO₃ and aminoethoxyvinylglycine on in vitro shoot and root organogenesis from seedling explants of recalcitrant Brassica genotypes. *Plant Cell Rep* **9**: 195–198
- Chupeau M-C, Granier F, Pichon O, Renou J-P, Gaudin V, Chupeau Y** (2013) Characterization of the Early Events Leading to Totipotency in an Arabidopsis Protoplast Liquid Culture by Temporal Transcript Profiling. *Plant Cell* **25**: 2444–2463
- Claude A, Fullman EF** (1945) AN ELECTRON MICROSCOPE STUDY OF ISOLATED MITOCHONDRIA: METHOD AND PRELIMINARY RESULTS. *J Exp Med* **81**: 51–62
- De Clercq I, Vermeirssen V, Van Aken O, Vandepoele K, Murcha MW, Law SR, Inze A, Ng S, Ivanova A, Rombaut D, et al** (2013) The Membrane-Bound NAC Transcription Factor ANAC013 Functions in Mitochondrial Retrograde Regulation of the Oxidative Stress Response in Arabidopsis. *Plant Cell* **25**: 3472–3490
- Clifton R, Lister R, Parker KL, Sappl PG, Elhafez D, Millar AH, Day DA, Whelan J** (2005) Stress-induced co-expression of alternative respiratory chain components in

- Arabidopsis thaliana*. *Plant Mol Biol* **58**: 193–212
- Colas des Francs-Small C, Falcon de Longevialle A, Li Y, Lowe E, Tanz SK, Smith C, Bevan MW, Small I** (2014) The Pentatricopeptide Repeat Proteins TANG2 and ORGANELLE TRANSCRIPT PROCESSING439 Are Involved in the Splicing of the Multipartite *nad5* Transcript Encoding a Subunit of Mitochondrial Complex I. *Plant Physiol* **165**: 1409–1416
- Cornejo-Martin MJ, Mingo-Castel AM, Primo-Millo E** (1979) Organ Redifferentiation in Rice Callus: Effects of C₂H₄, CO₂ and Cytokinins. *Zeitschrift für Pflanzenphysiologie* **94**: 117–123
- Crow ML, Serizet C, Thareau V, Aubourg S, Rouzé P, Hilson P, Beynon J, Weisbeek P, van Hummelen P, Reymond P, et al** (2003) CATMA: A complete *Arabidopsis* GST database. *Nucleic Acids Res* **31**: 156–158
- Curaba J, Moritz T, Blervaque R, Parcy F, Raz V, Herzog M, Vachon G** (2004) AtGA3ox2, a key gene responsible for bioactive gibberellin biosynthesis, is regulated during embryogenesis by LEAFY COTYLEDON2 and FUSCA3 in *Arabidopsis*. *Plant Physiol* **136**: 3660–3669
- Dahan J, Tcherkez G, Macherel D, Benamar A, Belcram K, Quadrado M, Arnal N, Mireau H** (2014) Disruption of the CYTOCHROME C OXIDASE DEFICIENT 1 gene leads to cytochrome c oxidase depletion and reorchestrated respiratory metabolism in *Arabidopsis thaliana*. *Plant Physiol*. doi: 10.1104/pp.114.248526
- Damri M, Granot G, Ben-Meir H, Avivi Y, Plaschkes I, Chalifa-Caspi V, Wolfson M, Fraifeld V, Grafi G** (2009) Senescing cells share common features with dedifferentiating cells. *Rejuvenation Res* **12**: 435–443
- Dröse S, Brandt U** (2012) Molecular Mechanisms of Superoxide Production by the Mitochondrial Respiratory Chain In Mitochondrial Oxidative Phosphorylation. **748**: 145–169
- Duclercq J, Ndong YPA, Guerineau F, Sangwan RS, Catterou M** (2011) *Arabidopsis* shoot organogenesis is enhanced by an amino acid change in the ATHB15 transcription factor. *Plant Biol* **13**: 317–324
- Dudkina N V., Heinemeyer J, Sunderhaus S, Boekema EJ, Braun HP** (2006) Respiratory chain supercomplexes in the plant mitochondrial membrane. *Trends Plant Sci* **11**: 232–240
- Earnshaw BA, Johnson MA** (1987) Control of Wild Carrot Somatic Embryo Development by Antioxidants. *Plant Physiol* **85**: 66–77

- Emery JF, Floyd SK, Alvarez J, Eshed Y, Hawker NP, Izhaki A, Baum SF, Bowman JL** (2003) Radial Patterning of Arabidopsis Shoots by Class III HD-ZIP and KANADI Genes. *Curr Biol* **13**: 1768–1774
- Esposti MD** (1998) Inhibitors of NADH – ubiquinone reductase: an overview. *Biochim Biophys Acta* **1364**: 222–235
- Faltin Z, Holland D, Velcheva M, Tsapovetsky M, Roedel-drevet P, Handa AK, Abu-abied M, Friedman-einat M, Eshdat Y, Perl A** (2010) Glutathione Peroxidase Regulation of Reactive Oxygen Species Level is Crucial for In Vitro Plant Differentiation. *Plant Cell Physiol* **51**: 1151–1162
- Fato R, Bergamini C, Bortolus M, Maniero AL, Leoni S, Ohnishi T, Lenaz G** (2009) Differential effects of mitochondrial Complex I inhibitors on production of reactive oxygen species. *Biochim Biophys Acta* **1787**: 384–392
- Feldmann KA, Marks MD** (1986) Rapid and efficient regeneration of plants from explants of Arabidopsis thaliana. *Plant Sci* **47**: 63–69
- Ferreira PCG, Hemerly AS, de Almeida Engler J, Van Montagu M, Engler G, Inzé D** (1994) Developmental expression of the Arabidopsis cyclin gene *cyc1At*. *Plant Cell* **6**: 1763–1774
- Fiorani F, Umbach AL, Siedow JN** (2005) The Alternative Oxidase of Plant Mitochondria Is Involved in the Acclimation of Shoot Growth at Low Temperature. A Study of Arabidopsis AOX1a Transgenic Plants. *Plant Physiol* **139**: 1795–1805
- Foyer CH, Noctor G** (2011) Ascorbate and Glutathione: The Heart of the Redox Hub. *Plant Physiol* **155**: 2–18
- Foyer CH, Ruban A V., Noctor G** (2017) Viewing oxidative stress through the lens of oxidative signalling rather than damage. *Biochem J* **474**: 877–883
- Frey TG, Mannella CA** (2000) Mannella - The Internal Structure of Mitochondria. *Trends Biochem Sci* **25**: 319–324
- Fromm S, Senkler J, Eubel H, Peterhansel C, Braun HP** (2016) Life without complex I: Proteome analyses of an Arabidopsis mutant lacking the mitochondrial NADH dehydrogenase complex. *J Exp Bot* **67**: 3079–3093
- Garmier M, Carroll AJ, Delannoy E, Vallet C, Day DA, Small ID, Millar AH** (2008) Complex I Dysfunction Redirects Cellular and Mitochondrial Metabolism in Arabidopsis. *Plant Physiol* **148**: 1324–1341
- Gazzarrini S, Tsuchiya Y, Lumba S, Okamoto M, McCourt P** (2004) The transcription factor FUSCA3 controls developmental timing in Arabidopsis through the hormones

Gibberellin and abscisic acid. *Dev Cell* **7**: 373–385

- Geigenberger P, Thormählen I, Daloso DM, Fernie AR** (2017) The Unprecedented Versatility of the Plant Thioredoxin System. *Trends Plant Sci* **22**: 249–262
- Gill SS, Tuteja N** (2010) Reactive oxygen species and antioxidant machinery in abiotic stress tolerance in crop plants. *Plant Physiol Biochem* **48**: 909–930
- Gong H, Jiao Y, Hu WW, Pua EC** (2005) Expression of glutathione-S-transferase and its role in plant growth and development in vivo and shoot morphogenesis in vitro. *Plant Mol Biol* **57**: 53–66
- Gordon SP, Heisler MG, Reddy GV, Ohno C, Das P, Meyerowitz EM** (2007) Pattern formation during de novo assembly of the Arabidopsis shoot meristem. *Development* **134**: 3539–3548
- Grafi G** (2004) How cells dedifferentiate: A lesson from plants. *Dev Biol* **268**: 1–6
- Grafi G, Barak S** (2015) Stress induces cell dedifferentiation in plants. *Biochim Biophys Acta - Gene Regul Mech* **1849**: 378–384
- Gray MW** (2012) Mitochondrial Evolution. *Cold spring Harb Perspect Biol* **4**: 1–17
- Guilfoyle TJ, Hagen G** (2007) Auxin response factors. *Curr Opin Plant Biol* **10**: 453–460
- Gupta KJ, Kaiser WM** (2010) Production and scavenging of nitric oxide by barley root mitochondria. *Plant Cell Physiol* **51**: 576–584
- Gupta SD** (2011) Role of free radicals and antioxidants in in vitro morphogenesis. *React Oxyg Species Antioxidants High Plants* 229–247
- Gupta SD, Datta S** (2003) Antioxidant enzyme activities during in vitro morphogenesis of gladiolus and effect on application of antioxidants on plant regeneration. *Biol Plant* **47**: 179–183
- Gutscher M, Pauleau A-L, Marty L, Brach T, Wabnitz GH, Samstag Y, Meyer AJ, Dick TP, Goi A, Trapido M, et al** (2008) Real-time imaging of the intracellular glutathione redox potential. *Nat Methods* **5**: 553–559
- Haberlandt G** (1902) Kulturversuche mit isolierten Pflanzenzellen. *Sitzungsber Akad Wiss Wien, Math-Naturwiss Kl, Abt 1*: 69–92
- Haïli N, Arnal N, Quadrado M, Amiar S, Tcherkez G, Dahan J, Briozzo P, Colas des Francs-Small C, Vrielynck N, Mireau H** (2013) The pentatricopeptide repeat MTSF1 protein stabilizes the nad4 mRNA in Arabidopsis mitochondria. *Nucleic Acids Res* **41**: 6650–6663
- Haïli N, Planchard N, Arnal N, Quadrado M, Vrielynck N, Dahan J, Francs-Small CC des, Mireau H** (2016) The MTL1 Pentatricopeptide Repeat Protein Is Required for Both

- Translation and Splicing of the Mitochondrial NADH DEHYDROGENASE SUBUNIT7 mRNA in Arabidopsis. *Plant Physiol* **170**: 354–366
- Hasanuzzaman M, Nahar K, Anee TI, Fujita M** (2017) Glutathione in plants: biosynthesis and physiological role in environmental stress tolerance. *Physiol Mol Biol Plants* **23**: 249–268
- Hatanaka T, Sawabe E, Azuma T, Uchida N, Yasuda T** (1995) The role of ethylene in somatic embryogenesis from leaf discs of *Coffea canephora*. *Plant Sci* **107**: 199–204
- Hatefi Y, Haavik AG, Griffiths DE** (1962) Studies on the electron transfer system. *J Biol Chem* **237**: 1676–1680
- He C, Chen X, Huang H, Xu L** (2012) Reprogramming of H3K27me3 Is Critical for Acquisition of Pluripotency from Cultured Arabidopsis Tissues. *PLoS Genet* **8**: 1–13
- Heinz S, Freyberger A, Lawrenz B, Schladt L, Schmuck G, Ellinger-Ziegelbauer H** (2017) Mechanistic Investigations of the Mitochondrial Complex i Inhibitor Rotenone in the Context of Pharmacological and Safety Evaluation. *Sci Rep* **7**: 1–13
- Hilson P, Allemeersch J, Altmann T, Aubourg S, Avon A, Beynon J, Bhalerao RP, Bitton F, Caboche M, Cannoot B, et al** (2004) Versatile Gene-Specific Sequence Tags for Arabidopsis Functional Genomics: Transcript Profiling and Reverse Genetics Applications Versatile Gene-Specific Sequence Tags for Arabidopsis Functional Genomics : Transcript Profiling and Reverse Genetics Applic. *Genome Res* 2176–2189
- Hirst J** (2013) Mitochondrial Complex I. *Annu Rev Biochem* **82**: 551–575
- Ho LHM, Giraud E, Uggalla V, Lister R, Clifton R, Glen A, Thirkettle-watts D, Aken O Van, Whelan J** (2008) Identification of Regulatory Pathways Controlling Gene Expression of Stress-Responsive Mitochondrial Proteins. *Plant Physiol* **147**: 1858–1873
- Hsieh W-Y, Liao J-C, Hsieh M-H** (2015) Dysfunctional mitochondria regulate the size of root apical meristem and leaf development in Arabidopsis. *Plant Signal Behav* **10**: e1071002
- Hu Y, Depaepe T, Smet D, Hoyerova K, Klíma P, Cuypers A, Cutler S, Buyst D, Morreel K, Boerjan W, et al** (2017) ACCERBATIN, a small molecule at the intersection of auxin and reactive oxygen species homeostasis with herbicidal properties. *J Exp Bot.* doi: 10.1093/jxb/erx242
- Huang S, Van Aken O, Schwarzländer M, Belt K, Millar AH** (2016) The Roles of Mitochondrial Reactive Oxygen Species in Cellular Signaling and Stress Response in Plants. *Plant Physiol* **171**: 1551–1559
- Hwang I, Sheen J** (2001) Two-component circuitry in *Arabidopsis* cytokinin signal

- transduction. *Nature* **413**: 383–389
- Ikeuchi M, Iwase A, Rymen B, Harashima H, Shibata M, Ohnuma M, Breuer C, Morao AK, de Lucas M, De Veylder L, et al** (2015a) PRC2 represses dedifferentiation of mature somatic cells in *Arabidopsis*. *Nat Plants* **1**: 15089
- Ikeuchi M, Iwase A, Sugimoto K** (2015b) Control of plant cell differentiation by histone modification and DNA methylation. *Curr Opin Plant Biol* **28**: 60–67
- Ikeuchi M, Ogawa Y, Iwase A, Sugimoto K** (2016) Plant regeneration: cellular origins and molecular mechanisms. *Development* **143**: 1442–1451
- Ivanova A, Law SR, Narsai R, Duncan O, Lee J-H, Zhang B, Van Aken O, Radomiljac JD, van der Merwe M, Yi K, et al** (2014) A Functional Antagonistic Relationship between Auxin and Mitochondrial Retrograde Signaling Regulates Alternative Oxidase1a Expression in *Arabidopsis*. *Plant Physiol* **165**: 1233–1254
- Iwase A, Harashima H, Ikeuchi M, Rymen B, Ohnuma M, Komaki S, Morohashi K, Kurata T, Nakata M, Ohme-takagi M, et al** (2017) WIND1 Promotes Shoot Regeneration through Transcriptional Activation of ENHANCER OF SHOOT REGENERATION1 in *Arabidopsis*. *Plant Cell* **29**: 54–69
- Iwase A, Mita K, Nonaka S, Ikeuchi M, Koizuka C, Ohnuma M, Ezura H, Imamura J, Sugimoto K** (2015) WIND1-based acquisition of regeneration competency in *Arabidopsis* and rapeseed. *J Plant Res* **128**: 389–397
- Johnston EJ, Rylott EL, Beynon E, Lorenz A** (2015) Monodehydroascorbate reductase mediates TNT toxicity in plants. *Plant Sci* **349**: 1072–1075
- Jopling C, Boue S, Belmonte JCI** (2011) Dedifferentiation, transdifferentiation and reprogramming: three routes to regeneration. *Nat Rev Mol Cell Biol* **12**: 79–89
- Joy IV RW, Patel KR, Thorpe TA** (1988) Ascorbic acid enhancement of organogenesis in tobacco callus. *Plant Cell Tissue Organ Cult* **13**: 219–228
- Junker A, Mönke G, Rutten T, Keilwagen J, Seifert M, Thi TMN, Renou JP, Balzergue S, Viehöver P, Hähnel U, et al** (2012) Elongation-related functions of LEAFY COTYLEDON1 during the development of *Arabidopsis thaliana*. *Plant J* **71**: 427–442
- Juszczuk IM, Rychter AM** (2003) Alternative oxidase in higher plants. *Acta Biochim Pol* **50**: 1257–1271
- Juszczuk IM, Szal B, Rychter AM** (2012) Oxidation-reduction and reactive oxygen species homeostasis in mutant plants with respiratory chain complex I dysfunction. *Plant, Cell Environ* **35**: 296–307
- Kareem A, Durgaprasad K, Sugimoto K, Du Y, Pulianmackal AJ, Trivedi ZB,**

- Abhayadev P V, Pinon V, Meyerowitz EM, Scheres B, et al** (2015) PLETHORA Genes Control Regeneration by a Two- Step Mechanism. *Curr Biol* **25**: 1–14
- Koprivova A, Francs-Small CC Des, Calder G, Mugford ST, Tanz S, Lee BR, Zechmann B, Small I, Kopriva S** (2010) Identification of a pentatricopeptide repeat protein implicated in splicing of intron 1 of mitochondrial nad7 transcripts. *J Biol Chem* **285**: 32192–32199
- Kühn K, Obata T, Feher K, Bock R, Fernie AR, Meyer EH** (2015) Complete Mitochondrial Complex I Deficiency Induces an Up-Regulation of Respiratory Fluxes That Is Abolished by Traces of Functional Complex I. *Plant Physiol* **168**: 1537–1549
- de la Paz Sanchez M, Aceves-Garcia P, Petrone E, Steckenborn S, Vega-Leon R, Alvarez-Buylla ER, Garay-Arroyo A, Garcia-Ponce B** (2015) The impact of Polycomb group (PcG) and Trithorax group (TrxG) epigenetic factors in plant plasticity. *New Phytol* **208**: 684–694
- Lall S, Mandegaran Z, Roberts A V.** (2005) Shoot multiplication in cultures of mature *Alnus glutinosa*. *Plant Cell Tissue Organ Cult* **83**: 347–350
- Lee B, Lee H, Xiong L, Zhu J-K** (2002) A Mitochondrial Complex I Defect Impairs Cold-Regulated Nuclear Gene Expression. *Plant Cell* **14**: 1235–1251
- Lei C, Wang H, Liu B, Ye H** (2014) Effects of silver nitrate on shoot regeneration of *Artemisia annua* L. *Plant Biotechnol* **31**: 71–75
- Li H, Soriano M, Cordewener J, Muino JM, Riksen T, Fukuoka H, Angenent GC, Boutilier K** (2014) The Histone Deacetylase Inhibitor Trichostatin A Promotes Totipotency in the Male Gametophyte. *Plant Cell* **26**: 195–209
- Li W, Liu H, Cheng ZJ, Su YH, Han HN, Zhang Y, Zhang XS** (2011) Dna methylation and histone modifications regulate de novo shoot regeneration in arabidopsis by modulating wuschel expression and auxin signaling. *PLoS Genet.* doi: 10.1371/journal.pgen.1002243
- Lurin C, Andrés C, Aubourg S, Bellaoui M, Bitton F, Bruyère C, Caboche M, Debast C, Gualberto J, Hoffmann B, et al** (2004) Genome-Wide Analysis of Arabidopsis Pentatricopeptide Repeat Proteins Reveals Their Essential Role in Organelle Biogenesis  *Plant Cell* **16**: 2089–2103
- Manna S** (2015) An overview of pentatricopeptide repeat proteins and their applications. *Biochimie* **113**: 93–99
- Matakiadis T, Kintzios S** (2005) The effect of ATP on cucumber (*Cucumis sativus* L.)

- regeneration from nodal explants: Association with ??-tocopherol, H₂O₂ and size of culture vessel. *Plant Growth Regul* **45**: 127–137
- Mcdonald AE, Gospodaryov D V** (2018) Mitochondrion Alternative NAD (P) H dehydrogenase and alternative oxidase: Proposed physiological roles in animals. *Mitochondrion* 1–11
- Meyer AJ, Brach T, Marty L, Kreye S, Rouhier N, Jacquot JP, Hell R** (2007) Redox-sensitive GFP in *Arabidopsis thaliana* is a quantitative biosensor for the redox potential of the cellular glutathione redox buffer. *Plant J* **52**: 973–986
- Meyer EH, Tomaz T, Carroll AJ, Estavillo G, Delannoy E, Tanz SK, Small ID, Pogson BJ, Millar AH** (2009) Remodeled Respiration in *ndufs4* with Low Phosphorylation Efficiency Suppresses *Arabidopsis* Germination and Growth and Alters Control of Metabolism at Night. *Plant Physiol* **151**: 603–619
- Meyer Y, Belin C, Delorme-Hinoux V, Reichheld J, Riondet C** (2012) Thioredoxin and Glutaredoxin Systems in Plants: Molecular Mechanisms, Crosstalks, and Functional Significance. *Antioxid Redox Signal* **17**: 1124–1160
- Mi H, Huang X, Muruganujan A, Tang H, Mills C, Kang D, Thomas PD** (2017) PANTHER version 11: Expanded annotation data from Gene Ontology and Reactome pathways, and data analysis tool enhancements. *Nucleic Acids Res* **45**: 183–189
- Mi H, Muruganujan A, Casagrande JT, Thomas PD** (2013) Large-scale gene function analysis with the panther classification system. *Nat Protoc* **8**: 1551–1566
- Millar AH, Whelan J, Soole KL, Day DA** (2011) Organization and Regulation of Mitochondrial Respiration in Plants. *Annu Rev Plant Biol* **62**: 79–104
- Mittler R** (2017) ROS Are Good. *Trends Plant Sci* **22**: 11–19
- Mohiuddin AKM, Chowdhury MKU, Abdullah ZC, Napis S** (1997) Influence of silver nitrate (ethylene inhibitor) on cucumber in vitro shoot regeneration. *Plant Cell Tissue Organ Cult* **51**: 75–78
- Møller IM** (2001) PLANT MITOCHONDRIA AND OXIDATIVE STRESS: Electron Transport, NADPH Turnover, and Metabolism of Reactive Oxygen Species. *Annu Rev Plant Physiol Plant Mol Biol* **52**: 561–591
- Moruš M, Baran M, Rost-Roszkowska M, Skotnicka-Graca U** (2014) Plant stem cells as innovation in cosmetics. *Acta Pol Pharm - Drug Res* **71**: 701–707
- Motte H, Galuszka P, Spichal L, Tarkowski P, Plihal O, Smehilova M, Jaworek P, Vereecke D, Werbrouck S, Geelen D** (2013) Phenyl-Adenine, Identified in a LIGHT-DEPENDENT SHORT HYPOCOTYLS4-Assisted Chemical Screen, Is a Potent

- Compound for Shoot Regeneration through the Inhibition of CYTOKININ OXIDASE/DEHYDROGENASE Activity. *Plant Physiol* **161**: 1229–1241
- Motte H, Vercauteren A, Depuydt S, Landschoot S, Geelen D, Werbrouck S, Goormachtig S, Vuylsteke M, Vereecke D** (2014a) Combining linkage and association mapping identifies RECEPTOR-LIKE PROTEIN KINASE1 as an essential Arabidopsis shoot regeneration gene. *Proc Natl Acad Sci* **111**: 8305–8310
- Motte H, Vereecke D, Geelen D, Werbrouck S** (2014b) The molecular path to in vitro shoot regeneration. *Biotechnol Adv* **32**: 107–21
- Ng S, De Clercq I, Van Aken O, Law SR, Ivanova A, Willems P, Giraud E, Van Breusegem F, Whelan J** (2014) Anterograde and retrograde regulation of nuclear genes encoding mitochondrial proteins during growth, development, and stress. *Mol Plant* **7**: 1075–1093
- Ng S, Giraud E, Duncan O, Law SR, Wang Y, Xu L, Narsai R, Carrie C, Walker H, Day DA, et al** (2013a) Cyclin-dependent Kinase E1 (CDKE1) Provides a Cellular Switch in Plants between Growth and Stress Responses. *J Biol Chem* **288**: 3449–3459
- Ng S, Ivanova a, Duncan O, Law SR, Van Aken O, De Clercq I, Wang Y, Carrie C, Xu L, Kmiec B, et al** (2013b) A membrane-bound NAC transcription factor, ANAC017, mediates mitochondrial retrograde signaling in Arabidopsis. *Plant Cell* **25**: 3450–3471
- Nishiwaki M, Fujino K, Koda Y, Masuda K, Kikuta Y** (2000) Somatic embryogenesis induced by the simple application of abscisic acid to carrot (*Daucus carota* L.) seedlings in culture. *Planta* **211**: 756–759
- Noctor G, Mhamdi A, Chaouch S, Han Y, Neukermans J, Marquez-Garcia B, Queval G, Foyer CH** (2012) Glutathione in plants: An integrated overview. *Plant, Cell Environ* **35**: 454–484
- Noctor G, Mhamdi A, Foyer CH** (2016) Oxidative stress and antioxidative systems: Recipes for successful data collection and interpretation. *Plant Cell Environ* **39**: 1140–1160
- Noctor G, Reichheld JP, Foyer CH** (2017) ROS-related redox regulation and signaling in plants. *Semin Cell Dev Biol*. doi: 10.1016/j.semcdb.2017.07.013
- O’Toole N, Hattori M, Andres C, Iida K, Lurin C, Schmitz-Linneweber C, Sugita M, Small I** (2008) On the expansion of the pentatricopeptide repeat gene family in plants. *Mol Biol Evol* **25**: 1120–1128
- Overmyer K, Brosché M, Kangasjärvi J** (2003) Reactive oxygen species and hormonal control of cell death. *Trends Plant Sci* **8**: 335–342
- Passmore JB, Pinho S, Gomez-Lazaro M, Schrader M** (2017) The respiratory chain

- inhibitor rotenone affects peroxisomal dynamics via its microtubule-destabilising activity. *Histochem Cell Biol* **148**: 331–341
- Peer WA, Cheng Y, Murphy AS** (2013) Evidence of oxidative attenuation of auxin signalling. *J Exp Bot* **64**: 2629–2639
- Perales M, Eubel H, Heinemeyer J, Colaneri A, Zabaleta E, Braun HP** (2005) Disruption of a nuclear gene encoding a mitochondrial gamma carbonic anhydrase reduces complex I and supercomplex I+III₂ levels and alters mitochondrial physiology in Arabidopsis. *J Mol Biol* **350**: 263–277
- Peres LEP, Amar S, Kerbauy GB, Salatino A, Zaffar GR, Mercier H** (1999) Effects of Auxin, Cytokinin and Ethylene Treatments on the Endogenous Ethylene and Auxin-to-cytokinins Ratio Related to direct Root Tip Conversion of *Catasetum fimbriatum* Lindl. (Orchidaceae) into Buds. *J Plant Physiol* **155**: 551–555
- Peterson G, Smith R** (1990) Effect of abscisic acid and callus size on regeneration of american and international rice varieties. *Plant Cell Rep* **10**: 35–38
- Pétriacq P, de Bont L, Genestout L, Hao J, Laureau C, Florez-Sarasa I, Rzigui T, Queval G, Gilard F, Mauve C, et al** (2017) Photoperiod Affects the Phenotype of Mitochondrial Complex I Mutants. *Plant Physiol* **173**: 434–455
- del Pozo JC** (2016) Reactive Oxygen Species: From Harmful Molecules to Fine-Tuning Regulators of Stem Cell Niche Maintenance. *PLoS Genet* **12**: 4–7
- Provart N, Tong Z** (2003) A Browser-based Functional Classification SuperViewer for Arabidopsis Genomics. *Curr Comput Mol Biol* 271–272
- Pullman GS, Mein J, Johnson S, Zhang Y** (2005) Gibberellin inhibitors improve embryogenic tissue initiation in conifers. *Plant Cell Rep* **23**: 596–605
- Purnhauser L, Medgyesy P, Czako M, Dix PJ, Marton L** (1987) Stimulation of shoot regeneration in *Triticum aestivum* and *Nicotiana plumbaginifolia* Viv. tissue cultures using the ethylene inhibitor AgNO₃. *Plant Cell Rep* **6**: 1–4
- Qiao M, Zhao ZJ, Xiang FN** (2012) Arabidopsis thaliana in vitro shoot regeneration is impaired by silencing of TIR1. *Biol Plant* **56**: 409–414
- Racchi M** (2013) Antioxidant Defenses in Plants with Attention to *Prunus* and *Citrus* spp. *Antioxidants* **2**: 340–369
- Radhakrishnan D, Kareem A, Durgaprasad K, Sreeraj E, Sugimoto K, Prasad K** (2018) Shoot regeneration : a journey from acquisition of competence to completion. *Curr Opin Plant Biol* **41**: 23–31
- Ramel F, Birtic S, Ginies C, Soubigou-Taconnat L, Triantaphylides C, Havaux M** (2012)

- Carotenoid oxidation products are stress signals that mediate gene responses to singlet oxygen in plants. *Proc Natl Acad Sci* **109**: 5535–5540
- Rao RSP, Salvato F, Thal B, Eubel H, Thelen JJ, Müller IM** (2017) The proteome of higher plant mitochondria. *Mitochondrion* **33**: 22–37
- Rashotte AM, Mason MG, Hutchison CE, Ferreira FJ, Schaller GE, Kieber JJ** (2006) A subset of Arabidopsis AP2 transcription factors mediates cytokinin responses in concert with a two-component pathway. *Proc Natl Acad Sci* **103**: 11081–11085
- Rasmusson AG, Geisler DA, Møller IM** (2008) The multiplicity of dehydrogenases in the electron transport chain of plant mitochondria. *Mitochondrion* **8**: 47–60
- Rasmusson AG, Soole KL, Elthon TE** (2004) Alternative Nad(P)H Dehydrogenases of Plant Mitochondria. *Annu Rev Plant Biol* **55**: 23–39
- Reape TJ, Molony EM, McCabe PF** (2008) Programmed cell death in plants: Distinguishing between different modes. *J Exp Bot* **59**: 435–444
- Rentel MC, Lecourieux D, Ouaked F, Usher SL, Petersen L, Okamoto H, Knight H, Peck SC, Grierson CS, Hirt H, et al** (2004) OXI1 kinase is necessary for oxidative burst-mediated signalling in Arabidopsis. *Nature* **427**: 858–861
- Rhoads DM, Umbach AL, Subbaiah CC, Siedow JN** (2006) Mitochondrial reactive oxygen species. Contribution to oxidative stress and interorganellar signaling. *Plant Physiol* **141**: 357–366
- Del Río LA** (2015) ROS and RNS in plant physiology: An overview. *J Exp Bot* **66**: 2827–2837
- Rosspopoff O, Chelysheva L, Saffar J, Lecorgne L, Gey D, Caillieux E, Colot V, Roudier F, Hilson P, Berthomé R, et al** (2017) Direct conversion of root primordium into shoot meristem relies on timing of stem cell niche development. *Development* **144**: 1187–1200
- Santuari L, Sanchez-Perez G, Luijten M, Rutjens B, Terpstra I, Berke L, Gorte M, Prasad K, Bao D, Timmermans-Hereijgers JLPM, et al** (2016) The PLETHORA gene regulatory network guides growth and cell differentiation in Arabidopsis roots. *Plant Cell* **28**: tpc.00656.2016
- Sazanov LA** (2015) A giant molecular proton pump: structure and mechanism of respiratory complex I. *Nat Rev Mol Cell Biol* **16**: 375–388
- Schapira AH V** (1998) Human complex I defects in neurodegenerative diseases. *Biochim Biophys Acta - Bioenerg* **1364**: 261–270
- Schertl P, Braun H-P** (2014) Respiratory electron transfer pathways in plant mitochondria. *Front Plant Sci* **5**: 1–11

- Schmitz-Linneweber C, Small I** (2008) Pentatricopeptide repeat proteins: a socket set for organelle gene expression. *Trends Plant Sci* **13**: 663–670
- Schmülling T, Werner T, Riefler M, Krupková E, Bartrina Y Manns I** (2003) Structure and function of cytokinin oxidase/dehydrogenase genes of maize, rice, Arabidopsis and other species. *J Plant Res* **116**: 241–252
- Schwarzländer M, Fricker M, Müller C, Marty L, Brach T, Novak J, Sweetlove L, Hell R, Meyer A** (2008) Confocal imaging of glutathione redox potential in living plant cells. *J Microsc* **231**: 299–316
- Schwarzländer M, Fricker MD, Sweetlove LJ** (2009) Monitoring the in vivo redox state of plant mitochondria: Effect of respiratory inhibitors, abiotic stress and assessment of recovery from oxidative challenge. *Biochim Biophys Acta - Bioenerg* **1787**: 468–475
- Schwarzländer M, König AC, Sweetlove LJ, Finkemeier I** (2012) The impact of impaired mitochondrial function on retrograde signalling: A meta-analysis of transcriptomic responses. *J Exp Bot* **63**: 1735–1750
- Schwarzländer M, Tobias DP, Meyer AJ, Morgan B** (2016) Dissecting Redox Biology using Fluorescent Protein Sensors. *Antioxid Redox Signal* **24**: 680–712
- Sechet J, Roux C, Plessis A, Effroy D, Frey A, Perreau F, Biniek C, Krieger-Liszakay A, Macherel D, North HM, et al** (2015) The ABA-deficiency suppressor locus HAS2 encodes the PPR protein LOI1/MEF11 involved in mitochondrial RNA editing. *Mol Plant* **8**: 644–656
- Sies H, Berndt C, Jones DP** (2017) Oxidative Stress. *Annu Rev Biochem* **86**: 25.1–25.34
- Singhi SK, Syamal MM** (2000) Anti-auxin enhance *Rosa hybrida* L. micropropagation. *Biol Plant* **43**: 279–281
- Skoog F, Miller CO** (1957) Chemical regulation of growth and organ formation in plant tissues cultured in vitro. *Symp Soc Exp Biol* **11**: 118–131
- Slesak I, Libik M, Karpinska B, Karpinski S, Miszalski Z** (2007) The role of hydrogen peroxide in regulation of plant metabolism and cellular signalling in response to environmental stresses. *Acta Biochim Pol* **54**: 39–50
- Songstad DD, Duncan DR, Widholm JM** (1988) Effect of l-aminocyclopropane-l-carboxylic acid, silver nitrate, and norbornadiene on plant regeneration from maize callus cultures. *Plant Cell Rep* **7**: 262–265
- Sousa JS, D’Imprima E, Vonck J** (2018) Mitochondrial Respiratory Chain Complexes. In: Harris J., Boekema E. (eds) *Membrane Protein Complexes: Structure and Function*. *Subcell Biochem* **87**: 167–227

- Srivastava P, Panda D** (2007) Rotenone inhibits mammalian cell proliferation by inhibiting microtubule assembly through tubulin binding. *FEBS J* **274**: 4788–4801
- Stasolla C** (2010) Glutathione redox regulation of in vitro embryogenesis. *Plant Physiol Biochem* **48**: 319–327
- Staswick PE, Serban B, Rowe M, Tiryaki I, Maldonado MT, Maldonado MC, Suza W** (2005) Characterization of an Arabidopsis Enzyme Family That Conjugates Amino Acids to Indole-3-Acetic Acid. *Plant Cell* **17**: 616–627
- Stone SL, Braybrook SA, Paula SL, Kwong LW, Meuser J, Pelletier J, Hsieh T-F, Fischer RL, Goldberg RB, Harada JJ** (2008) Arabidopsis LEAFY COTYLEDON2 induces maturation traits and auxin activity: Implications for somatic embryogenesis. *Proc Natl Acad Sci* **105**: 3151–3156
- Su YH, Su YX, Liu YG, Zhang XS** (2013) Abscisic acid is required for somatic embryo initiation through mediating spatial auxin response in Arabidopsis. *Plant Growth Regul* **69**: 167–176
- Su YH, Zhang XS** (2014) The hormonal control of regeneration in plants. *Curr Top Dev Biol* **108**: 35–69
- Su YH, Zhao XY, Liu YB, Zhang CL, O'Neill SD, Zhang XS** (2009) Auxin-induced WUS expression is essential for embryonic stem cell renewal during somatic embryogenesis in Arabidopsis. *Plant J* **59**: 448–460
- Subrahmanian N, Remacle C, Hamel PP** (2016) Plant mitochondrial Complex i composition and assembly: A review. *Biochim Biophys Acta - Bioenerg* **1857**: 1001–1014
- Sugimoto K, Gordon SP, Meyerowitz EM** (2011) Regeneration in plants and animals: Dedifferentiation, transdifferentiation, or just differentiation? *Trends Cell Biol* **21**: 212–218
- Sugimoto K, Jiao Y, Meyerowitz EM** (2010) Arabidopsis Regeneration from Multiple Tissues Occurs via a Root Development Pathway. *Dev Cell* **18**: 463–471
- Sugiyama M** (2015) Historical review of research on plant cell dedifferentiation. *J Plant Res* **128**: 349–359
- Sugiyama M** (2013) Molecular genetic analysis of organogenesis in vitro with temperature-sensitive mutants. *Plant Biotechnol Rep*. doi: 10.1007/s11816-013-0292-1
- Szarka A, Horemans N, Kovács Z, Gróf P, Mayer M, Bánhegyi G** (2007) Dehydroascorbate reduction in plant mitochondria is coupled to the respiratory electron transfer chain. *Physiol Plant* **129**: 225–232

- Takase T, Nakazawa M, Ishikawa A, Kawashima M, Ichikawa T, Takahashi N, Shimada H, Manabe K, Matsui M** (2004) ydk1-D, an auxin-responsive GH3 mutant that is involved in hypocotyl and root elongation. *Plant J* **37**: 471–483
- Takebe I, Labib G, Melchers G** (1971) Regeneration of whole plants from isolated mesophyll protoplasts of tobacco. *Naturwissenschaften* **58**: 318–320
- Tanaka M, Kikuchi A, Kamada H** (2008) The Arabidopsis Histone Deacetylases HDA6 and HDA19 Contribute to the Repression of Embryonic Properties after Germination. *Plant Physiol* **146**: 149–161
- Thimm O, Bla O, Gibon Y, Nagel A, Meyer S, Kru P, Selbig J, Mu LA, Rhee SY, Stitt M** (2004) MAPMAN : a user-driven tool to display genomics data sets onto diagrams of metabolic pathways and other biological processes. *Plant J* **37**: 914–939
- Thorpe TA, Stasolla C** (2001) Somatic Embryogenesis. *Curr Trends Embryol Angiosperms*. doi: https://doi.org/10.1007/978-94-017-1203-3_12
- Tian M, Gu Q, Zhu M** (2003) The involvement of hydrogen peroxide and antioxidant enzymes in the process of shoot organogenesis of strawberry callus. *Plant Sci* **165**: 701–707
- Tisserat B, Murashige T** (1977) Effects of Ethephon, Ethylene, and 2,4-Dichlorophenoxyacetic Acid on Asexual Embryogenesis in VitroL' 2. *Plant Physiol* **60**: 437–439
- To JPC, Haberer G, Ferreira FJ, Deruère J, Mason MG, Schaller GE, Alonso JM, Ecker JR, Kieber JJ** (2004) Type-A Arabidopsis response regulators are partially redundant negative regulators of cytokinin signaling. *Plant Cell* **16**: 658–671
- To JPC, Kieber JJ** (2008) Cytokinin signaling: two-components and more. *Trends Plant Sci* **13**: 85–92
- Trehan S** (2017) Plant stem cells in cosmetics : current trends and future directions. *Futur Sci OA*. doi: [10.4155/fsoa-2017-0026](https://doi.org/10.4155/fsoa-2017-0026)
- Triantaphylides C, Krischke M, Hoerberichts FA, Ksas B, Gresser G, Havaux M, Van Breusegem F, Mueller MJ** (2008) Singlet Oxygen Is the Major Reactive Oxygen Species Involved in Photooxidative Damage to Plants. *Plant Physiol* **148**: 960–968
- Tsukagoshi H, Busch W, Benfey PN** (2010) Transcriptional Regulation of ROS Controls Transition from Proliferation to Differentiation in the Root. *Cell* **143**: 606–616
- Vandepoele K, Raes J, De Veylder L, Rouze P, Rombauts S, Inze D** (2002) Genome-wide analysis of core cell cycle genes in Arabidopsis. *Plant Cell* **14**: 903–916
- Vanlerberghe GC** (2013) Alternative oxidase: A mitochondrial respiratory pathway to

- maintain metabolic and signaling homeostasis during abiotic and biotic stress in plants. *Int J Mol Sci* **14**: 6805–6847
- Verkhovskaya ML, Belevich N, Euro L, Wikstrom M, Verkhovsky MI** (2008) Real-time electron transfer in respiratory complex I. *PNAS* **105**: 3763–3767
- Wang C, Aubé F, Planchard N, Quadrado M, Dargel-Graffin C, Nogué F, Mireau H** (2017) The pentatricopeptide repeat protein MTSF2 stabilizes a nad1 precursor transcript and defines the 3' end of its 5'-half intron. *Nucleic Acids Res* **45**: 6119–6134
- Wang H, Caruso L V., Downie AB, Perry SE** (2004) The Embryo MADS Domain Protein AGAMOUS-Like 15 Directly Regulates Expression of a Gene Encoding an Enzyme Involved in Gibberellin Metabolism. *Plant Cell* **16**: 1206–1219
- Wang Z, Fan M, Candas D, Zhang T, Eldridge A, Wachsmann-Hogiu S, Ahmed KM, Chromy BA, Nantajit D, Duru N, et al** (2014) CyclinB1/Cdk1 Coordinates Mitochondrial Respiration for Cell Cycle G2/M Progression. *Dev Cell* **29**: 217–232
- Waszczak C, Carmody M, Kangasjarvi J** (2018) Reactive Oxygen Species in Plant Signaling. *Annu Rev Plant Biol* **69**: 1–28
- Welchen E, García L, Mansilla N, Gonzalez DH** (2014) Coordination of plant mitochondrial biogenesis: keeping pace with cellular requirements. *Front Plant Sci* **4**: 551
- Wheaton WW, Weinberg SE, Hamanaka RB, Soberanes S, Sullivan LB, Anso E, Glasauer A, Dufour E, Mutlu GM, Scott Budigner GR, et al** (2014) Metformin inhibits mitochondrial complex I of cancer cells to reduce tumorigenesis. *Elife* **3**: 1–18
- Williams L, Zhao J, Morozova N, Li Y, Avivi Y, Grafi G** (2003) Chromatin reorganization accompanying cellular dedifferentiation is associated with modifications of histone H3, redistribution of HP1, and activation of E2F-target genes. *Dev Dyn* **228**: 113–120
- Winer J, Jung CKS, Shackel I, Williams PM** (1999) Development and Validation of Real-Time Quantitative Reverse Transcriptase–Polymerase Chain Reaction for Monitoring Gene Expression in Cardiac Myocytes *In Vitro*. *Anal Biochem* **270**: 41–49
- Woo JW, Kim J, Kwon S II, Corvalán C, Cho SW, Kim H, Kim S, Kim S, Choe S, Kim J** (2015) DNA-free genome editing in plants with preassembled CRISPR-Cas9 ribonucleoproteins. *Nat Biotechnol* **33**: 1162–4
- Wrzaczek M, Brosché M, Kangasjärvi J** (2013) ROS signaling loops - production, perception, regulation. *Curr Opin Plant Biol* **16**: 575–582
- Xu L, Huang H** (2014) Genetic and Epigenetic Controls of Plant Regeneration, 1st ed. *Curr Top Dev Biol*. doi: 10.1016/B978-0-12-391498-9.00009-7

- Yamamoto Y, Kamiya N, Morinaka Y, Matsuoka M, Sazuka T** (2007) Auxin Biosynthesis by the YUCCA Genes in Rice. *Plant Physiol* **143**: 1362–1371
- Yang L, Zhang J, He J, Qin Y, Hua D, Duan Y, Chen Z, Gong Z** (2014) ABA-Mediated ROS in Mitochondria Regulate Root Meristem Activity by Controlling PLETHORA Expression in Arabidopsis. *PLoS Genet.* doi: 10.1371/journal.pgen.1004791
- Yang X, Trumpower BL** (1986) Purification of a three-subunit ubiquinol-cytochrome c oxidoreductase complex from *Paracoccus denitrificans*. *J Biol Chem* **261**: 12282–12289
- Yao N, Eisfelder BJ, Marvin J, Greenberg JT** (2004) The mitochondrion - An organelle commonly involved in programmed cell death in *Arabidopsis thaliana*. *Plant J* **40**: 596–610
- Yusoff AAM, Ahmad F, Idris Z, Jaafar H, Abdullah JM** (2015) Understanding Mitochondrial DNA in Brain Tumorigenesis. *Mol Considerations Evol Surg Manag Issues Treat Patients with a Brain Tumor* 3–28
- Zeng J, Dong Z, Wu H, Tian Z, Zhao Z** (2017) Redox regulation of plant stem cell fate. *EMBO J* e201695955
- Zhang CH, Zhang BB, Ma RJ, Yu ML, Guo SL, Guo L** (2015) Isolation and expression analysis of four HD-ZIP III family genes targeted by microRNA166 in peach. *Genet Mol Res* **14**: 14151–14161
- Zhang H, Zhang TT, Liu H, Shi DY, Wang M, Bie XM, Li XG, Zhang XS** (2017a) Thioredoxin-mediated ROS Homeostasis Explains Natural Variation in Plant Regeneration. *Plant Physiol.* doi: 10.1104/pp.17.00633
- Zhang T-Q, Lian H, Zhou C-M, Xu L, Jiao Y, Wang J-W** (2017b) A Two-Step Model for de novo Activation of WUSCHEL during Plant Shoot Regeneration. *Plant Cell* **29**: 1073–1087
- Zheng Y, Ren N, Wang H, Stromberg AJ, Perry SE** (2009) Global Identification of Targets of the Arabidopsis MADS Domain Protein AGAMOUS-Like15. *Plant Cell Online* **21**: 2563–2577
- Zwack PJ, De Clercq I, Howton TC, Hallmark HT, Hurny A, Keshishian EA, Parish AM, Benkova E, Mukhtar MS, Van Breusegem F, et al** (2016) Cytokinin Response Factor 6 Represses Cytokinin-Associated Genes during Oxidative Stress. *Plant Physiol* **172**: pp.00415.2016

Résumé substantiel

La régénération *in vitro* repose sur des mécanismes complexes contrôlés par de multiples facteurs, dont divers stress. Dans ce réseau, les mitochondries jouent un rôle important dans la mesure où elles participent à l'intégration des signaux de stress survenant lors de divers défis environnementaux et relaient ces signaux pour influencer sur les processus de développement des plantes. Au cours de mon doctorat, j'ai étudié les effets des déficiences mitochondriales sur des processus biologiques spécifiques: la croissance *in vitro* de cellules dédifférenciées (cals) et la caulogénèse *in vitro* à partir de cals issus de protoplastes.

Le chapitre I du présent travail consiste en une introduction bibliographique divisée en trois grandes parties. La première partie rappelle quelques définitions sur la régénération et plus précisément les principaux modes de régénération chez les plantes : l'embryogenèse somatique et la caulogénèse (régénération de bourgeons). La seconde partie de cette introduction générale concerne la respiration mitochondriale. Dans cette partie est rappelé le système OXPHOS et la chaîne de transport des électrons avec une sous partie détaillée sur le complexe I. La deuxième moitié de cette partie décrit la famille des protéines PPR avec une section dédiée aux phénotypes de croissance et développement des mutants PPR qui sont affectés dans le complexe I de la chaîne de transport des électrons. Enfin, la troisième partie fait le lien entre la signalisation redox (oxydo-réduction) et le développement des plantes avec un rappel des principales espèces réactives d'oxygène (ERO) chez les plantes et les modes de détoxification des différentes ERO. Un focus est fait sur les ERO et leur détoxification au sein de la mitochondrie. Ainsi, cette troisième partie finie en présentant la régulation redox du développement des plantes.

Le chapitre II décrit notre analyse de quatre mutants d'*Arabidopsis* affectés dans le complexe I mitochondrial, qui est le premier complexe de la chaîne de transport des électrons mitochondriale. Ces mutants du complexe I ont été choisis car ils présentent des phénotypes de retard de croissance gradués et dans le but de d'analyser une corrélation potentielle entre la croissance *in vitro* et la formation de bourgeons dans les cals.

Le chapitre III explique comment nous avons pu phénocopier les mutations du complexes I en utilisant la roténone, un puissant inhibiteur chimique du complexe I mitochondrial. Nous avons appliqué l'inhibiteur à trois moments différents au cours de la séquence de régénération du cal et à différentes concentrations pour trouver le mode d'application qui induit le plus efficacement l'organogénèse. Les processus impliqués d'une

part dans la croissance des cals et d'autre part dans la régénération de bourgeons ont été étudiés en utilisant cet inhibiteur. Nous avons également utilisé un biosenseur redox cytosolique pour analyser l'état redox des cals suite au traitement à la roténone.

Comme détaillé dans le chapitre IV, les résultats obtenus dans certaines de nos expériences ont été marqués par un niveau de variabilité persistant, en particulier pour les traitements dont les concentrations en roténone sont les plus efficaces pour induire la formation de bourgeons. Nous avons étudié les cause(s) plausibles de cette variabilité en recherchant des paramètres qui seraient éventuellement corrélés au taux de régénération de bourgeons dans les cals sauvages non traités. Nous avons également étudié s'il y avait une corrélation entre la taille et le taux de croissance des cals avec le taux de régénération des bourgeons. Nous avons clôturé cette partie de notre travail de recherche en analysant l'effet de deux autres inhibiteurs de la respiration mitochondriale - ciblant le complexe IV mitochondrial et l'oxydase alternative - sur la croissance des cals et la régénération des bourgeons.

Enfin, dans le but de mieux comprendre le lien entre l'organogenèse et la déficience du complexe I, nous avons caractérisé les changements moléculaires qui se produisent au moment des étapes clés de la séquence de régénération et cela grâce à une analyse transcriptomique approfondie en utilisant des puces à ADN (microarrays) tel que présenté dans le chapitre V. Cette étude est la base de plusieurs hypothèses de travail expliquant les phénotypes d'augmentation du taux de régénération observés chez les cals issus des mutants du complexe I et les cals traités avec la roténone, décrits dans le chapitre VI.

Titre : L'inhibition du complexe I mitochondrial améliore l'organogenèse végétale *in vitro*

Mots clés : *Arabidopsis thaliana*, régénération, stress oxydatif, mitochondrie, bourgeon.

Résumé : La régénération *in vitro* est un processus complexe largement utilisé pour la multiplication végétative ainsi qu'en recherche fondamentale pour étudier l'organogenèse. Malgré les diverses applications de la caulogenèse *in vitro*, les mécanismes de régulation impliqués restent mal caractérisés. Avant le début de mon doctorat, nous avons identifié un mutant d'*Arabidopsis thaliana* chez lequel un défaut du complexe I de la chaîne de transport d'électrons mitochondriale (CTEm) entraîne une augmentation du taux de régénération comparé au sauvage, mesurée sur des cals issus de protoplastes. Au début de mon projet doctoral, j'ai confirmé le lien entre le dysfonctionnement respiratoire et l'augmentation des taux de régénération en utilisant un inhibiteur spécifique du complexe I appelé rotenone. Pour comprendre ce phénomène, j'ai étudié les mécanismes moléculaires et biochimiques liant la respiration mitochondriale et l'organogenèse *in vitro*. J'ai analysé différents mutants affectés dans l'activité du complexe I et conclu que le

retard de croissance qui en découle est positivement corrélé avec le taux de régénération. Pour comprendre comment les perturbations de la CTEm affectent la formation des bourgeons, j'ai comparé les profils d'expression des gènes dans des tissus mutants du complexe I et dans des cals traités avec la rotenone. Les résultats obtenus montrent, d'une part, que le profil d'expression des gènes est différent chez le sauvage et chez les mutants du complexe I et, d'autre part, que la rotenone induit un stress oxydatif, inhibe la prolifération cellulaire et module les régulations hormonales. J'ai confirmé que la réponse oxydative induite par la rotenone est rapidement relayée dans le cytosol en utilisant un bio-senseur de l'état redox cellulaire. Nos résultats suggèrent un lien de causalité entre un stress oxydatif induit par des perturbations respiratoires et la hausse du taux de régénération. Nos travaux pointent vers des méthodes alternatives pour améliorer l'efficacité de l'organogenèse *in vitro* par inhibition transitoire d'activités mitochondriales.

Title: Mitochondrial complex I dysfunction enhances *in vitro* plant organogenesis

Keywords: *Arabidopsis thaliana*, regeneration, oxidative stress, mitochondria, shoot meristem.

Abstract: *In vitro* shoot regeneration is a complex process routinely used for vegetative propagation and to study plant organogenesis. Despite multiple applications of *in vitro* shoot initiation, the regulatory mechanisms involved remain poorly understood. Prior to the beginning of my PhD thesis, we identified an *Arabidopsis thaliana* mutant in which a defect in the complex I of the mitochondrial electron transport chain (mETC) results in a higher shoot regeneration rate compared to wild type, measured on protoplast-derived calli. At the beginning of my PhD project, I confirmed the link between the respiratory defect and the shoot regeneration boost with a specific complex I inhibitor called rotenone. To understand this phenomenon, I investigated the molecular and biochemical mechanisms linking mitochondrial respiration and shoot organogenesis. For this purpose, I analyzed different mutants affected in

the complex I activity and concluded that the resulting growth retardation is positively correlated with the regeneration rate. To understand how mETC perturbations promote shoot regeneration, I compared gene expression profiles in complex I mutant tissues and in calli treated with rotenone. Our data show, on the one hand, that gene expression profiles are different in complex I mutants and, on the other hand, that rotenone induces an oxidative stress, inhibits cell proliferation, and modulate hormonal regulations. I confirmed that the oxidative response induced by rotenone is rapidly relayed in the cytosol with a redox-sensitive biosensor. Altogether, our results suggest a causal link between an oxidative stress caused by respiratory impairments and shoot regeneration enhancement. Our findings point to alternative methods to promote *in vitro* organogenesis via transient inhibition of mitochondrial activities.

